



Bestar Cekrezi

Hydro-morphology, channel change and sediment transport dynamics of major Albanian Rivers



UNIVERSITY OF TRENTO - Italy
Department of Civil, Environmental
and Mechanical Engineering



Doctoral School in Civil, Environmental and Mechanical Engineering
Topic 1. Civil and Environmental Engineering - XXXV cycle 2019/2022
Doctoral Thesis - April 2024

Bestar Cekrezi

**Hydro-morphology, channel change and sediment transport
dynamics of major Albanian Rivers**

Supervisor

Guido Zolezzi, University of Trento

Co-Supervisor

Klodian Skrame, Polytechnic University of Tirana

Credits of the cover image: *Bestar Cekrezi*

*View of the Erzen River in the lowland part, five km downstream of
Ndroq hydrometric station,
12 November 2022*



Contents on this book are licensed under a Creative Common
Attribution Non Commercial - No Derivatives
4.0 International License, except for the parts already published by other publishers.

University of Trento
Doctoral School in Civil, Environmental and Mechanical Engineering
<https://www.dicam.unitn.it/en>
Via Mesiano 77, I-38123 Trento
Tel. +39 0461 282670 / 2611 - dicamphd@unitn.it

Acknowledgments

At the culmination of a four-year chapter, I find myself reflecting on an experience that has left an indelible mark on my life. This period, focused on pursuing my doctoral studies, has been a journey of profound transformation. It has been a mosaic of encounters, trials, and delightful surprises that have reshaped my view of the world. Unlike anything I've known before, the pursuit of my doctoral degree has sparked a deep intellectual curiosity within me and a desire to explore new realms of knowledge. Along this path, I've immersed myself in various intellectual, cultural, and social contexts, each contributing to my personal and academic growth in its own unique way.

First and foremost, I want to extend my deepest gratitude to my supervisor, Guido Zolezzi. Guido has been more than just a mentor; he's been a trusted friend, a colleague, and a master in his field. His unwavering dedication to my development, even at the expense of his own family time, has been truly remarkable. Through his guidance, he has not only enhanced my critical thinking abilities but also equipped me with invaluable skills necessary for success in my field. Guido's infectious passion for his work, his ability to remain composed under pressure, his positive outlook, and his unwavering motivation have served as beacons of light throughout this journey. Without his unwavering support and encouragement, I would not have had the opportunity to delve into the beauty of research, expanding my knowledge in engineering while living in the breathtaking city of Trento, in the heart of the Italian Alps, surrounded by the stunning peaks of the Dolomites and embraced by picturesque lakes.

I express immense gratitude to my family, my dad, mum, and my sisters for their unwavering support throughout my Ph.D. journey and my life decisions over the past 31 years. Their encouragement and willingness to listen have been invaluable. I particularly want to thank my grandfather, whose valuable advice has been a guiding light in my life. I also cherish the memory of my grandmother, who sadly passed away last July, and I wish she could have been here to see the completion of this journey.

To all my colleagues at DICAM, especially Marta Crivellaro, who has been a big support in my thesis by improving my skills in Python, visualization figures, and utilizing her code to support some of my findings and data analysis in my PhD Thesis. I apologize Marta for the numerous times I may have disrupted you from your work by asking many questions and seeking suggestions to improve my work and learn. It has been a gift to work alongside you, great talent in research, and I am sure you will become a world class researcher in your field.

I also extend my gratitude to the internal Ph.D. committee at the University of Trento (DICAM), Prof. Marco Toffolon, and Annunziato Siviglia, for their critical thinking and feedback every year, which has helped improve the quality of my research work. I am thankful to my co-supervisor, Klodian Skrame, at the Polytechnic University of Tirana, for his assistance with data and the classification of Albanian rivers' geology. Additionally, I appreciate the efforts of Prof. Andrea Andreoli and Simone Bizzi, who have provided invaluable feedback on my thesis review, enhancing its quality.

Special thanks to Prof. Marco Bezzi, whom I first met with my supervisor in Albania in July 2015 while studying coastal erosion in Lazy Bay. At that time, I was a master's student at the Faculty of Civil Engineering, Polytechnic University of Tirana. I appreciate his character of working hard with full energy 24 hours per day and the synergy we have created together. His suggestions and supportive comments during my application for the PhD program were instrumental in enrolment of PhD programme.

To all my friends and colleagues in Albania, professors at the Polytechnic University of Tirana, especially the Institute of Geosciences of Albania, specially to Prof. Liljana Lata I am immensely thankful for providing crucial historical data that was instrumental in my research work.

I extend my gratitude to the administration staff of the University of Trento, especially Daniela Tosi at the International Office Unitn, who was my first point of contact upon arriving in Trento. Additionally, I want to thank PhD Secretary Cristina at DICM for her invaluable assistance throughout this journey.

And last but not least, to the Agenzia Italiana per la Cooperazione allo Sviluppo (AICS), I express my sincere gratitude for the Ph.D. grant awarded during the three years of my Ph.D. journey. Without their financial support, I would not have been able to pursue my Ph.D.

Trento, 12 April 2024

B.C

Contents

Abstract	4
1. Introduction and research design.....	5
1.1 General overview of Albanian Rivers.....	5
1.2 Anthropic pressures.....	10
1.3 Methodological framework for hydromorphological assessment.....	15
1.4 Institutional framework of river management in Albania	15
1.5 Reference hydro-morphological concepts for the present thesis study work....	18
1.6 Short review of studies on Albanian rivers	22
1.7 Aim and outline of the thesis.....	23
2 Country-wide analysis of the present and historical morphology of major Albanian rivers	26
Abstract	26
2.1 Introduction	26
2.2 Overview of the studied river catchments.....	29
2.3 Material and Methods	33
Choice of the IDRAIM method	33
Overview of the adopted module of the IDRAIM method.....	34
Workflow of the method	36
2.4 Results and discussion.....	51
2.5 Conclusion.....	73
3 Intense channel modifications in the Erzen River following rapid socio-economic changes: reconstructing channel incision and narrowing in a data-scarce context....	75
Abstract	75
3.1 Introduction	76
3.2 Study Area.....	78
3.3 Material and methods.....	82
3.3.1 Automated Landsat image analysis (1985-2020).....	82
3.3.2 Analysis of Corona Satellite images (1968).....	90
3.3.3 Indirect methods to estimate channel incision.....	92
3.3.4 Mapping of main hydromorphological pressures.....	94

3.4.1	Changes in the active river corridor width.....	98
3.4.2	Changes in Active Channel Width	102
3.3.3	Vertical channel adjustments.....	106
3.4.5	Analysis of the possible drivers of channel adjustments	110
3.5	Discussion	119
3.5.1	Channel adjustments in the Erzen river and relation other contexts	119
3.5.2	Possible driving factors of change	122
3.5.3	Limitations of the work.....	125
3.5.4	Management implications.....	126
3.6	Conclusion.....	127
4.	Assessing the role of recent channel adjustments of Albanian rivers and of climatic oscillations on fluvial sediment inputs to the Adriatic Sea.	128
	Abstract	128
4.1	Introductions	129
4.2	Study Area and relevant gauging stations.....	132
3.3	Material and Methods.....	135
4.3.1	Methods for historical hydrometric and sediment transport measurements in Albania	136
4.3.2	Collection of historical discharge time series and digitalization for Erzen river in Albania	137
4.3.3	Flow Data processing.....	139
4.3.4	Estimate of incipient sediment mobility conditions	144
4.3.5	Estimation of Sediment Transport capacity	148
4.3.6	Calibration of the simplified model for sediment transport capacity.....	152
4.4	Results	154
4.4.1	Discharge statistics	154
4.4.2	Return times analyses of discharge.....	159
4.4.3	Estimates of Sediment transport capacity	161
4.5	Discussion	165
4.5.1	Suspended Sediment Load Analysis	166
4.5.2	Discharge Trends and Statistics.....	166
4.5.3	Effects of Channel Adjustments on Sediment Transport Capacity.....	167

4.6 Conclusion.....	167
5. Conclusion	169
Appendix.....	172
References	178
List of figures.....	187
List of tables.....	193

Abstract

This dissertation offers a comprehensive exploration into the hydromorphological transformations of major Albanian rivers, situated within the unique ecosystem of the Western Balkans. Covering the Mat, Ishmi, Erzen, Shkumbin, Seman, and Vjosa rivers, the research spans critical facets of river dynamics, contributing vital insights for effective river basin management in line with the European Union Water Framework Directive and Floods Directive. Examining nearly 80% of the Albanian river network, with catchment areas exceeding 650 km², the study reveals the present dominance of single-thread (22%) and sinuous (17%) river morphologies. Notably, a distinct trend towards channel narrowing emerges, with historical analyses showcasing substantial shifts, including transformations from braided to wandering (39%) and braided to sinuous (10%). Meandering reaches experience a 21% alteration, with 20% transitioning into abandoned reaches. Over five decades, approximately 53 km of river channels shift into abandoned status, emphasizing the impact of channelization, land cover changes, and natural river cut-offs. This country-wide analysis establishes a foundational understanding for river basin management, flood prevention, and restoration, crucial as Albania moves towards EU membership.

Focusing specifically on the Erzen River, a major watercourse passing near Tirana and Durrës, the research delves into meticulous analyses of channel adjustments, incision, and narrowing. Utilizing remote sensing, historical image analyses, DEM, and field surveys, the study reveals rapid changes in channel morphology, including up to 75% channel narrowing and significant riverbed incision. Sediment mining emerges as a primary driver, with 22 mining sites detected between 1995-2015. These observed channel modifications contribute to coastal erosion and potential downstream freshwater shortages, emphasizing the urgent need for effective sediment transport management. Accurate data and predictive calculations play a crucial role in achieving sustainable river management.

Further exploring sediment transport dynamics, the study analyses historical hydrology data from 1949 to 1992 for the Erzen River. A calibrated sediment transport capacity predictor offers insights into the impact of channel changes on sediment transport rates. Comparison with the nearby Shkumbin River reveals important baselines to understand the intricate relationship between human activities, sediment transport, and coastal erosion. The research addresses a critical question: to what extent have modifications in channel morphology affected sediment transport capacity in selected Albanian rivers? The findings underscore the pivotal role of predictive calculations in developing basin management plans aligned with EU directives.

In essence, these integrated findings provide a nuanced understanding of hydromorphological changes in major Albanian rivers, offering comprehensive insights into the evolving river dynamics. The research serves as a foundational resource for policymakers, scientists, and stakeholders, advocating for sustainable river basin management practices to preserve the ecological significance of the Western Balkans' unique river systems for future generations.

Chapter 1

1. Introduction and research design

1.1 General overview of Albanian Rivers

In the most industrialized countries of the world, rivers and streams have undergone significant alterations by human activities since more than 150 years, following the industrial revolution of the mid 1800s, bringing a wide set of benefits to human societies, while at the same time affecting with increasing intensity the freshwater and terrestrial environments and becoming a major causes of ecosystem degradation, habitat and biodiversity loss. In Europe, this phenomenon has been evident for centuries, allowing for various uses of water resources such as drinking water, irrigation, and hydropower. In the nearby Balkan region, many rivers and streams, including several large ones, have instead maintained a high degree of naturalness and their free-flowing character due to a different socio-economic development dynamics, which has been also lagged in time, if compared to Western Europe. Despite limited available studies and data on these valuable river environments, recent research (Schiemer et al., 2020) has revealed extremely high levels of biodiversity, also leading, among other ecosystem values, to the discovery of new animal species unknown to science.

This region has also been named the "blue heart of Europe" (RiverWatch, 214, EuroNatur, 2015, Wieser, C. 2019, IUCN, 2022). Besides its intrinsic values in terms of ecosystem integrity, the minimal anthropic disturbance on many of the river systems in the Western Balkans also bears a relevant economic development potential for the region in terms of attractiveness for tourism, especially when oriented to seek pristine environments, increasingly rare in the western part of Europe. However, massive exploitation and regulation projects, often based on a limited understanding of these river systems and their dynamics, have been emerging since 10-15 years with increasing intensity due to the growing political stability in the region after major socio-economical changes brought by the collapse of the communist regimes in the early 1990s. While the potential for exploitation through dams and barriers, sediment extraction from riverbeds as construction material, water supply for irrigation and other uses can provide substantial benefits to the human society, the widespread lack or fragmentation of knowledge, data and information on the functioning of freshwater systems in the Western Balkans pose a considerable threat to their natural value and, at the same time, also high risk to the economical investments required for infrastructure development. This, in turn, jeopardizes an environmental value that is almost unique in Europe and also considering that landscape and environmental planning are in the process of being more systematic and structured only since a relatively short time.

The development of data, studies, and scientific information on the dynamics of the rivers in the blue heart of Europe is a crucial contribution that can only come from the scientific community. This effort is essential to ensure a sustainable future for this unique environmental heritage on our doorstep. Through a quantitative understanding of river flows,

sediment transport, and the evolution of forms and habitats, it becomes possible to propose "win-win" solutions that balance socio-economic development, water resource utilization, and environmental quality.

The present thesis focuses on the hydromorphology and river channel change of Albanian rivers, which represent a paradigmatic example of several river systems in the Western Balkan area.

Albania boasts an extensive network of rivers and streams, with eight primary river catchments draining into eight main rivers: Drin, Mat, Ishmi, Erzen, Shkumbin, Seman, Vjosa, and Bistrica (Fig. 1.1). Among these, the Drin River holds the distinction of being the longest, coursing through the country for 285 km. Notably, the Vjosa River stands out as one of Europe's last remaining wild rivers, with huge ecological value and recently declared a "Wild river national park". The hydrographic characteristics of Albanian rivers include a notably high flow rate, as documented by (Cullaj et al., 2005) and summarized in Table 1.1, which provides hydrographic data for seven rivers based on information collected prior to 1990. According to available data, the average total annual river discharges range between 39 billion m³/y and 42 billion m³/y. Approximately 95% of these discharges find their way into the Adriatic Sea, with the remaining 5% flowing into the Ionian Sea. Groundwater resources, estimated to be between 9 billion m³/y and 13 billion m³/y (UNECE, 2018), contribute significantly to the overall hydrological dynamics of the region.

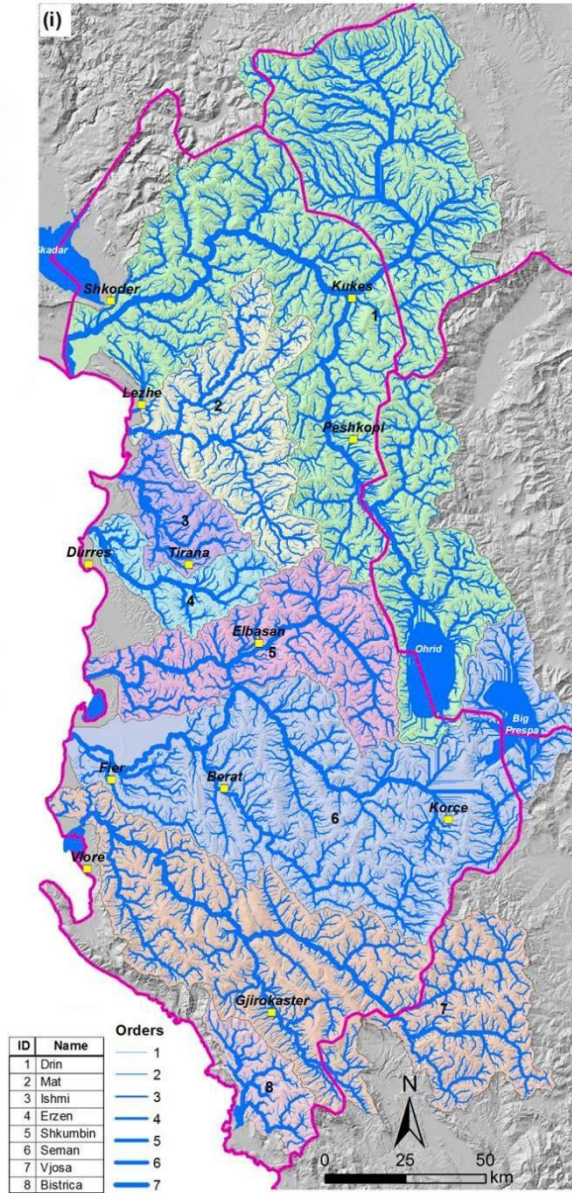


Figure 1. 1. Hydrological map of Albania (Ozdemir, 2013). The eight river basins are highlighted by different colours.

Basin	Length (km)	Drainage basin (km ²)	Mean altitude (m.a.s.l)	Average flow (m ³ /s)	Annual sediment yield to sea (tons/km ²)
¹ Drin	285	11756	971	352	1129
Mat	115	2 441	746	103	1032
Ishmi	74	673	357	20.9	3715
Erzen	109	760	435	18.1	5222
Shkumbin	181	2 444	753	61.5	2938
Seman	281	5 649	863	95.7	2876
Vjosa	272	6 706	855	195	1249

Table 1. 1. Main characteristic of major Albanian rivers (Kabo. M, 1990; Hydrology of Albania, 1979).

Albania, despite its modest size, encompasses diverse climate regions. The coastal plains exhibit a mediterranean climate, while the highlands predominantly experience a continental climate.

Across much of the country, the climate is characterized by mild and wet winters alternating with hot and dry summers. Precipitation is abundant, with a multi-annual mean ranging from approximately 1,300 mm/y in the southern regions to over 2,000 mm/y in the northern areas, gradually decreasing in an easterly direction. Winter accounts for around 40% of the total rainfall, followed by 32% in spring, and the remaining precipitation distributed between autumn and summer. Notably, rain showers are brief yet intense, capable of transforming into torrents of water within minutes, leading to the erosion of soil that is subsequently carried to the sea (Kabo. M, 1990; World Bank, Climate Change Knowledge Portal, 2023)

Mean monthly climate data for Albania are reported in Figure 1.2 using data from World Bank (2023), with reference to average minimum, average mean and average maximum surface temperature and mean monthly precipitation referred to the 1991-2020 period.

¹ The annual sediment yield to sea for the Drin river considers only the contribution of the Drin river at Vau i Dejes station without the contribution of the Buna river.

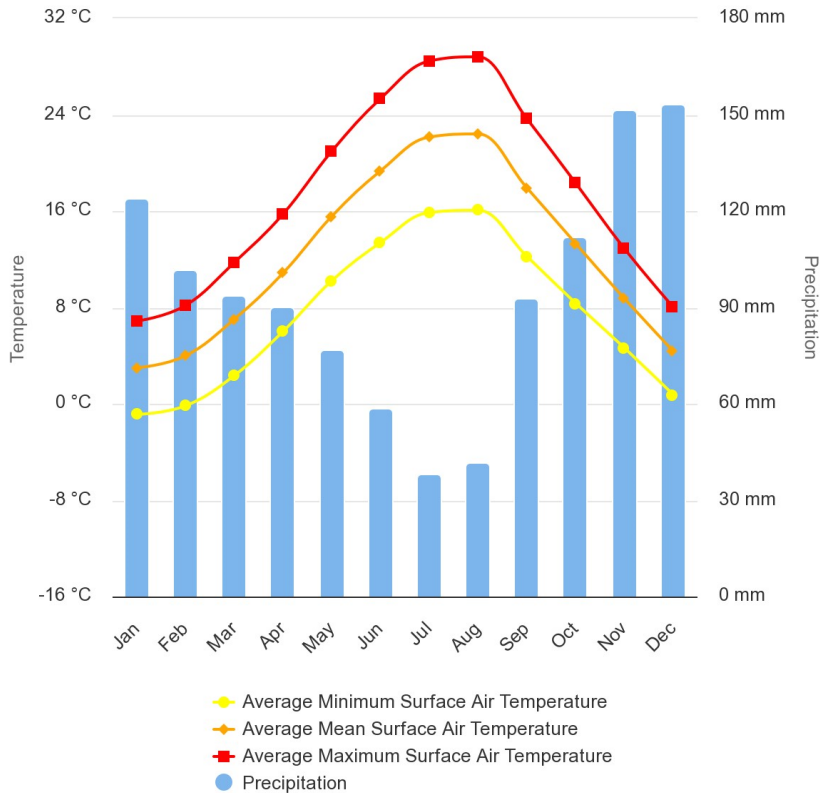


Figure 1. 2. Monthly climate information of Albania based on the 1991-2020 period, data from the World Bank, Climate Change Knowledge Portal (2023)

Albanian rivers present a highly significant natural value attributable to their diverse geomorphological features, ecological significance, and hydrological dynamics (Cullaj et al., 2005). Nestled within rugged terrains and verdant landscapes (Figure 1.3), these water bodies play a fundamental role in supporting regional biodiversity and promoting health and integrity of a variety of ecosystems. Several studies have shown how the hydrological and morphological complexity and diversity of these river systems contribute to a dynamic aquatic, riparian and also terrestrial environment (Eftimi, 2010; Miho et al., 2008).



Figure 1. 3. Illustrative images of the landscape of the Buna river in the left (a), part of Drin basin (source <https://medwet.org/>) and of the Vjosa river (b), (source: <https://www.muchbetteradventures.com/magazine/vjosa-national-park-now-announcement/>)

The aquatic ecosystems of these rivers serve as habitats for a diverse array of flora and fauna, including rare and endemic species, as evidenced by research findings on the Vjosa River (Drescher, 2018). Thorough biodiversity assessments underscore the critical importance of these waterways as essential habitats and migration corridors. The need for conservation extends beyond their scenic beauty (Figure 1.3), encompassing their crucial role in sustaining a variety of valuable, yet poorly quantified, ecosystem services.

1.2 Anthropic pressures

Albanian rivers, fundamental to the nation's ecological equilibrium, have undergone substantial transformations since the 1960s, largely propelled by ambitious dam construction projects. Though relevant for some river systems, initial changes were focusing only on localized areas. The initiation of major dams along the Drin River, primarily for electricity generation, started in the 1960s. Originally conceived to address growing energy demands, these dams caused changes in the river's natural flow, ushering in alterations in sediment transport and influencing the integrity of river habitats. The consequences of these interventions extended far beyond immediate locations, setting in motion a series of ecological transformations that persistently shape the course of Albanian rivers. An illustrative example of these transformations is the city of Kukes (Figure 1.4). In 1962, the city underwent a relocation to accommodate the construction of the Fierza Dam, a significant hydropower project along the Drin River. This relocation not only altered the urban landscape but also resulted in the creation of a vast artificial lake. The Fierza Dam represents an interesting example of the interplay between human interventions, societal needs, and environmental impacts.

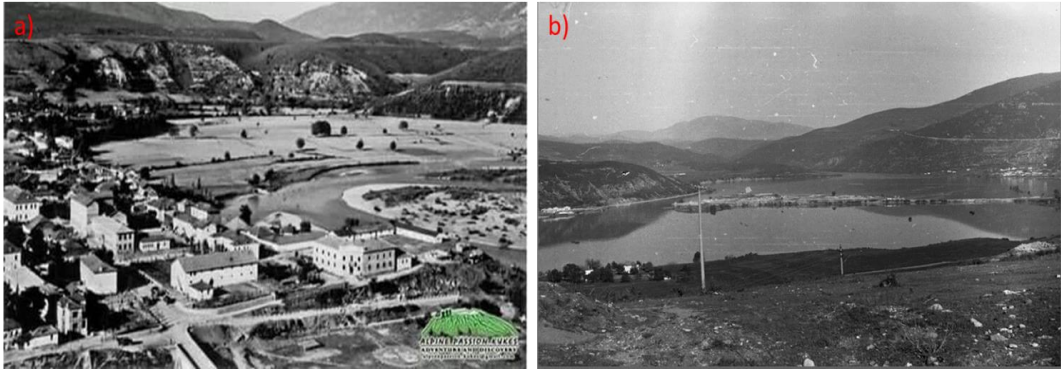


Figure 1. 4. Kukes City located in the North-East of Albania. (a) the city before creation of the Fierza hydropower dam in 1978. (b) the city after the completion of the dam.

Simultaneously, in the pre-1990 landscape, an increase in small dams construction unfolded across various streams of other rivers, motivated by agricultural expansion and the increasing need for irrigation; these dams likely caused some alterations of the low flow regimes in some streams, while probably not affecting too much the sediment transport regime and the channel morphology, though studies on such issue are widely lacking.

In the post-1990 landscape of Albania, the practice of sediment extraction (Figure 1.5) from rivers has emerged as a significant concern, disrupting the natural sediment transport regime, inducing habitat destruction, and triggering coastal erosion. This prevalent activity not only alters river morphology but also results in a deficit of sediment supply, impacting the replenishment of riverbeds and downstream areas. This has likely triggered processes of channel narrowing and incision, which have not been quantified so far but that are visually evident particularly to the local populations and stakeholders.



Figure 1. 5. (a) Sediment mining in Shkumbin river. (b) Exposure of the “Bridge Zogu” foundation in Mat River associated with channel incision.

Urbanization, particularly in cities like Tirana and Dures, has transformed riverine landscapes in Albania (Figure 1.6). The construction of houses in lowland areas near rivers

has increased the flooding risks. The absence of comprehensive flooding studies and urban planning intensifies the vulnerability of the rapidly growing, mainly unplanned settlements across the major urban centres of the country (Figure 1.7). Such unregulated floodplain development in the lowland parts of rivers indeed represents a major source of risk. The demand for housing and land, coupled with urbanization, has led to the construction of many houses near the banks of rivers. This urban expansion occurred without adequate regulation or urbanistic requirements, exacerbating the vulnerability of these areas to flooding.



Figure 1. 6. Terkuze River (Ishem river basin) near Tirana Airport. (a) Corona images 1973 (reach 5) and (b) satellite image of 2015, showing urbanization and buildings very close to the river channel, which at the same time has been dramatically narrowed.



Figure 1. 7. Examples of flooding in Albania. (a) flooding in lower part of Drin River, south of Shkodra city 23.11.22. (b) flooding in city of Tirana 03.11.2023, Lana River.

In recent years, the riverine landscape, especially in the mountain reaches, has evolved with the advent of run-of-river hydropower projects (Figure 1.8). These projects, while providing renewable energy, came with impacts for the downstream environment. Alterations in river

morphology and habitat composition, coupled with sediment extraction for construction, contribute additional ecological impacts, yet largely unquantified, to Albanian rivers.



Figure 1. 8. Run off river hydro power plant in Valbona River (tributary of Drin River) in Albania. Valbona valley is a National Park. (a) construction phase in 2018 of hydropower plants in Valbona valley. (b) people from NGO that protest against hydropower plants that are being built in the same national Park (2022).

Albanian rivers stand out for their remarkable sediment transport values, as for instance, reported by Ciavola (1990). The Erzen River, for instance, exhibits an annual sediment transport of 5222 tons/km², while the Ishem River and the principal tributary of the Seman River, the Devoll River, display values of 3715 tons/km² and 3589 tons/km² per year, respectively. Notably, T. Mulder and J. Syvitski (1995) underscore the global significance of Albanian rivers as noteworthy contributors to sediment transport on a regional scale in the Mediterranean area, with specific sediment yields among the largest at global level.

This complex combination of high natural value, high resource availability, rapid transformation by anthropogenic stressors, and of little data availability, accentuates the urgency for adopting sustainable river management practices, particularly in light of the extensive dam construction and sediment mining activities by both the private and public sector. The construction of dams along Albanian rivers has initiated a substantial reduction in sediment transport, possibly inducing shifts in river morphodynamics. This transformative alteration might carry profound consequences for both river ecosystems and coastal areas. The tandem effects of sediment extraction, particularly notable in Albanian rivers emitting high sediment transport per catchment area, and dam impoundment, disrupt the natural flow of sediments. This can compromise the river's inherent capacity to replenish and sustain its channel morphology that was established as a dynamic equilibrium over time, therefore not only inducing a noticeable shift in river morphology and habitat availability, but also, possibly, significantly amplifying susceptibility to coastal erosion. An interesting example is the one of Lalzi Bay (Figure 1.9), where the reduction in fluvial sediment transport, has likely been a major factor that facilitated the coastal erosion, with a stark loss of approximately 800 meters of land over the last three decades, as presented by De Leo (2016).

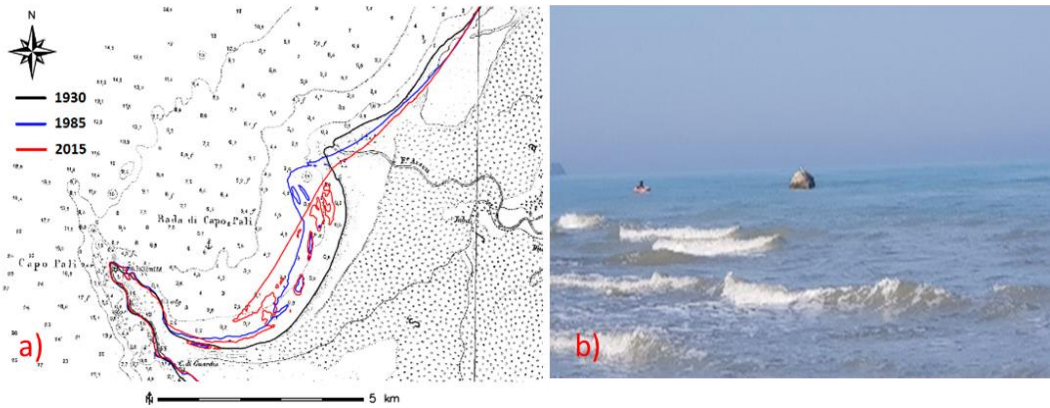


Figure 1.9. Coastal Erosion Impact, Lalzi Bay, Albania (Leo et al., 2017). (a) depicts the notable movement of Lalzi Bay's coastal line from 1985 to 2015, indicating an 800-meter loss. (b) photo taken in 2020, a bunker built before the 1990s on the local sand beach, is now submerged in the sea, illustrating the drastic effects of coastal erosion.

The European Union Water Framework Directive (WFD) is a key international environmental legislation that aims to ensure the sustainable and integrated management of water resources across EU member states. Adopted in 2000, the WFD outlines a holistic approach to water policy, emphasizing protection, improvement, and sustainable use of water ecosystems. Its overarching goal is to achieve and maintain a so called "good ecological status" for all surface waters, including rivers, lakes, coastal waters, and groundwater, by 2027, a deadline that, though having progressively been shifted, has allowed member states to develop country-wide assessments of the ecological conditions of their water bodies and, based on that, to develop comprehensive river basin management plans to achieve those targets. The WFD indeed encourages member states to implement river basin management plans as key tools, fostering a coordinated approach to water management, focusing on the river catchment as the fundamental spatial unit. It incorporates principles of stakeholder involvement, adaptive management, and consideration of the economic dimension of water use. The directive places a strong emphasis on preventing further deterioration of water quality, promoting the restoration of degraded ecosystems, and ensuring the sustainable use of water resources for both present and future generations. A key element of the WFD to assess the overall "ecological status" of water bodies is represented by hydro-morphology, the integrative discipline that accounts for the mutual role of hydrology and morphology on the overall environmental functioning of river systems. To assess the ecological status, the evaluation of "hydro-morphological quality elements" is required, which implies the need of a detailed knowledge of the morphology, the flow and sediment supply regimes of all water bodies, and how this might have been altered with respect to some "reference conditions", assumed as those corresponding to minimal human impact-

The other key EU directive with major management implications for river management is the EU Floods Directive (FD), designed to enhance the EU's capacity to manage and mitigate

the impacts of floods. Published in 2007, it addresses the challenges associated with flood risk, emphasizing a comprehensive and cooperative approach among member states. Following analogous principles to the WFD, the FD promotes a holistic flood risk management cycle, encompassing risk assessment, mapping, prevention, protection, and preparedness, also focusing on the river catchment as the fundamental spatial unit on a both conceptual and management level. Member states are required to develop flood risk management plans, fostering collaboration across borders and ensuring coordinated actions to address shared risks.

1.3 Methodological framework for hydromorphological assessment

Assessment of river hydromorphology is a crucial element for complying with both the WFD and the FD, and therefore serves at least two major regulatory purposes. Different EU countries have adopted different specific methods for such assessment, and some of these methods have been implemented within comparative analyses to test their suitability for application also in other countries. An example is the IDRAIM methodological framework for hydromorphological assessment, analysis and monitoring (M. Rinaldi et al., 2015), which was originally developed as the reference method in Italy and which has further undergone a comparative analysis at a European level within the REFORM FP7 project (M. Rinaldi et al., 2015). IDRAIM represents a significant advancement in hydromorphological assessment, analysis, and monitoring. Specifically designed for the Italian context, it aligns with the objectives of the Water Framework and Floods Directives. Built upon contemporary, state-of-art geomorphological concepts and methods, the IDRAIM framework was initially tailored to addresses Italy's specific characteristics in terms of river channel morphologies, observed channel adjustments and types and timing of human pressures, qualitatively considering hazards related to fluvial dynamics. Tailored for use by national environmental and water agencies, the IDRAIM framework encompasses four key phases: (1) catchment-wide characterization of the fluvial system; (2) evolutionary trajectory reconstruction and assessment of present river conditions; (3) prediction of channel evolution; (4) identification of management options. The REFORM project, spanning four years and involving 26 partners from 15 European countries, aimed to address challenges in achieving ecological objectives for European rivers mandated by the EU Water Framework Directive (REFORM, 2015). With many rivers regulated for flood protection, navigation, and hydropower, the ecological impacts of these modifications were still to be understood at the beginning of the implementation of such framework. REFORM sought to provide cost-effective tools for implementing restoration measures and monitoring. The project focused on improving existing tools and developing new ones to enhance the success and cost-effectiveness of restoration procedures. In the same time, supporting River Basin Management Plans of the WFD and other European environmental directives.

1.4 Institutional framework of river management in Albania

As Albania progresses toward EU membership, ongoing projects relevant to national-scale river and water resources management focus on enhancing the legal and institutional

framework while, at the same time, increasing and coordinating the biophysical knowledge base for effective policy preparation, planning, implementation, and evaluation. The objective is to establish clear and transparent responsibilities, aligning with the implementation of the EU Acquis. Water management legislation and regulations are categorized into four major sections: primary legislation, secondary legislation, inter-sector legislation, and EU Directives. This comprehensive approach aims to ensure alignment with European standards and facilitate the integration of Albania into the EU framework.

Regarding to the primary legislation, since November 15, 2012, water resources in Albania have been regulated by Law No. 111, "*On Integrated Management of Water Resources*," subsequently amended by Law No. 6/2018. These legal provisions aim to:

- Protect and enhance the aquatic environment, encompassing surface waters (temporary or permanent), sea water, territorial waters, exclusive economic zones, continental shelf, and groundwater, ensuring their sustainable status.
- Ensure the security, protection, development, and sustainable utilization of water resources crucial for life and the socio-economic development of the country.
- Facilitate the equitable distribution of water resources through effective management.
- Safeguard water resources from pollution and overuse, promoting consumption in line with actual needs.
- Establish the necessary institutional framework at both national and local levels to implement a comprehensive national policy for the administration and management of water resources. This framework is designed to benefit communities and align with the social and economic interests of the country.

Administration and management structures for water management are provided at national and local level. *Figure 1.10* shows the current relationship between government ministries and local agencies. At the national level, the National Water Council (NWC) is the central executive body. Albania being a candidate country for EU Accession, it needs to approach compliance with a significant number of EU directives related to water management. The country is divided into six river basins, each one having a River Basin Council (RBC) and an Administration Office of Water Basin. This structure is favourable, in principle, to counteract the current fragmentation of water resources management and promote an effective administration at local level (*source: AMBU website*²).

The ministry of Agriculture and Rural Development is responsible for setting national policies, supervising legal and financial aspects of related organizations, and overseeing the technical aspects of infrastructure. Additionally, the ministry conducts audits, inspections, and maintains databases to ensure effective operation and quality monitoring of irrigation and drainage systems.

² <http://www.ambu.gov.al/misioni/>

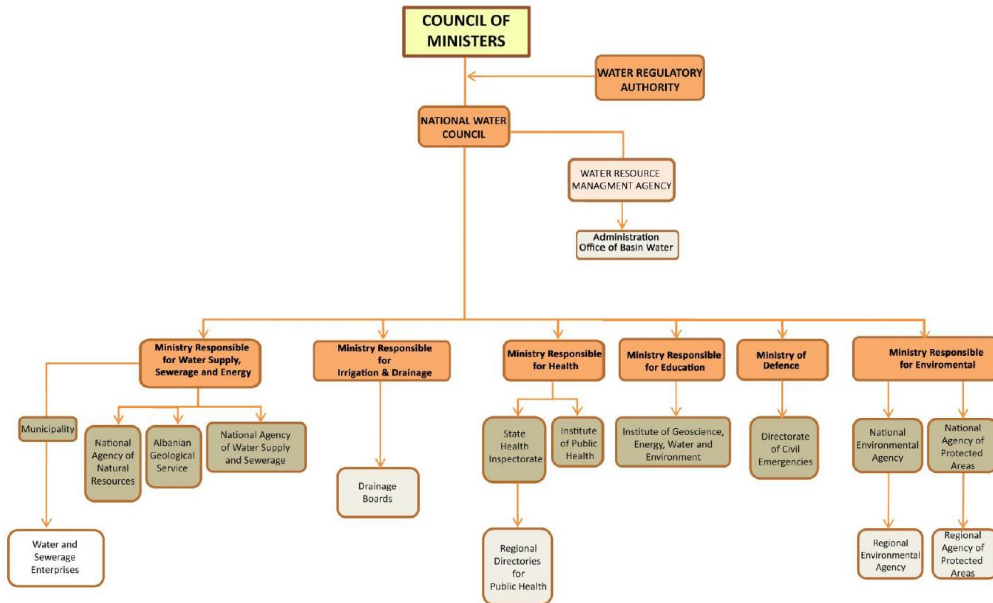


Figure 1. 10. Organizational chart for institutional framework on water resources management, Albania (Ministry of Agriculture and Rural Development, Albania, 2019).

National Water Council and Water Resource Management Agency

The National Water Council (NWC), established in 1996, serves as the central body for integrated water resources management planning. It leads the Integrated Policy Management Group and sub-thematic groups for specific water-related areas. The NWC is supported by the Water Resource Management Agency (AMBU), functioning under the Prime Minister's Office, responsible for implementing water policies, managing permits, promoting water user participation, and coordinating river basin activities (AMBU, website).

Water Monitoring

Water monitoring in Albania involves a complex network of over 20 government institutions. The National Environmental Agency (NEA) plays a central role in overseeing water quality and quantity monitoring, collaborating with institutions such as the Institute of GeoScience, the Albanian Geological Survey, the National Agency of Natural Resources, the Institute of Public Health, and the Water Regulatory Authority. These organizations collectively monitor hydro-meteorological parameters, surface and underground water quality, hydropower plants, public health aspects, and regulatory compliance in the water sector.

Administration Offices of Water Basins

Following the 2015 local elections and the implementation of Law No. 115/2014 on administrative-territorial division, Albania now has 61 municipalities as basic units of local government, replacing the previous structure of villages and municipalities. Local

Government Units (LGUs) are organized within these municipalities, maintaining administrative subdivisions based on former villages. The decentralization of water management occurs at the River Basin level through six River Basin Councils (RBC) and their corresponding Administration Offices of Basin Water. River Basin Council –(i) Drin Buna, (ii) Mat, (iii) Ishem-Erzen, (iv) Shkumbin, (v) Seman and (vi) Vjose. Chaired by responsible Prefects, each RBC aims to ensure rational protection, development, and fair distribution of water resources within its designated basin boundaries, emphasizing the prevention of pollution, misuse, and overuse, in alignment with national legislation.

1.5 Reference hydro-morphological concepts for the present thesis study work

Albania lacks crucial baseline information on the morphological dynamics and changes in its rivers. The understanding of how river morphology evolves over time, including the consequences of these changes, remains inadequately documented, despite being a fundamental prerequisite for sustainable river and water resources management. Recognizing the essential role of quantifying and comprehending the dynamic nature of river morphology, especially in accordance with the Water Framework Directive (WFD), is pivotal for a comprehensive assessment of the hydromorphological status of Albanian rivers. Moving from a management to a scientific level, this gap is also more fundamentally related to the lack of knowledge about the key biophysical processes that are most relevant in the dynamics of Albanian rivers and that are important to control their rapid morphological responses to rapidly evolving anthropogenic stressors. This information and scientific gap hinders our ability to assess the current state and to predict the potential future trajectories of river morphology in Albania in response to different management choices, and therefore, limits the possibility to wisely choose sustainable management alternatives.

A first needed information in this respect is a census of the channel morphologies that appear in the major rivers of the country. An analogous study has been recently performed by compiling the Alpine rivers' morphology (Hohensinner et al., 2021), investigating 143 major rivers in the European Alps, which underscored a considerable change between pre-regulation and present channel patterns. For Alpine rivers, major hydro-morphological regulation occurred since the mid-1800s, while for Albania, major river alteration by human effects is likely to have started nearly one century later. Hohensinner et al. (2021), analyzing historical cartographic data spanning the 1750s to nearly 1900, reveal that in the early 19th century, about one-third of major Alpine rivers displayed multi-channel configurations, while 28% featured single-bed channels oscillating between valley sides. Variations in historical river patterns were linked to slope, floodplain width, and distance from sources, reflecting tectonic/orographic conditions. The present river morphology in the same Alpine region has been strongly modified. Channel straightening resulted in a 4.3% loss (510 km) of river course length. Currently, multi-channel stretches represent only 15% of their historical length, a percentage that has been halved after major regulation, and 45% of larger Alpine rivers have undergone intensive channelization or transformation into reservoirs (Figure 1.11).

A similar analysis for Albanian rivers would be particularly needed to set a key baseline on which to ground sustainable river management plans for the near future.

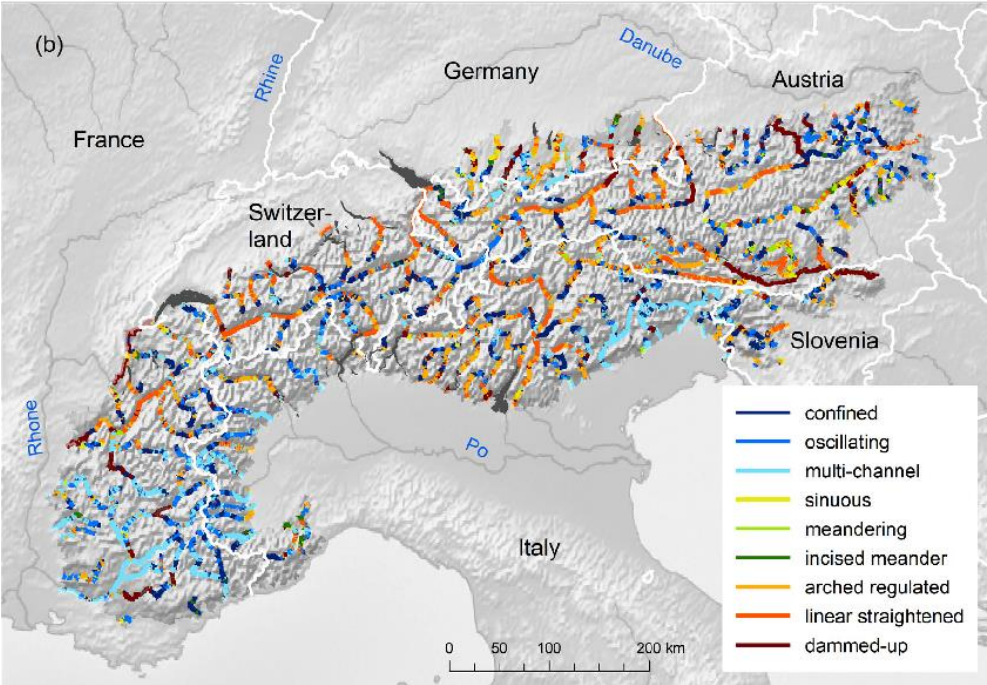
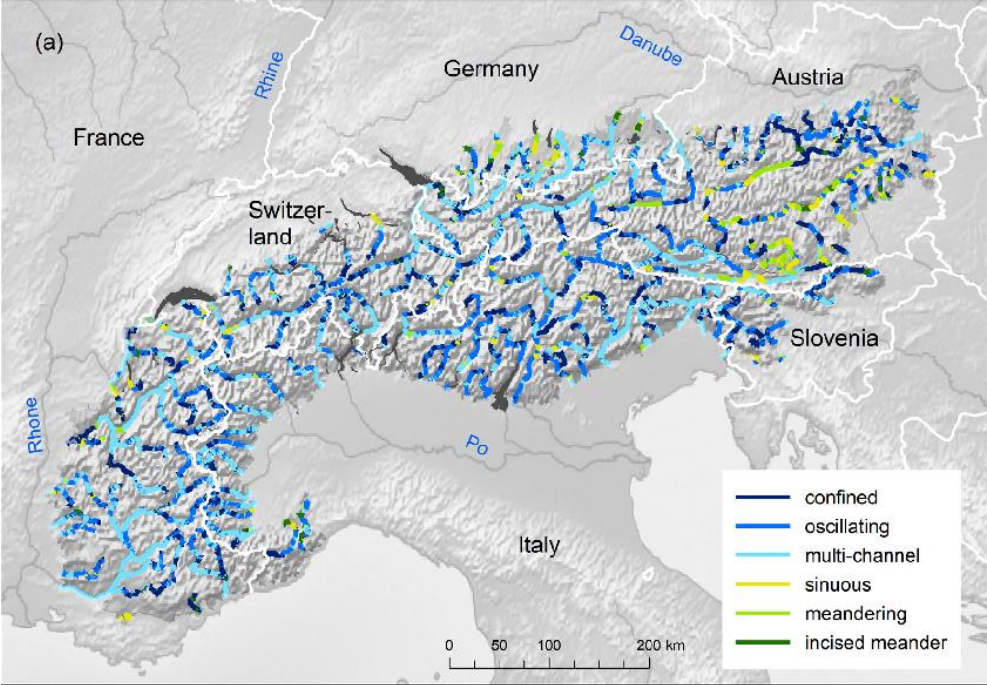


Figure 1. 11. Morphological patterns of major Alpine rivers (Hohensinner et al., 2021) (a) historical patterns in the early 19th century; (b) present-day patterns as detected in a 2017 satellite image.(Hohensinner et al., 2021)

A census of the past and present morphologies of the major rivers in a region is a fundamental starting point but can hardly provide insight on the main (bio)physical processes that control the evolution of the same rivers at the reach scale, and their response to anthropogenic stressors and management actions. The River Trajectory Concept, as explored by several authors (e.g. Ziliani and Surian, 2012), allows important insights into the dynamic relationship between the river dynamics and its external drivers at multiple scales, and take the form of the temporal evolution of representative river dynamics indicators such as the bed elevation and the channel width over time. This concept provides a valuable framework for understanding the morphological evolution of rivers, particularly in the context of changes in bed elevation and channel width. Examining such trajectories has been recognized as an important step in understanding the complex interplay of environmental factors that influence river systems. At present, morphological evolutionary trajectories for Albanian rivers have been very poorly investigated, and there is a strong need to reconstruct and interpret them at the river reach, catchment and country scales.

For instance, the Tagliamento River has undergone significant channel narrowing, with changes in channel width of up to 700 meters over the past 200 years. This narrowing phenomenon is a dynamic aspect of the river's trajectory, as described by Ziliani and Surian (2012). Understanding such alterations in channel width is crucial for managing the Tagliamento's evolving morphology and implementing strategies to address environmental impacts.

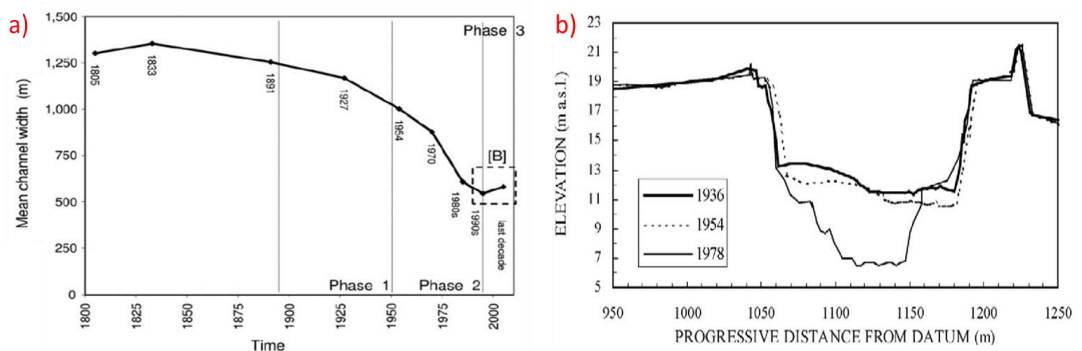


Figure 1. 12. Channel Trajectory concept. (a) Tagliamento river (Italy) channel width evolution in time (Ziiani, and Surian, 2012). (b) incision of Arno River (Italy) as documented by the comparison of the cross-sectional bed elevations over time in different years (Surian and Rinaldi 2002).

In contrast, the Arno River has experienced channel incision, with the riverbed lowering by 7 meters from 1936 to 1978 (Surian and Rinaldi, 2002). This substantial incision along the Arno exemplifies the channel evolutionary trajectory using the bed elevation as representative indicator of the channel morphology. The incision reflects the occurrence of

anthropogenic sediment deficit causing dominant erosional processes, and provide a comprehensive understanding of the river's trajectory for effective management.

In conjunction with this concept, the notion of Dynamic Equilibrium and Channel Pattern, as articulated by several authors since the late 1960s (e.g. Eaton et al., 2010), contributes significantly to our comprehension of river systems processes and response to external drivers. The dynamic equilibrium concept posits that rivers strive to achieve a balance between erosion and deposition over time, influencing their overall channel pattern, which appears similar through time though in continuous local modifications under the action of competent flood events to drive sediment transport and morphological change.

Understanding the changing dynamics of rivers is crucial for effective and sustainable river management, encompassing both environmental protection and hazard mitigation. The concept of trajectories, or the paths rivers follow in their morphological evolution, is essential for informed decision-making. In Italy, for instance, awareness of the changing course of most of the river systems at the country level, including the largest Po River, has been pivotal in implementing measures within river basin management plans. Similarly, in France, monitoring the evolving morphology of most river systems has informed strategies to balance ecological preservation with human activities; here, pivotal studies at the country level referred to the Rhone river basin. In Poland, the Vistula River's trajectory analysis guides efforts to mitigate flood risks and preserve the integrity of river ecosystems.

The importance of tracking river changes lies in anticipating and mitigating potential environmental impacts. For instance, alterations in river morphology can affect habitats, biodiversity, and water quality. By comprehending these changes, authorities can implement proactive measures to safeguard ecosystems and biodiversity. Additionally, understanding the trajectory of river channels is crucial for hazard mitigation. Identifying areas prone to erosion or flooding allows for the implementation of protective measures, such as riparian vegetation restoration or the construction of flood defences.

The trajectories of rivers are intimately connected to the driving variables, primarily the flow and sediment supply regimes, as well as human interventions at catchment or local scales. In the field of river morphology, these relationships are extensively studied (e.g. Brierley, and Fryirs, 2005; Kondolf and Piégay, 2016). From a physical viewpoint, variations in flow patterns directly impact river trajectories. Changes in precipitation, snowmelt, or alterations in land use that affect runoff can modify the flow regime. High flows during intense rainfall events or snowmelt contribute to erosion and sediment transport, influencing channel morphology. Conversely, reduced flow, often associated with altered hydrological regimes due to human activities, can lead to channel downcutting and changes in bed elevation Hooke, J. M. (2018).

Sediment supply is another critical driver of river morphology. Natural processes such as weathering, erosion, and sedimentation influence sediment availability. However, human activities, such as deforestation, agriculture, or construction, can alter sediment supply significantly. For instance, land-use changes that increase soil erosion may enhance sediment delivery to rivers, affecting channel morphology and trajectory Schumm, S. A.

(1977); Eaton et al., (2010). Human interventions, like channelization, directly impact river trajectories. Channel straightening or narrowing, often undertaken for flood control or navigation purposes, disrupts the natural equilibrium between flow, sediment transport, and channel morphology. These alterations can lead to increased erosion or deposition, changing the trajectory of the river.

The causes of alterations in flow and sediment supply regimes are diverse. Climate change, land-use changes, urbanization, and anthropogenic modifications to river systems (e.g., dams, reservoirs) are major contributors. These alterations often result in shifts in hydrological patterns, affecting both flow and sediment dynamics.

1.6 Short review of studies on Albanian rivers

It has to be noted that there are very few river hydromorphological studies at the country scale published internationally in the entire Balkan area (Stefanidis et al., 2020) and at the country scale in Albania. The focus of existing hydro-morphological studies is on a general, broad overview of Albanian rivers (Pepa et al., 2023; Ozdemir, 2013) which describe the geomorphometric analysis of Albania river basins.

Among the few published papers on Albanian rivers hydro-morphology, a recent increase in scientific and management interest has been growing also in relation to the ecology, flow and sediment regimes especially in one river catchment that gained a high international interest, the Vjosa river in the south of Albania, which sources in Greece (Hauer et al., 2021, Schiemer et al., 2020, Bizzi et al., 2021). The Vjosa is now widely recognised as a wild, near natural and free-flowing river system as it represents a reference system for large, Mediterranean braided rivers. Earlier the year preceding the publication of this PH.D thesis (spring 2023) the Vjosa river has been declared a National Park by the Albanian Government, stopping, at least temporarily, several announced plans for hydropower development of its main stem, which could have dramatically compromised the ecological integrity of the Vjosa river system. This has been assessed by Peters et al. (2021), which focuses on assessment of sustainable hydropower planning in the Vjosa river, and supports the view that major hydropower development could result in a “lose-lose-lose” situation, opposite to a “win-win” desired scenario, in terms of reservoirs operation sustainability, ecosystem health and downstream coastal erosion.

In comparison to hydro-morphology, perhaps more, though less recent studies have been published internationally on river water quality for Albanian rivers. A look at the dates in which these studies have been published suggests that a major trigger for these studies has been an increasing awareness of rapidly declining river water quality caused by the combination of rapid urban, industrial and population growth, with the absence or limited development of water treatment plants and sewage infrastructure. Studies on river water quality focus on the Shkumbin River (Paparisto et al., 2014; Çomo et al., 2013), on the Mat River, considering the use of bacteria and benthic macroinvertebrates as water quality parameters (Hamzaraj et al., 2014), on assessing water quality indexes in the Seman River (Zela et al., 2020), and also on the Vjosa river (Hamzaraj et al. 2014), based on biological

and chemical parameters. A more recent study on the Ishem River by Gjyli et al. (2023) investigates plastic pollution in different tributaries of the Ishëm River. Another study has been recently published in relation to the Erzen river, focused on the assessment of the abundance and composition of macroinvertebrates (Gjyli et al., 2022).

The few studies on river sediment transport in the country have been mainly driven by interests to assess the potential effects of intense sediment loads for the sustainability of planned or recently build hydropower reservoirs and related infrastructures. Most of these studies focus on the Devoll river, a main tributary of the Osum river. Ardicioglu et al., 2011 focus on assessment of suspended sediment transport of the Devoll river; the MSc thesis by Sørås (2017) explores the use of new techniques of estimating sediment transport at Banja dam, the first dam in Devoll river, and Guerrero et al. (2016) looked at suspended load monitoring through ADCP-based measurements in the same context. Perhaps the only study that links sediment transport with the river morphological pattern is that by Bizzi et al. (2021) combining the sediment transport at the river network scale through the CASCADE model with the channel pattern at the reach scale. Direct, reported bedload measurements are very rare at the regional Balkan scale, with the exception of Pessenlehner et al., (2022) on the increasingly studied Vjosa river. Also hydrological studies published at international level are quite few. A study work presented at the EGU General Assembly by Pesci et al. (2020) takes in consideration ERA5 data to look at the water balance modelling of the Devoll river, while Nicandrou et al. (2004) looked at the hydrological modelling of the Fan river (tributary of Mat river).

Related studies to those on river hydromorphology are those referring to the coastal morphological evolution, taking in consideration river delta and costal dynamics in Albania. Ciavola et al. (1999) looked at the relation between river dynamics and coastal changes in Albania, based on satellite imagery with historical data; Fouache et al. (2001) focused on delta geomorphological evolution of the Seman and Vjosa rivers. Dollma (2010) looked at the human impact on the coastal area of Ishem-Shengjin, while Deleo et al. (2016) addressed the recent erosion of the Lalzi Bay north of the city of Durres.

1.7 Aim and outline of the thesis

The general goal of this thesis is to make an important step forward in developing systematic information, quantitative and structured knowledge base on the morphology of Albanian rivers, and to support understanding of the main processes and possible drivers of recent changes in the river morphology, and the possible connection with sediment transport and its potential changes in the same time frame. This is expected to contribute a relevant advance in the support to the development and implementation of effective river basin management plans at the national level.

To achieve such goal, after this introductory chapter, the thesis is structured into three main chapter and a concluding one, as follows:

Chapter 2 addresses a significant research gap by investigating the hydromorphology of Albanian rivers in a country scale, and quantifying the changes in channel patterns

distribution following the collapse of the previous communist regime and the onset of rapid socio-economic changes. Specifically, it aims at providing some first answers to the following questions:

- (i) What are the morphologies of Albanian rivers, and how are they distributed in the different physiographic regions?
- (ii) To which extent and in which ways have river reaches changed their channel patterns after rapid socio-economic development occurring after the 1990s?
- (iii) How can the concept of “reference conditions” be conceptually and operationally developed in the case of Albanian rivers?

This chapter focuses on the main stems and largest tributaries of the Vjosa, Devoll, Osum, Seman, Shkumbin, Erzen, Ishem, and Mat rivers and provide a quantitative assessment of the channel morphology with resolution at the reach scale.

Chapter 3 addresses in depth the morphological changes occurring in one of the river systems analysed in Chapter 2, the Erzen River, which is the one historically reported to have the highest annual average sediment yield per unit catchment area to the sea. The study analyses the channel adjustments, mainly incision and channel narrowing occurring in selected representative reaches of the river, by using a combination of remote sensing, historical image analyses, DEM and survey in the field. Major hydromorphological pressures potentially affecting the flow and sediment supply regime are mapped and then the role of the potentially driving factors on the observed changes is discussed. The specific goal of the work presented in this chapter is to quantify the characteristics of the channel adjustments and river trajectories occurring in the lowland reaches of a representative river system in the western Balkan area in terms of timescales, magnitude, possible drivers, and to relate it to analogous processes that have been documented in westernized countries, to understand similarities and differences among contexts characterized by different phases of development.

Chapter 4 addresses a comprehensive analysis of sediment transport along the Erzen River in Albania, focusing on discerning the impact of recent channel adjustments and climate variations on the transport of fluvial sediments into the Adriatic Sea. The investigation spans the period from 1949 to 1992, employing established sediment transport methodologies. The primary objective is the calibration of a sediment transport capacity predictor, using reach-averaged input parameters and an instantaneous normal flow approximation. Key considerations include variations in channel slope and width, particularly significant in lowland river regions experiencing heightened anthropogenic activities and related channel adjustments. The analysis integrates historical data on suspended sediment transport rates and forecasts variations under diverse scenarios. The methodology entails thorough data collection of historical discharge time series, statistical analyses, and the computation of sediment transport capacity at discharge gauging stations. The chapter concludes by underscoring the pivotal role of precise sediment transport data and predictive tools in shaping basin management plans aligned with EU directives. The work presented in this chapter has to be viewed as a preliminary investigation of the Erzen river system, and also for the entire country, in which the historical practice of direct sediment transport

measurements was routinely performed and should be foreseen again in river management plans.

Finally, **Chapter 5** (Conclusions) summarizes the main findings of the thesis in the light of the overarching research questions summarized in this introduction, and discusses them also in the light of the needed developments and remaining open questions for future research.

Chapter 2

2 Country-wide analysis of the present and historical morphology of major Albanian rivers

Abstract

This chapter addresses a significant research gap by investigating hydromorphological changes in Albanian rivers, covering nearly 80% of the river network with catchment areas exceeding 650 km² from 1960 to 2015. A total of 1300km of river length has been analysed, with presently the dominant river morphologies being single thread (276 km, 22%) and sinuous (221 km, 17%), which occur mainly in the mountain and hill physiographic units, respectively. The historical analysis reveals substantial shifts, primarily affecting braided and wandering reaches, for which the changes to a different pattern referred to 59% and 52% of the initial morphologies.

In 1960, the dominant morphologies were single thread (247 km, 19%) and meandering (244 km, 19%), with wandering covering 217 km (17%). Emphasizing a distinct trend towards channel narrowing, our study highlights a 39% shift from braided to wandering and a 10% transformation from braided into sinuous. Changes include 20% from wandering to sinuous, 13% to sinuous visible bedforms (VB), and 9% to meandering. Meandering reaches encountered a 21% alteration, with 20% transforming into abandoned reaches. Notably, approximately 53 km of river channels transitioned into abandoned (channel lost) reaches over five decades due to channelization, alterations in land cover, and natural river cut-offs.

This comprehensive quantification of channel adjustments serves as a crucial foundation for supporting river basin management, flood prevention, and restoration. As Albania pursues EU membership, compliance with water-related directives becomes crucial for its environmental legislation, pointing at the development of River Basin Management Plans, which require the reach-scale information of the morphologies of the river network as a fundamental information, together with its historical evolution of river dynamics to support effective river basin management plans. The study is among the first comprehensive diachronic evaluation of channel pattern types in major Albanian river basins, quantifying the changes in channel patterns distribution following the collapse of the previous communist regime and the onset of rapid socio-economic changes.

2.1 Introduction

In recent decades, strong scientific progress has been made in our understanding of the morphological dynamics of rivers. This has resulted in the development of methodological frameworks of analysis and quantitative predictive tools for the investigation of the river dynamics, which are needed to effectively support the sustainable management of river systems in the medium and long term. More specifically, the classification of channel

patterns or of “river styles” (Brierley and Fryirs, 2005) is of particular relevance for supporting river management because the knowledge of channel patterns is integrative (Hohensinner et al., 2020) of both their geomorphological and ecological functioning (e.g. Church, 2022, Amoros and Petts, 1996). Therefore, knowing channel patterns at the catchment or even regional scale, and how this has been evolving over time, is a key information required to set realistic goals and action plans for their sustainable management,

This is particularly relevant in Albania as the national approach to river management is following the key principles of the EU Water Framework Directive (2000/60), to align the national regulations to EU member states in the process of EU integration. Specifically, evaluating hydro-morphologically quality elements” is a key component of river basin management plans, which are presently being structured and developed in these years for all Albanian catchments. This implies the need of a detailed knowledge of the morphology, the flow and sediment supply regimes of all water bodies, and how this might have been altered with respect to some “reference conditions”, assumed as those corresponding to minimal human impact. How to establish the reference period against which assessing the recent morphological changes needed for quantifying the degree of human impacts and the consequent need of future restoration / management / mitigation measures is an open issue in the country.

A common requirement of these approaches and tools is that they rely on the availability of structured datasets on the hydrology, morphology and sediment size distributions in the target rivers. As a consequence, the application of these methods and tools has mainly focused in the so-called “western” or highly industrialized countries, while their use in other regions has been way more limited. The present thesis focuses on rivers in the South-Eastern European region, and more specifically on rivers draining the Albanian Alps. Here rivers have been reported as some of the highest sediment transporting streams worldwide, when compared with other rivers in similar climatic - geomorphic settings. Despite this, quantitative, structured information of their hydro-morphological dynamics as well as understanding of the most dynamic and sensitive river reaches to anthropogenic activities is very limited so far. A first attempt to fill this knowledge gap has been motivating the analysis of the first research element of this thesis.

Rivers in the Western Balkans, and especially those in South-East Europe, differently from major rivers in Western Europe, didn't undergo systematic river regulation programmes in the first half of the 19th century (Brown et al., 2018). While anthropogenic pressures were surely present, but very local and minimal, before World War II, it has been intensified during the communist regime 1950-1990, though mainly concentrating on the effects of local large dams and channelization of some lowland reaches. As population growth and urban growth were not massive, it can be hypothesized that such effects were present but not able to cause dramatic effects. Instead, after 2000, major development occurred, and many reaches in the mostly anthropized regions present severe modifications. Many upper and middle reaches of rivers in the area, in contrast, are known to have a very high natural value with also a high potential for biodiversity, cultural and recreational ecosystems services, also possible resources for sustainable tourism in rural areas with unique landscapes.

However, very few data collection and detailed studies are at present available to support such hypotheses, and, in general, information on the present and past hydromorphological conditions and evolution of Albanian rivers is heavily lacking.

It has to be noted that there are very few river hydromorphological studies at the country scale published internationally in the entire Balkan area (Stefanidis et al., 2020) and at the country scale in Albania the focus of existing studies is on general overview of Albanian rivers (Pepa et al., 2023; Ozdemir, 2013) which describe the geomorphometric analysis of Albania river basins. A recent increase in scientific and management interest has been focusing on the Vjosa river (Hauer et al., 2021, Schiemer et al., 2020, Bizzi et al., 2021), one of the last larger free-flowing river in Europe and recently declared as one of the few river-based National Parks in Europe. Studies related to river hydro-morphology may be found in those assessing sediment transport in Albanian rivers, like those on suspended load on the Devoll river (e.g. Ardiclioglu et al., 2011, Sørås, 2017, Guerrero et al. 2016) the work of Pessenlehner et al., (2022) on bedload and suspended load measurements on the Vjosa river.

The work presented in this chapter aims at start filling the country-wide knowledge gap on river hydromorphology, by developing a country-wide assessment of the morphological patterns of selected major rivers of Albania. Specifically it aims at providing some first answers to the following questions:

- (i) What are the morphologies of Albanian rivers, and how are they distributed in the different physiographic regions?
- (ii) To which extent and in which ways have river reaches changed their channel patterns after rapid socio-economic development occurring after the 1990s?
- (iii) How can the concept of “reference conditions” be conceptually and operationally developed in the case of Albanian rivers?

It focuses on the main stems and largest tributaries of the Vjosa, Devoll, Osum, Seman, Shkumbin, Erzen, Ishem, and Mat rivers and provide a quantitative assessment of the channel morphology with resolution at the reach scale, with reference to present conditions and an historical condition before the collapse of the dictatorial regime, as it can be extracted from a selection of historical sources: military maps (1928-1944) from the Italian Geographic Military Institute in Florence, the maps compiled by the Military Institute of Albania (1959-1985), and the available Corona spy Satellite mission (1960-1972).

The IDRAIM (Rinaldi et al., 2013) methodological framework is adopted to guide the analysis, from the initial segmentation of the river network into hydromorphologically homogenous reaches, up to the extraction of reach-averaged values of the channel slope, active corridor width, reach length, sinuosity, elevation, together with indicators of lateral confinement and of the main geological layers in which every reach is found. Results offer a regional-level quantitative picture of the most typical channel patterns and allow us to explore possible dominant catchment-scale controls. The findings are also compared with previous studies at similar scales focused on the European Alps (Hohensinner et al., 2021).

The outputs of the work contribute a substantial advancement for the management of South-Eastern European rivers, thanks to the development of spatially explicit and diachronic information. It represents an important baseline for setting management targets that are coherent with major EU Directives and allows to understand which specific river reaches may be targeted for restoration or conservation actions, having been either most or least modified in the last decades.

2.2 Overview of the studied river catchments

The work is focused on six main river catchments of Albania: Mat (including Fan), Ishem, Erzen, Shkumbin, Seman (including Devoll and Osum), Vjosa.

Table 2. 1. Main characteristic of River studied.

River Name	Length (Km)	Basin area (km ²)	Riverbed elevation at upper analysed section (m asl)	Mean annual flow (m ³ /s)	Annual sediment yield to sea (tons/km ²)
Mat	115	2441	402	103	1032
Ishem	74	673	360	20.9	3715
Erzen	110	760	560	18	5222
Shkumbin	181	2444	782	61.5	2938
Devoll	196	3130	637	49.5	3589
Osum	161	2073	768	32.5	2417
Seman*	85	5649	649	95.7	2876
Vjosa	272	6706	544	195	1249

*Seman river included two big tributaries Devoll and Osum River. For riverbed elevation and river length is taken Devoll river as longest river course. (Ciavola et al., 1999)

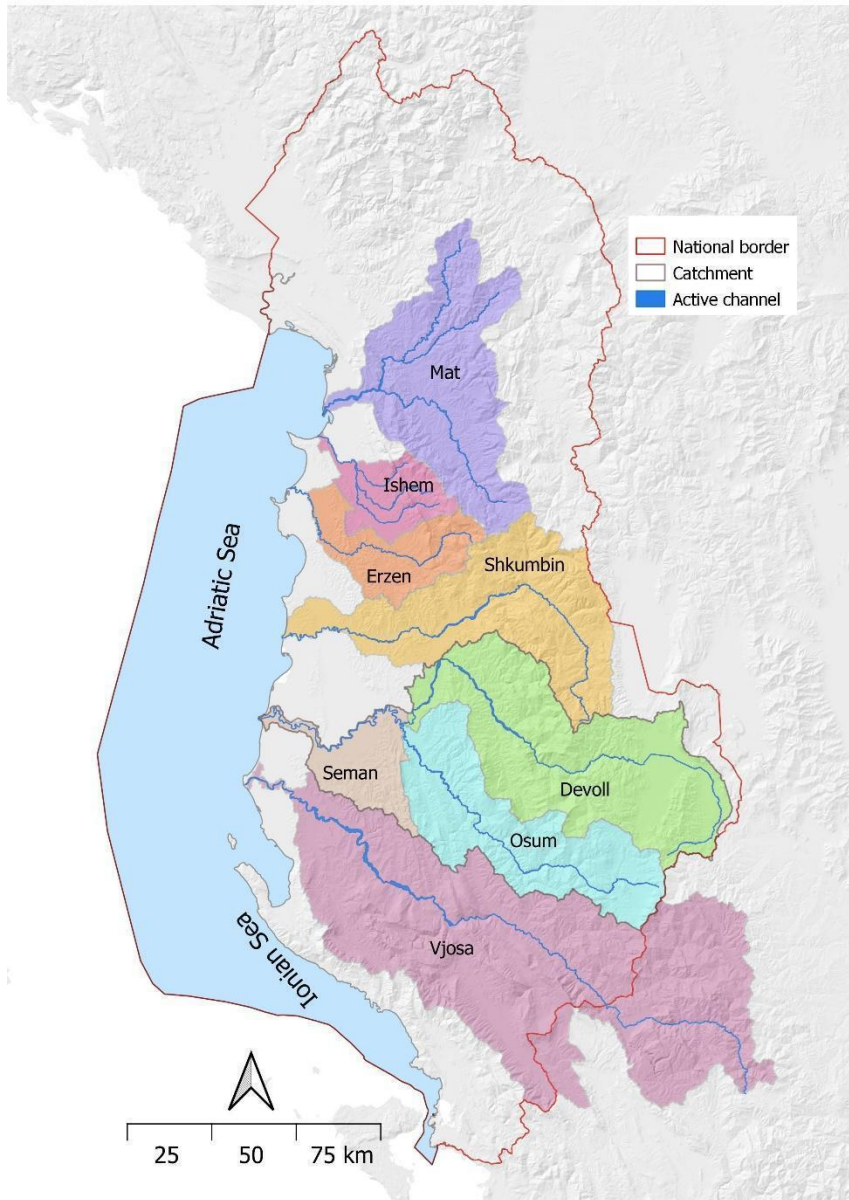


Figure 2. 1. Map of the analysed river catchments

Despite a critical lack of information and data is often claimed in relation to Albanian rivers and, in general, to Western Balkans' rivers, an important issue needs to be highlighted. Standard hydro-meteorological data, including measurements of sediment transport, were systematically collected by state institutions until the early 1990s, when the previous communist regimes collapsed. These measurements allowed to estimate average sediment fluxes from Albanian rivers to the sea. After such monitoring was interrupted, it started again mostly in the early 2000s, though it has often been less systematic and continuous. In both

cases, before and after the 1990s, data are not straightforward to be retrieved, and a thorough investigation in sparse historical source has to be developed. More details on which type of sediment transport measurements, which tools and methods were used and which type of sediment transport data have been retrieved for the present study are reported in Chapter 4.

The analysed river catchments cover a total area of about 28750 km², and nearly 80% of the entire territory of Albania, when accounting for the area (mainly belonging to the Greek portion of the Vjosa river basin) that is under in foreign territories. The only missing large catchment relevant for Albania in this analysis is the Drin river catchment, which has a considerable proportion of land in Kosovo and Northern Macedonia, for which a complete, transnational dataset could not be developed within the timeframe of the present work. Nevertheless, the total size of the analysed catchment characterizes the work as a country-scale analysis.

All the six rivers catchment have main stems flowing from East to West and discharging to the Adriatic Sea. A short overview of the main characteristics of each of the examined catchments is provided in Table 2.1, in Figure 2.2 and also summarized below. The main sources of information for Table 2.1 and for the description of the river catchments are Kobo (1990); Hydrology of Albania, 1979; Ciavola et al. (1999).

Mat catchment. The Mat is a river flowing in north-central Albania. Its overall length is 115 km, while its catchment is 2,441 km² and has an average discharge is 103 m³/s, and estimated total sediment transported 2,519, 635 ton/ year. The main tributary is Fan and Fan itself has two main tributaries: Big Fan and Small Fan (Fani Madh and Fani i Vogel in Albanian), flowing from the northeast, while the Mat flows from the southwest down to the confluence with Fan and then towards the Adriatic Sea.

Ishëm catchment. The Ishëm River is a significant waterway in western Albania. It serves as a primary water source for the region to the north of the Albanian capital, Tirana. The river is part of a broader watercourse known as the Tiranë-Gjole-Ishëm system, whose lowland part, corresponding to nearly 1/3 of the river length, is referred as the Ishëm River, which originates from the confluences of several upper streams. The proper Ishëm River originates from the confluence of two other rivers, the Gjole and Zezë, situated a few km northwest of Fushë-Krujë. It eventually flows into the Adriatic Sea near the town of Ishëm. Gjole river is composed by two other tributaries: Tirana and Terkuze river. Historically, the Tirana and Zeza rivers may not have always been tributaries of the Ishëm. They might have flowed into the Erzen River. It's believed that, at some time, they altered their course due to geological changes in the landscape, like those associated with earthquakes. The Ishëm River's drainage basin covers an area of 673 km², with an average discharge of 20.9 m³/s and total sediment transport estimated as 2,500,306 ton/year. The river experiences significant variations in discharge, with the highest annual discharge being more than six times the annual minimum.

Erzen catchment: River has catchment area approximately 760 km² and is located in the central part of the country. The river originates in the western slopes of the Gropa Mountain, at an altitude of 1200 m above sea level, and flows westwards towards the Adriatic Sea, passing through the lowland transitional and meandering reaches before entering Lalzi Bay.

The main river length is around 110 km, average discharge 18 m³/s and average elevation of the riverbed in the catchment at about 440 m above sea level. Total sediment transported 3,968,827 ton/year.

Shkumbin catchment: The Shkumbin River, also known as Shkëmbi (which means "Stone" in English), stretches across a length of 181.4 km. Originating in the eastern Valamara Mountains at an elevation of 2375 meters above sea level, it flows westward, eventually emptying into the Adriatic Sea. With a drainage basin covering an area of 2,444 km² and an average discharge of 61.5 m³/s, total sediment transport 7,181,039 ton/year the river is a significant geographical feature of central Albania. It is often recognized as a natural border dividing between northern and southern Albania.

Seman Catchment: Seman river is formed by the confluence of the rivers Devoll and Osum, a few km west of Kuçovë. It is 85 km long, 281 km with its longest source, river Devoll, and its drainage basin is 5,649 km². Average discharge is 95.7 m³/s and total sediment transport 16,244,350 ton/year. It meanders generally westwards through a flat lowland. Near Fier it receives Gjanica river from the left. It flows into the Adriatic Sea at the southern margin of Divjakë-Karavasta National Park.

Devoll river, it is one of the source rivers of Seman, it is 196 km long and its drainage basin is 3,130 km² with an average discharge 49.5 m³/s. Its source is in the southwestern corner of the Devoll municipality, close to the Greek border. It flows initially northeast, through Miras, then north through Bilisht, and northwest through Progër, Pojan (in the northern Korçë internal Plain which was marshy until right after the World War II), Maliq, Moglicë, Kodovjat, Gramsh, where two major hydropower dams are located (Moglica dam and Banja dam). It joins the Osum river near Kuçovë, to form the Seman.

Osum river is the second source of the Seman. It is 161 km long and its drainage basin is 2,073 km². Average discharge is 32.5 m³/s. Its source is in the southwestern part of the Korçë County, near the village Vithkuq at an altitude of 1,050 m.a.s.l. It flows initially south to the Kolonjë municipality, then west to Çepan, and northwest through Çorovodë where it flows through the famous Osum Canyon, Poliçan, Berat and Urë Vajgurore. It joins the Devoll near Kuçovë, to form the Seman.

Vjosa catchment: The Vjosa or Aoös (Greek: Αώος) is located in northwestern Greece and southwestern Albania. Total length is about 272 kilometres of which the first 80 kilometres are in Greece, and the remaining 192 kilometres in Albania. The total drainage basin is 6,706 km², of which 2154 km² (32%) are in Greece. The average annual discharge of the Vjosa is 195 m³/s. Sediment transport estimated is 8,376,776 ton/year. The main tributaries are Voidomatis, Sarantaporos, Drino and Shushicë.

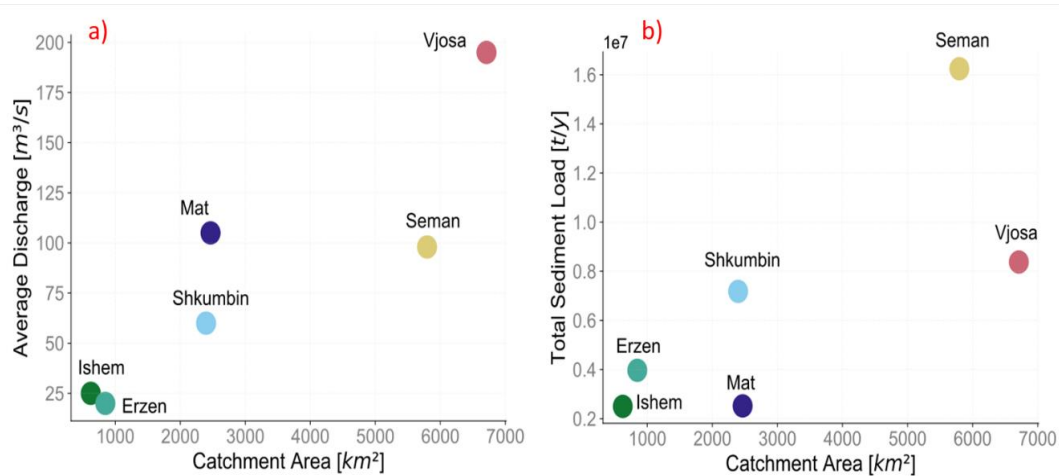


Figure 2. 2. a) Average annual discharge (m^3/s) per catchment area; b) Total sediment load (ton/year) for each analysed catchment.

The Vjosa River has the highest discharge among the other studied rivers of Albania with an average of $195 m^3/s$ and the largest catchment area of $6,706 km^2$, followed by the Mat River with a discharge of $103 m^3/s$ and the Seman River with $95.7 m^3/s$. The Shkumbin River has an average discharge of $61.5 m^3/s$, while the Ishem and Erzen rivers have discharges of $20.9 m^3/s$ and $18.1 m^3/s$, respectively (Hydrology of Albania, 1979).

In terms of sediment transport, the Seman River leads with the highest average sediment load per year at $162,443.50$ tons, and the second-largest catchment area of $5,649 km^2$ after Vjosa (Hydrology of Albania, 1979). The Vjosa River follows as the second-highest sediment transporter, moving approximately $837,677.6$ tons yearly. Additionally, the Shkumbin River demonstrates substantial sediment transportation, accounting for $718,103.9$ tons annually. The Erzen River transports $396,882.7$ tons, the Mat River $251,963.5$ tons, and the Ishem River $250,030.6$ tons of sediment annually (Ciavola et al., 1999).

2.3 Material and Methods

The following main sources of information have been used for the present analysis, available from ASIG – Albanian national Geoport. The EU-wide freely available DEM with 25m resolution; the orthophoto of Albania of 2015 having a spatial resolution of 20 cm; the DTM of Albania with resolution of 10 m, its visualization as a raster hill shade of the same geoport. Albania, and the hydrogeology map of Albania.

Choice of the IDRAIM method

The European Union's Water Framework Directive (WFD) introduced the concept of 'hydromorphology' to address modifications in flow regime, sediment transport, river

morphology, and lateral channel mobility (Rinaldi et al., 2013). Hydromorphological Quality Elements have been introduced as one of the three pillars for the definition of the “Ecological status”, together with biological and chemo-physical quality elements. European nations, including Italy, implement the WFD through methods like the River Habitat Survey (Raven et al., 1997) and Germany's (Lawa, 2000). However, many these approaches have limitations, such as small survey areas, over-reliance on field surveys, and a static view of river processes, not properly accounting for the geomorphological dynamics of rivers.

To overcome these limitations, there is a growing emphasis on geomorphological methodologies that consider physical processes at appropriate spatial and temporal scales. Notable approaches include the River Styles Framework (Brierley and Fryirs, 2005), SYRAH (Chandesris et al., 2008), IHG (Ollero et al., 2011), and the method by Wyzga et al. (2012). While these methodologies have merits, they may not fully align with each country's specific requirements for WFD application, including quantitative assessment, usability by authorized bodies, and adaptation to the national specific characteristics of river systems.

Human activities including urbanization and industrialization in developed countries in the past but recently, also in the Balkan region, have modified hydromorphological conditions of the river bodies. The IDRAIM method (Rinaldi et al., 2013) has proved to be relevant for river assessment in Italy first, and it has further been adapted for application at a wider European context. Considering the many similarities between river styles in Italy and Albania, with particular reference to similar proportions of mountain / hilly / plain areas in the two countries and similar climatic settings, especially referring to the Italian Appennines, the IDRAIM method has been chosen as suitable for its adoption in the present country-scale analysis of the morphologies of Albanian rivers. IDRAIM, developed by ISPRA (Istituto superiore per la protezione e la ricerca ambientale), is a comprehensive framework for river analysis, post-monitoring evaluation, and the design of restoration and mitigation measures in line with WFD and the Flood Directive 2007/60/CE. It includes specific methods for the assessment environmental quality and flood risk mitigation, making it a valuable decision support tool for river management.

For the purposes of this study, the river morphology at the river reach scale is evaluated using the Orthophoto of 2015, having 20 cm resolution from Geoportal Albania as the present reference and historical military maps produced by the Geographic Institute of Florence between 1928 and 1944, with a scale 1:50,000. In cases where older maps were unavailable for assessing small streams, military maps of Albania from 1959 to 1985 (1:25,000 scale) and Corona images from 1968 to 1972 are being used for morphology evaluation (“ASIG Geoportal,” n.d.). This approach therefore offers a historical, diachronic perspective on major river morphological changes and reference conditions.

Overview of the adopted module of the IDRAIM method

For the purpose of the present country-scale analysis of Albanian rivers morphology, the initial “module” of the broader IDRAIM methodological approach has been adopted. This

allows to partition the selected river systems into hydro-morphologically homogeneous river reaches, for which several morphometric properties (active channel width, mean slope, sinuosity, etc.) are computed and a channel pattern is classified. A short summary of this module is presented below, followed by a detailed description of the specific steps required by this type of analysis.

The initial phase of the IDRAIM framework (as presented in the deliverables form the REFORM EU project) involves the delineation of spatial units, as outlined in Gurnell et al. 2015. This process begins with the division of the catchment into landscape units, primarily determined by geological features and topography. These landscape unit boundaries serve as the initial segmentation of the river valley network. However, for larger segments, further subdivision may be necessary, considering factors such as significant changes in valley gradient, catchment area, the confluence of major tributaries, and lateral confinement.

Based on the work of Brierley and Fryirs (2005) and Rinaldi et al. (2012, 2013), three distinct valley settings are identified:

- Confined: In these settings, more than 90% of the river banks directly interact with hillslopes or ancient terraces.
- Partly Confined: River banks in these settings are in contact with the alluvial plain for a portion of their total length, ranging from 10% to 90%.
- Laterally Unconfined Channels: Here, less than 10% of the river bank length is in contact with hillslopes or ancient terraces.

The fundamental spatial unit within this framework is the "reach," which represents a section of the river and its floodplain where boundary conditions exhibit sufficient uniformity to maintain consistent internal process-form interactions. While the boundaries of river segments initially define reaches, subdivision of these segments may be required to identify reaches with similar channel and floodplain morphology, reflecting local changes in bed slope, sediment particle size, discharge (e.g., from minor tributaries), and sediment supply that might be too subtle to define as distinct segments.

At the reach scale, the primary factors influencing delineation are reflected in the planform characteristics of the river channel and floodplain, including the presence of geomorphic units. Consequently, a morphological classification serves as the foundation for reach delineation. This initial classification offers insight into the spatial distribution and connectivity of morphological patterns, facilitating the interpretation of processes occurring from the catchment to reach scales and their morphological impacts over time.

The basic river typology (BRT) is the initial, simplified level of morphological classification for river reaches, adapted from Rinaldi et al. (2013). BRT categorizes river reaches into seven types (plus a type 0 for highly altered reaches) based on river channel planform characteristics (such as the number of threads and planform pattern) within the context of valley confinement. This classification relies on readily available information, primarily obtained through remotely sensed imagery.

Workflow of the method

The implemented module of the IDRAIM method foresees the following five main steps, which are then described in detail:

- a) Catchment landscape units and segmentation of the river network
- b) Assessment of the lateral confinement of the river segments
- c) Planimetric-based morphological classification of the river
- d) Outline of discontinuity and controlling factors along the river network
- e) Homogeneous river reaches subdivision

Table 2. 2. Summary of general setting and segmentation procedure in the IDRAIM approach (modified from Rinaldi et al., 2013).

Steps	Criteria	Outputs
<i>Step 1:</i> general setting and identification of landscape (or physiographic) units and segments	geological and geomorphological characteristics	Landscape units Segments
Step 2: definition of confinement typologies	lateral confinement	Confinement typologies: confined (C) partly confined (PC) unconfined (U)
Step 3: identification of morphological typologies	planimetric characteristics (sinuosity, braiding, and anabranching indices)	Morphological typologies: Confined: single thread, wandering, braided, anabranching, partly confined - unconfined: straight, sinuous, meandering, wandering, braided, anabranching
Step 4: other elements for reach delineation	further discontinuities in hydrology, bed slope, characteristic geomorphic units, bed sediment size, channel width, floodplain width	Reaches

Step 1- Landscape units

The first step foresees the division of the catchment area in three types of physiographic units. For each catchment are the EU-DEM v1.1 with resolution 25 m and with vertical accuracy: +/- 7 meters is used in to delineate the watershed area in sub-basins. First the DEM is reprojected to WGS 84/ UTM zone 34N EPSG: 32634 as a reference system for Albania. With plugin GRASS 8 processing at QGIS software and the command *r.watershed* used to delineate the river network. The *r.watershed* allows to extract the hydrographic network directly from the DEM. From the input raster map (DEM) which represents the elevation, the algorithm needs some parameters to operate. The most important is the minimum size of exterior watershed basin which has been set to a value between 20,000-30,000 for each watershed. This indicates a threshold parameter that specifies a minimum size of an exterior watershed basin in cells. It is only relevant for those watersheds with a single stream having at least the threshold of cells flowing into it. After parameters set up, the algorithm returns several raster maps, three of which are used in the next steps:

- Drainage direction;
- Stream segments;
- Unique label for each watershed basin;

The first of the three maps allow to observe that the algorithm has not made typical errors such as failure to remove areas that do not drain further and pits. The *r.watershed* contains, internally, an algorithm that minimizes the impact of any errors in the DEM, improving the results produced in areas with a low slope where, classically, the algorithms for calculating outflows encounter particular difficulties so the procedure of pit filling is not necessary if this functions is used.

The second map generates a binary map in which the value 1 identifies the hydrographic network and 0 identifies what is not a river. Through two more geo-algorithms (*r.stream.extract* and subsequently *r.to.vect*) this raster map is transformed into a vectorial one, obtaining river segments in a line format.

The third map divides into basins the area giving a label for each watershed basin. Since it still is a raster map it requires the same transformation of the stream segments to turn it in a vectorial map.

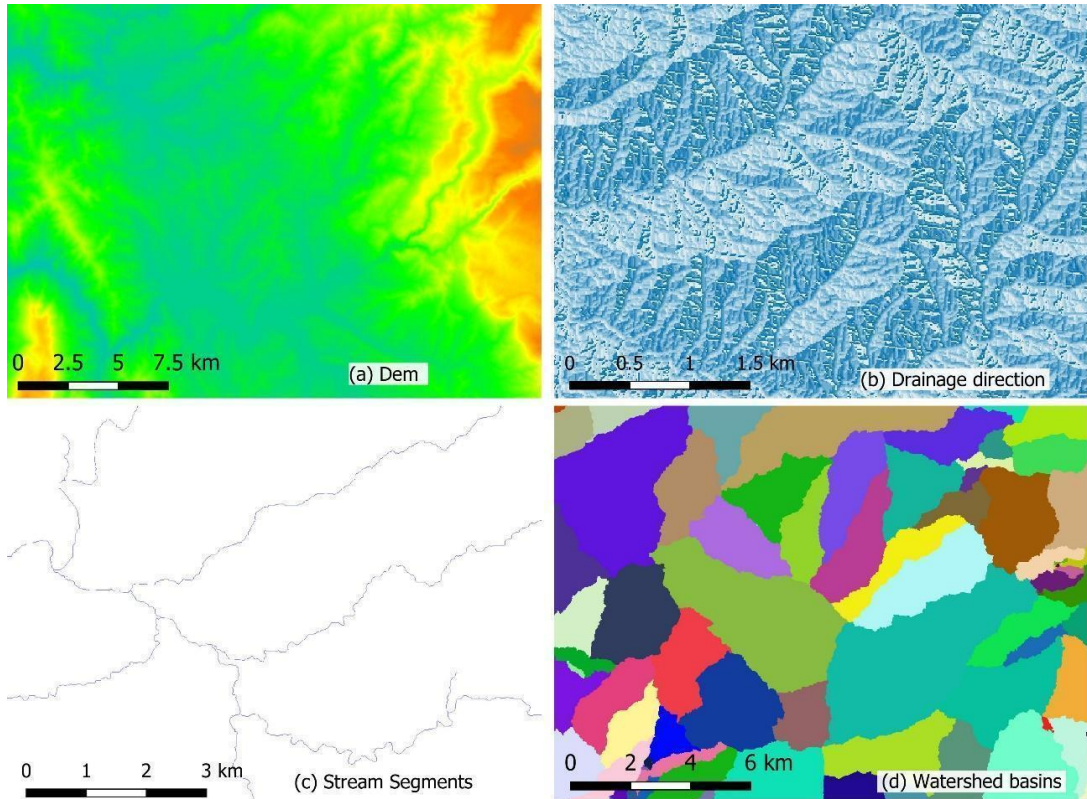


Figure 2. 3. Results of the main steps of the watershed delineation workflow.

In order to extract all the catchment area the command *r.water.outlet* is used with an input layer indicating the drainage direction. From this the coordinate of the river outlet is chosen, i.e., the location where the main river discharges into the sea, which allows to get all the catchment area of the basin. The output layer is then used as a mask for the watershed area, drainage direction and stream network.

To compute the average elevation of each basin inside the catchment area, the command *v.rast.stats* is used. A new column with elevation data is generated in the attribute table for each statistic elevation chosen. In order to get the elevation average per each sub basin we use the same DTM as per watershed declination.

As a first step of the IDRAM method, the detection of the main physiographic units within the catchment area is foreseen. After having the elevation for each basin, a classification of elevation of the basins in three main physiographic settings: mountains, hills, plains (Rinaldi et al., 2016).

Table 2. 3. Criteria used to outline the main physiographic units by the IDRAIM method (*e-elevation*).

<i>Unit</i>	<i>Criteria</i>
Mountain	$e > 600$ m.a.s.l.
Hill	$200 < e < 600$ m.a.s.l.
Plain	$e > 200$ m.a.s.l.

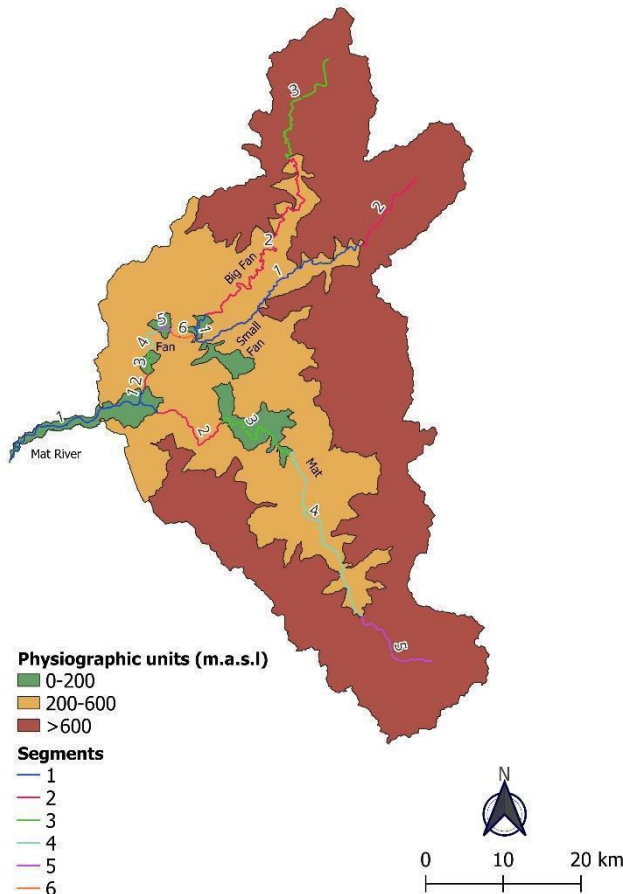


Figure 2. 4. Example of the output of the subdivision of a river catchment area into landscape or “physiographic” units (Mat River, Albania).

The output of the first phase of the method yields the river segments, which are the portions of the river channel included in each physiographic unit. In the illustrative case of the Mat River (Figure 2.4) there are six different segments. Furthermore, these initially identified river segments can be further separated into smaller segments on the basis of homogeneous characteristics in terms of floodplain, of the geology, big confluences or dysconnectivity such are dams or other barriers. In case of the Mat River six segments are defined.

Step 2- Confinement typologies

The lateral confinement of the analysed rivers is evaluated through two indicators: the Confinement degree (Cd) and the Confinement Index (CI).

- *Confinement degree*

The confinement degree Cd evaluates the lateral confinement in the longitudinal valley direction. It corresponds to the percentage of river banks not directly in contact with the plain but with hillslopes or ancient terraces, relative to the total length of the two banks (Brierley and Fryirs, 2005). The plain is here identified as the entire floodplain, generally constituted by alluvial sediments (also indicated as alluvial plain), and it is normally identified using a combination of information derived from a Digital Terrain Model (DTM), when available at a high enough resolution, from an orthoimage of the area and from geological maps with present alluvium or Holocene alluvium, while ancient terraces are older. In the present analysis, the floodplain has been identified through the combined use of the available 10m resolution DTM for Albania and of the aerial orthoimage, and considering as floodplain flat areas with an elevation that did not exceed the detectable nearby channel bed elevation of a threshold value of few (2-3, depending on river reach width, occasionally slightly higher) meters. The initially extracted floodplain areas have been visually checked against the information that could be retrieved from the orthophoto and, finally from the (coarse scale) geological map, only for the largest river reaches. Recent terraces generated by historical bed incision (e.g., during the last 100-200 years, as it has been frequently documented for several European countries) are not considered as ancient terraces and, for the purpose of the confinement, they are part of the entire floodplain. This choice is motivated by the visual evidence of recent channel incision in most lowland segments of Albanian rivers, which is locally well known though it still needs proper quantification. In addition to a chronological criterion, further factors for defining the confinement can be the difference in elevation and the erodibility of the material. In these cases, the floodplain is intended in a broader sense, as a surface that does not constrain the river dynamics (in terms of flooding and/or lateral erosion), and the altimetric and erodibility criteria should be used (i.e., the difference in elevation with the channel bed should be limited to a few meters, and the material should not be strongly consolidated or cemented). No information on the floodplain / terrace material erodibility could be retrieved for this study. The difference in elevation between the channel bed and the nearby surfaces has been assessed through the 10m resolution available DTM. Once the elements of confinement (hillslopes and ancient terraces) have been delimited, three cases can be distinguished based on the confinement degree (Rinaldi et al., 2014)

- *Confined channels*: more than 90% of the banks are directly in contact with hillslopes or ancient terraces. The floodplain is limited to some isolated “pockets” for a percentage length $\leq 10\%$.
- *Partly confined channels*: banks are in contact with the floodplain for a length from 10 to 90%.
- *Unconfined channels*: less than 10% of the bank length is in contact with hillslopes or ancient terraces. In fact, the floodplain is nearly continuous, and the river has no lateral constraints to its mobility.

- *Confinement index*

In some cases, the confinement degree is not sufficient to appropriately define the confinement characteristics. In fact, it is not infrequent (particularly in mountain areas) to have streams with a very narrow (some meters) but quite continuous floodplain on the sides of the river contacting the hillslopes. Therefore, an additional parameter is used here which considers the width of the floodplain and is defined as follows. The confinement index C_i is defined as:

$$C_i = \frac{W_p}{W} \quad (1)$$

Where W_p is the floodplain width of the plain (including the channel) and W is the channel width. Consequently, the index is inversely proportional to the confinement: a minimum value of 1 indicates that the floodplain and channel coincide (i.e. there is no floodplain), while the index increases when the floodplain increases its width relatively to the channel width. Based on the confinement degree and confinement index, the following three classes of confinement are defined as shown in Tab 2.5 and illustrated in Fig. 2.5.

Table 2. 4. Selected criteria for physiographic categorization.

Confinement index	Range
High	$1 \leq C_i < 1.5$
Medium	$1.5 \leq C_i < n$
Low	$C_i > n$

Where $n = 5$ for single thread channels and $n = 2$ for multi-thread or transitional (wandering) morphologies. Based on the confinement degree and confinement index, the following three final classes of confinement are defined as shown in figure 2.5.

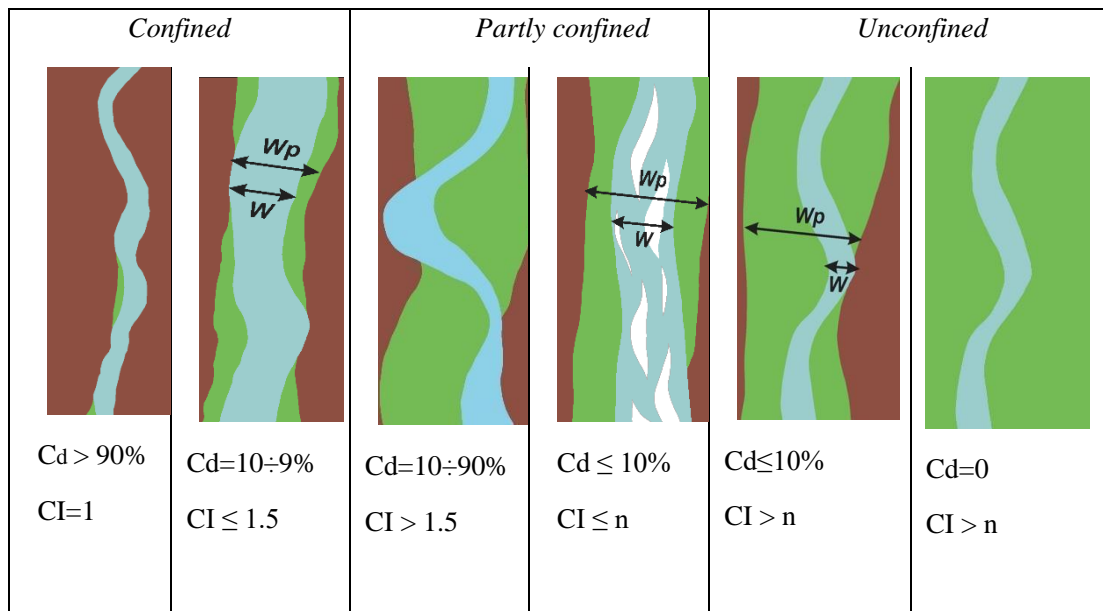


Figure 2. 5. Illustration of the employed confinement parameters. Floodplain denoted in green, hillslopes / ancient terraces denoted in brown. From Rinaldi et al. (2014). Cd; Confinement degree; CI: Confinement index

Table 2. 5. Definition of final confinement classes as obtained by combining the value ranges of confinement degree and confinement index. Reworked from Rinaldi et al., (2014)

Confinement class	Description
Confined	All cases with $Cd > 90\%$ Cd from 10% to 90% and $CI < 1.5$
Partly confined	Cd from 10% to 90% and $CI > 1.5$ $Cd \leq 10\%$ and $CI \leq n$
Unconfined	$Cd \leq 10\%$ and $CI > n$

In order to define the confinement index (C_i) and confinement degree (C_d) the active channel width has been mapped digitally from Geoportal Albania – layer “water course”, which is produced from orthophoto 2015 having a spatial resolution of 20 cm. The flood plain has been defined by using the combination of: the DTM of Albania with resolution of 10 m, a raster hill shade of the geoportal Albania, and the hydrogeology map of Albania and the same RGB orthophoto with resolution of 20 cm.

From the active channel layer, using the *GRASS GIS 8.1* software with command *v.voronoi*, the centerline of the river has been extracted. Along the river centerline several transects have been extracted with a longitudinal spacing of 200 m distance, by using the command

v.transects. The lateral limits of the originally generated transects are defined by their intersections with the left and right boundaries between the floodplain and the active channel width. The resulting transects lengths are the local active channel widths. The ratio between the floodplain width and the active channel transects widths give us the confinement index per each transect, the Cd has been instead visually evaluated by carefully scrutinizing the flood plain and the active channel width boundaries with the abovementioned data sources.

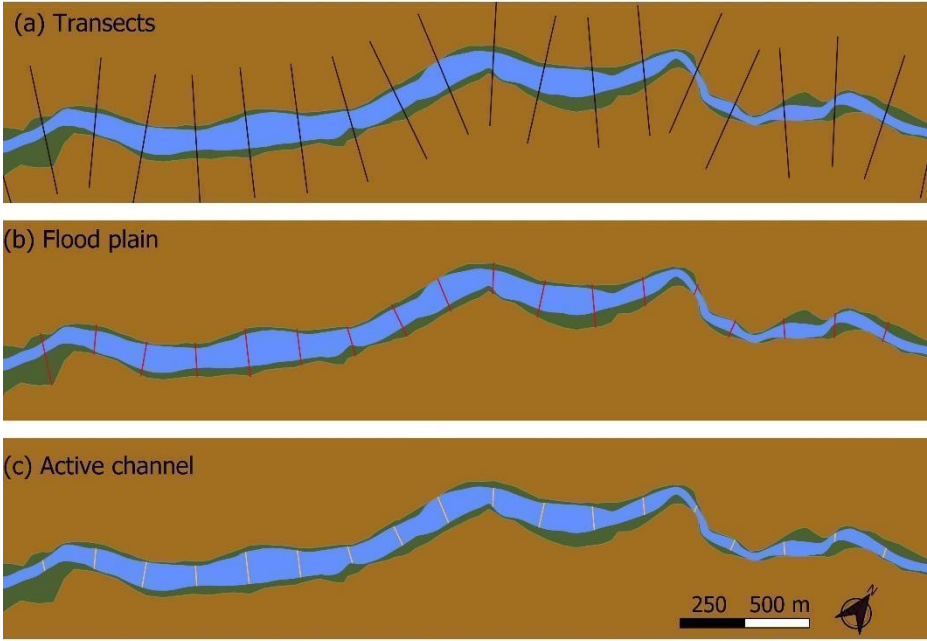


Figure 2. 6. Transects generated for calculating the Confinement Index, Reach 13, Mat river.

The output is classification of the confinement classes of the river as shown in figure 1.7 which refers to the example of the Mat River basin. In this specific case the procedure yields 116 km (50% of the total length) of the main river channel as confined, 84 km (37%) as partly or semi-confined and 29 km (13 %) unconfined.

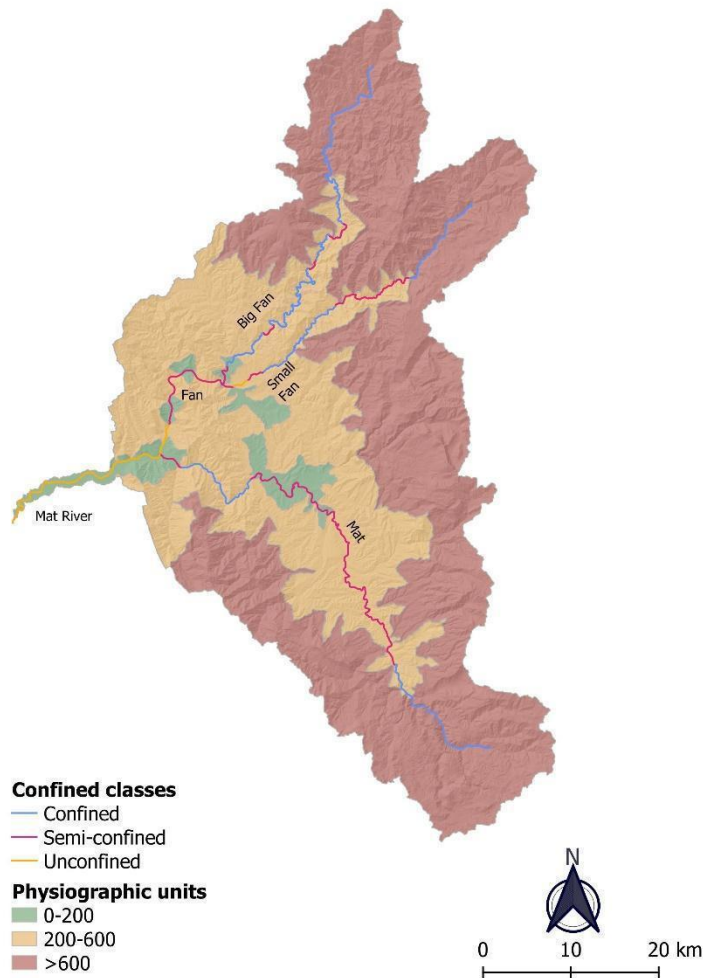


Figure 2. 7. Map of confinement classes (Mat River, Albania)

Step 3- Reach-scale channel morphology

In the third step the characterization becomes finer, the is defined and classified for every reach. The first level of morphological classification used for the delineation of river reaches is based on river channel planform character (number of threads and planform pattern) in the context of valley setting (confinement). This *Basic River Typology* (BRT) (Rinaldi et al., 2015) defines seven river types using readily available information, mainly by remotely-sensed imagery. Based on these parameters, the following six Basic River Types of partly confined and unconfined channels are defined Fig. 2.8.

- *Single-thread channels*: straight, sinuous, meandering
- *Transitional channels*: wandering
- *Multi-thread channels*: braided, anabranching

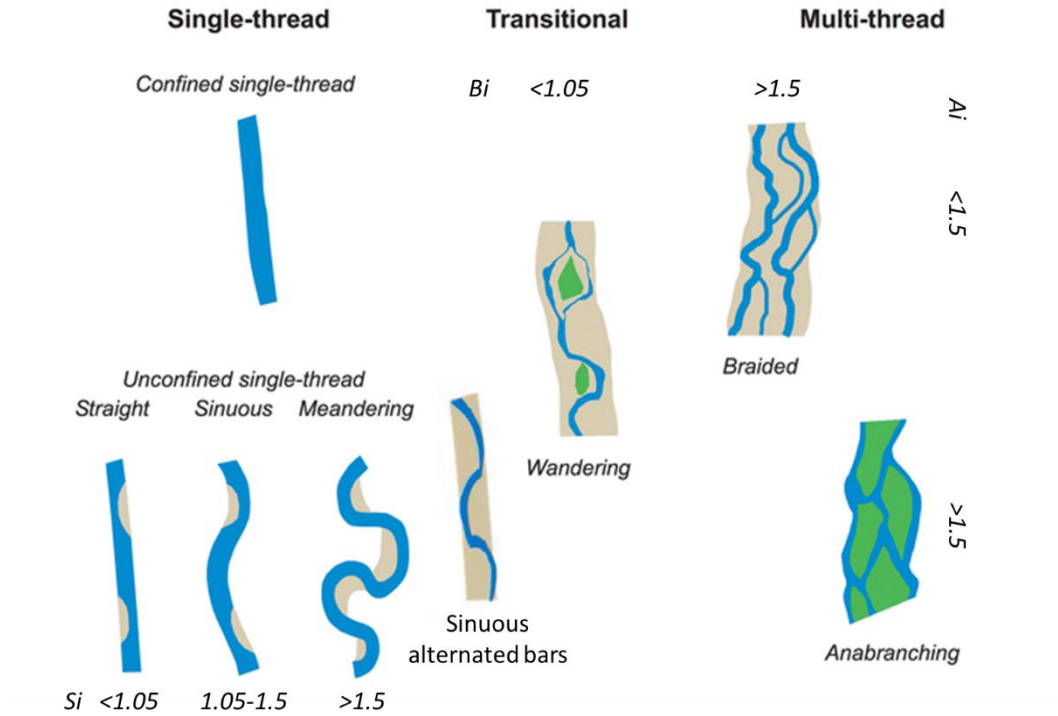


Figure 2. 8. The eight river types of the Basic River Typology (BRT) defined by Rinaldi et al., (2016)

Based on subjective expert judgement and on the assessment of channel sinuosity, and also with reference to the recent work of Hohensinner et al. (2020), with the aim to fully encompass the entire spectrum of channel morphologies of Balkan Region, with particular focus of those that can be encountered in Albanian rivers, other 4 typologies have been proposed for a total of ten typologies to evaluate the reaches' morphology: dammed-up, channelized, abandoned (Figure 2.9) The channelized type has further been divided into "channelized" and "channelized with bedforms".

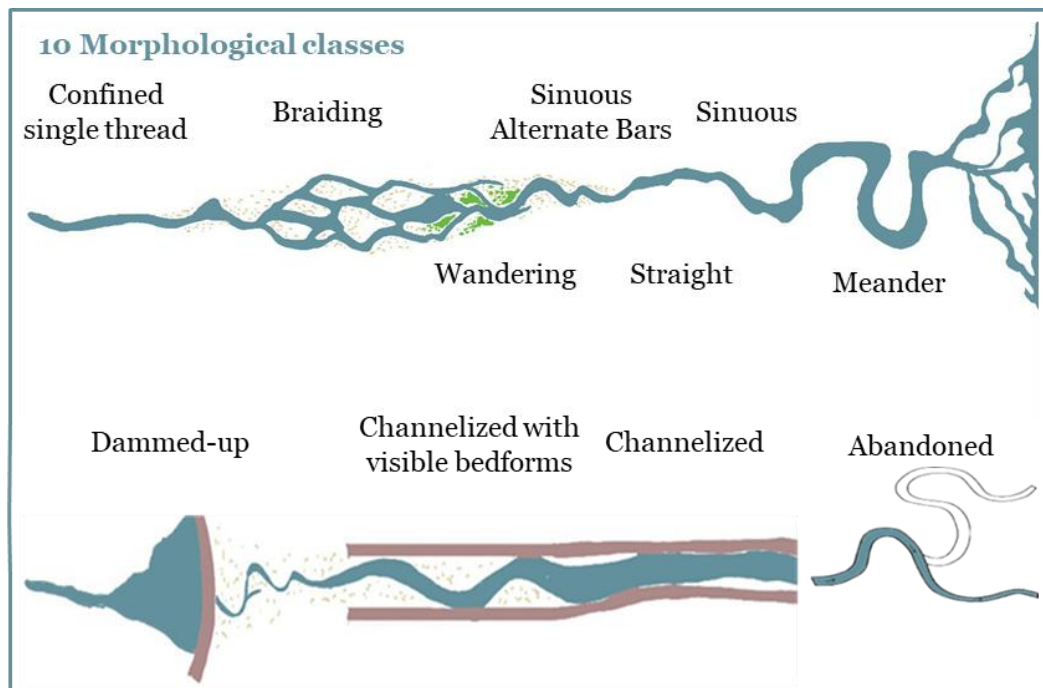


Figure 2. 9. Nine typologies of the morphology to quantify the present morphology of Albanian river.

To develop a consistent evaluation of both the past and present morphologies, the “abandoned” type has been introduced, which was part of the river before, but due to channelization, artificial or natural cut off of the previously meandering channel it has been disconnected from the main stem and is inundated only under some flood events, while the main channel changed the direction to another path.

The IDRAIM methods indicates the use of three indices to assess the reach channel morphology: the sinuosity, braiding and anabranching indices. They are defined below. In the present work the channel morphology has been assessed using a combination of the channel sinuosity and subjective expert judgment on available orthophotos to classify the morphologies of the river’s reaches. Some examples of the assessment based on expert judgement for each morphology have been reported in Figure A1 in the appendix. Other examples are also reported in figure 2.29, 2.30.

For this work the Sinuosity Index (SI) is calculated for every reach. *SI* is expressed as the ratio between the distance la measured along the (main) channel and the sum of the n cartesian distances ln measured following the direction of the overall river planform, as illustrated in Figure 2.10.

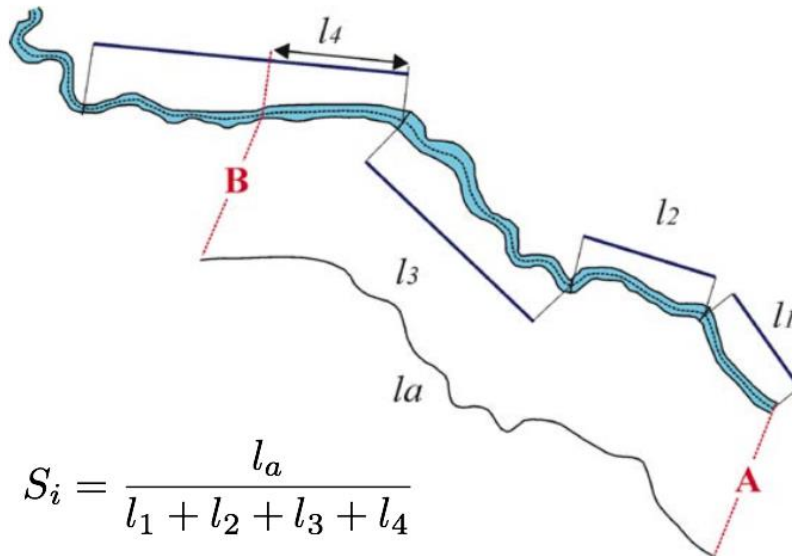


Figure 2. 10. Measurement of the Sinuous Index

The *Braiding index (Bi)* is defined as the number of wet channels at baseflow in a cross-section that are separated by bars; The *Anabranching index (Ai)* is instead defined as the number of active channels at the baseflow separated by vegetated islands.

Step 4. Other elements for reach delineation

Step 4 aims to finalize the delineation of reaches accounting for additional factors. In this phase segments are divided into reaches, representing the basic spatial unit for different application. To subdivide segments into reaches some additional criteria (figure 2.11) must be considered:

- *Change in geomorphological units:* Within a reach having a same Basic River Type, a distinct change in the typical assemblage of geomorphic units can be noted and used as an additional criterion for sub-dividing the reach. Changes in geomorphological units and/or in sediment size are reflected in a change of river type, and therefore implies partition into two or more reaches of the original one.
- *Discontinuities in bed slope:* This is particularly important in the case of confined channels where important and abrupt changes in bed slope can be noted from the longitudinal profile.
- *Tributaries:* Tributaries determining significant changes in flow discharge or sediment transport can be considered in this step, as possibly setting a border between two reaches.
- *Dams and other artificial elements:* Artificial discontinuities are mainly identified with dams, which are always assumed as a limit between reaches. Similarly, check

dams or diversion structures of relevant sizes are normally considered as a limit of the reach.

- *Change in confinement and/or size of the floodplain:* In some cases, this can be considered as an additional criterion.
- *Changes in sediment size:* Cases of a considerable and sudden change in sediment size, e.g. a passage from gravel-bed to sand-bed, can be considered a criterion of separation in different reaches.

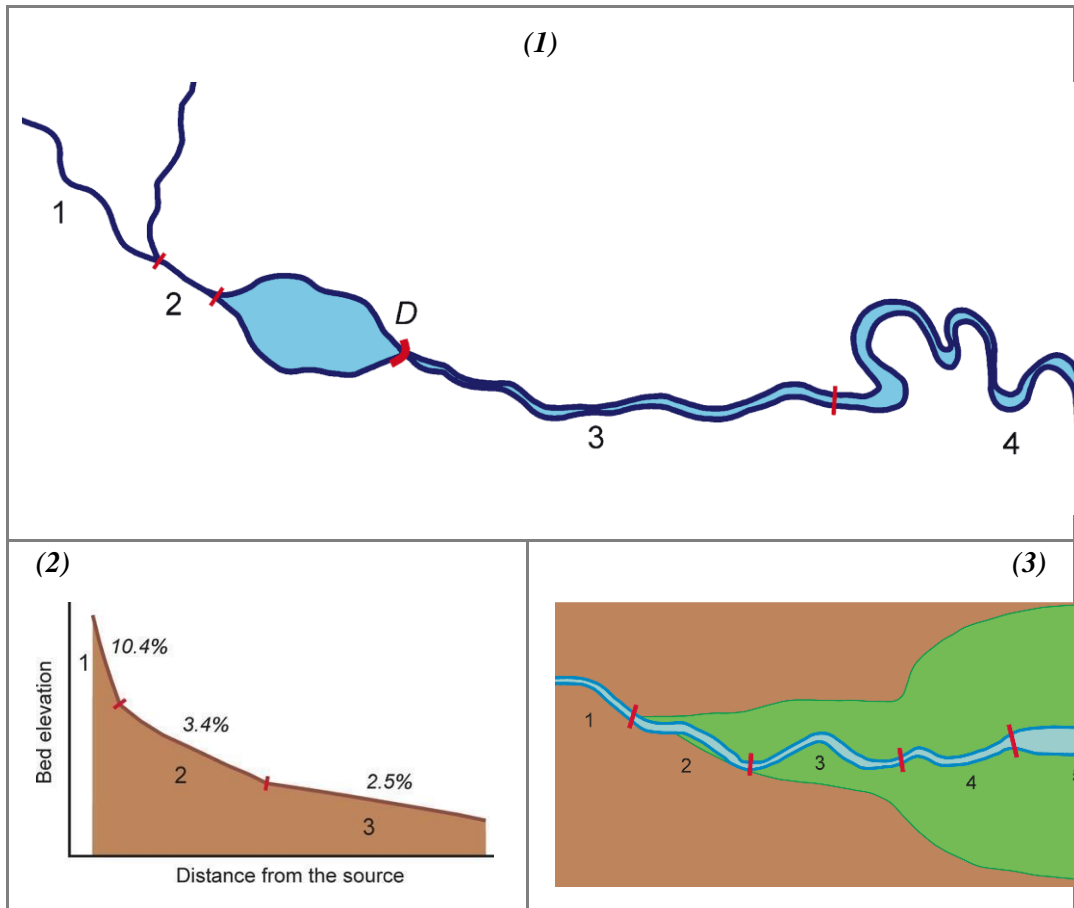


Figure 2. 11. (1) Hydrological discontinuity due to a major tributary; (2) discontinuity in bed slope; (3) change in size of the floodplain; change in channel width. From Rinaldi et al., (2015)

Data sources

Map	Date	Scale/Resol.	Coverage
Istituto Geografico Militare, Florence	1928-1944	1:50,000	All Albania

Topographic Military Institute, Albania	1959-1985	1:25,000	All Albania
Topographic Military Institute, Albania	1980-1984	1:10,000	West Albania
Corona Images*	1960-1972	2-12 m	Ex. USSR countries
Aerial orthophoto grayscale	1994	1:10,000	West Albania
Orthophoto RGB	2007	20 cm	All Albania
Orthophoto RGB	2015	20 cm	All Albania
Google Earth	2008-2022	-	All Albania
Geology Map	-	1:200,000; 1:100,000	All Albania
EU Digital Elevation Model v1.1	2011/16	25 m	All Albania

Table 2. 6. Special data source used for the study

* United States Geological Survey, Corona spy satellite mission.

For data processing and visualisation QGIS, Grass GIS and python are used. For this work for data processing and visualization are used this main software: QGIS, GRASS GIS, Python, and Inkscape. All the military maps, orthophotos and geology maps are available at Geoportal Albania through webGIS platform.

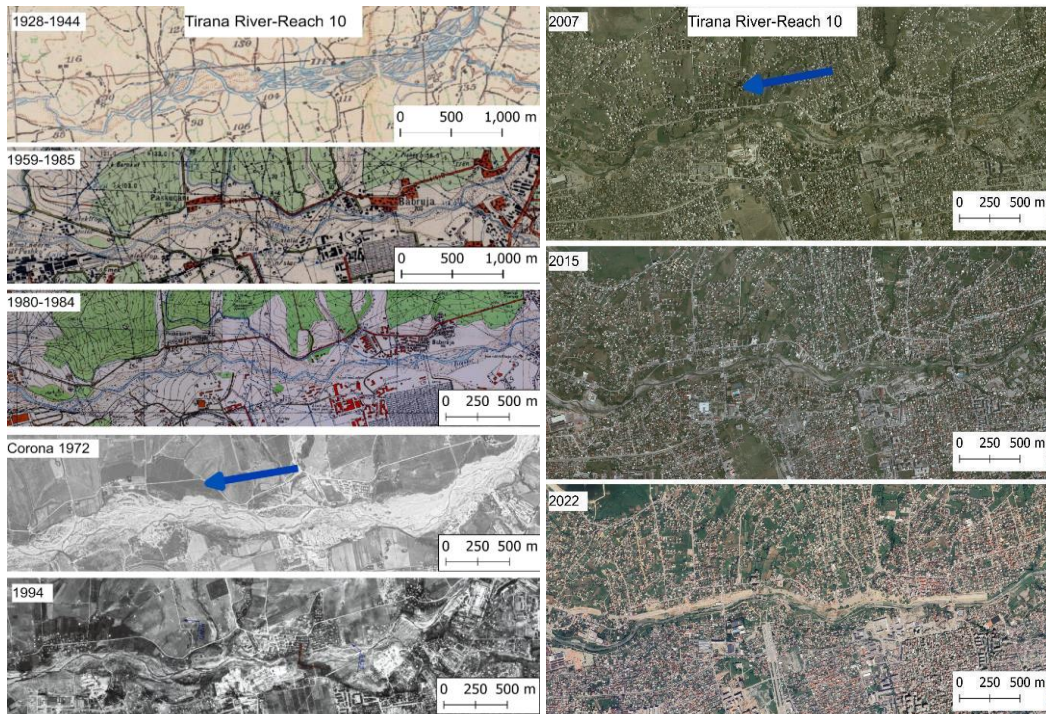


Figure 2. 12. An illustrative example of the used cartographic and satellite / aerial imagery sources. The example shows the evolution of river morphology and urban areas for a reach of the Tirana river, Ishem river basin.

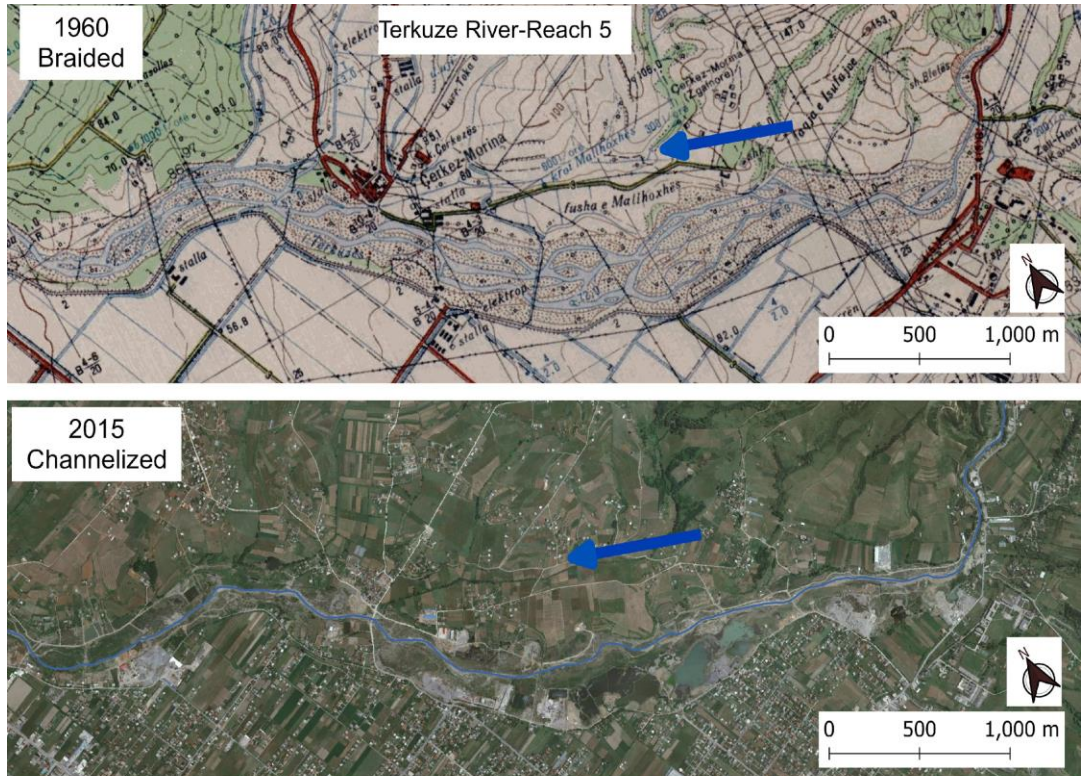


Figure 2.13. Change of River Morphology from Braided to Channelized, Terkzue River, Ishem basin.

2.4 Results and discussion

The present section is organized as follows. First, an overview of the main geological formations of the analysed catchment is presented and related to the information on the catchment sediment yield. Afterwards, the results of the segmentation procedure are presented, in terms of the landscape units classification and river confinement for each catchment. A diachronic “Morphological Atlas” is then presented, with reference to the detected historical morphologies, prior to 1968, and to the present channel morphologies. The chapter is concluded with an analysis of the major observed changes between the two periods, also examining the implications of these findings for river management in Albania.

Geology characterization in catchment scale

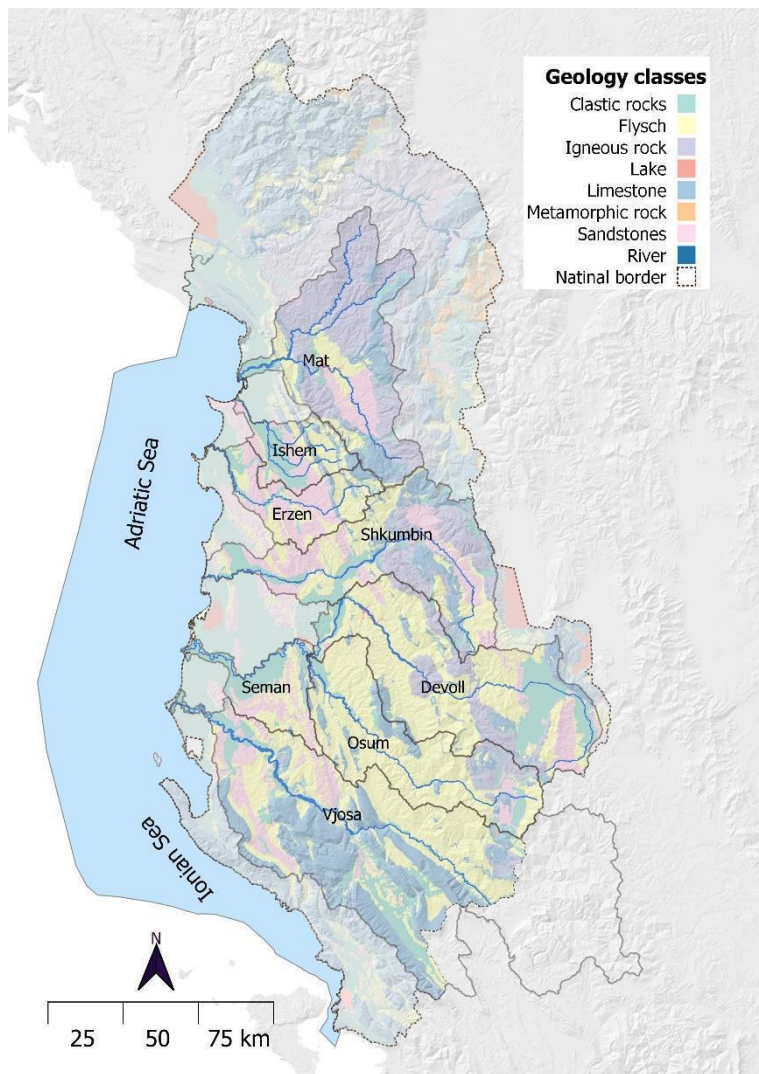


Figure 2. 14. Geology characterization at catchment scale for rivers analysed.

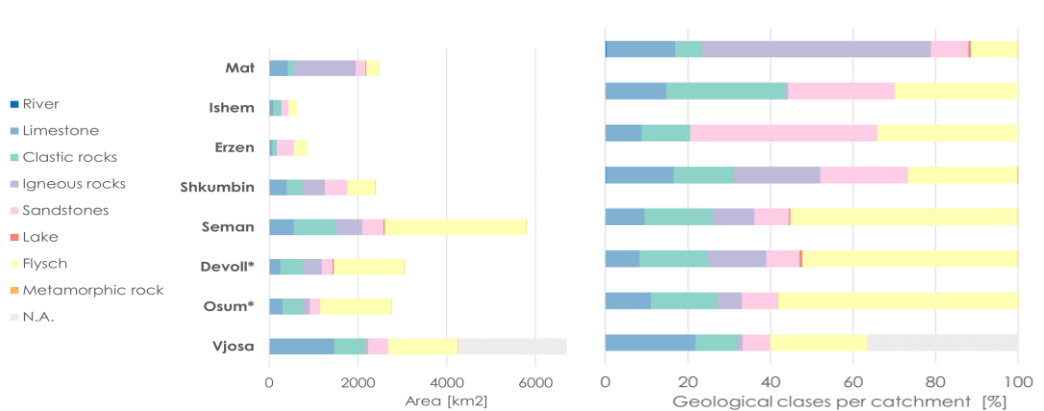


Figure 2.15. Main geology classes (km² and percentage of the total area) per catchment. *Devoll and Osum river are catchments of Seman river.*

The Geological Map of Albania at a scale of 1:200,000, prepared by the Geological Albanian Service, categorizes the 88 geological classes based on their rock formation characteristics. These classes have been grouped into six main broader categories, each of which includes several of the detailed classes: 1-Flysch; 2- Limestone; 3- Igneous rock; 4- Sandstone; 5- Clastic rocks; 6-Metamorphic rocks. In addition to these six categories, two other classes, 'River' and 'Lakes,' have been included to provide a comprehensive overview of the geological features in the region.

Flysch is a geological formation characterized by alternating layers of fine-grained and coarse-grained sedimentary rocks, typically found in regions with active tectonics. These formations provide valuable insights into the complex geological history of an area. The alternation of sediment types can influence erosion patterns and sediment transport dynamics in the region, impacting the overall landscape. They are easily erodible and typically determine high sediment-productive draining river channels. Flysch occupies nearly 50% of the catchments of Osum, Devoll and Seman rivers.

Limestone is a common rock type that has a significant influence on the geological features of an area. Its solubility in water can lead to the formation of unique landscapes such as caves, sinkholes, and underground river systems. Limestone's presence can affect groundwater flow and water quality in the region, making it a key consideration in geological studies.

Igneous rocks, often associated with volcanic activity, can shape the topography of an area, leading to rugged terrains and steep gradients. Additionally, the mineral composition of igneous rocks can have implications for water chemistry and the overall geological character of the region.

Sandstone is a sedimentary rock that can contribute to the formation of sandbars, riverbanks, and other sedimentary features along river courses. Sandstone's porous nature allows for water storage, impacting groundwater availability and influencing local hydrology.

Clastic rocks, which include sandstone and shale, can break down into sediments that are transported by natural processes, affecting the region's topography and sediment load. Clastic rocks also play a role in influencing water chemistry and nutrient content in local bodies of water.

Metamorphic rocks, shaped by intense heat and pressure, can have diverse characteristics depending on their mineral composition. Some metamorphic rocks may contain minerals that influence water chemistry, while others may exhibit resistance to erosion, impacting the overall geological landscape of an area.

Looking at the catchment scale for each river, the following dominant geological formations emerge. Mat river catchment is dominated by igneous rocks, followed by limestone and flysh. In the Ishem river clastic rocks dominate, followed by flysh, sandstones and limestone. In the Erzen river catchment the predominant geology is made by sandstones and flysh. The Shkumbin catchment sees a rather balanced presence of igneous rocks, sandstones, flysch, clastic rocks and limestone. The Seman river catchment, which includes Devoll and Osum river basins, have as more predominant geological classes flysch and clastic rocks. Vjosa river, in its Albanian part, sees limestone, flysch and clastic rocks as the main geological formations.

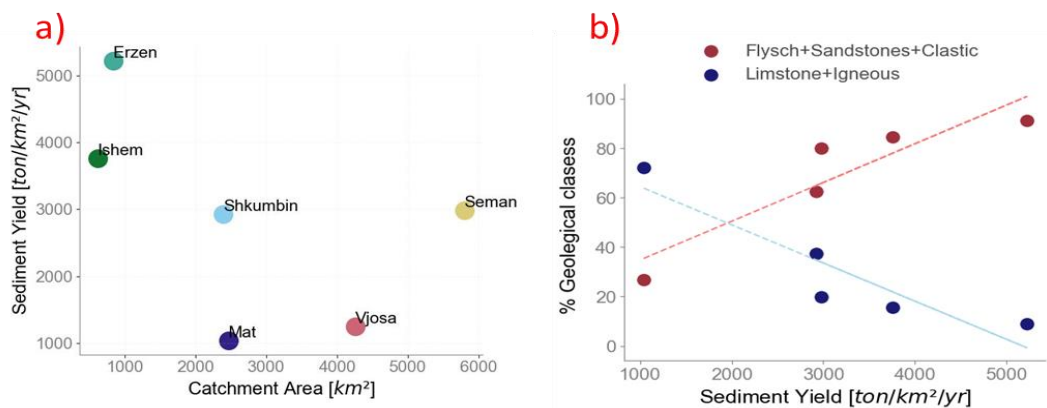


Figure 2.16. (a) Annual Sediment yield , per catchment area. (b) Annual sediment yield plotted against the % of some chosen geological categories, expected to be more erodible (red circles) and less erodible (blue circles).

The geological composition of a river's catchment area plays a pivotal role in sediment transport. In the case of the Erzen and Ishem rivers, their catchment area is characterized by the presence of two significant rock types: flysch and sandstone, Ishem river clastic rocks as well. These rock types have distinct properties that make them highly susceptible to erosion and subsequent sediment transport.

Flysch is a sedimentary rock formation that is characterized by its alternating layers of fine-grained materials such as shale and sandstone. The fine-grained nature of flysch rock makes it highly erodible, especially when exposed to the relentless forces of water flow. This

characteristic makes flysch an abundant source of sediment in these river systems, especially of fine material that is mainly transported as suspended load during the highest floods.

Sandstone, on the other hand, is composed of compacted sand grains. While it is more resistant to erosion compared to flysch, it can still be weathered and eroded over time. Its presence in the catchment area contributes to the overall sediment load carried by the rivers.

On the other hand, Erzen and Ishem river are short rivers (around 100 km) compared to the other longer and larger rivers such as Shkumbin, Osum and Vjosa. These rivers are relatively short in length, which means that they have limited distance to transport sediments downstream. Shorter rivers tend to accumulate sediment more quickly since there is less distance for sediment to travel before settling. This is particularly significant in their upper mountainous reaches. The high slopes in the mountainous sections of these rivers lead to faster water flow and increased erosional power. Steeper gradients result in more turbulent water, which is highly effective in dislodging and transporting sediment., in the case of the Ishem river.

Analysis of the detected Physiographic Units

Physiographic Units are the baseline information for river segments subdivisions, along with major tributaries.

<i>Unit</i>	<i>Criteria</i>
Mountain	$e > 600$ m.a.s.l.
Hill	$200 < e < 600$ m.a.s.l.
Plain	$e > 200$ m.a.s.l.

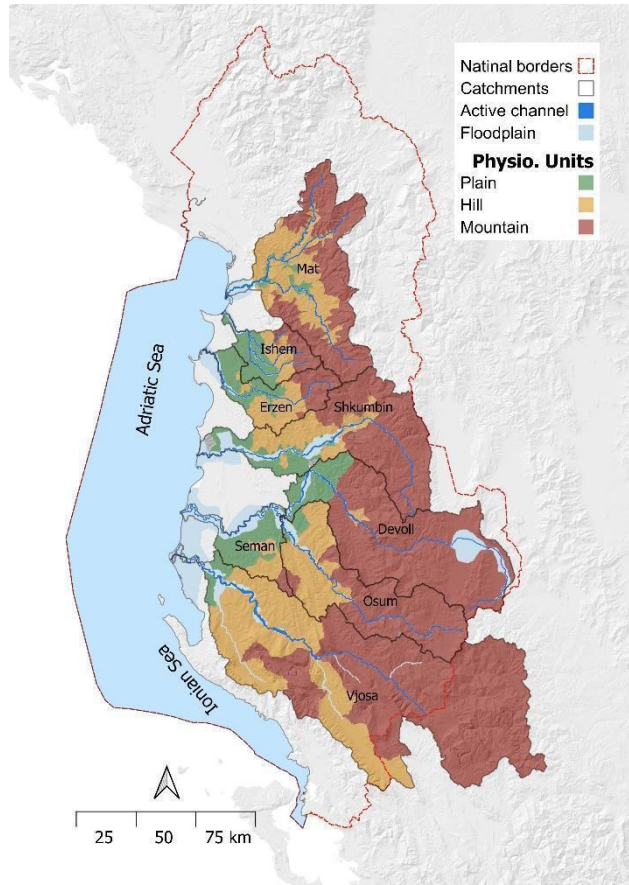


Figure 2. 17. Map of the physiographic units of the analysed river catchments.

Physiographic unit are classified in three classes: “Mountain” (elevation higher than 600 m.a.s.l, “Hill” (between 200 and 600 m.a.s.l) and “Plain” (elevation lower than 200 m.a.s.l.). Albanian rivers, which mainly flow from east to west and ultimately discharge into the Adriatic Sea, possess significant mountain units in their catchment areas. Among the catchment areas examined, about 63% are classified as mountainous, 26% as hilly, and a mere 11% as plains. This implies that roughly 63% of these catchment areas are situated at elevations exceeding 600 meters above sea level (m.a.s.l), 26% fall within the range of 200-600 m.a.s.l, and the remaining 11% are situated below 200 m.a.s.l (Figure 2.18).

This distribution helps elucidate the high sediment transport rates observed in Albanian rivers per unit catchment area. The prevalence of mountainous rivers, known for their steep gradients, is a primary contributing factor to this phenomenon, together with the relatively high rainfall occurring in the mountain landscape units up to 2,800-3,000 mm per year (Climate change post, 2023)

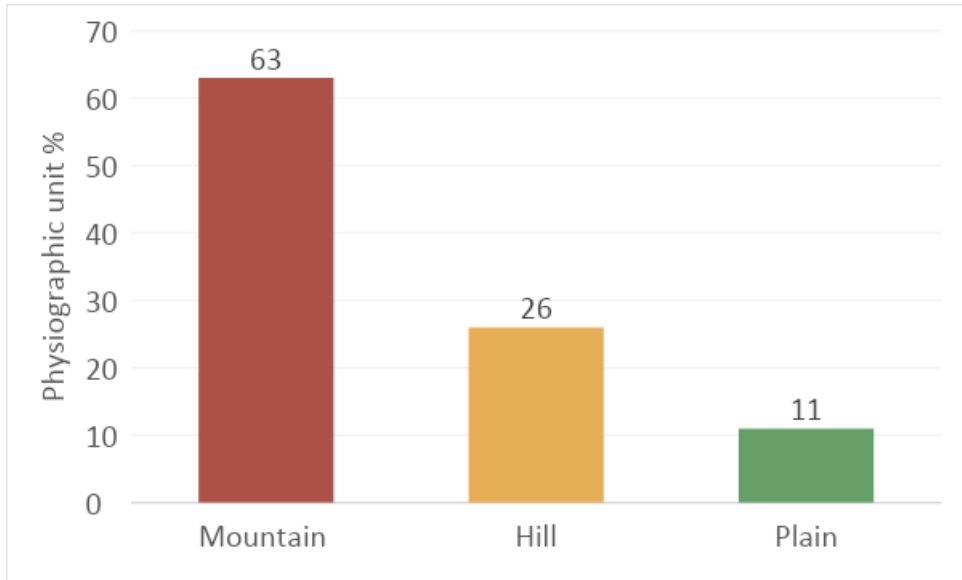


Figure 2. 18. Percentage area of each physiographic unit type relative to the total catchment area of the examined Albanian rivers.

Figure 2.18 reports the same information per each river catchment, allowing to illustrate inter-catchment differences. The Vjosa River, encompassing a vast catchment area of 6,655 km², stands out with 64% of its catchment above 600 meters above sea level (m.a.s.l). Originating in Greek territory, it includes 33% hilly terrain and a mere 3% in plains. These geographic features significantly influence the Vjosa River's hydrological behavior, with a predominant mountainous catchment. The Seman River, covering 5,755 km², is primarily characterized by mountainous catchment, making up 67% of its total area. It also features 16% hilly terrain and 17% plains, contributing to the diverse hydrological patterns observed in the Seman River. The Mat River, ranking as the third largest among the studied rivers with a catchment area of 2,505 km², exhibits a catchment that is 59% mountainous, 37% hilly, and 4% plain.

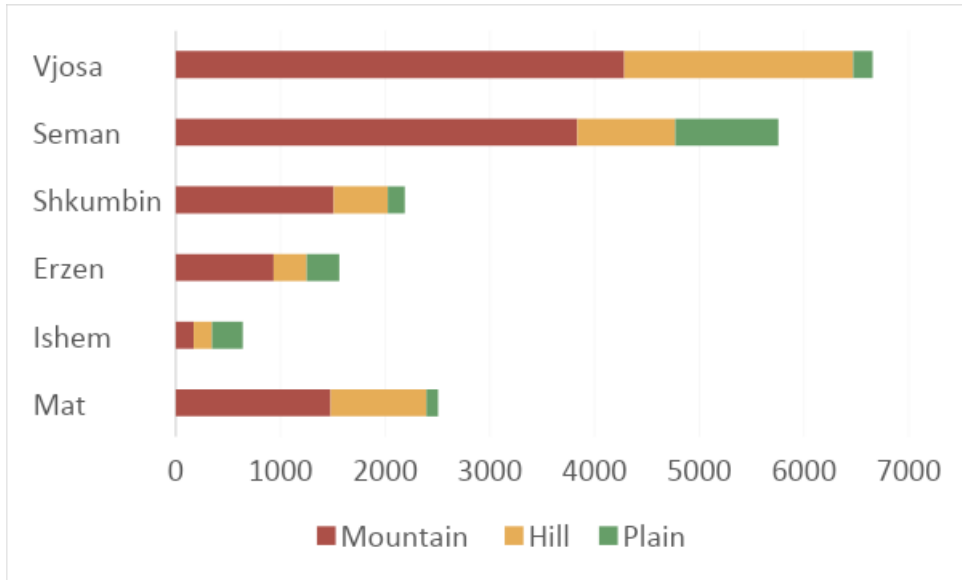


Figure 2. 19. Physiographic unit of the Albanian rivers in km²

With a catchment area of 2,187 km², the Shkumbin River is predominantly mountainous (69%), followed by hilly physiographic unit (24%), and plains (7%). The Erzen River, covering 1,562 km², features a catchment area that is 60% mountainous, 20% hilly, and 20% in plains, being the river with the highest percentage of catchment area in the plain physiographic unit, like the Seman, after the Ishem.

In contrast, the Ishem River, with a total catchment area of 640 km², consists of 27% mountainous terrain, 27% hilly areas, and 46% plains. The distinct composition of the Ishem River's catchment area has a notable impact on the processes controlling its channel morphology.

These diverse catchment characteristics provide support for interpreting differences in the morphological types observed in these Albanian rivers.

Confinement characterization of the Albanian rivers

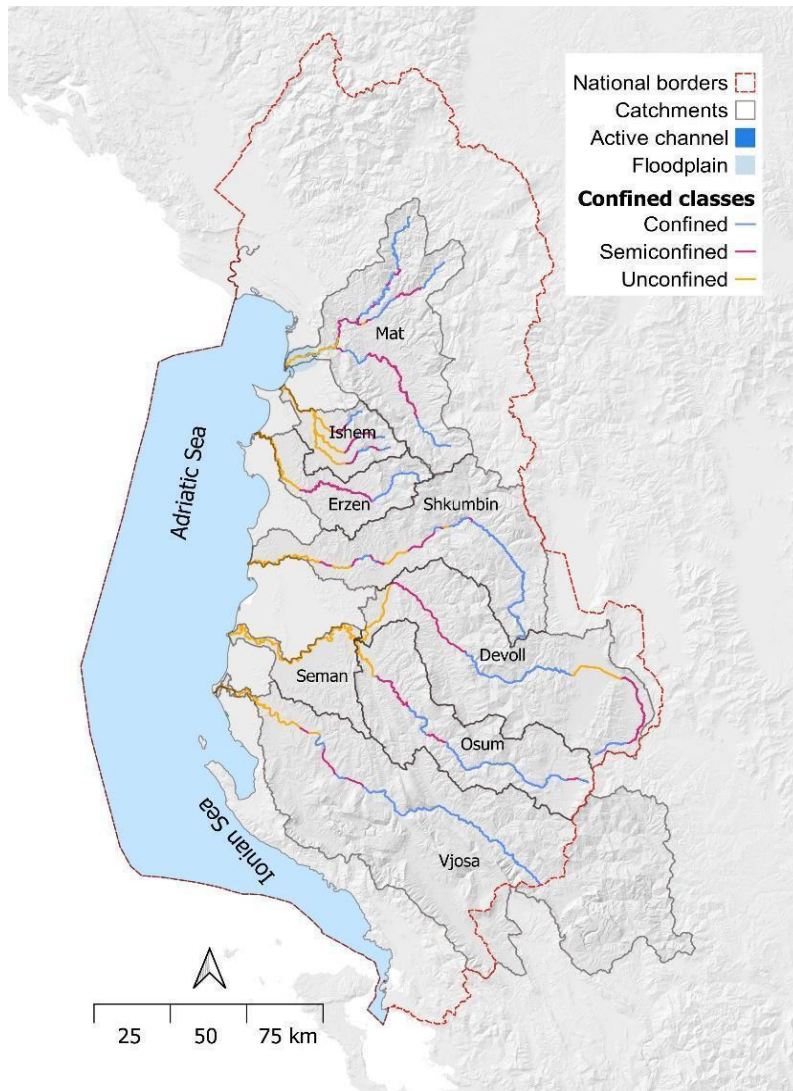


Figure 2. 20. Confinement map for major Albanian rivers.

The light blue colour on the map in Figure 2.20 represents confined rivers, which are primarily located in the eastern and central regions of Albania. These rivers flow through narrow valleys and often form canyons. The confined sections are predominantly found in the hilly and mountainous areas of the river catchments, as indicated on the map. The purple colour shows semi-confined or partially confined river segments, which are located mostly in the central part of Albania and hill unit of the river catchments.

Unconfined rivers are depicted in orange on the map and are typically situated in hilly and lowland regions. These rivers are characterized by wide floodplains. An exception to this pattern is the Devoll River, which, at an elevation of 800 meters above sea level (m.a.s.l),

features an unconfined section. This is due to the presence of a substantial floodplain in the Korca district, formed by clastic rock geology. This flat area is surrounded by mountains and primarily used for agricultural purposes.

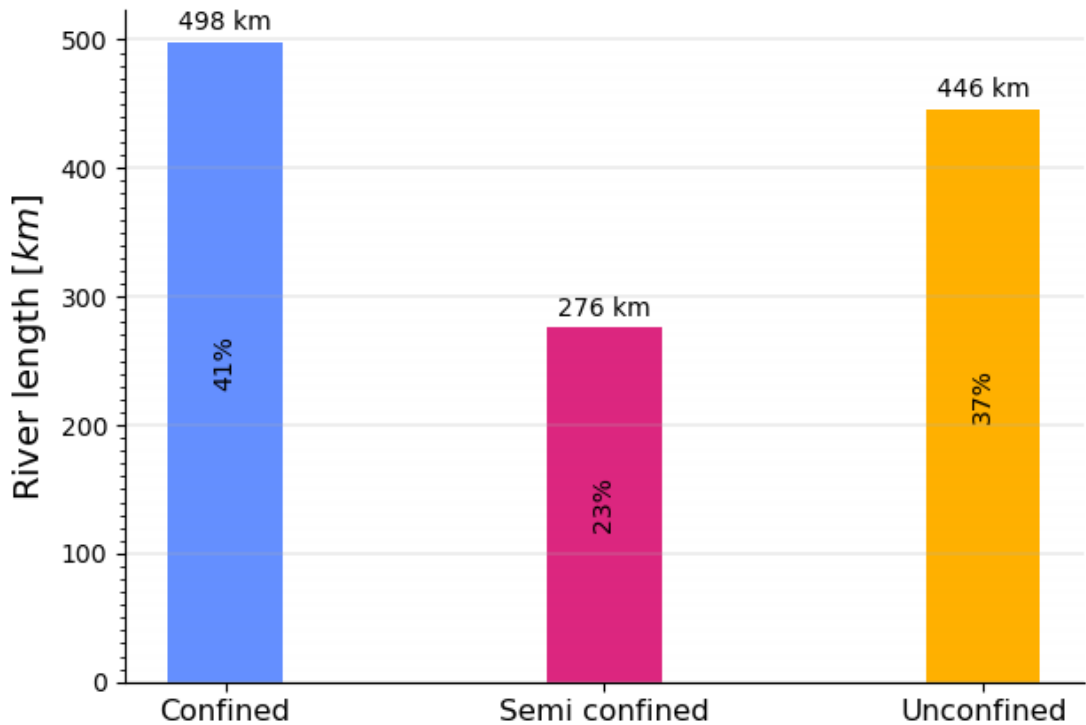


Figure 2. 21. Length of confinement classes in km

Among the rivers studied, covering a total length of 1,240 km, 41% of them, equivalent to 498 km are confined rivers. Semi-confined make up 27% of the total, accounting for 276 km. Unconfined rivers represent the remaining 37% of the studied rivers, with a total length of 446 km (Figure 2.21).

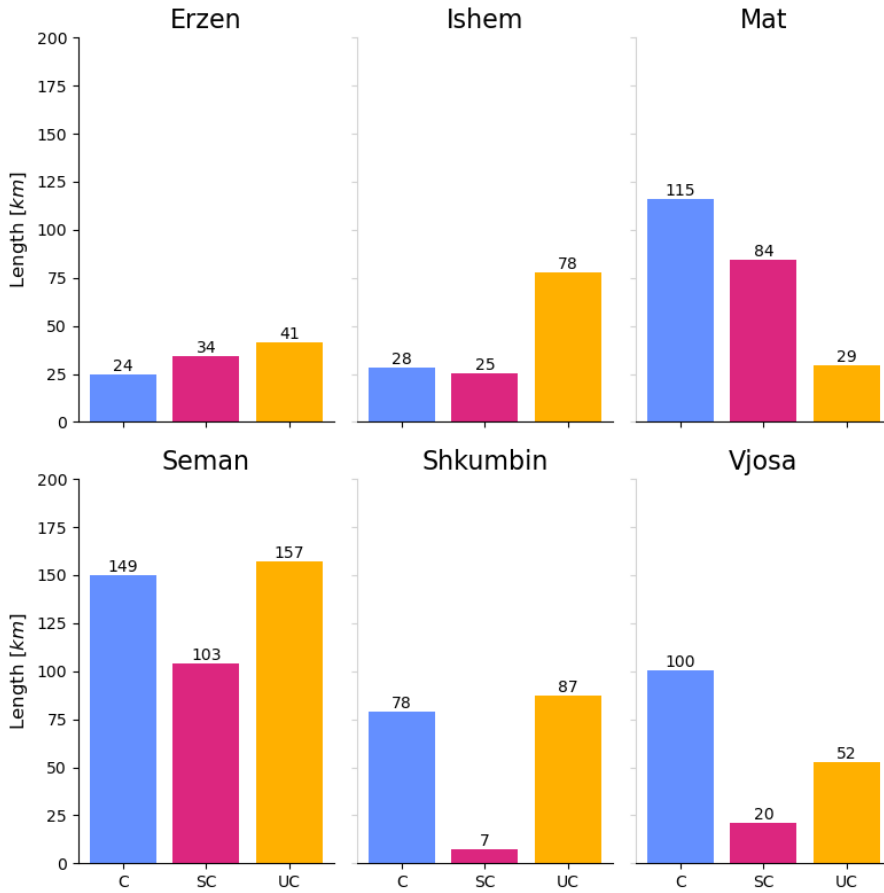


Figure 2. 22. Confined classes per each catchment (C-confined; SC- semi-confined; UC-unconfined)

Figure 2.22 shows the difference in confinement classes within each catchment. Among these rivers, the Erzen River, with a studied length of approximately 100 km, displays a rather balance combination of confined, semi-confined, and unconfined reaches, amounting to 24 km (24%), 34 km (34%), and 41 km (41%), respectively. In the case of the Ishem River, covering 131 km and including four major tributaries (Tirana, Trerkuze, Gjole and Zeze rivers), its course primarily consists of unconfined segments, encompassing 78 km (60%), while confined and semi-confined sections account for 28 km (21%) and 25 km (19%), respectively.

The Mat River, spanning 228 km and featuring four major tributaries (Mat, Fan, big Fan and small Fan River), presents a predominantly confined river channel for 115 km (50%), along with 84 km (37%) of semi-confined sections and 29 km (13%) of unconfined areas. The Seman River, with an extensive 407-km length and two major tributaries, is predominantly classified as unconfined, covering 157 km (39%), while confined and semi-confined sections make up 149 km (37%) and 103 km (25%), respectively.

The Shkumbin River, studied over 172 km, is characterized by a significant unconfined portion of 87 km (51%), 78 km (45%) of confinement, and just 7 km (4%) of semi-confined areas, making it particularly unique for having the shortest length of semi-confined sections among the studied rivers.

Lastly, the Vjosa River, the mainstream within Albania, analysed over a length of 172 km, features 100 km (58%) of confinement, 20 km (12%) of semi-confined segments, and 52 km (30%) of unconfined areas.

Morphology characterization

River morphology in the 1960s

Albanian rivers exhibit a diverse morphology within a relatively small territory, characterized by high hydrodynamic rivers. By comparing historical maps available from different periods, specifically from 1928-1944 (Istituto Geografico Militare, Florence) and the Topographic Military Institute of Albania (1959-1985), Corona images at the end of the 1960s – early 1970s, it was possible to map the channel morphology of all the analysed river reaches.

From the analysis of six catchment rivers, totalling around 1310 km in river length, eight distinct morphologies have been identified. These include: (i) single-thread rivers, (ii) straight rivers, (iii) meandering rivers, (iv) sinuous rivers with alternate bars, (v) sinuous rivers, (vi) wandering rivers, (vii) braided rivers, and (viii) dammed-up rivers. It's important to note that the 'dammed-up' morphology, as defined here, represents only one reach in the Devoll river that used to be a lake in 1960 and has since then been channelized.



Figure 2. 23. River morphology atlas 1960 for majority rivers in Albania

As shown on the map of Figure 2.23, the purple colour represents the single-thread morphology, which is primarily found in the confined (mountainous) areas of the river, covering a total length of 247 km (19%). The second most prominent morphology is the meandering one, stretching over 244 km (19%). Together, these two morphologies account for 38% of the river's features.

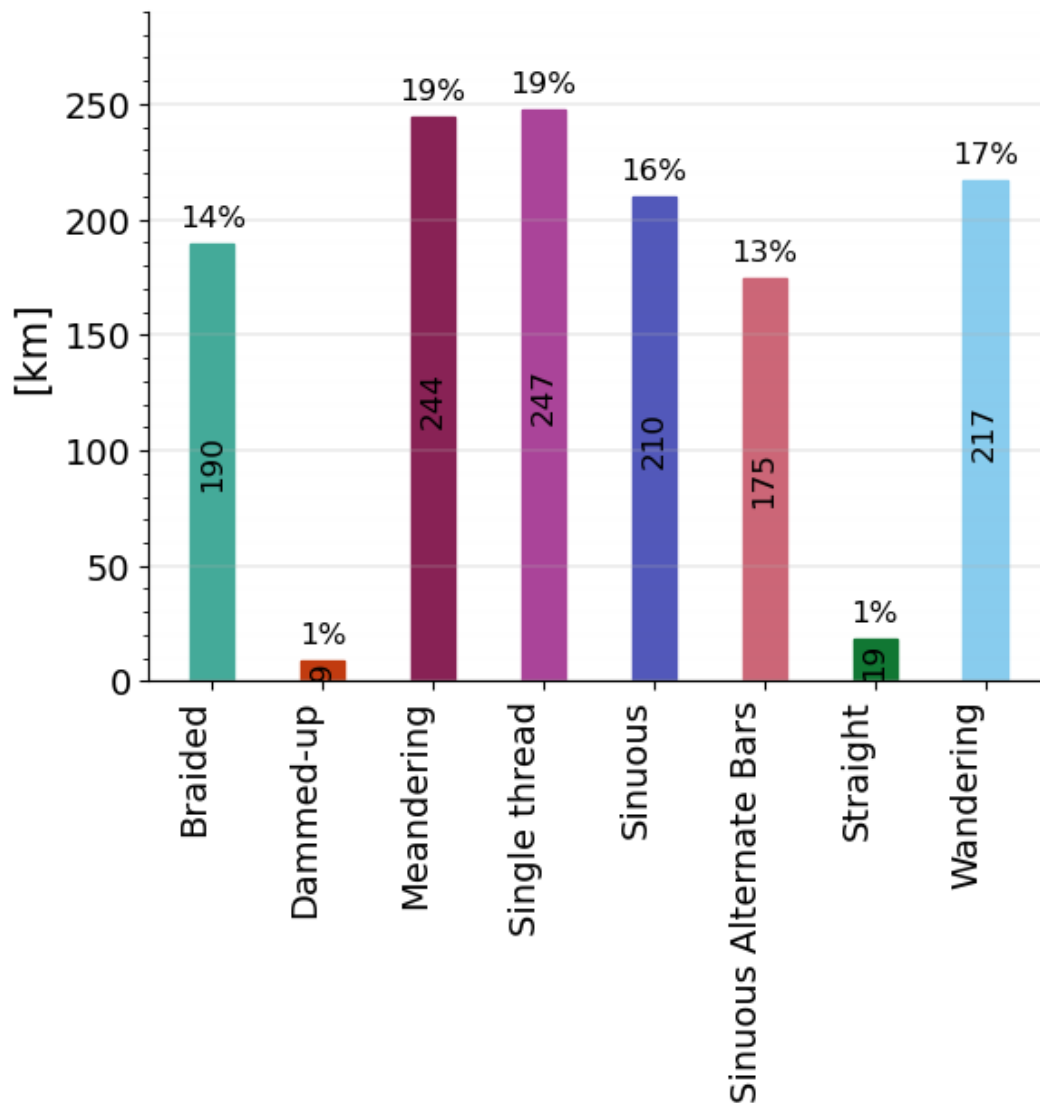


Figure 2. 24. Albanian River morphological classes 1960

The third significant morphology is the wandering type, spanning 217 km (17%), followed closely by the sinuous morphology at 210 km (16%). The rivers also shows that braided morphology covered 190 km (14%), sinuous morphology with alternate bars accounting for 13%, straight morphology over a length of 19 km (1%), and finally, dammed-up, which make up 1% of the investigated river network (Figure 2.24).

River morphologies in 2015

To assess the river's morphologies, we conducted an analysis using orthophoto data from 2015, which covers the entire Albania. The total length of the studied rivers spans 1,260 km, and it's worth noting that this number is approximately 50 km less compared to the 1960s, implying that in the 70-year period since 1960, the original river network length has been

reduced by almost 5%. As a result, four new morphologies have been identified, bringing the total count to ten morphology characterization. The updated map of the river morphological types is shown in Figure 2.25.



Figure 2. 25. Albanian river morphological atlas for 2015

The new morphologies that recently appeared in the river network of Albania and that, therefore, needed to be introduced are (i) Channelized, (ii) Channelized with Visible Bedforms, and (iii) Abandoned, which represents a river that has transitioned from an active channel into abandoned, much like a meandering river that has cut-off from the main waterway.

The dominant morphology remains single thread extending across 276 km (22%). Close behind is sinuous, covering 221 km (17%), and meandering, which encompasses 190 km (15%). wandering morphologies extend for 179 km (14%), while sinuous with alternate bars occupies 152 km (12%) (Figure 2.26).

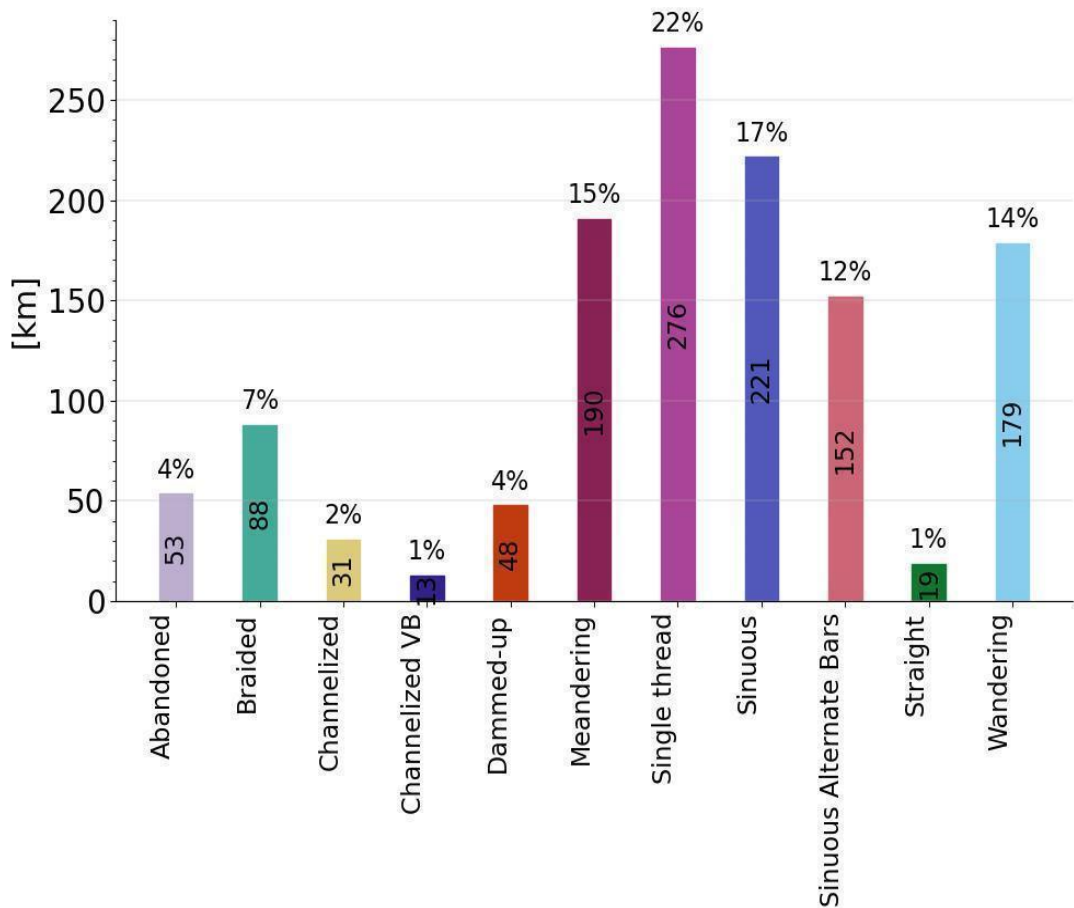


Figure 2. 26. Albanian River Morphology classes 2015

Furthermore, braided reaches span now 88 km (7%), Dammed-Up reaches represent 48 km (4%), and three other morphologies that were not present in the past, abandoned reaches cover 53 km (4%). channelized reaches encompass 31 km (2%) and channelized with visible bedforms extends over 13 km (1%). This comprehensive analysis not only highlights the evolving morphologies of the river but also underscores the dynamic nature of this natural landscape over the decades.

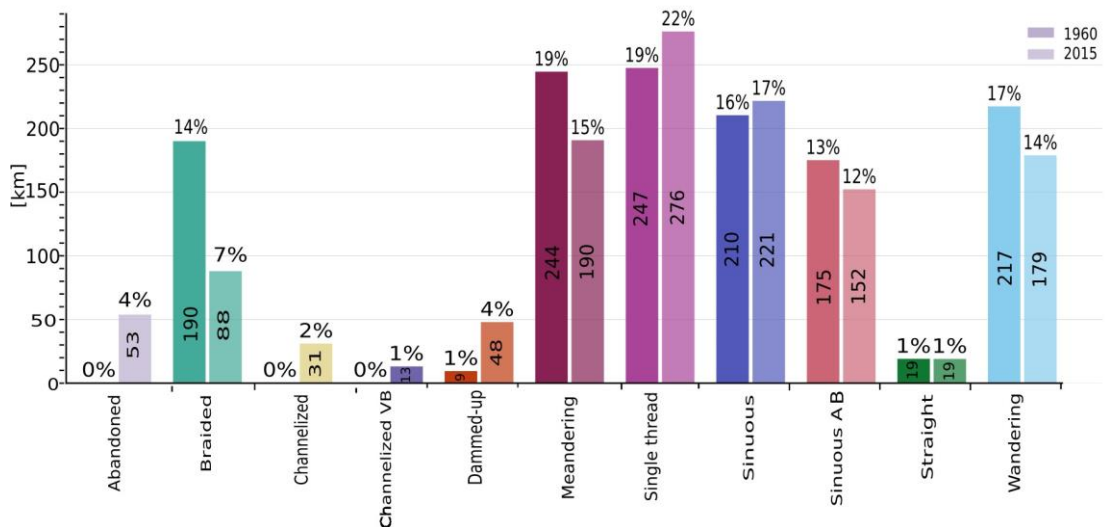


Figure 2. 27. Morphology classes for two periods 1960 in the left and 2015 on the right with lighter colour.

Figure 2.27 compares the frequency distribution of the morphologies in the two periods. Overall, a reduction in the more complex morphologies is evident. Braided morphology is reduced by half 50%, lost with a total loss of 102 km of formerly braided patterns; meandering reaches reduced their length by 4%, corresponding to a net loss of 54 km of meandering rivers. Wandering morphologies also consistently reduced by 38 km (3% of their original length). Sinuous channel pattern does not undergo a major net change, by 1% (11 km), like sinuous with VB, which reduced by 1% (23 km); straight morphologies are basically constant, remaining of the same length, of 19 km. Dammed-up increased by 3% or 39 km more. Three other morphologies that were not present in 1960, appeared: channelized (31 km), channelized with visible bedforms (12 km) and abandoned (53 km).

In the past six decades, Albanian rivers have therefore undergone significant changes in their morphologies. The primary alterations observed between 1960 and 2015 indicate a transformation in the braided and wandering river types: the initially braided and wandering morphologies changed by 59% and 52% respectively (figure 2.28). The shifts in braided reaches show that 39% transformed into wandering, 10% into sinuous, 5% became dammed up, while 3% developed sinuous alternate bars (AB) and 2% turned channelized. On the other hand, wandering reaches experienced a conversion of 20% into sinuous, 13% into sinuous visible bedforms (VB), 9% into meandering, and 5% into braided morphologies.

Additionally, 2% became both channelized and dammed up, while 1% displayed channelized visible bedforms VB (figure 2.28 and 2.29).

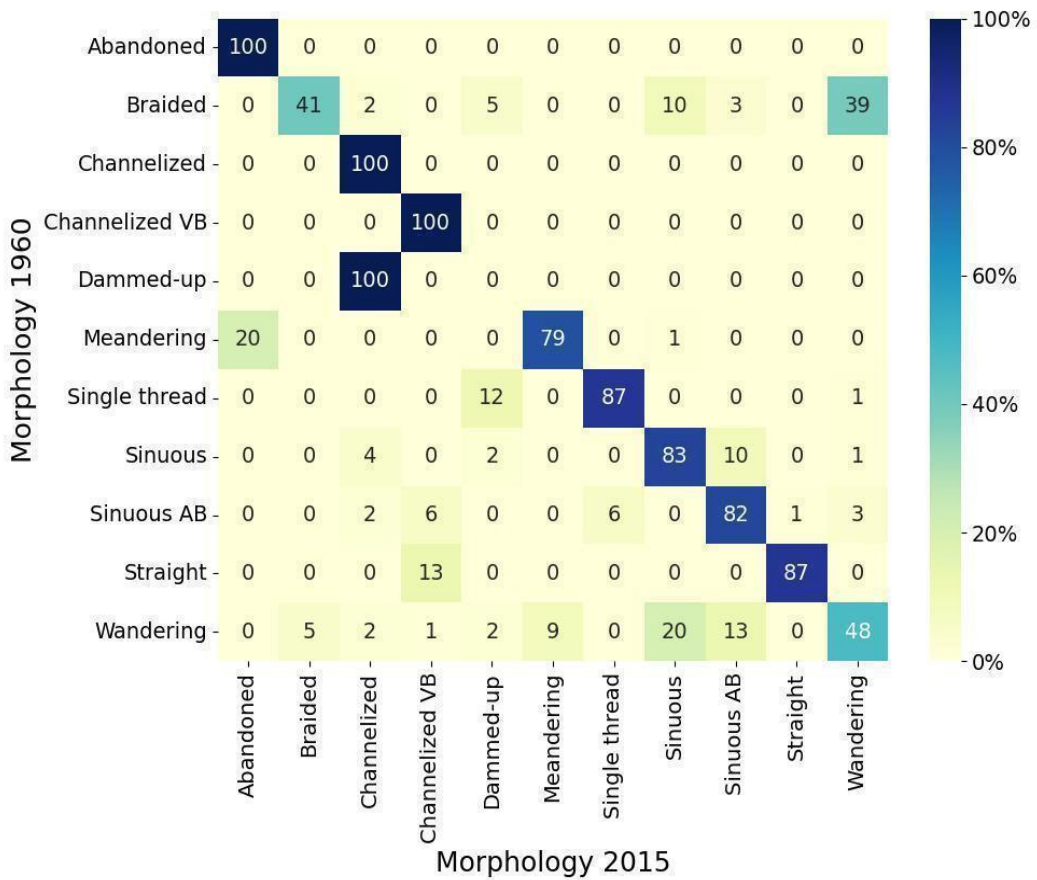


Figure 2. 28. The Metamorphosis of Main Albanian River Morphologies: A Heat map comparison between 1960 and 2015.

Meandering reaches encountered a 21% alteration, with 20% transforming into abandoned configurations and 1% evolving into sinuous forms. Sinuous reaches with alternate bars (AB) experienced an 18% change, with 6% transitioning into channelized with visible bedforms (VB), 6% transforming into single-thread patterns, 3% becoming wandering, 2% channelized, and 1% straight morphologies. Sinuous reaches transformed by 17%: 10% evolved into sinuous AB, 4% into channelized, 2% into dammed up, and 1% into wandering.

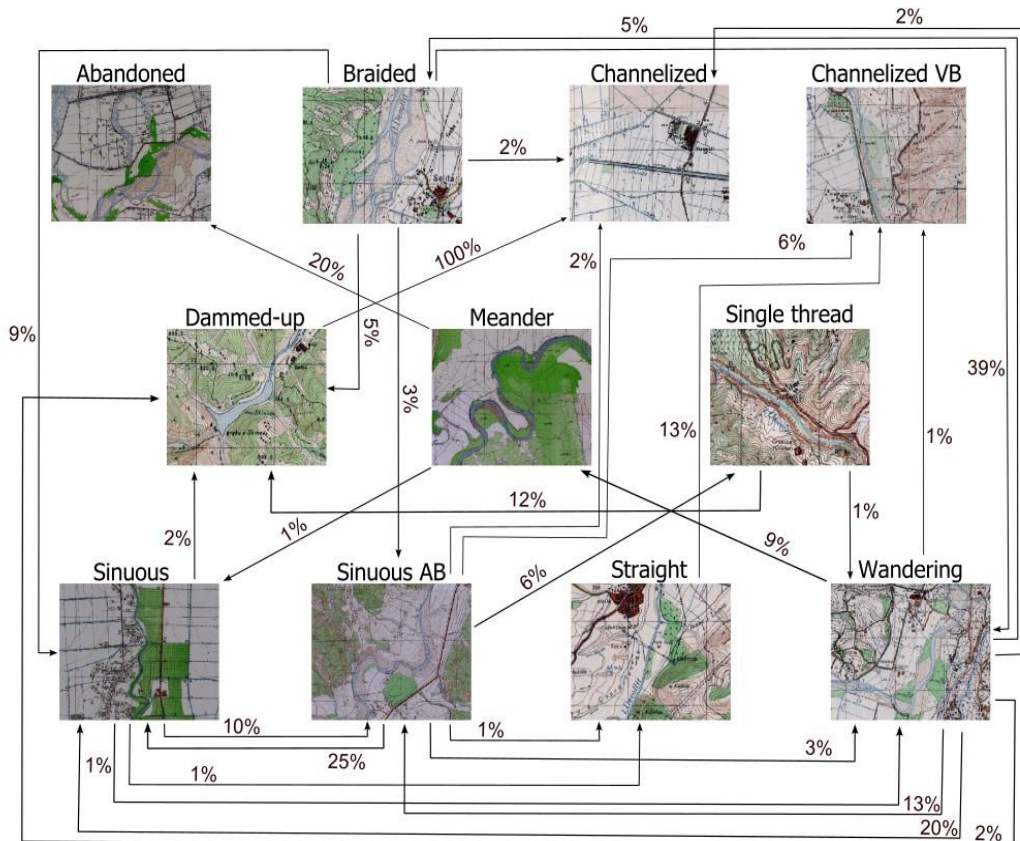


Figure 2. 29. Sequence relation diagram of river morphology changes from 1960 to 2015 changes

Figure 2.29 is a relational diagram of the changes between different channel morphologies. Each arrow indicates the direction of changes and the percentage of the initial morphological class that was modified into the arriving morphological class. Single-thread and straight reaches both underwent a 13% change. Single-thread reaches saw a 12% transformation into dammed up and 1% into wandering. Straight reaches entirely transitioned into channelized with visible bedforms (VB). Notably, one reach in the Devoll River (9), previously dammed up as a lake primarily for irrigation near Korca city in southeast Albania, shifted into a channelized form due to land reclamation, resulting in the drying up of the lake and its conversion into agricultural land.

- *Historical maps, similar study, example Alps, the time covered much longer and in Albanian river short period, but the magnitude of changes has been higher.*

The analysis highlights a prominent trend wherein various morphological classes of rivers tend to shift towards a more constricted/ narrowed channel morphology. This shift is observable in the transformations from braided to wandering morphologies and from wandering to sinuous patterns, as well as from meandering to abandoned states. The majority

of these alterations are concentrated in the transitional regions of rivers, specifically the areas between hill (braided-wandering) and lowland reaches (meander-abandoned). These transitional zones often bear the brunt of human-induced stressors, leading to more pronounced changes in the river's form and behaviour.

Notably, in the mountainous areas, a significant change occurred over time. Single-thread, confined reaches, which were predominant in these regions, evolved into dammed-up configurations post-1960. This transformation was primarily driven by the advantageous suitability of these locations for the construction of hydropower plants aimed at energy generation or dams for water irrigation.

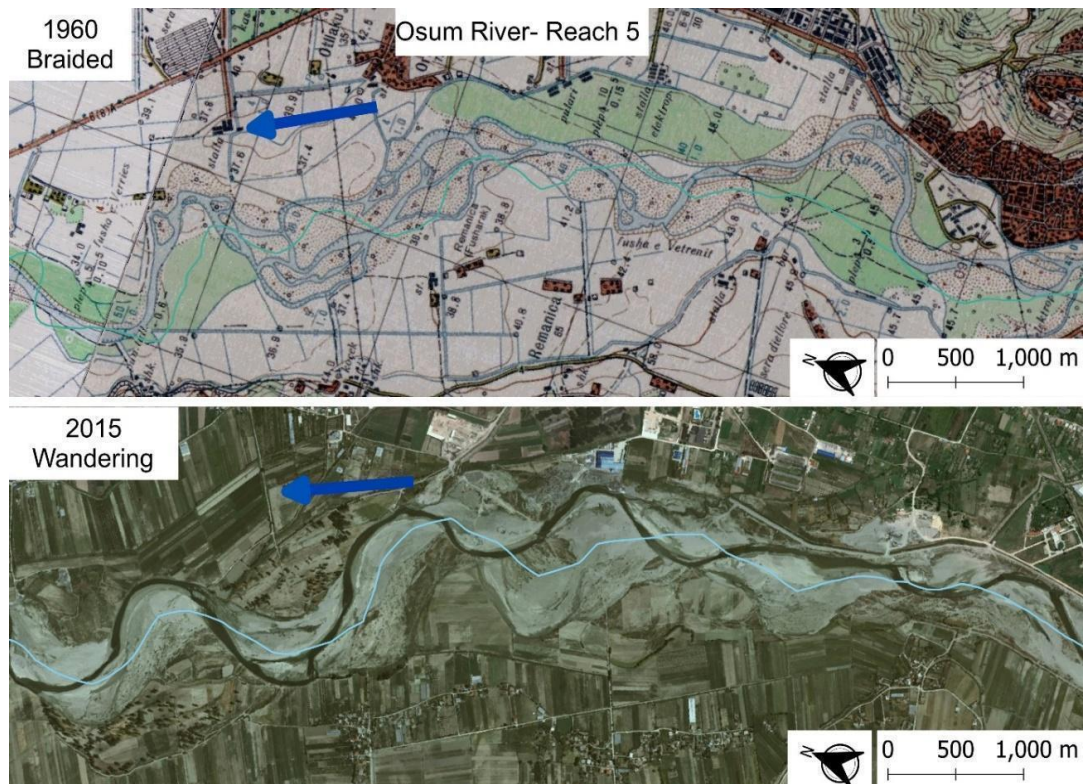


Figure 2. 30. Osum River-Reach 5, changes from braided to wandering morphology

Figure 2.30 provides an illustrative example of one of these changes, from braided to wandering affecting reach no.5 of the Osum river, which is one of the main tributary of the Seman river. Braided reaches, that are reduced by half comparing last 60 years, turned into wandering morphologies for 39% of their initial lengths, which is dominantly located in the hill part of the river. Here, the multi-thread typology (braided and wandering) is predominant among Albanian rivers. According to Piégay et al. (2009) and Hohensinner et al. (2021) braided rivers in the French Alps also reduced in length by 50%, though this was reported to occur in a time frame of more than 150 years, while in Albania the same proportion of change occurred in less than 60 years, i.e., 2.5 times faster. The main reason of the river alps of multichannel transforming to single channel has been the obstruction on the upstream

of the rivers, such are dams and channelization for flood protection. While the analysis of the main driving factors for these rapid changes in Albania is still to be developed, it can be reasonably assumed that the construction of dams, occurring after the 1960s, and the intense sediment extraction in the rivers, occurring after the 1990s, can be two key hydromorphological pressures that contributed to the observed significant changes in the river morphologies. As it will be examined in the next Chapter for the case study of the Erzen river, river narrowing (and very likely, incision) occurred especially in hilly and lowland parts of the river network, with the complete change (“metamorphosis”) in the morphological pattern representing the ultimate variation that happened when the narrowing process became too intense for either local or catchment-scale controls.

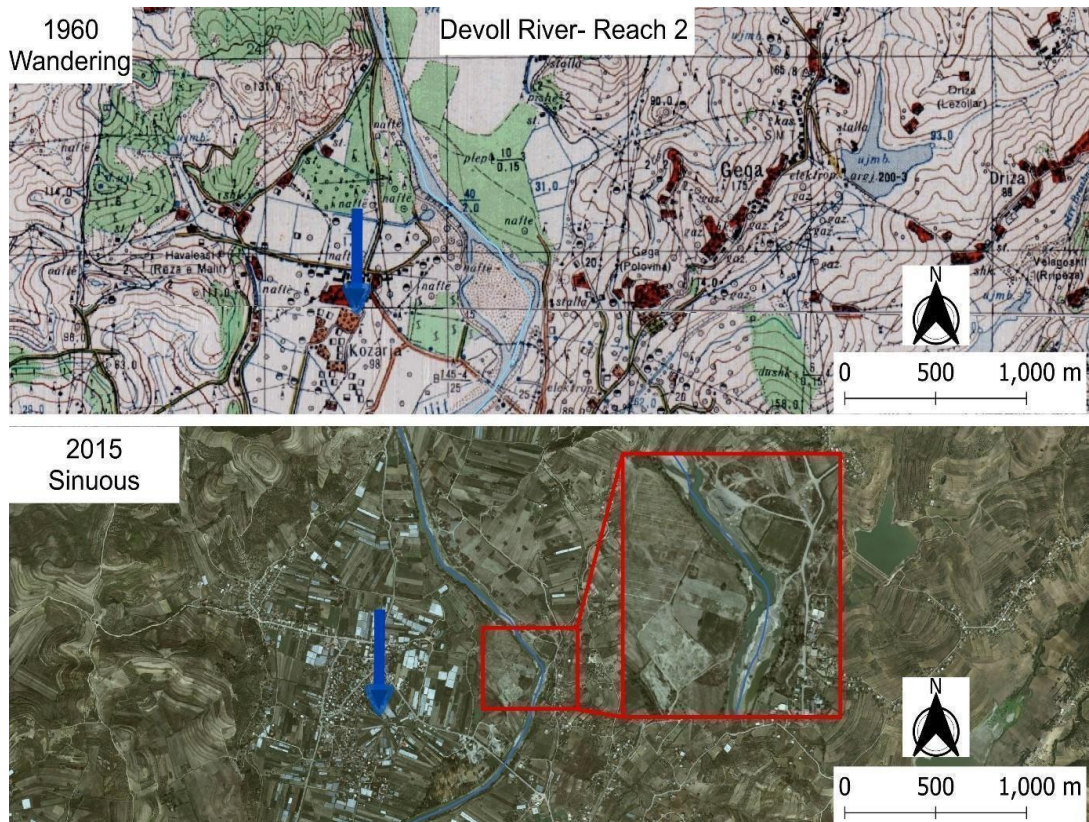


Figure 2. 31. Devoll River-Reach 2, changes from wandering to sinuous morphology

Figure 2.31 shows the transformation of morphology from wandering to sinuous reaches (one of the morphologies that changed the most), particularly in reach no. 2 of the Devoll River, a tributary of the Seman River. Approximately 20% of the wandering reaches shifted to sinuous, with an additional 13% transitioning into sinuous with visible bedforms (VB).

Over a period of five decades, roughly 53 km of river channels in Albania transitioned into abandoned reaches, resulting in lost channels. This trend indicates a significant shift in river resources. Nearly the same length percentage (5%) of rivers in the European Alps (Hohensinner et al., 2021), approximately 510 km of rivers, accounting for 4.3%, were

similarly loss due to channel straightening over a, much longer, 150-year period. In Albania, the abandonment of reaches was primarily caused by channelization, alterations in land cover, artificial river cut-off.

Comparatively, the trends in Albania suggest a more concentrated and rapid change in river morphology over a shorter time frame, with causes more closely related to direct human interventions, in contrast to the longer-term gradual changes observed in the Alpine regions.

Comparative studies with the Alps rivers (Hohensinner et al., 2021) indicate that while 4.3% or 510 km of channels were lost over two centuries in the Alps, approximately 4% or 53 km of the Albanian river channels have been lost in the last six decades, transitioning from meandering to abandoned rivers. Notably, the primary alterations observed between 1960 and 2015 indicate a transformation in the braided and wandering river types, accounting for 59% and 52% of the changes, respectively. The shifts in braided reaches show that 39% transformed into wandering, 10% into sinuous, 5% became dammed up, while 3% developed sinuous alternate bars (AB) and 2% turned channelized. On the other hand, wandering reaches experienced a conversion of 20% into sinuous, 13% into sinuous visible bedforms (VB), 9% into meandering, and 5% into braided morphologies. Additionally, 2% became both channelized and dammed up, while 1% displayed channelized visible bedforms VB.

This highlights a higher tendency for channel narrowing compared to the Alps study, where only 15% of multichannel rivers have shifted to single channels, and in France, approximately 50% of braided rivers have been reduced over two centuries. Comparatively, in Albania, the reduction of braided rivers by the same percentage occurred in almost half a century, highlighting a threefold higher magnitude of changes in morphology. The tendency of the morphology shifting towards channel narrowing is apparent. For example, from braided to wandering, there is a 39% out of 59% transformation of braided; from wandering to sinuous, a 20% out of 52% transformation; and from meandering to abandoned, 20%. This demonstrates a consistent progression towards channel narrowing, with shifts occurring from one morphology to another.

Considering the socioeconomic changes in Albania, such as agricultural and industrialization developments, and how these have been intensified especially after the 1990s, the end of the 1960 might be a good candidate for a reference period against which to examine the recent morphological variations that are a key part of the assessment of the river morphological quality for example within the IDRAIM method used in Italy, for the application of the WFD assessments.. As a reference year to assess the recent river morphological change, the end of the 1960s is a good candidate in the case of Albanian rivers. It combines the availability of data for most rivers in the country, thanks to the Corona images, with being in a period in which major hydromorphological pressures have not started yet to affect the rivers in most catchments. Whether or not this may represent a useful reference against which to assess recent morphological changes has to be assessed through more detailed analysis aimed at reconstructing the historical morphological evolutionary trajectories

This work signifies the primary quantification of the main Albanian rivers in terms of their hydromorphology, bridging a critical knowledge gap for river management. As Albania aspires to EU membership, compliance with various legislation, notably the Water Framework Directive (WFD 2000/60/EC), and the Flood Directive (Directive 2007/60/EC), becomes crucial. These directives mandate the evaluation of water body status and the preparation of a River Basin Management Plan (RBMP) in line with EU standards. Understanding the river morphology and its changes, such as the observed 50% reduction in braided morphology over the past six decades, proves an important information for the Agency Management Basin Authority (AMBU) to develop targeted intervention measures, which shall depend on the channel morphology and cannot prescind from knowing its recent trend. For instance, braided reaches have a higher capacity to accumulate water during flash floods. With the reduction of these braided reaches, the downstream areas become more vulnerable to flooding. Water management agencies (AMBU) should consider this when preparing water management plans and developing flood protection downstream. Similarly, abandoned reaches should be considered when planning future construction, particularly for housing, as there could be an increased risk of flooding and related events in areas that were initially part of active river corridors.

Future research is presently ongoing to finalize the present version of the Albanian Morphological Atlas, to include the very large Drin River in North Albania, with a length of 285 km, a discharge of 352 m³/s, and a basin area of 11,756 km². The Drin is a critical transnational waterway connecting Albania, North Macedonia, and Kosovo. This study primarily focuses on the main stem of the targeted river courses. Subsequent phases will need to encompass the major river tributaries in Albania. This extended analysis promises a deeper understanding of the dynamic river network, offering increased information and insights for comprehensive strategic river basin management. Further analysis of the main tributaries will also provide critical data for understanding the morphological quality of the region's rivers, which is particularly important in the light of the numerous small hydropower plants that are being constructed or planned in the higher order streams in the area.

2.5 Conclusion

This research marks a pioneering attempt to quantitatively assess the morphological evolution of six major Albanian rivers: Mat, Ishem, Eren, Shkumbin, Seman (Devoll and Osum) and Vjosa, covering over 1300 km of river length and focusing on two periods: the 1960s and 2015. This has been obtained by applying the IDRAIM methodological framework that is commonly used for Italian rivers and is perfectly aligned with the Water Framework Directive, it facilitates a comprehensive evaluation of Albanian river morphology.

The findings of this study provide a country-scale picture of the Albanian rivers' hydromorphology in two different periods. An historical time, approximately corresponding to the 1960s, and the present time, set at 2015. The total length of the examined rivers, spanning nearly 1300 km, offers a comprehensive overview of the hydromorphological

landscape that was not available so far. All catchments with area exceeding 650 km² have been examined.

River channel patterns are dominated by of single thread 22% (276 km) and sinuous 17% (221 km) river morphologies, particularly in mountain and hill physiographic units. Meandering reaches, covering 190 km, are predominantly located in lowland areas within plain physiographic units. Wandering reaches exhibit a diverse distribution, with 51% (92 km) in hill regions, 28 % (50 km) in lowland, and 21% (37 km) in mountainous areas. The presence of braided reaches is most significant in hill physiographic units 38% (33km), followed by lowland 35% (31km) and mountainous areas 27% (24km).

Relevant changes over the 60 years studied period are evident, with the length of the initially braided and wandering reaches subject to changes of 59% and 52%, respectively, highlighting significant changes in river morphology. A discernible trend towards channel narrowing emerges, highlighted by a 39% shift from braided to wandering and a 10% transformation from braided to sinuous reaches. The study also draws attention to the direct man-made changes in the river morphology that occurred in the last 60 years. Approximately 53 km of river channels underwent swift transitions into abandoned reaches over five decades due to channelization, changes in land cover, and natural river cut-offs.

Thanks to the diachronic analysis that clarifies the main morphological modifications occurring in the target rivers between the late 1960s and 2015, the outcomes of this work also provide some support to the historical period that could be used as a reference to assess recent morphological changes, as required in many indicators of morphological quality (e.g. Rinaldi et al., 2016) for the assessments of hydro-morphological quality elements sensu the EU Water Framework Directive.

Chapter 3

3 Intense channel modifications in the Erzen River following rapid socio-economic changes: reconstructing channel incision and narrowing in a data-scarce context.

Abstract

Channel adjustments that occurred on the Erzen River in the last 60 years have been investigated. The Erzen passes nearby the two major urban centres in Albania of Tirana and Durrës, is 109 km long, drains a catchment area of 760 km² and it flows approximately westwards towards its mouth in the Adriatic Sea, near the Lalzi Bay. We have analysed both channel incision and channel narrowing occurring mainly in the lower part of the river by using remote sensing, historical image analyses, DEM and survey in the field. Major hydromorphological pressures potentially affecting the flow and sediment supply regime have been also analysed. Specifically, sediment mining has been reconstructed by identifying the mining sites in contact with the active river corridor between 1990-2015 along 42 km river length from aerial images, and from technical reports providing estimation of sand and gravel removed from the river.

Findings indicate two phases of adjustments, a slower phase until the 1990s, followed by a faster phase. Especially in this second phase, changes of channel morphology, have been quite rapid. Channel narrowing between 20% and up to 75% affected the transitional and meandering reaches between 1968-2015 and high riverbed incision at the reach scale have been indirectly estimated up to 5-6 m, which is also revealed by visual signs like increasing bed rock and bridge foundations exposure. Two cut-offs have been artificially created in the meandering reaches of the river. Most of the main bridges in Albanian rivers have shown exposed foundations with 3-4 m on the last 15-20 years, where some of them are replaced by other bridges due to unstable structure condition. Compared with previous studies, narrowing and incision rates are among the highest observed in Europe after the 1950s, particularly if focusing on the second adjustment phase. While on the upstream segment of the river two dams have been built, sediment mining appears as the main driving factors of the observed channel narrowing and incision. Twenty-two mining sites have been detected between 1995-2015 and 457,380 m³/year of sediments have been reported as withdrawn from the riverbed. The rapid channel incision may have also contributed to the increasing salty water intrusion and subsequent freshwater shortage in lowland part of the river. The observed narrowing and incision have likely played a key role also in the reduction of river sediment supply to the sea, which probably explains most of the very rapid coastal erosion that has been observed in the same period in the Lalzi Bay (De Leo et.al, 2019).

3.1 Introduction

Rivers are complex and dynamic systems that are critical for the ecological, social, and economic well-being of communities worldwide (Vörösmarty et al., 2010). However, human pressures such as damming, channelization, mining, and urbanization have significantly altered the morphology and hydrology of many rivers, leading to a decline in their ecological and socio-economic services (Nilsson et al., 2005). While many studies have focused on the impacts of human activities on rivers in Western Europe, North America, and other high-income countries (Poff et al., 1997) there are limited information on the historical transformations of rivers in the Balkan area. This lack of systematic information on river hydro-morphological dynamics in the region limits the development of sustainable river management strategies in this area, which is undergoing rapid environmental transformations.

Human activities have impacted rivers for centuries, even spanning thousands of years (Petts et al., 1989; Downs and Gregory, 2004; Hooke, 2006; Comiti, 2012; Brown et al., 2018; Comiti and Scorpio, 2019). Fluvial changes have been investigated deeply in Europe, mostly in France, Italy, Spain and Poland (Surian, 2022). The majority of studies focused on key aspects such as the types and magnitudes of changes, the causes behind these changes (e.g., human activities in catchment areas and along river reaches, as well as climate changes), and the practical implications of geomorphic transformations in terms of human safety, environmental quality and river management. Understanding and quantifying the processes of channel adjustments, such as channel narrowing and incision, and to detect the main driving factors such as channelization, sediment mining, dams, land use change, climate changes (Surian, 2022) is an important prerequisite when aiming to predict the present morphological trends of the rivers and to hypothesize likely future river patterns, a key information for river managers to make informed decisions. Understanding the relation between the intensity (magnitude) of morphological changes associated to channel adjustment and the magnitude, temporal and spatial extent of occurrence of the possible driving factors is a main open issue, and still it has proven often unfeasible to isolate the role of each individual change driver on specific channel adjustment processes, because multiple human stressors often overlap in the same river catchment.

The temporal variability of biophysical river parameters that can be used to describe the historical channel adjustment is commonly referred to as river “evolutionary trajectories” (Fryirs and Brierley, 2016). To reconstruct meaningful portions of these trajectories it is crucial to get the longest time available evidence of representative parameters of the river morphology, such as, for instance, the mean reach-scale bed elevation, active corridor width, percentage riparian vegetation cover of the active corridor. As clearly explained in Surian (2022), analysis of river trajectories encompassing very short temporal scales (e.g., a few years or a decade) can lead to inaccurate interpretations of fluvial changes. Rivers that seem stable over a brief period may exhibit significant instability over a longer time span (e.g., 40-50 years). Analysing long-term trends provides a more accurate understanding of river behaviour and morphological transformations, helping to assess their dynamic nature and

responses to different forces and disturbances over time (Ziliani and Surian, 2012; Arnaud et al., 2019).

Only a few studies have reported about multi-decadal scale modifications in the channel morphology of Eastern European rivers. Despite the growing attention on rivers in the Balkan area (see Introductory Chapter of this thesis), studies providing relevant hydro-morphological information are still very limited (Bizzi et al., 2021; Hauer et al., 2021; Pessenlehner et al., 2022), and almost no systematic investigation refer to their morphological evolutionary trajectory. This limited research can be attributed to a combination of different factors the region's social-political situation, transitional economy, lack of knowledge in this area, and insufficient structural data for reconstructing the behaviour of river systems. The occurrence of such modification in many of these river systems in the Balkan area is evident, but quantitative information on their occurrence, and main characteristics are mostly lacking so far. As a result, our understanding of fluvial changes in the Balkans remains relatively limited. There is a need for more comprehensive and focused research efforts to address these gaps and gain insights into the dynamics of river morphology in the region. Improving data availability and overcoming the challenges posed by the social and economic context will be crucial in advancing our knowledge of Balkan rivers, thus to support their sustainable management for harmonizing environmental protection with hydraulic safety and flood hazard mitigation.

A specific gap in historical information refers especially to data on the river topography and on the river sediment size. Such information were collected also systematically by the former Hydrometeorology Institute of Albania but their availability at present is often scattered and uncertain. This limits our possibilities to reconstruct the evolutionary trajectories of these river systems, particularly in relation to the vertical channel adjustments, riverbed degradation / incision or aggradation.

The specific goal of the work presented in this chapter is to quantify the characteristics of the channel adjustments occurring in the lowland reaches of a representative river system in the western Balkan area in terms of timescales, magnitude, possible drivers, and to relate it to analogous processes that have been documented in westernized countries, to understand similarities and differences among contexts characterized by different phases of development.

To this aim, we investigate the multi-decadal channel adjustments of the Mediterranean Erzen River in Albania, which originates at 1200 m asl from the Gropa mountain, and flows westwards towards the Adriatic Sea near Lalzi Bay with a total length of 109 km. Using a combination of aerial and satellite images, digital elevation models, targeted topographic surveys and collection of historical data sources, we analyse changes in the river morphology that occurred from 1950 onwards, with reference to the IDRAIM hydromorphological approach (Rinaldi et al., 2015). Findings reveal rapid trajectories of change, with channel narrowing, incision, and artificial meander cut-offs occurring in the lowland meandering reaches. The intense human pressures, including sediment mining, dam construction, deforestation, and urbanization after 1990, have played a critical role in affecting the

multidecadal river dynamics, posing significant challenges for the future management of the Erzen River.

3.2 Study Area

The study area is the Erzen River basin in Albania (Figure 3.1), which covers an area of approximately 760 km² and is located in the central part of the country. The river originates in the western slopes of the Gropa Mountain, at an altitude of 1200 m above sea level, and flows westwards towards the Adriatic Sea, passing through the lowland transitional and meandering reaches before entering Lalzi Bay. The main river length of around 110 km and an average elevation of the riverbed at about 440 m above sea level.

Conventionally, the Erzen River is usually classified together with the Ishëm River in the same basin, which is one of the six main river basins in Albania (Albanian Hydrometeorology Institute, 1979). The average gradient of the riverbed elevation is about 0.6%, while the average gradient of the valley side slopes is around 2.6% (Albanian Hydrometeorology Institute, 1979). In the upper part of the Erzen River, it exhibits the characteristics of a steep, confined mountain river with a high energy. The surface riverbed sediment composition is characterized by large rock boulders up to 1 m linear size and more. Downstream the confluence with the first mountainous tributary (river Qafe Molle), the riverbed is characterized by a typical downstream fining with sediment diameter reducing to 20-30 cm. In the narrowed, confined reach of the Skorana gorge, the river sediments have mean diameters of 60-10 cm, and alluvial deposits become evident. Downstream the narrowing of the Skorana gorge, the river passes through hilly and flat areas until it reaches the sea, showing the gravel-sand transition nearly 43 km of river length upstream its mouth to the sea (Albanian Ministry of Agriculture and food, Institute of Land Studies, 2004).

The flow regime of the Erzen is typical of a Mediterranean river, characterized by a highly variable flow with maximum discharge in winter and minimum in summer. As a general feature, the mean annual discharge of the lower part of the Erzen River is around 15-20 m³/s, corresponding to a specific discharge of about 20 l/s/km². The maximum recorded daily discharge was about 960 m³/s at Ndroq (1966) and 1100 m³/s at Sallmonaj (1966), while the minimum can be lower than 1 m³/s (Albanian Hydrometeorology Institute, 1979). The water of the Erzen River has low mineralization, of the bicarbonate-calcium type, with an overall average mineralization of around 300-350 mg/l.

Climate characterisation

The Erzen River Basin, despite its small size, is situated in different climatic zones due to its elongated shape, extending from east to west. The evident climatic zones in this region are: the sub-Mediterranean lowlands (from the river's source to the Mullet area), the hilly Mediterranean climate (which extends to the Killojka area), and the pre-mountainous Mediterranean climate (stretching from Killojka to the Erzen's source in the Shëngjergji area).

The average climatic parameters for the different physiographic regions are relatively comparable to the main annual temperature and precipitation values, with small variations in magnitude. As a general feature, the main annual temperatures and precipitation values in the coastal, hilly, and mountainous areas are, respectively, 16°C with 1000 mm, 14°C with 1500 mm, and 12-13°C with 2000-2500 mm of precipitation. The minimum and maximum values of precipitation are, respectively, around 640 mm and 1540 mm for the coastal area, around 850 mm and 1670 mm for the hilly area, and around 970 mm and 3500 mm for the mountainous area (Albanian Agency of Water Resources Management, 2022).

River Discharge and Sediment Transport

There are three main hydrometric gauging stations in the Erzen river catchment. moving from the headwaters to the sea, the historical stations of Ibe, Ndroq and Sallmone can be found. They respectively cover a basin area of 247 km², 663 km² and 755 km². The average discharge on these stations are 8.6 m³/s (Ibe, 1972-1990), 14.5 m³/s (Ndroq, 1952-1990) and 18 m³/s (Sallmone, 1949-1992)

The measurements of sediment transport reported from Institute of Geoscience Albania (1950-1975), suspended sediment transport rate for Ndroq station is 68.4 kg/s and Sallmone 101 kg/s, while the turbidity 4270 gr/m³ in Ndroq and 5610 gr/ m³ in Sallamonaj.

Study area focus

The study is focused on 5 reaches along the main stem of the Erzen river, which have been named R2, R5, R8 ,R11 ,R13, R17 in the country scale morphological analysis presented in Chapter 1, using the methodological IDRAIM framework (Rinaldi, et.al 2015). Out of the selected five reaches (Table 1), four are located in the lowland part, and one in the mountain part of the river catchment (Figure 3.1)

Following the IDRAIM multi-scale hierarchical framework (Rinaldi et al. 2015) the Erzen River system has been segmented at the reach scale using the 2015 ASIG National Orthophoto (Fig. 3.1). The three main Physiographic Units (Mountain, Hill, Lowland) have been defined, and the river floodplain delineated; the main stem of the Erzen river has finally been partitioned into seven hydro homogeneous river segments (see Chapter 1 for more details). Furthermore, confinement index and confinement degree were evaluated according to Rinaldi et al. (2015). This analysis resulted in the subdivision of the Erzen River into hydro-morphologically homogeneous reaches, from which the 5 target reaches listed above were selected.

Several criteria were used to select the target reaches. First, at least one representative reach for each dominant morphological pattern in the entire catchment has been selected. The choice was also restricted to lowland, mainly unconfined reaches where more intense modifications caused by anthropic stressors are more likely to be reflected in decadal scale channel adjustments. One of the reaches is found in the confined segments, upstream of a main dam, to have the possibility to analyse the morphological changes occurring not only in the lowland part of the catchment, but also to get information on possible adjustments

occurring in the mountain upstream reaches subject to much less anthropic effects. This could offer the possibility to better highlight the role of climatic variability with respect to direct human effects. Furthermore, because of the resolution of the used image sources, only reaches having an active channel width largely exceeding 30 m could be considered for the classification of river corridor macro-morphological units (water, bare sediments, vegetation) from Landsat images. Only one reach (R2, Table 3.1) had a lower average active channel width compared to the Landsat image resolution (25x25 m) and it was therefore analysed using a higher resolution orthophoto 2015 (20 cm resolution orthoimage from ASIG, Albanian Geoportal), the Corona satellite images and old military maps (1950-1985), as reported in section 3.3.2 in more detail.

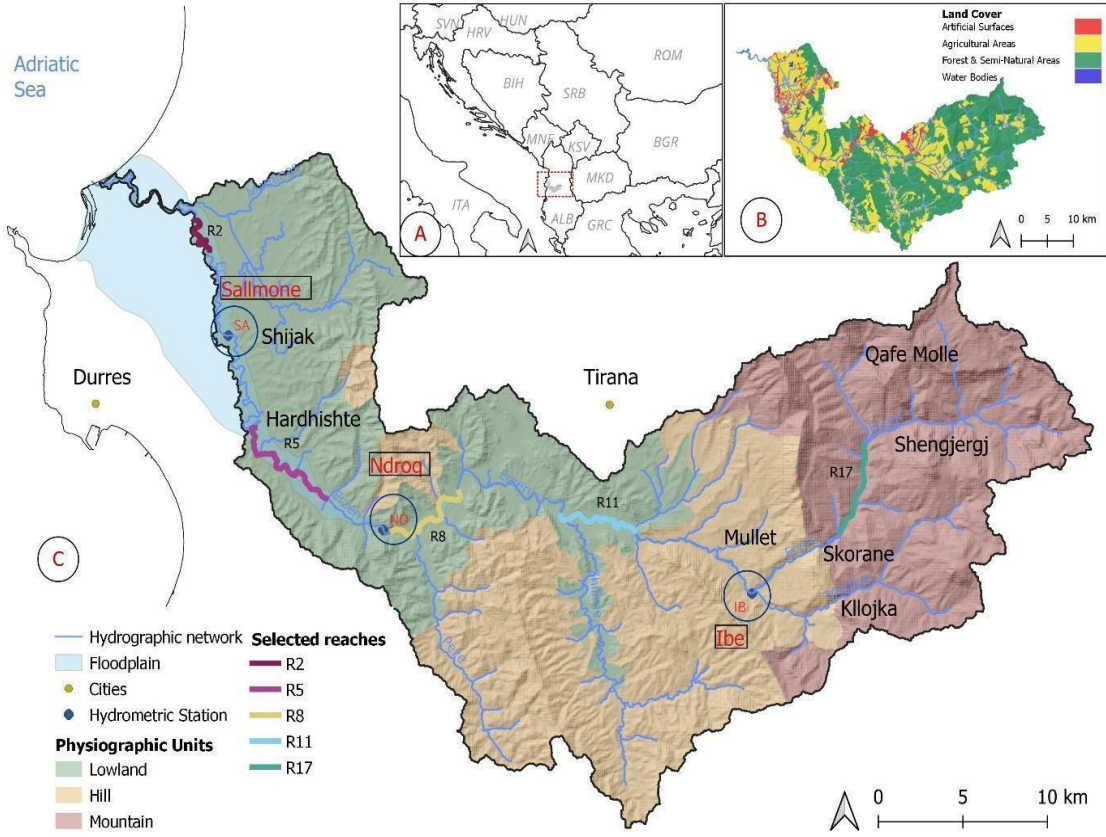


Figure 3. 1. Erzen River catchment area

Reach Number	Physiographic Unit	Confinement	Confinement Index	Distance from the sea (km)	L (km)	Reach average elevation (m asl)	SI (2015)	Morphology (2015)	Slope m/km	Floodplain width (m)	Active Channel width (m)
2	Lowland	UN	427.2	10.1	3.18	0.7	1.6 9	Meander	1.4	7528	18
5	Lowland	UN	43.78	31.1	8.07	11.7	1.4 0	Sinuuous	1	1325	42
8	Lowland	PC	8.07	41.6	6.57	28.1	1.4 7	Sinuuous	2.3	327	47
11	Lowland	PC	4.17	54.9	5.77	75.6	1.3 0	Sinuuous	4.8	246	67
17	Mountain	C	1.4	81.7	5.45	304.1	1.0 8	Braided	14. 7	245	160

Table 3. 1. Main morphological properties of the selected reaches for the analysis. Confinement: UC- Unconfined, PC – Partially Confined, C- Confined, CI- Confinement Index; L- reach Length (km); Reach average elevation taken from DEM 10 m ASIG Albania; SI- Sinuosity index, Floodplain W- Floodplain average width in (m) are old terraces of the river created during the years, Active channel W- average width in m is the river corridor including water, gavel and sometimes vegetation.

Geological characterisation

The Erzen River originates in the Shëngjergj Mountains, to the west of the carbonate rocks of Mali me Gropa. It cuts through the Cretaceous carbonate rocks of the Krastë zone, east of Qafë Molla and Derja. Then, it flows through the Paleogene fluvial deposits of the Qafë Molla, Darshen, and Killojka regions, and further to the west, it enters the Paleogene and Cretaceous limestone rocks of the Dajti mountain range, passing through the Skorana and Pëllumbas gorges, which are characterized by incredibly beautiful canyons (Kamza Municipality, 2020).

To the northwest of Pëllumbas, the Erzen River interrupts the Neogene terrigenous deposits, mainly alluvial, and passes through the Ibë, Mullet, Stërmas, Arbanë, Ndroq, and Varri i Ashikut areas. In this stretch, the river widens its bed, depositing large amounts of riverine sediments, while along its banks, there are thick terraces with inert materials (Kamza Municipality, 2020).

In the area below Hardhishtë, the Erzen River enters and meanders through the Quaternary deluvial-alluvial deposits of the Shijak, Sukth, Katundi i Ri, and Rrushkull fields, until it finally discharges into the Adriatic Sea in the Bay of Lalzi.

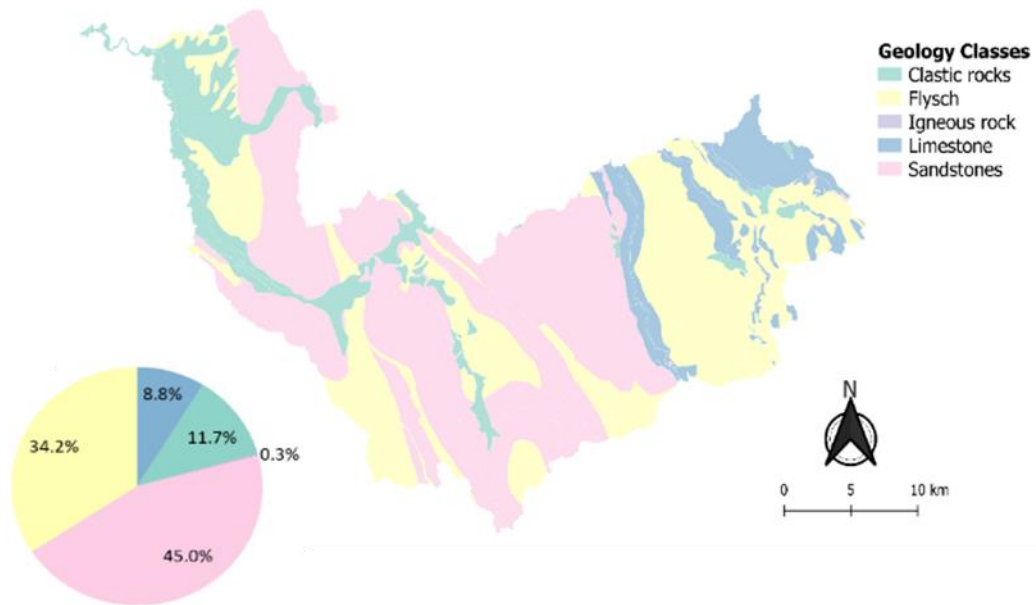


Figure 3. 2. Geological map of Erzen basin according to the reclassified six classes described in Chapter 2

The geological characterization of the Erzen River basin presents a diverse landscape that exerts significant influence on its hydrological and geomorphic features. The dominant presence of sandstone, accounting for 45% of the geological composition, suggests the prevalence of a sturdy and porous rock type that can substantially affect sediment transport and water infiltration processes. The substantial representation of flysch, comprising 34.2%, underscores the intricate arrangement of alternating sedimentary layers, potentially influencing erosion patterns and sediment supply dynamics. Limestone, constituting 8.8% of the basin, holds implications for the formation of karst topography and interactions between surface water and groundwater systems. The 11.7% of clastic rock points to a varied range of fragmentary rock types that can significantly impact sediment behaviour and transport. The limited presence of igneous rock, at 0.3%, implies a minor contribution to sediment load and distinctive lithological characteristics.

3.3 Material and methods

3.3.1 Automated Landsat image analysis (1985-2020)

In this work, Google Earth Engine (GEE) was used to extract information on river planform morphodynamics from multi-temporal, multi-spectral, satellite imagery, namely Landsat Surface Reflectance products (Landsat 5 Thematic Mapper, Landsat 7 Enhanced Thematic Mapper, and Landsat 8 Operational Land Imager), having spatial resolution of 30 m. The method was used on the four wide enough reaches (R5, R8, R11, R17 (Table 3.1), while

reach channel adjustments of reach R2 was analysed using different sources because of its small active channel area in recent years.

The implemented morphological assessment procedure used a combination of the normalized difference vegetation index (NDVI) and of the modified normalized difference water index (MNDWI) (Xu, 2006) to extract the active channel and the vegetation cover. Figure 3.3 reports the detailed workflow of the procedure developed by Crivellaro et al. (2023). The active channel is here defined as the region of the domain showing recent hydromorphological activity, i.e., the area that includes bar sediments and low flow channels, following the definitions used in previous work (Crivellaro et al., 2023, Henshaw et al., 2013, Monegaglia et al., 2018, Spada et al., 2018, Boothroyd et al., 2021, Harezlak et al., 2020).

A time resolution of 5 years has been chosen to assess the reach-scale evolutionary trajectories, requiring the use of a total of eight Landsat observation scenes from 1985 to 2020. Per each observation, the collection of all available Landsat images in the year of observation is considered. Then, per each image of the collection, the NDVI and MNDWI maps are computed. From these, a synthetic image, representative of each year of observation, was computed, applying a median reducer to aggregate all spatially overlapping non-cloud pixels, as proposed by Boothroyd et al. (2021)a. The synthetic image was calculated at pixel scale, with the median value of all the input images at that location, calculated independently for NDVI and MNDWI maps. Thus, the annual active channel (ACy) was mapped with relational operators applied to the two synthetic images. Specifically, $MNDWI \geq -0.35$ (Boothroyd et al, 2020) and $NDVI < 0.15$ (Bertoldi et al., 2011) were the conditions for active channel masking. The domain envelope mask (EM mask) for each reach was then defined as the envelope computed from the eight yearly ACy. After envelope computing, a noise manual removal was done, using expert judgment to refine the domain.

To properly map the dynamics of the riparian vegetation excluding seasonal fluctuations, we limited the image collection of each year to the vegetation growing season (May to October), and we extracted and analysed active channel changes considering the growing season derived data as the reference for planform dynamics. Analogously to the annual active channel computation, a synthetic median image for both NDVI and MNDWI were produced. Inside the domain envelope (EM mask), pixels were classified as active channel (AC) when $NDVI < 0.15$, vegetation (VEG) otherwise. Within the computed domain, we investigated the planform changes of selected reaches.

The EM mask per each river reach, along with the seasonal AC and VEG maps were exported from Google Earth Engine and processed through the GRASS GIS software. A single reference reach centerline was extracted from the domain envelope (v.voronoi) and used to generate transects (v.transects) at 200 m intervals (as in Jézéquel et al., 2022).

To assess the accuracy of the semi-automatic method, its outputs have been compared with active channel extracted manually from orthophotos in two different years, like 2015 in which both a high-resolution orthophoto (geoportal Albania, or Google Earth) and the active

channel extracted from the Landsat at the same reference year were available. Since Landsat resolution is 30 m, the range of applicability of the *active_width* extraction should prefer “large” rivers, for which an acceptable error could be achieved (Monegaglia et al., 2018). In the Erzen case study, the average river corridor width of selected reaches goes from 220 m (R8, 7 times pixel resolution) to 150 m (R5, 5 times pixel resolution), referring to image collection 1985 Landsat. Considering this, a misclassification from 3 to 20% is the expected error range. This was compared with manual digitalisation of different time series starting from the Corona satellite images dating about 1968 till the 2015 orthophoto with 20 cm resolution (Albanian Geportal). The detail workflow is described below.

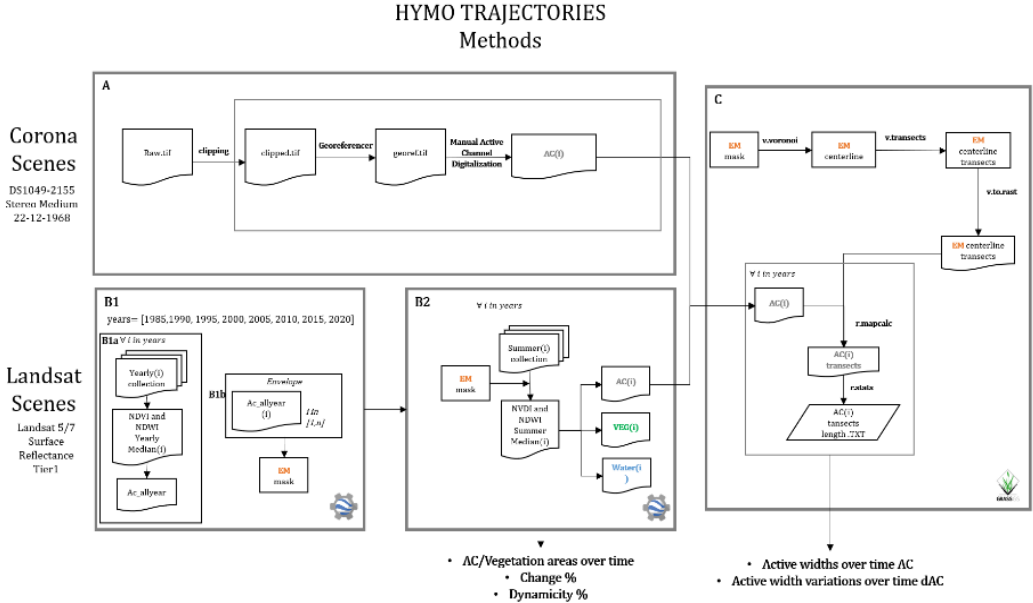


Figure 3. 3. Semi-automatic method to study extract of the hydromorphological evolutionary trajectories of a reach (reproduced from Crivellaro et al., 2023).

Workflow procedure

Identification of the computation domain: For each analyzed year, the entire collection of available images was considered. After initially creating a cloud mask (only for Landsat 7 and 8) for each image, NDVI and MNDWI maps were generated from these images. From these maps, a representative image of the active channel was computed for each year of observation. This was achieved by applying a median reducer to aggregate all pixels identified as “non-cloud” [Crivellaro et al., 2022], as determined previously by the cloud mask. This process resulted in one image per year, spanning from 1985 to 2021. The representative image for each observed year was obtained by calculating the median value of NDVI and MNDWI for each overlapping pixel from the available images. To create the mask of the active channel, threshold values of NDVI and MNDWI from the literature (Table 2) Boothroyd et al., 2021 were used.

NDVI	MNDWI
<0.15	>-0.35

Table 3. 2. Threshold values of NDVI and MNDWI used for determining the computation domain.

The NDVI (Normalized Difference Vegetation Index) is an index that has been correlated to the presence of vegetation on land and it is calculated as the ratio of the difference to the sum of the near-infrared and red radiation reflected by plants, specifically at wavelengths around 2.4 micrometers.

$$NDVI = \frac{NIR-RED}{NIR+RED} \quad (1)$$

The index ranges from -1 to 1, where a negative value represents bare soil or clouds, and a positive value close to 1 indicates vegetation cover with very high and dense vegetation (Table 3.2).

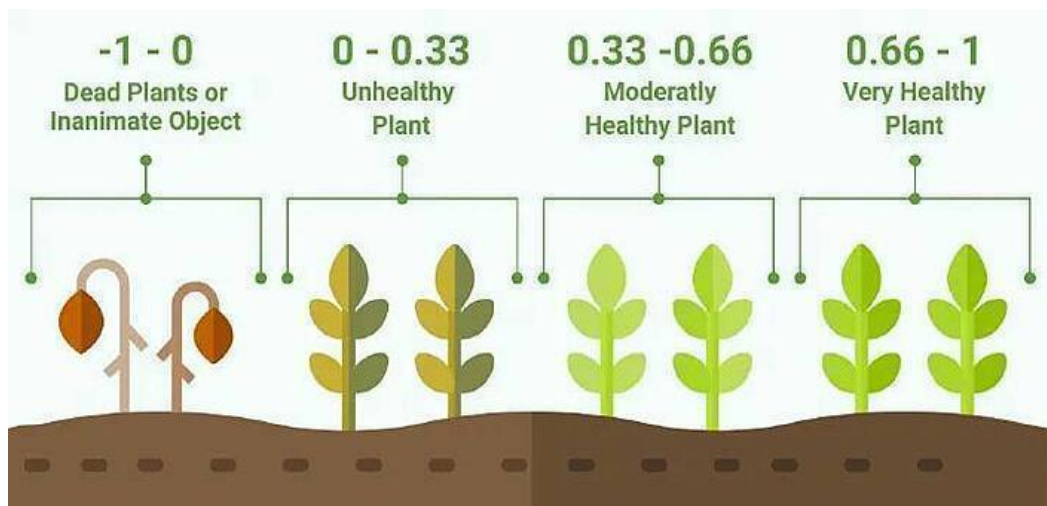


Figure 3. 4. Visualization of the correspondence between the normalized difference vegetation index NDVI and the likely presence and type of vegetation. (source: <https://eos.com/blog/ndvi-faq-all-you-need-to-know-about-ndvi/>)

The MNDWI (Modified Normalized Difference Water Index) utilizes the green and shortwave infrared (SWIR) bands to map water bodies. Negative values in MNDWI represent the absence of water, while positive values indicate the presence of water.

$$MNDVI = \frac{GREEN-SWIR}{GREEN+SWIR} \quad (2)$$

The masks of annual active channels were subsequently aggregated using an enveloping algorithm, enabling the automatic generation of the preliminary investigation domain. Subsequently, through expert judgment, the preliminary investigation domain was refined and improved in the GIS environment, resulting in a more compact mask (figure 3.5).

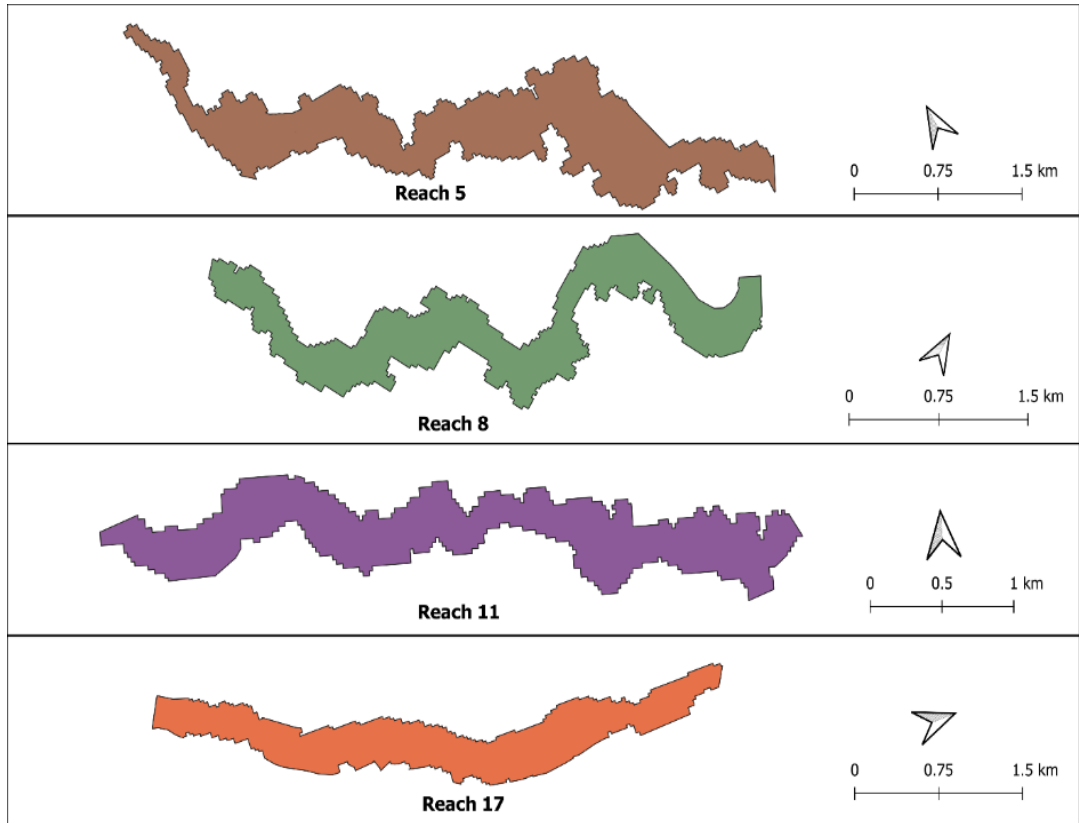


Figure 3. 5. Envelope of active channel extracted for the selected reaches.

Using the obtained computation envelope (figure 3.5) masks were created for four classes: water, sparse vegetation, dense vegetation, and the active channel. The analyzed period for each year ranged from May to September, covering the vegetative season to capture vegetation accurately. Literature-based NDVI and MNDWI thresholds values were used for the classification. For the collection of images acquired between May and September, a median operation was performed on overlapping pixels, resulting in binary maps, with each pixel attaining values of 0 or 1, thus yielding a representative classified image for each year (figure 3.6).

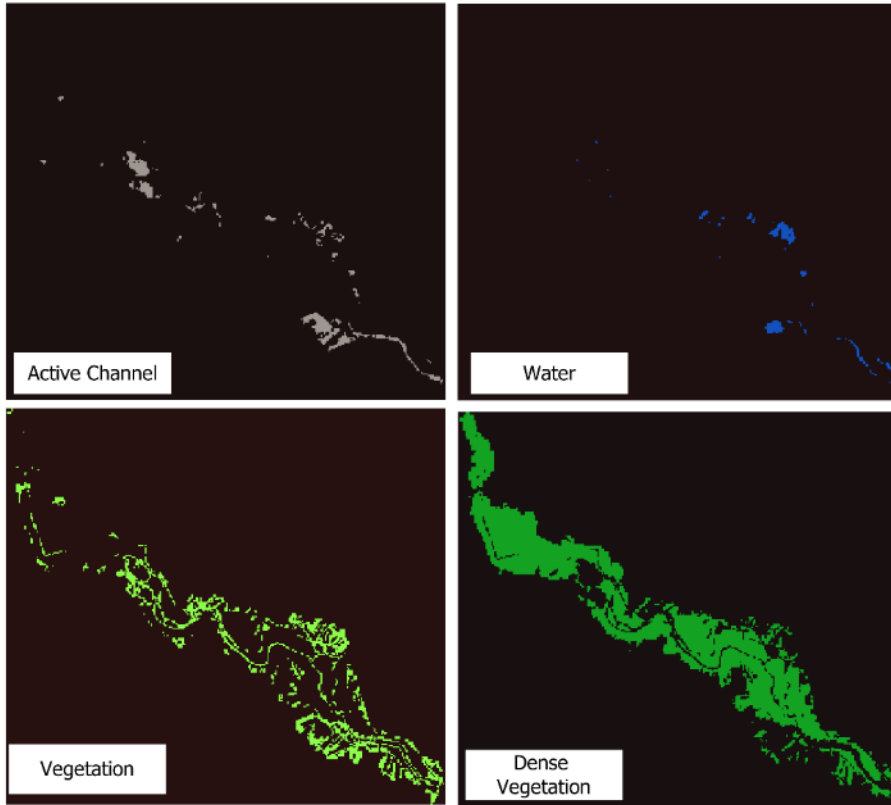


Figure 3. 6. Classification in four classes on reach 5, referring to year 2020.

To obtain an overall view of the classification, the four maps were merged using the expression (3) and then the output was reclassified by assigning values from 1 to 4 to the pixels, where 1 indicated water, 2 indicated gravel, 3 indicated sparse vegetation, and 4 indicated dense vegetation.

$$Class = 10 \times RW + 2 \times RAC + 3 \times RVS + 4 \times RVD \quad (3)$$

Where:

- 3.3.2 RW = Water mask raster;
- 3.3.2 RAC = Active channel mask raster;
- 3.3.2 RVS = Sparse vegetation mask raster;
- 3.3.2 RVD = Dense vegetation mask raster.

Classes	Pixel Value after Reclassification	Pixel Value Merged
Water	1	value >-10

Gravel	2	5-< value <10
Vegetation	3	3
Dense Vegetation	4	4

Table 3. 3. Pixel values after reclassification with their respective classes and pixel values before reclassification after merging the masks using the expression (3)

To address the considerable volume of maps generated, one map was produced for each year within selected reaches. To facilitate visualization, the decision was made to focus on maps created at intervals of every 5 years from 1985 to 2020. The process of merging and reclassifying these maps was automated using the *rasterio* package in Python for Landsat images (refer to Figure 3.6). Following the merging and reclassification, distinct maps were obtained for each year, and this procedure was executed for each analyzed reach. Subsequently, the areas corresponding to each class (four classes each year) were computed, allowing for the assessment of their temporal trends.

The evolution of the river channel width over time was calculated considering the classified active channel every 5 years, from 1985 to 2020. The width of the active river channel was computed as an average of the widths of several transects that were delineated at a spacing of 200 m. The spacing was decided based on the transects length not to overlap with each other in the meandering sections, based on the reaches length, so to obtain an accurate representation of the channel width. Such spacing was kept constant for all the analysed reaches. The chosen spacing of 200m has been selected after several trials in which the analysis was run for spacing of transects of 100 m, 200 m and 300 m, with 200m optimally performing for the Erzen river case study. To obtain these transects, the envelope of the active channel was converted to vector format to derive a channel centerline using the "v.voronoi" command in GRASS. From the centerline, transects were then generated using the "v.transects" command (Figure: 3.7a) and subsequently converted to raster format.

The decision was made to use the same centerline to ensure precise overlap of the transects across different years, allowing for local variations in width. The transects were then adjusted to the width of the river channel using the GRASS "r.mapcalc" command, where the expression "=if(raster active channel, raster transects)" was used. This expression returns the pixels of the transect that are inside the active channel raster (Figure: 3.7c).

To obtain the transect width in meters, the pixels for each transect were counted using the "r.stats" command and then multiplied by the resolution of the raster. This process allowed for the analysis of the river channel width changes over the specified years.

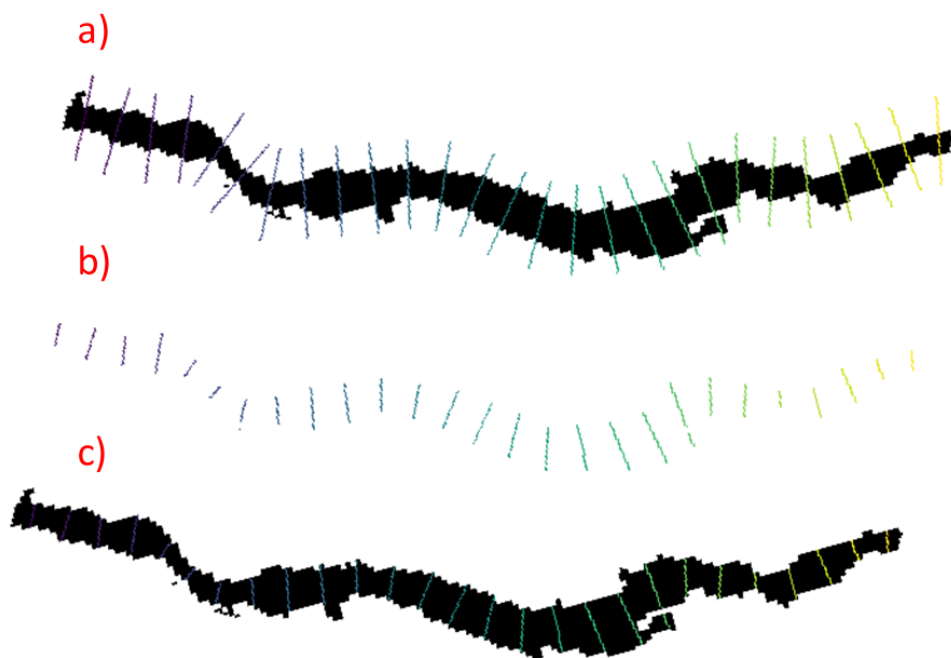


Figure 3. 7. Transects generated by mask for active channel (reach 17, 1985 Landsat). (a) transects generated with a spacing of 200m along the river centerline. (b) transects with length determined after the `r.mapcalc` command has been applied, which cuts the transects cut based on the active channel mask. (c) transect are inside the active channel and ready to export and calculated the average length. This is done for every 5 years of active channel.

For reach 2 Landsat images could not be used because the active channel is smaller than the pixel resolution. Active channel was manually digitized using the available higher-resolution images from Geoportal Albania. These images referred to years 1985, 1994, 1999, 2007 and 2015; the available Google satellite image of 2022 was also used. The same procedure described above is used to evaluate the reach trajectory for all reaches analysed, listed in table 3.1. and a comparison between manual digitalisation and semi-automated method using Landsat is carried out.

Mann-Kendell trend test

Once the evolutionary trajectories in terms of the four main classes were obtained for every reach, a trend analysis was applied to the extracted trajectories to assess whether the observed trends were statistically significant for every reach.

The likelihood of the observed outcome occurring randomly can be evaluated through the application of the Mann-Kendall trend test. A p-value derived from this test below 0.05 indicates statistical significance, while a p-value exceeding 0.05 suggests a lack of

significance. This assessment helps the validity of the observed trends and their potential implications within the given context.

Value of P	Inference
$P > 0.10$	No evidence against the null hypothesis
$0.05 < P < 0.10$	Weak evidence against the null hypothesis
$0.01 < P < 0.05$	Moderate evidence against the null hypothesis
$0.05 < P < 0.001$	Good evidence against null hypothesis
$0.001 < P < 0.01$	Strong evidence against the null hypothesis
$P < 0.001$	Very strong evidence against the null hypothesis

Table 3. 4. Mann-Kendell trend test P Value range

3.3.2 Analysis of Corona Satellite images (1968)

The Corona program was a series of American strategic reconnaissance satellites produced and operated by the Central Intelligence Agency Directorate of Science and Technology with substantial assistance from the U.S. Air Force. The Corona satellites were used for photographic surveillance of the Soviet Union (USSR), the People’s Republic of China, and other areas beginning in June 1959 and ending in May 1972. Photos were collected with a system of twin cameras called KH-4A (KeyHole), which allows the acquisition of images in stereoscopic format. The frames have a high ground coverage, about 17x232 km, and a 2.75m spatial resolution (Spada et al., 2018).

Two medium resolution grayscale Corona Images acquired on 22-12-1968 were added to the analysis to extend the investigated time interval. The Images available were downloaded at the website of the United States Geological Survey. The images cover the four reaches R2, R5, R8, R11, while it was not available for reach R17.

Each image was georeferenced using 12 Ground Control Points (GCPs) identified on a 2015 orthophoto (available as WMS through the Geoportal Albania) with a second-degree polynomial transformation and nearest neighbour resampling (Table 3.5), and a spatial post-georeferenced spatial resolution of 2.5 m.



Figure 3. 8. View of the available Corona images covering the Erzen river catchment.

Image ID	Acquisition date	RMSE (m)	Covered reaches
DS1049-2155DA041	1968/12/22	4.6	R2, R5
DS1049-2155DF040	1968/12/22	5.2	R8, R8, R11, R17

Table 3. 5. Image ID, Acquisition date, Root-mean square error and covered reaches of the Corona Images Georeferencing procedure.

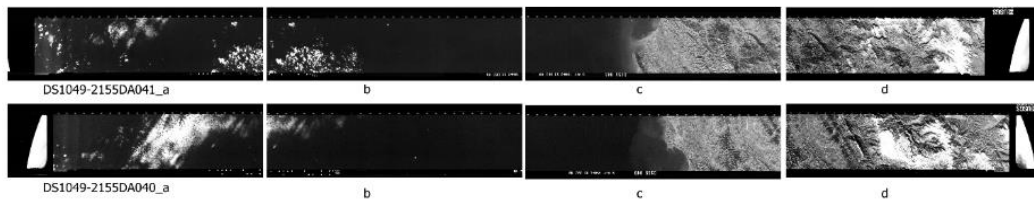


Figure 3. 9. Low-res view of the full spectrum of Corona images used for our reaches. Original images were further georeferenced.

Manual active channel digitizing was performed on a GIS (QGIS 3.10) for each of the four georeferenced reaches, producing the active channel masks. Analogously to the Landsat GRASS-based procedure, longitudinal distributions of active channel widths were computed for the date of photo acquisition (1968).

3.3.3 Indirect methods to estimate channel incision

A visual look at the present lower alluvial reaches of the Erzen river (Figure 3.11 show a deeply incised, narrow channel in the floodplain and a marked vegetation encroachment, suggesting that a relevant process of channel adjustment occurred in the past years, occurring at the river segment scale.



Figure 3. 10. A visual impression of channel incision occurred in the lower Erzen river. (A) photo taken in November 2022 near Hardhishte village, in reach 4, at cross section 6 (B) photo taken in September 2020, in reach 1, at cross section 3 (figure 3.13 for cross-sections location).

However, assessment of vertical channel adjustments in the Erzen, like in many Albanian rivers, can be problematic because historical topographic data are either absent, or difficult to be found, or referred to hydrometric gauging stations that are mainly located in relatively stable, often confined sections of rivers, which are therefore less prone to processes of vertical or lateral adjustments. Furthermore, the few available historical topographic cross-sectional data might suffer from incomplete or highly uncertain metadata, like the reference elevations to which vertical coordinates of surveyed points are referred, making it problematic to compare with present-days topographic surveys. For these reasons, indirect methods for the reconstruction of possible morphological trajectories of the riverbed elevation have to be developed and applied based on the site-specific data availability.

To (i) verify the occurrence of and to (ii) attempt at quantifying the magnitude of such segment-scale channel incision, and based on the specific hydromorphological conditions of the lower Erzen river, three, partially related, complementary methods have been used. These are:

- a) Comparing the present, surveyed riverbed elevation with the “bed” elevation of an abandoned meander due to an artificial cutoff made in the 1970s, before relevant channel adjustments processes could be detected and before the widespread development of major hydro-morphological pressures;
- b) Computing the (presently surveyed) vertical differences between the floodplain elevation and the water surface elevation at low flows with low-flow to bankfull

flow stage differences that are typically observed in single-thread alluvial rivers of similar size, and

- c) Comparing the bankfull width-to-depth ratio of the present river channel with the typical range of observed bankfull width-to-depth ratios of meandering alluvial channels

All these three approaches (with b) and c) being mutually related) required the availability of information on the present riverbed topography. Such information was collected through targeted field surveys between 10 and 14 November 2022, in which ten cross sections were measured along the main stem of Erzen river, mostly located in its lowermost segment, where qualitative evidence of channel incision and of channel narrowing is visually observable, and where most of the selected reaches are located. The GPS survey started at the river mouth and proceeded upstream up to the confluence with the Mudhar river (cross section 10 in figure 3.12), nearby the Ibe village. Here an historical hydrometric station Ibe) is found, at about 52.8 km upstream the river mouth.

Topographic surveys were carried out mainly in the lowest segment of the Erzen river, up to a distance of 52 km from the river mouth, measured along the river channel. Such focus area, is indeed the area where the effects of the incision process are more visible.. That section is quite close to the upstream end of the “plain” physiographic unit, and just upstream a main transition from unconfined to partially confined reaches. The measured points included the floodplain areas nearby the river channel, and within the n river channel, allowing to obtain the floodplain average elevation, the level of the water surface at (low) flow conditions occurring in the measurement period and the maximum depths of the riverbed. The device used to measure the cross section along the river was a Sokkia GRX2 model having a vertical accuracy on elevation +/-2 cm. The equipment and technical support was provided by a local engineering company.



Figure 3. 11. Images of the GPS Sokkia GRX2 used for the topographic survey(Sokkia GRX2 Operator Manual, 2012)

For a high accuracy of survey, the GPS were connected with GNSS ALBCORS network which enables a new realization of the Land System of the European Reference ETRS89 for the territory of Albania and at the same time serves for the maintenance of this reference for the same territory. The error of the condition tested is +/- 1-2 cm.

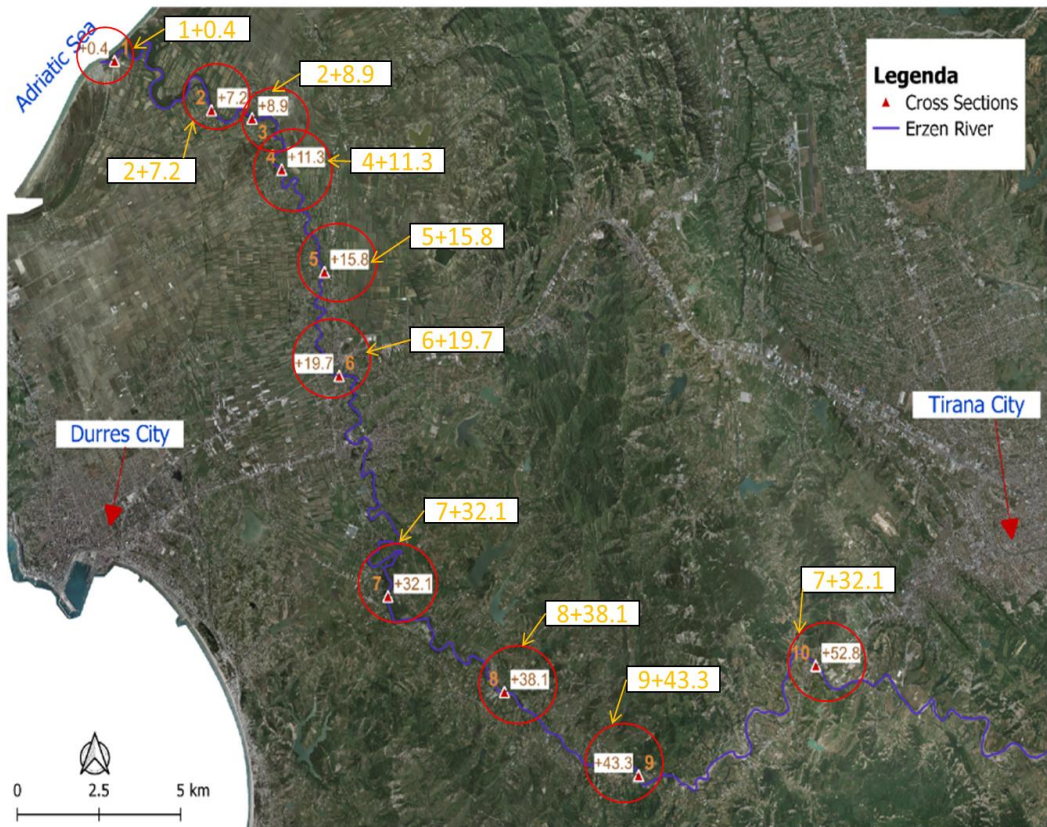


Figure 3. 12. Location of the surveyed cross sections. Cross-sections number and distance along the river are progressively measured starting from the mouth. The first number in each white box indicates the cross-section number and the second number (+xy) indicate the distance (km) from the mouth measured along the river course.

3.3.4 Mapping of main hydromorphological pressures

To understand the possible causes for the observed channel adjustments, the known hydromorphological man-made stressors present in the catchment and potentially producing effects on the river corridor dynamics have been mapped together with their temporal development. These include sediment extraction from the riverbed, presence of artificial structures, dams and associated reservoirs construction, land use – land cover change, changes in the flow regime. As a complementary information to support the analysis of the

temporal evolution of these hydromorphological pressures, some broader information on recent demographic and development indicators at the country scale are also provided.

Land use – land cover change

Changes in forest cover

To evaluate forest cover changes in Erzen catchment area, the initial attempt using military maps from Geoportal Albania 1960-1986 and Orthophotos RGB 2007 and 2015 (Geoportal Albania) proved impractical due to extended image processing times and incomplete temporal coverage. Consequently, Landsat satellite images were employed for their continuous coverage from 1986 onwards. Supervised classification through Google Earth Engine was utilized to analyze and categorize forest cover changes 1986-20 (Harezlak et al., 2020 and Azzari and Lobell, 2017). Landsat medium resolution images have been considered as the most suitable source to assess forest cover dynamics in the last decades (CORINE Land Cover), as the data requirements of approaches based on historical maps and aerial orthophotos were not satisfied. This also seems functional to capture the main landcover changes, which have been occurring mostly after the 1980s with gradual increase of the agricultural area occurring progressively along 1960-1990 and with a marked growth of urbanisation after the 1990s.

Firstly, a land cover supervised classification was implemented. A synthetic, growing season (May to October) representative image of 1986 was computed using *Landsat.simpleComposite* GEE command, over which a supervised classification was applied. Two classes were identified: forest and non-forest, using a set of 100 training pixels. Then, to assess the progressive forest change from 1986, we used the *LandTrendr* algorithm (Kennedy et al, 2010), which employs the Landsat-based detection of trends in disturbance and recovery algorithm to generate a simplified pixel-based spectral-temporal forest cover trajectory. Model output considered in this study was the spatially explicit data on forest loss and recovery with embedded the information of the year of disturbance, allowing to detect spatial and temporal patterns in net forest loss (loss minus recovery) within the catchment.

Changes in urbanized areas

Approximately 40% of Albania's population resides in the two major cities of Tirana and Durrës located in the Erzen catchment area, with Tirana alone accounting for almost 30% of the national population (National Institute of Statistics of Albania-INSTAT, 2022). Major urban growth has come with marked political and social changes, with analogies to the processes occurring in the so called “westernized countries” and a time lag of 40 to 50 years.

To assess urbanization, historical military maps from 1986 were examined alongside the 2015 orthophoto obtained from the Geoportal Albania, comparing the spatial scale of urban areas. The Corine Land Cover maps for the years 1990-2000, 2000-2006, 2006-2012, and 2012-2019 (Copernicus Land Monitoring Service, 2022) each with a 100-meter resolution, were used as well. These maps were reclassified into four categories: Artificial areas

(including urban zones), agricultural regions, forests and semi-natural areas, and water bodies using GIS raster classification.

In addition to spatial analysis, demographic trends were explored by considering population growth since 1960, using data from the World Bank database (World Bank Open Data, 2022). Furthermore, statistical data from INSTAT Albania (2022) were incorporated to examine the regional evolution of both population and urbanization.

Sediment mining

Sediment mining sites found in the active river corridor and artificial structures are visually mapped using the Google Earth free images also using the orthophotos after 1990 available to the Geoportal Albania since the Google Earth images do not provide good information at high enough resolution before 2004. The spatial mapping of sediment mining sites is compared with a local technical report referred to the Erzen and Ishem river basins (Ministry of Agriculture Albania, Institute of Earth Studies, 2009)

Dams

The assessment of hydropower plants (HPPs) within the Erzen basin is based on Euronatur -RiverWatch 313 – Fluvius 2020 Database (Euronatur, 2020), which reports the ensemble of operating, under construction, and 314 planned structures for the entire Balkan Region. Also, for mapping the HPPs, using the Geoportal Albania database (Geoportal Albania) and National Agency of Natural Resources Albania database of the existing construction of HPPs and them that are on permitting stage (Hydro- Energetic Potential of Albania - AKBN, 2019)

To estimate the sediment trapped from the Skorane dam (water irrigation) which has a total volume 2.3 million m³ and is built in 1973. The dam is filled with sediment on in 2005-2010 from Landsat images and actual photo of 2009 on the dam. To calculate the sediment volume, we multiply with a coefficient 0.65 (porosity of sediment 0.3-0.4).

Analysis of flow records

Data available of the flow of Erzen river were taken from Institute of Geosciences of Albania scanned and manually digitize for three station available. The flow discharge is daily and covers a period for Salamone station 1049-1992, Ndroq station 1952-1990 and Ibe station upstream 1972- 1990.

REPUBLIKA POPULLORE SOCIALISTE E SHQIPERISE
AKADENIA E SHKENCIVE
Instituti Hidrometeorologjik

TH-10/1

PRURJA E UJIT m³/s

Lumi: Prurja e Ujit Vendndorja: Sallmona Viti: 1982

Data	I	II	III	IV	V	VI	VII	VIII	IX	X	XI	XII
1	25.2	8.28	10.2	8.65	11.0	5.202	0.185	0.123	0.165	0.285	2.27	3.85
2	26.1	7.68	10.2	8.20	10.4	5.220	0.185	0.123	0.165	0.285	2.27	4.03
3	26.7	8.00	10.2	8.20	9.80	5.150	0.185	0.123	0.165	0.285	2.27	3.20
4	27.6	8.60	10.2	8.20	8.90	5.050	0.185	0.123	0.165	0.285	2.27	3.20
5	28.2	8.80	10.2	8.20	8.20	5.125	0.185	0.123	0.165	0.285	2.27	3.40
6	28.1	8.20	10.2	7.80	7.80	5.185	0.185	0.123	0.165	0.285	2.27	3.20
7	28.1	8.72	10.2	8.20	7.20	5.165	0.185	0.123	0.165	0.285	2.27	3.20
8	28.1	8.80	10.2	7.80	6.80	5.175	0.185	0.123	0.165	0.285	2.27	3.20
9	28.2	8.20	10.2	6.80	6.80	5.280	0.185	0.123	0.165	0.285	2.27	3.20
10	28.3	8.40	10.2	6.80	6.15	5.215	0.185	0.123	0.165	0.285	2.27	3.40
11	28.3	8.20	10.2	5.80	5.80	5.185	0.185	0.123	0.165	0.285	2.27	3.80
12	28.3	8.00	10.2	5.80	6.20	5.185	0.185	0.123	0.165	0.285	2.27	4.25
13	28.3	8.40	10.2	5.80	5.80	5.185	0.185	0.123	0.165	0.285	2.27	4.03
14	28.1	8.60	10.2	5.80	4.80	5.240	0.185	0.123	0.165	0.285	2.27	4.03
15	28.7	8.60	10.2	5.80	6.20	5.185	0.185	0.123	0.165	0.285	2.27	4.03
16	28.6	8.60	10.2	5.80	6.20	5.185	0.185	0.123	0.165	0.285	2.27	4.03
17	28.3	8.60	10.2	5.80	6.20	5.185	0.185	0.123	0.165	0.285	2.27	4.03
18	28.3	8.60	10.2	5.80	6.20	5.185	0.185	0.123	0.165	0.285	2.27	4.03
19	28.2	8.60	10.2	5.80	6.20	5.185	0.185	0.123	0.165	0.285	2.27	4.03
20	28.2	8.60	10.2	5.80	6.20	5.185	0.185	0.123	0.165	0.285	2.27	4.03
21	28.2	8.60	10.2	5.80	6.20	5.185	0.185	0.123	0.165	0.285	2.27	4.03
22	28.2	8.60	10.2	5.80	6.20	5.185	0.185	0.123	0.165	0.285	2.27	4.03
23	28.2	8.60	10.2	5.80	6.20	5.185	0.185	0.123	0.165	0.285	2.27	4.03
24	28.2	8.60	10.2	5.80	6.20	5.185	0.185	0.123	0.165	0.285	2.27	4.03
25	28.2	8.60	10.2	5.80	6.20	5.185	0.185	0.123	0.165	0.285	2.27	4.03
26	28.2	8.60	10.2	5.80	6.20	5.185	0.185	0.123	0.165	0.285	2.27	4.03
27	28.2	8.60	10.2	5.80	6.20	5.185	0.185	0.123	0.165	0.285	2.27	4.03
28	28.2	8.60	10.2	5.80	6.20	5.185	0.185	0.123	0.165	0.285	2.27	4.03
29	28.2	8.60	10.2	5.80	6.20	5.185	0.185	0.123	0.165	0.285	2.27	4.03
30	28.2	8.60	10.2	5.80	6.20	5.185	0.185	0.123	0.165	0.285	2.27	4.03
31	28.2	8.60	10.2	5.80	6.20	5.185	0.185	0.123	0.165	0.285	2.27	4.03
MES	35.7	8.00	10.2	10.0	4.97	0.199	0.185	0.123	0.165	0.285	2.27	4.03
MIN						0.168	0.140	0.100	0.120	0.200	1.500	2.200
MAX						0.220	0.200	0.140	0.180	0.300	2.500	3.500

Prurja mesazore: 8.01 m³/s

No veshje: 0.00 m³/s

Data:

Figure 3. 13. Illustrative example of scanned sheet of daily flow record in 1982 for Sallmona hydrometric station

To test possible changes in the flow regime with potential effects on the river dynamics, the presence of possible trends in the historical flow records has been analysed. The hypothesis behind this analysis is that changes in the magnitude, duration and frequency of flood events able to drive morphological change can result in relevant channel adjustments over time scale of decades. As a simplified proxy for the multidecadal scale variability of these morphologically relevant hydrologic indicators, the trends in monthly and annual flow water volumes have been computed, assuming that periods with more intense, frequent and longer floods overall correlate with generally more wet hydrological periods.

Trend analysis is a crucial aspect of studying time series data, offering valuable insights into patterns and changes over time. In this context, researchers often employ both parametric and non-parametric tests. Parametric tests necessitate the assumption that the data is independent and follows a normal distribution. Conversely, non-parametric trend tests only require the data to be independent and can accommodate outliers without significantly affecting the analysis (Hamed and Ramachandra Rao, 1998).

In assessing the flow trend of three stations, the Mann-Kendall trend test proves instrumental in analyzing monthly and yearly flow regimes. For this purpose, the *pyMannKendall* Python

package is employed, leveraging its pure Python implementation and vectorization techniques to enhance performance. Remarkably, the package comprises 11 different Mann-Kendall tests, as elaborated by Hussain and Mahmud (2019). This extensive range of tests allows for comprehensive and robust trend analysis, making it a valuable tool for researchers and practitioners in the field of time series data analysis (Hussain and Mahmud, 2019). For yearly trend the *Original Mann-Kendall* trend test is used that is a nonparametric test, which does not consider serial correlation or seasonal effects. While for the monthly trend the *Seasonal Mann-Kendall* test is used that is suitable for seasonal time series data.

3.4 Results

The results section is organized as follows. First, reconstructed channel adjustments, related to the change in the active river corridor and in the mean reach-scale bed elevation are presented. This is followed by the analysis of the main possible drivers of channel adjustments.

3.4.1 Changes in the active river corridor width

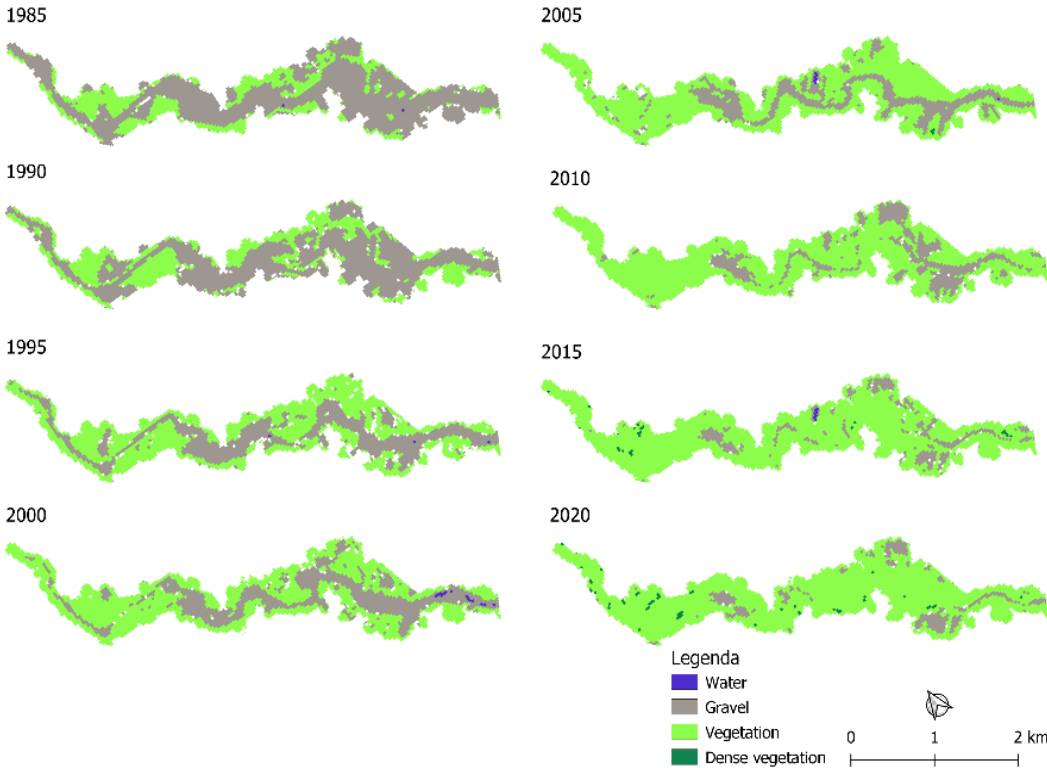


Figure 3. 14. Evolution of land cover in reach 5 visualized by images obtained every five years from the analysis of Landsat imagery.

Multi-temporal sequences of the different land cover classes resulting from the automated Landsat image analysis (section 3.3.1) for reaches 5 (sinuous in 2015) and 17 (braided) are reported in Figures 3.14 and 3.15. Examining the images referred to Reach 5 (Figure 3.14), a distinct pattern emerges, revealing that gravel and vegetation dominate the active channel corridor at low flow, summer conditions. Coherently, water and dense vegetation are mapped for very few pixels in each image due to the constrained size of the active channel and low flow. A clear temporal variability occurs in land cover from 1985 to 2020: a noticeable shift is evident, whereby gravel / bare sediment areas progressively diminish while vegetated areas expand. This shift implies a progressive narrowing of the active river channel.

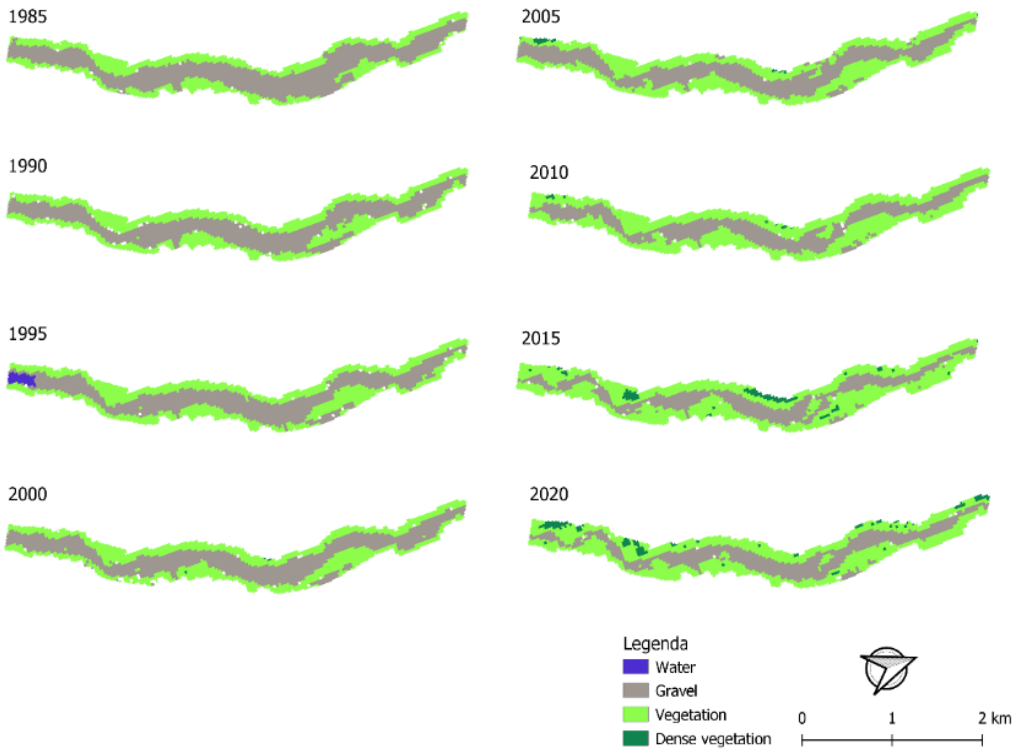


Figure 3. 15. Evolution of land cover in reach 17 (upstream of the Skorana dam) visualized by images obtained every five years from the analysis of Landsat imagery.

A different behaviour is instead exhibited by reach 17 (Figure 3.15), which is located upstream of the Skorana dam, towards the headwaters of the basin. Here the decrease in the bare sediment surfaces in favour of the vegetation cover is much smaller compared to reach 5. The gravel areas were occupying almost the entire active river corridor envelope in 1985,

while it has reduced to nearly half of it in 2021. This reduction does not follow the same marked trend observed in the lowland reaches.

The analogous maps for the other analysed reaches using Landsat imagery (reaches 8,11, located in the middle – lower Erzen) can be found in the Appendix. Their evolution is much more similar to that of reach 5 than that of reach 17. Here, we present only two reaches for illustrative purposes, allowing for better visualization.

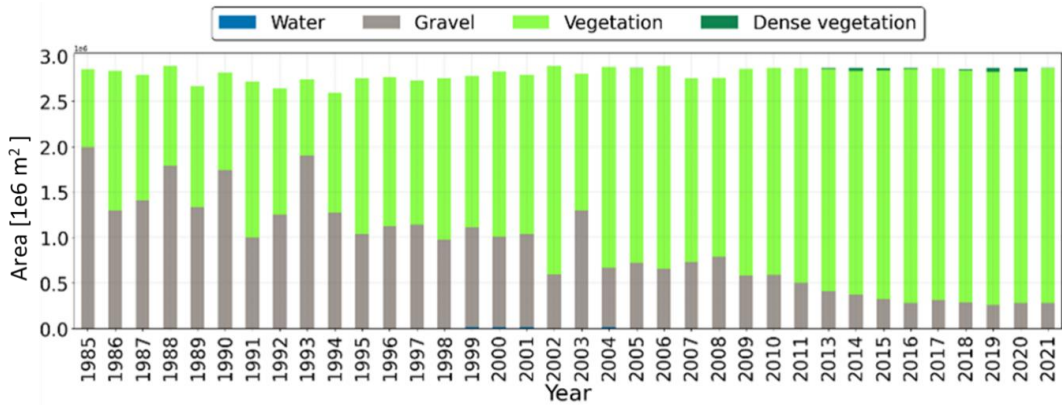


Figure 3. 16. Annual time series of land cover classes in reach 5 obtained from the analysis of Landsat imagery.

The temporal trend in land cover for reach 5 is visualized in a more comparable form in Figure 3.16, which depicts the relative proportion of the different land cover classes in the active channel on an annual basis (in square meters). Through the visualization, it becomes evident that the area occupied by gravel classes has experienced a strong reduction over the analysed years from nearly 2 Mm³ in 1985 to less than 0.3 Mm³ in 2021, an almost 7-fold reduction. Notably, there are instances of increased area in select years (e.g., 1998, 1993, and 2003); however, the overarching trend demonstrates a consistent decrease. In contrast, the vegetation class has exhibited growth over the same timeframe, from about 0.7 to nearly 2.5 Mm³ from 1985 to 2015. Qualitatively speaking, a first phase of reduction appears since the early 1990s and then after 2008. The proportions of the different classes look quite stable after 2016, when also some small parts of the initially active corridor are classified as “dense vegetation”, further supporting the presence of a more stable, less dynamic condition.

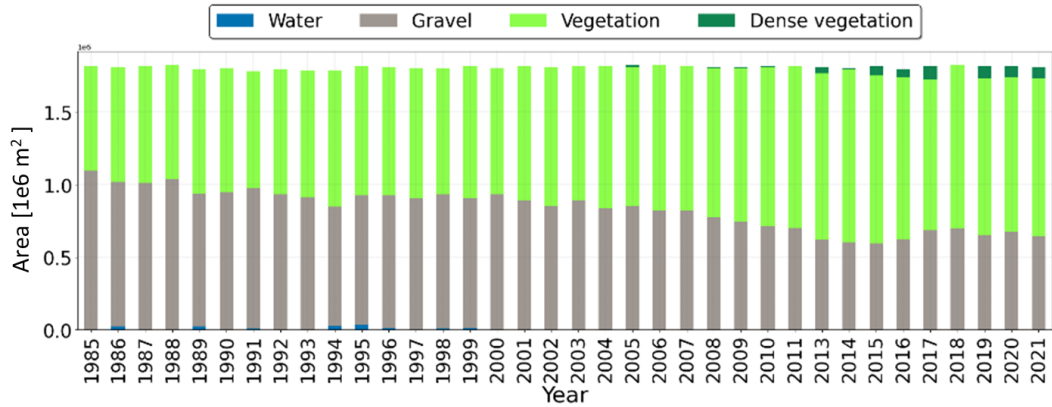


Figure 3. 17. Annual time series of land cover classes in reach 17 obtained from the analysis of Landsat imagery.

Though also showing a decrease in the gravel area and an increase of the vegetated area, differently from all the other analysed reaches, reach 17 shows a less rapid and less intense reduction in gravel areas and corresponding increase in vegetated areas. Notably, for reach 17 located at the headwaters and upstream of the Skorana dam, the trend of gravel reduction is not particularly pronounced and follows a more stable trajectory. Bare sediment areas occupied nearly 1.1 Mm^3 in 1985 and 0.6 Mm^3 in 2021, a reduction that is not even half of the initial value. Such reduction is 3.5 times smaller than the reduction observed in reach 5, which is qualitatively similar, though quantitatively slightly different, to those experienced by all the other reaches. At the same time, in these reaches, dense vegetation starts to be more evident in the last years and progressively continues to grow.

Table 3. 6. Results of the Mann-Kendall trend test for the time series of the different land cover classes for all reaches analysed.

Reach	Gravel			Vegetation			Dense Vegetation		
	Trend	P value	Slope	Trend	P value	Slope	Trend	P Value	Slope
R5	-	7.31 e-12	-40225	+	1.29 e-11	45134	+	6.65 e-06	0
R8	-	1.29 e-11	-27715	+	2.26 e-11	28498	+	9.32e-06	0
R11	-	4.82 e-10	-22556	+	1.59e-09	23723	+	0.006	0
R17	-	0.0009	-11635	+	1.12 e-08	10707	+	1.19 e-05	426

To assess the existence of possible trends in time series of the different annual land covers, the Mann-Kendall original trend test was employed. A P-value below 0.05 indicated a significant trend. Here the 0.05 is threshold value chosen as default (alpha value). Slope is an indicator of the strength and direction of that trend. Throughout the analysed periods from 1985 to 2021, distinct and meaningful trends were observed. These trends were negative for the reducing gravel surfaces and positive for a simultaneously increasing vegetated and densely vegetated areas.

Among the lowland reaches (Table 3.6), the analysis revealed a substantial and statistically significant decrease in gravel surfaces for all reaches. Specifically, the p-values for these reaches were $7.31e-12$ and $1.29e-11$, respectively. These decreasing gravel trends were aligned with a concurrent growth in areas occupied by sparse vegetation for the same reaches. However, observed, statistically significant trends were much milder in reach 17, which experiences a much slower reduction (increase) in gravel (sparse vegetation) areas, which are also statistically significant though with higher p-values (0.0009 and $1.12e-8$, respectively). Looking at the slope values in Table 2.6, it appears that the slope of the linear trends for reach 17 were about one fourth (one half) compared to the trends of the same quantities for reach 5 (8 and 11).

3.4.2 Changes in Active Channel Width

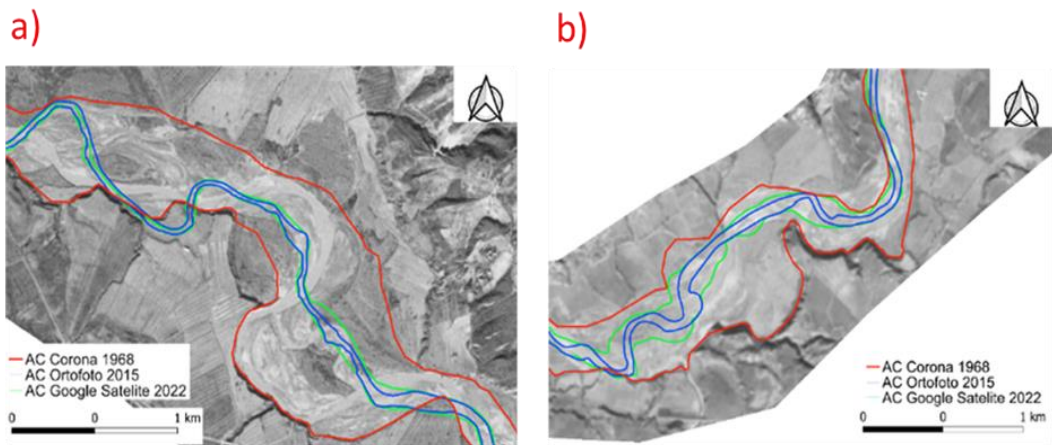


Figure 3.18. Background image: Corona image (1968). Boundaries of the active river channel indicated in red (1968), blue (2015) and green (2022). (a) Reach 5; (b) reach 8.

Available Corona satellite images (1968) are used as reference point to map the active channel width before the occurrence of major, rapid socio-economic changes at the country level. The boundaries of the active river corridor for reaches 5 and 8 are shown in red colour in Figure 3.18. I overlapped on the same Corona images, the blue and green lines indicate the boundaries of the active river corridor as mapped on the orthophotos of 2015, obtained from Geoportál Albania (Asig), and from the Google image of 2022 (Source: Google Earth).

A strong active channel width reduction is observed in both reaches, which is analogous to what can be observed also in reach 11. Figure 3.18 also highlight an important, striking effect of the strong active channel width reduction: the change in the channel pattern, from a multi-thread to a sinuous channel. The 1968 active channel showed a wandering behaviour, with bifurcation, confluences and a tendency to even a braided morphology locally. The 2015 and 2022 active channel, instead, clearly outline a sinuous, single-thread channel morphology.

Combining the Corona images and Landsat images the results are represented with boxplots in Figure 3.20.

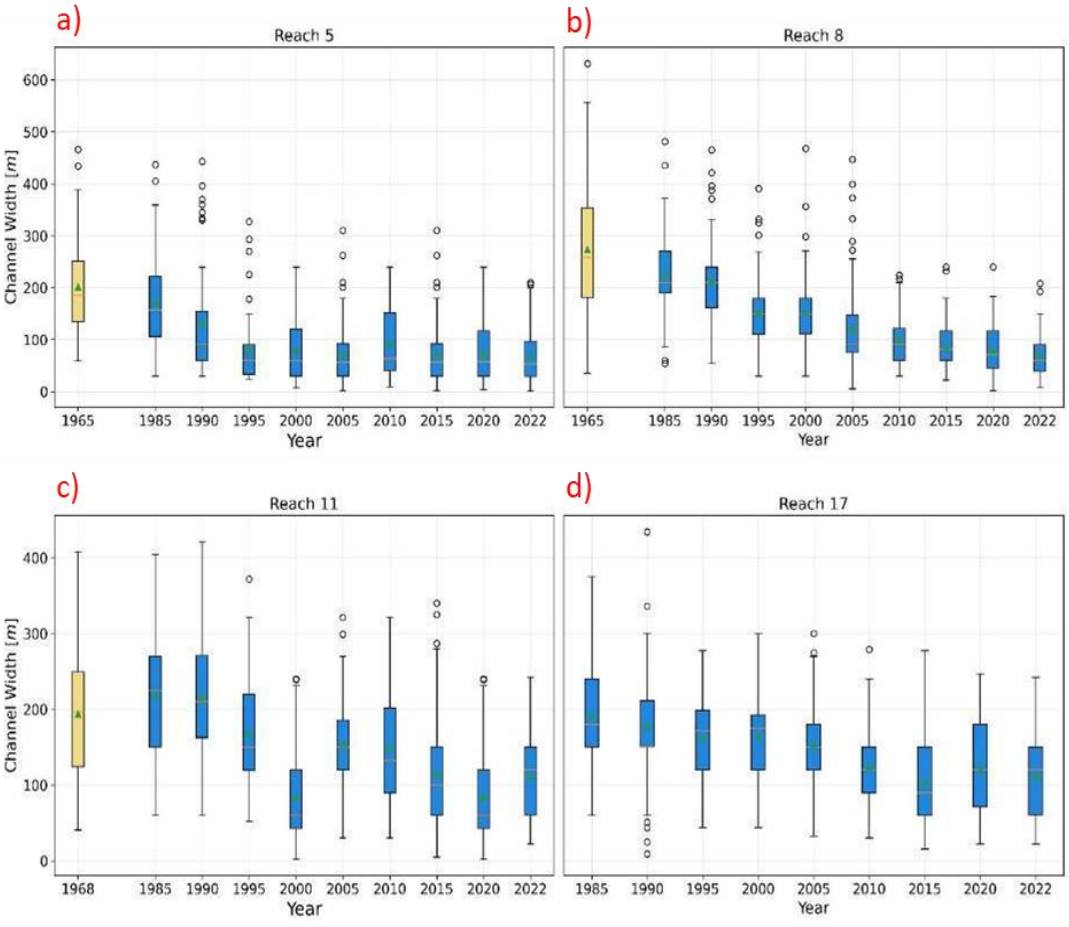


Figure 3. 19. Evolution of the distributions of reach-scale active channel width. Reach 5 (a), reach 8 (b), reach 11 (c) and reach 17 (d).

The Corona images were used for three reaches (5, 8, 11), while data for reach 17 was not available. In reach 5, the active channel width was 180 m in 1968, followed by a decrease to 150 m in 1985, eventually dropping to 50 m in 2022. This indicates a reduction in active channel width of around 130-100 m (73% of its initial value) over the span of 50 years.

Reach 8 exhibited a consistent trend of reduction, with the channel width diminishing from 260 m in 1968 to 60 m in 2022 (a total reduction of 200 m, 77% of its initial value). When considering only Landsat images from 1985 to 2022, the reduction in active channel width is 150 m (71.4%). For reach 11, the active channel width measured 195 m in 1968, reaching 230 m in 1985, and then experienced a decline, reaching its narrowest point at 80 m in both 2000 and 2020. The extracted active channel width was 120 m in 2022. Overall, a reduction of over 100 m in active channel width was observed. The integration of the information from the Corona satellite imagery (1968) with the one extracted from the Landsat imagery (1985 – 2021) for all reaches 5,8 and 11 suggests a milder narrowing (if any) occurring between the end of the 1960s and the mid 1980s, and a much more pronounced narrowing between the 1990s – the start of the strong socio-political changes in the country – and the present years.

Reach 17, located upstream of the dam, demonstrated a smaller reduction in active channel width compared to the other reaches, with a decrease of 60 m (33% of its initial value). This is evident in measurements of 180 m in 1985, and 120 m in 2022.

In the case of the meandering reach number 2, due to the limited size of the active channel, manual digitalization was carried out using available orthophotos (from 1968, 1984, 1994, 1999, 2007, 2015, available from ASIG Geoportal, and 2022 via Google Earth). Reach 2 displayed a narrowing of the channel, decreasing from 40 m in 1968 to 15 m in 2022 (63% of its initial value; figure 3.20). An important observation on the evolution of meandering reach 2 is that, differently from the initially wandering reaches 5,8,11, reach 2 kept its meandering pattern, though with a much-reduced width.

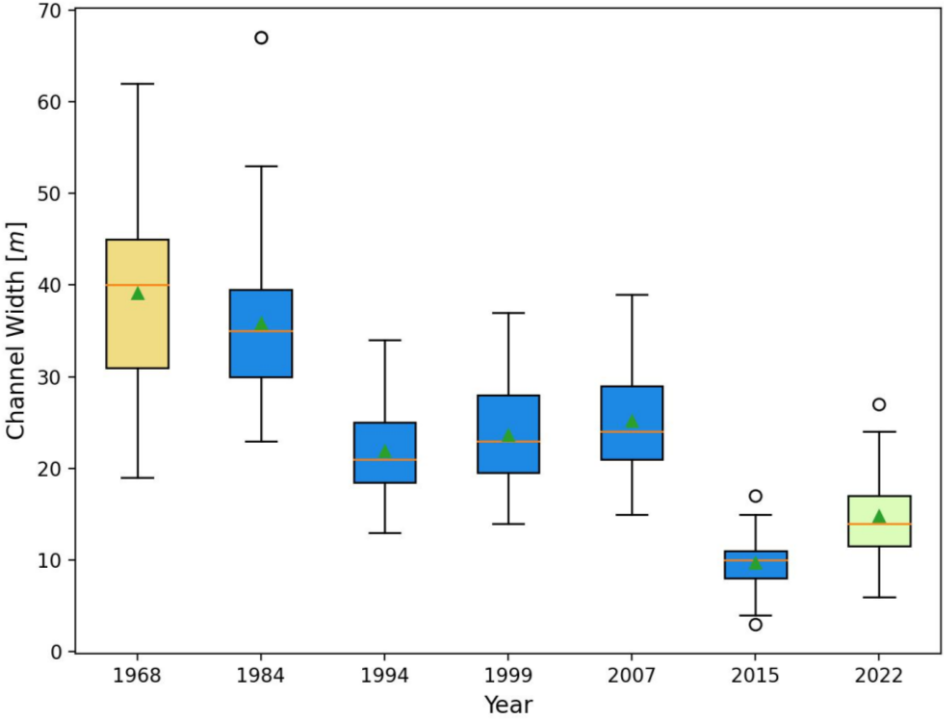


Figure 3. 20. Time series of the active channel width distributions obtained from manual digitalisation of ASIG imagery reach 2. Year 2022 with light green colour, active channel width is extracted from google maps imagery.

Manual digitization from available orthophotos at Geoportal Albania and 2022 Google Maps was conducted for all reaches and using the same method in Grass GIS and QGIS. Automated classification was instead performed when analysing the Landsat imagery. By comparing the results of the automated analysis of Landsat imagery and of the manual digitalization of active channels (AC) on the other sources, it's evident that the differences are minimal (Figure 3.21), suggesting a good consistency between the two methods. For illustrative purposes, Figure 3.21 showcases the results of both analyses on reach number 5, using manual extraction from Geoportal (Figure 3.21a) and automated extraction from Landsat imagery (Figure 3.21b). Both methods consistently reveal a similar reduction in the reach-averaged active channel width, though showing differences in the within-reach channel width frequency distributions, as highlighted by the different size of the corresponding boxplots.

An estimate of the accuracy of the semi-automated method has been obtained by comparing some percentiles of the distributions reported in the boxplots of Figure 3.21. Results are shown in Table 3.7, referring to Reach 5. It appears that when the channel is large enough, i.e., several pixels of the Landsat image, the accuracy of the classification is around 10%. However, for reaches whose width is close to one of very few Landsat pixels, as expected, the accuracy becomes poor (see the same reach 5 in 2015, after intense narrowing).

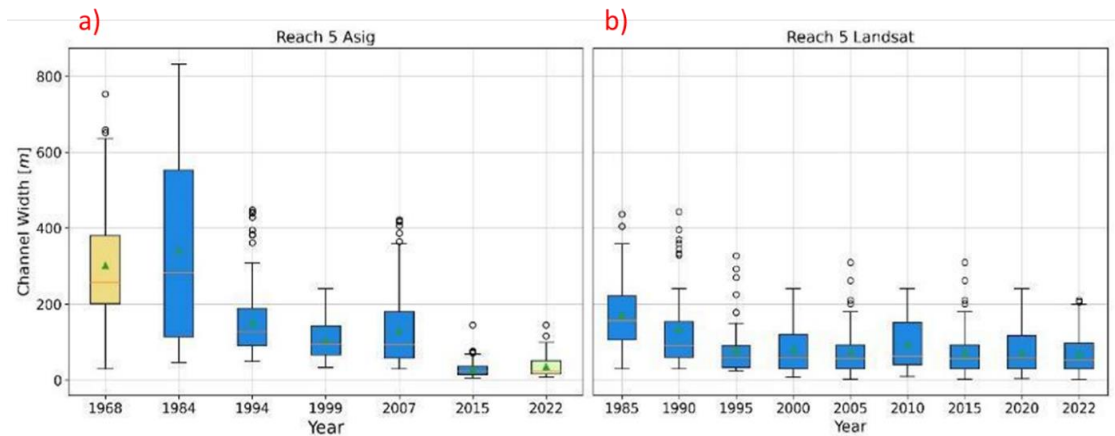


Figure 3. 21. Time series of the active channel width distributions obtained from manual digitalisation of ASIG imagery (a) and from the automated analysis of the Landsat imagery (b) for reach 5.

Reach 5	Year	Method	25 Percentile	Mean	75 Percentile
	1994-1995	Landsat (m)	60	131	210
		Manual (m)	85	149	194
		Difference	29 %	12 %	8 %
	2015	Landsat (m)	28	42	74
		Manual (m)	13	22	38
		Difference	115 %	91 %	95 %

Table 3. 7. Values of the 25th, 50th and 75th percentiles of the reach-scale distributions of the active channel width as obtained from the semi-automated method (Landsat imagery) and from manual extraction on high-resolution orthophoto. Data refer to reach 5, which has experienced a strong narrowing in the period of observation.

3.3.3 Vertical channel adjustments

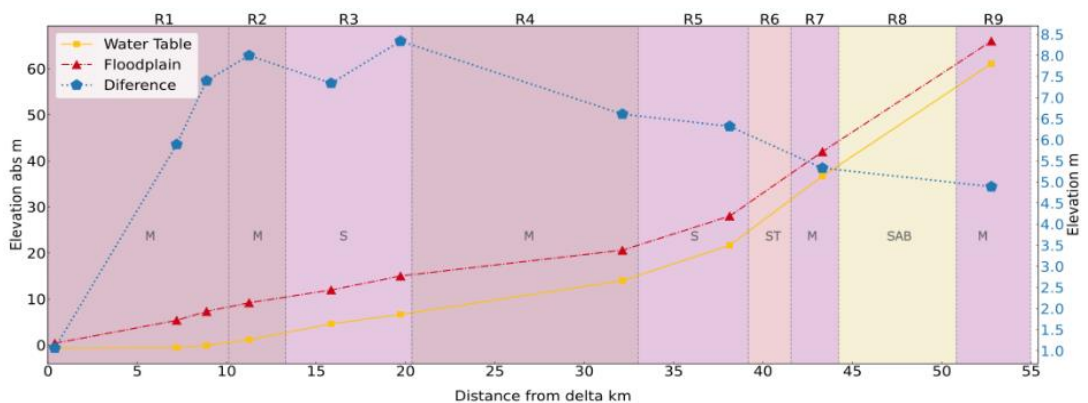


Figure 3. 22. Longitudinal (instream coordinate) profiles of a representative low flow water level, of the floodplain elevation in the same transects and of their difference. The location of reaches R1 – R9 is reported on the top of the figure, together with the corresponding channel morphology, as it results from the analysis of Chapter 2 (M= Meander, S= Sinuous, ST= Straight, SAB= Sinuous with alternated bars).

The difference between the floodplain elevation and the water surface levels surveyed at a representative low flow condition has been measured for ten cross sections covering the lower river segment, in which the visual signs of channel incision and the strongest active channel narrowing have been observed (Figures 3.15 and table 3.6). The results are shown in Figure 3.22, where the red and yellow line (values on the left vertical axis) represent the floodplain and water surface elevation, respectively, and the blue line their difference (values on the right vertical axis) It appears that reach 2 and 3 exhibit the highest differences, with 8 meters for reach 2 (where the artificial cutoff was realized) and 8.4 meters for reach number 3. When moving upstream along the river, this difference progressively diminishes. Another perspective to look at such geometrical configuration of the surveyed cross-sections is to compute the ratio between the channel width at a hypothetical bankfull stage, corresponding to the floodplain elevation, and a measure of the bankfull channel depth, taken as the vertical distance between the floodplain elevation and the low flow water surface elevation. The low flow depth could not be measured in high detail for all cross sections, due to the muddy and unsafe conditions of many parts of the riverbed, but the few measured values yield an estimate of maximum water depths of about 0.5 m during the survey. It's worth noting that such width to depth ratio is particularly low for the upstream portion of reach 1, for reaches 2 to 4 and, likely, for part of reach 5, where such ratio is below 4 (Figure 3.23). Reported studies on alluvial, laterally unconfined sand-bed meandering rivers, like the lower Erzen was originally, indicate a typical range of bankfull width to depth ratios generally of the order of above 10, up to even 100, as supported by data from real rivers (e.g. width/depth equal to: 7.5, Embarras River, Frothingham and Rhoads, 2003; 11, River Bollin UK, Luchi et al., 2010; 15, Wabash River, US, Konsoer et al., 2021)) and physically based modelling (Monegaglia and Tubino, 2019, Haito and Parker, 2020).

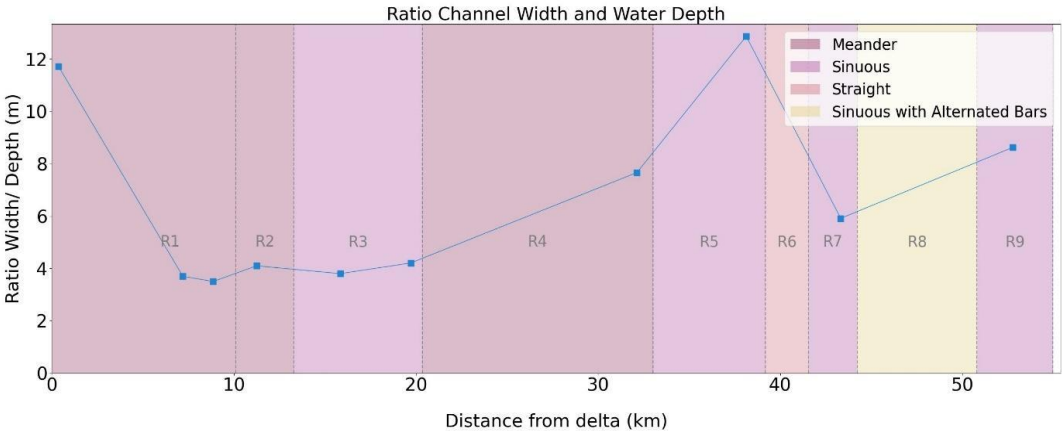


Figure 3. 23. Ratio channel width and channel depth in m

The graphical representation in Figure 3.23 displays the ratio between the channel width and channel depth for the lowland reaches up to reach 9. In the meandering and sinuous reaches between nearly 5 and 35 km river length, the ratio ranges between 3 and 4. This feature deviates from the typical conditions observed in a natural river, particularly within the meandering reaches (Wyżga, 2001).

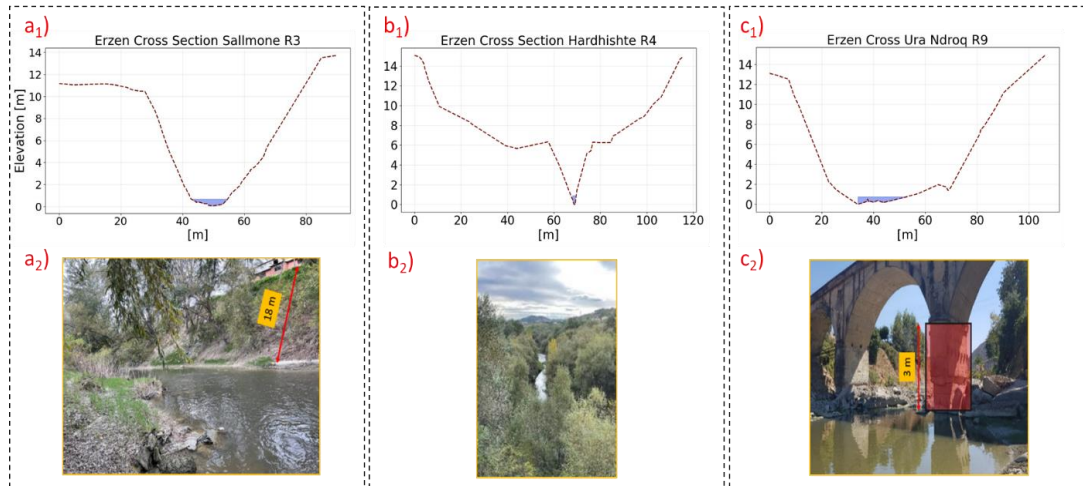


Figure 3. 24. Cross-section Sallmone reach 3, 15 km from mouth (a1), cross-section Hardhishte reach 4, 19.7 km from mouth (b1), cross section Ura e Beshirit reach 9, 43.3 km from mouth (c1). Figures A2, B2 9(taken in November 2022) and c2 (taken September 2020), represent the photos per each cross-section.

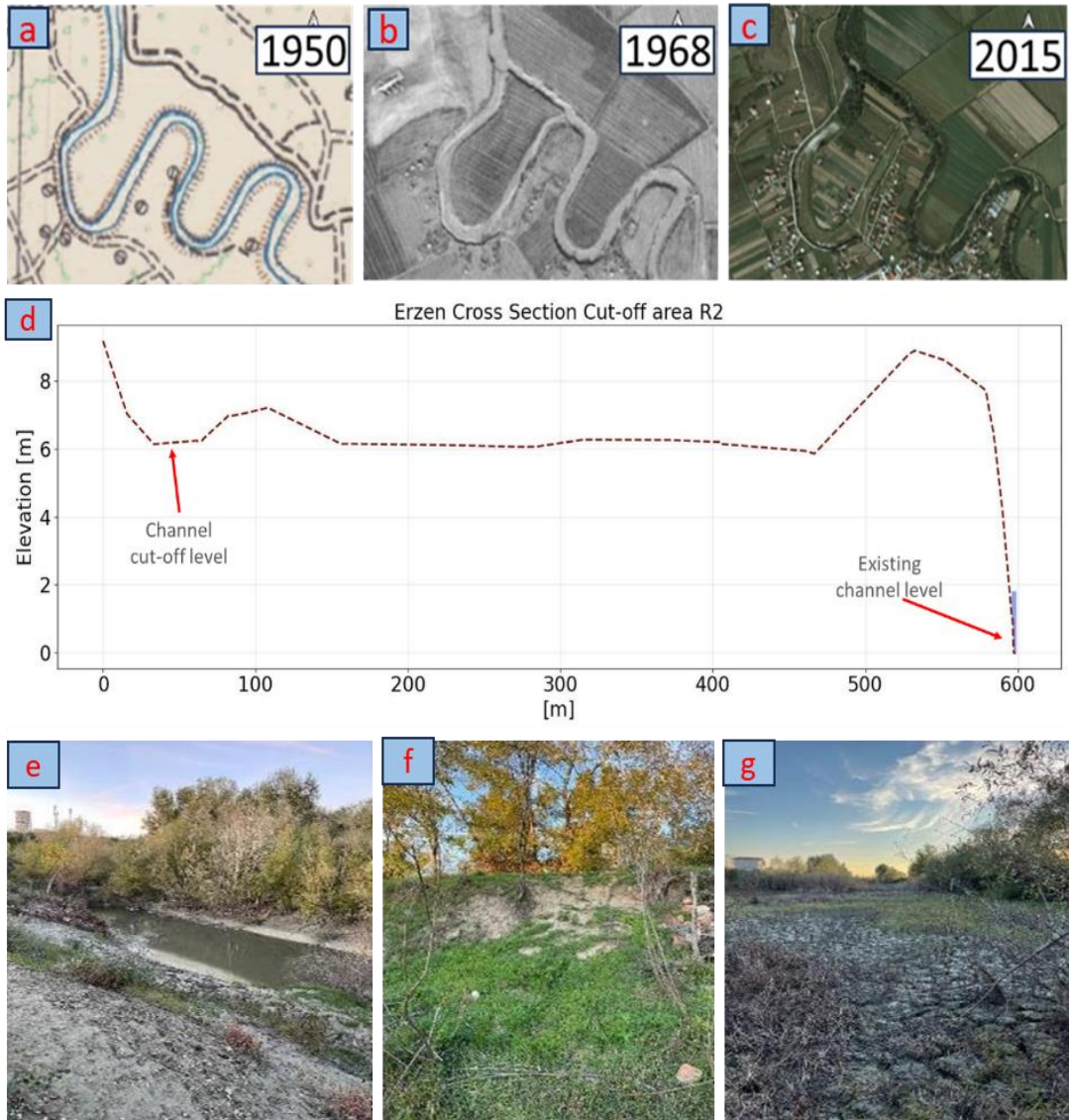


Figure 3. 25. Illustrations of the artificial cutoff occurred in the meandering reach 2, and of the related indirect estimation of channel incision occurring afterwards. (a-c) Historical evolution of the artificial meander cut-off that occurred in reach 2 at the end of the 1960s; (d) Cross-section surveyed in November 2022, reach 2, which extends into the floodplain until the abandoned meandering channel, showing the difference in elevation between the former channel bed in the abandoned meander and the present riverbed of the active channel. (e) view of the present channel from the left bank of the right bank; (f) view of the banks in the right of the cross-section; (g) middle portion of the cross-section of the abandoned arm of the river.

Figure 3.25 illustrates the artificial cutoff that was made in reach 2 (figure 3.25a-c) and how this has been used to develop another indirect estimate of the incision process, which most likely occurred in parallel with the observed channel narrowing (Sections 2.4.1 and 2.4.2).

In addition to the difference between the present floodplain level, the difference between the present riverbed level in the abandoned, old meandering channel and the existing riverbed channel topography has been surveyed (figure 3.25d) on this section to have a understanding of the channel topography now and in the past. The difference between existing riverbed channel (old river) and the actual riverbed is nearly 6 m. While it is likely that some natural or artificial sedimentation has been occurring in the abandoned channel, in the order of 3-4 meters, such difference may lead to estimate the magnitude of the incision process in this reach of about 4 to 5 meters.

Assuming such estimate (4 to 5 m) for the magnitude of the channel incision, coupling this estimate with the presently observed difference between the floodplain elevation and the present riverbed (nearly 8 m in this reach 2, Figure 3.25), and accounting for an average, present low flow depth of 0.5 m, this would lead to estimate a cross-sectional average bankfull channel depth between 3.5 to 4.5 m under least disturbed conditions by major anthropic effects, before the intense channel adjustment started. This would therefore correspond to an average, least disturbed bankfull width to depth ratio of 10, using the estimated bankfull width of reach 2 in 1968, at the time the artificial cutoff was constructed, as it can be extracted from the Corona image (Figure 3.25b)

3.4.5 Analysis of the possible drivers of channel adjustments

This last subsection of the Results presents the outputs of the analysis of the possible direct human and indirect - climatic drivers of channel adjustments.

Sediment mining

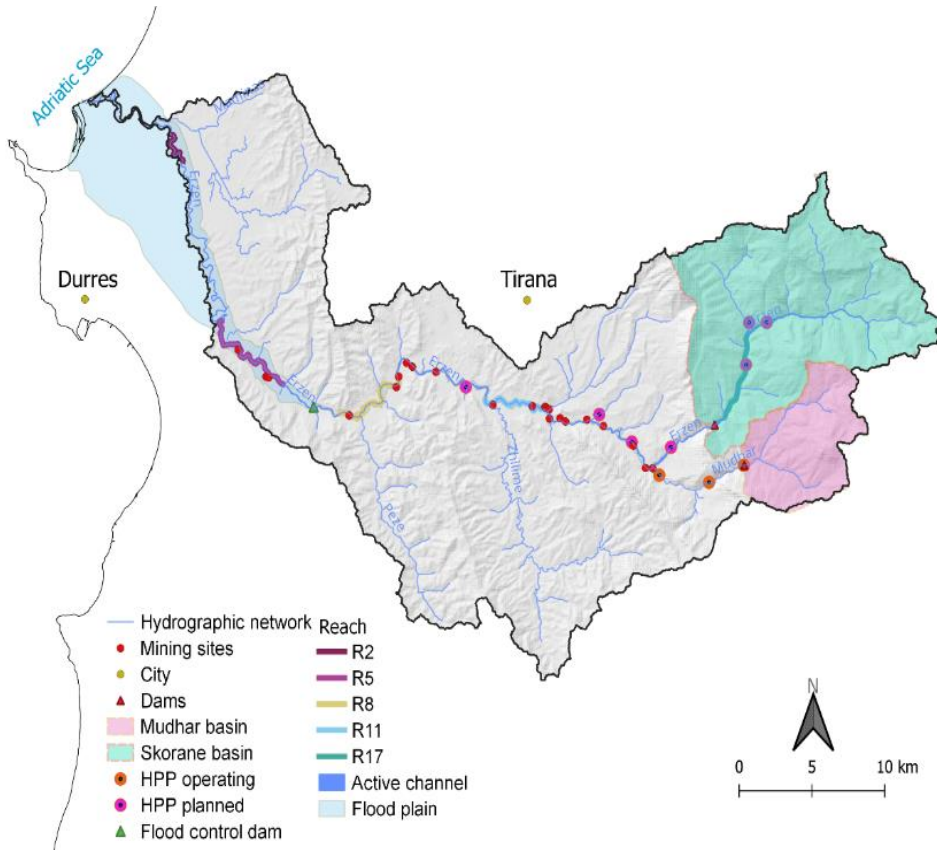


Figure 3. 26. Map of anthropic pressures Erzen Basin

A total of 22 sediment mining sites were visually recognized on the historical images available in Google Earth and mapped and geo-referenced after 1990. from Cukalla, M (2009) has reported 22 mining sites for Erzen River, some of them without having full permission to extract sediment from the river. Though the study of Cukalla (2009) is named: “*Study on small scale sediment mining in Albania*”, it focuses primarily on the Erzen River and reports a survey of 22 mining sites (mapped from Google Earth images as well), a corresponding estimate of 6 million m³ of total sediment extraction. Such estimated value accounts for approximately 15% of the total, long term historical average sediment transport of the Erzen River. Also, Cukalla (2009) states that official data reported by mining companies in the 2000-2008 period were 40% less than what has been actually estimated through such analysis. Which amounts to 6 million m³. From the data Hydrometeorology Institute of Albania, 1979 for Erzen River bedload transport is 636, 000 ton/year, so 15% of the of sediment extraction are 95,400 ton/year.

The mapped sediment mining sites are represented with red dots in Figure 3.26. The sediment mining sites are mostly located along the partly confined and unconfined reaches where the diameter of the gravel is suitable for use as primary material for construction. It

must be pointed out that, the information that could be reported is a cumulative information of the sites that could be recognized on the Google Earth imagery and on the available orthophotos on the ASIG geoportal Albania. Therefore a complete, quantitative history of the development of sediment mining cannot be provided.

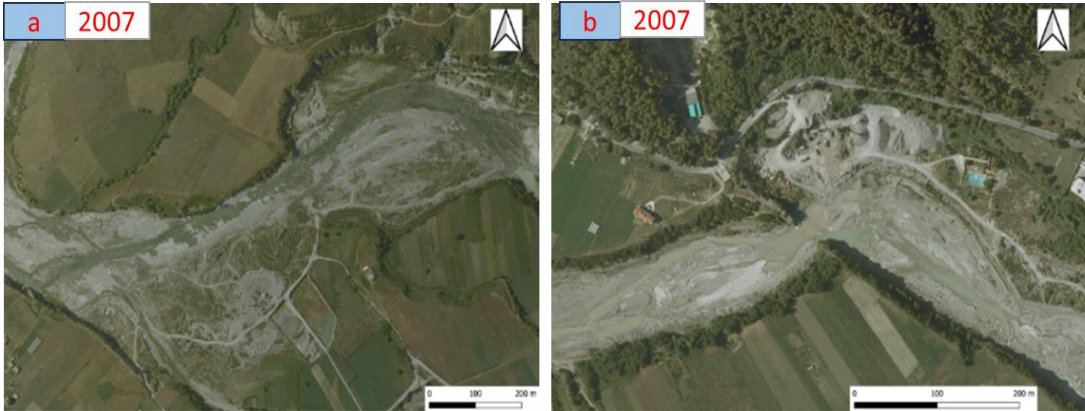


Figure 3. 27. View of some representative sediment mining sites in the Erzen River from the Orthophoto 2007. (a), reach 11, (b) reach 12). Source Geoportal Albania.

Illustrative examples of the sediment mining sites along the Erzen are reported in Figure 3.27. The location of the displayed portion of the 2007 orthophoto at reach 11 is 60 km from the mouth (figure 3.27a) and at reach 12 (figure 3.27b) is 66.4 km from the mouth. In both cases we see exposure of the riverbed and the artificial holes created from sediment mining along the river.



Figure 3. 28. Visual signs of the riverbed incision downstream of the reaches where the strongest concentration of sediment mining sites is observed. Both images show emergence of the bedrock. (a) Photo Riverbed Erzen River reach 7, November 2022. (b) Photo riverbed Erzen River reach 11, 2020.

The photo Figure 3.28a, located 43.3 km upstream the river mouth shows clearly the exposure of the bedrock of the river. Along this part of the river the signs of lack of sediment supply are visually evident for almost 70 km of the channel length upstream the river mouth to the sea. Also, in the photo in the right (b), located 60 km from river delta (reach 11) shows a riverbed that is not in natural status, with anomalous the exposure of the big rocks in the middle of the channel.

Dams

In the upper Erzen River catchment area, two dams can be found: the Skorana irrigation dam, constructed in 1973, and the Mudhar hydroenergy dam, built in 2014. Despite covering only 30% of the catchment area, it is worth examining whether these dams might have had a significant impact on the sediment supply, and therefore on the channel adjustment of the Erzen River further downstream, by trapping sediments that cannot reach anymore the lower part of the river. The Skorana dam has a catchment area of 166 km², accounting for 22% of the basin, and is located 15.3 km away from the study area (R11). On the other hand, the Mudhar dam has a catchment area of 51 km², accounting for 8% of the basin, and is situated 17.8 km away from the study area (R11).

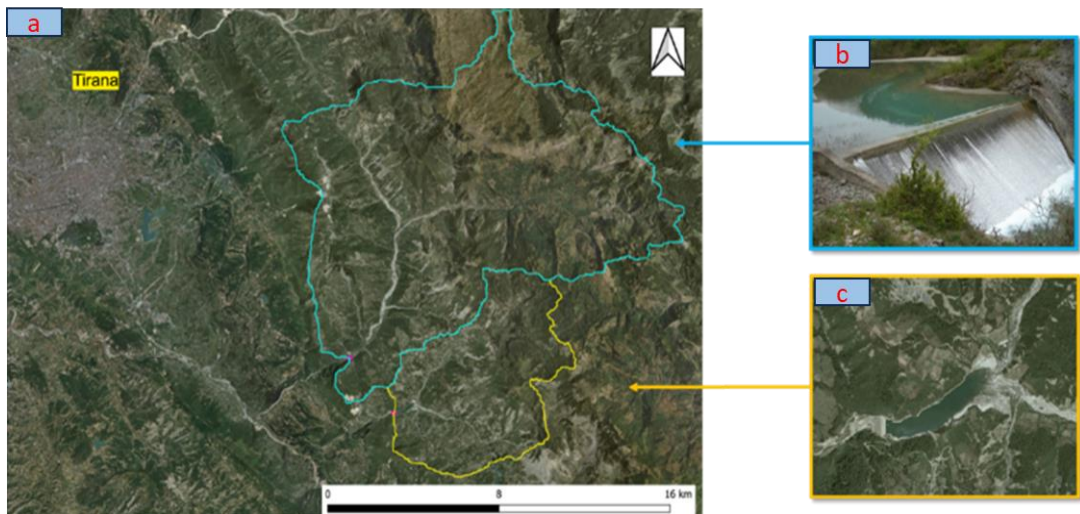


Figure 3. 29. Catchment areas covered by dams. (a) areas drained by the two dams. (b) view of Skorana dam, used for irrigation and built in 1972; (c) Mudhar dam, built in 2014 for hydroelectricity.

Figure 3.29 shows an overview of the two dams in the catchment. The irrigation dam looked as in Figure 3.29b in 2009. The analysis of changes in land cover based on the Landsat imagery is reported in Figure 3.30, which shows a progressive decrease until complete disappearance of the water land cover, followed by the disappearance of the bare sediment surfaces, with the entire reservoir area that became completely covered with sparse vegetation in the image of 2015. Furthermore, dense vegetation started to appear in the 2020 image, while it was almost completely absent in previous years. From the showed temporal

evolution, it can be reasonably hypothesized that the reservoir might have been completely filled with sediments in the period 2007-2012.

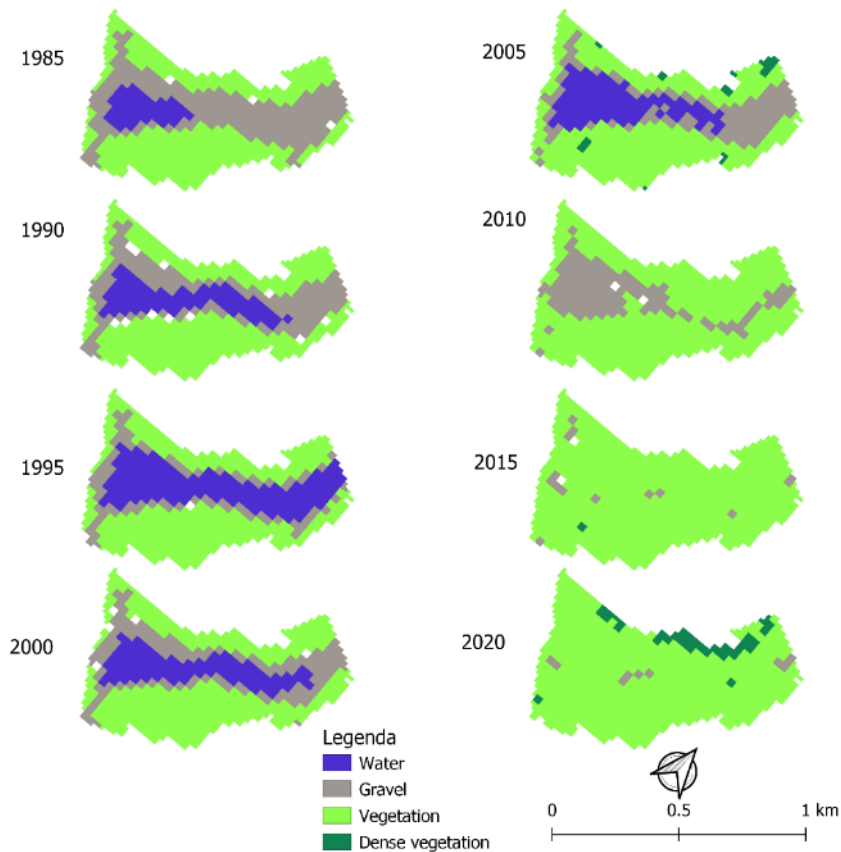


Figure 3. 30. Reach 16, immediately upstream the irrigation Skorana dam. Results of the Landsat imageries analysis showing the temporal changes in the land cover classes.

Knowing the reservoir volume of 2.3 million m^3 , it is possible to roughly estimate the amount of sediments trapped yearly by the dam. To account for the porosity of sediment in the range of 0.3 to 0.4, and therefore multiplying the reservoir volume by a coefficient of 0.65 yields a total sediment volume trapped by the dam of approximately 1.495 million m^3 , which can be rounded to 1.5 million m^3 .

By analysing Landsat images, and assuming a constant sedimentation rate in the entire period from dam construction to complete reservoir filling, the following estimates can be made. The available photo from 2009 suggested the dam's complete filling with sediment. Taking into consideration the dam's construction year as 1973 and assuming a 35-year span until reaching full sediment capacity in 2008-2013 (for possible uncertainties associated with water level oscillations in the reservoir, an annual sediment accumulation rate could be derived. This rate was calculated by dividing the total sediment volume in the dam (1.5 million m^3) by the 35-year period, resulting in 0.06 million m^3 /year or 60,000 m^3 /year (equivalent to 159,000 ton/year).

The estimate of the long term annual average sediment flux for the Sallmone gauging station of the lower Erzen river is 3810000 tons/year. This refers to the 1950-1975 period and includes the total suspended matter. Bedload was estimated at 20% (see Chapter 4). On dividing these numbers by the catchment areas of the Sallmone Station and of the dam, the two unit contributions are 6.05 tons/year/km² (Sallmone: 1949 – 1975, measured) and 0.96 tons/year/km² (Dam: 1973 – onwards, estimated). It must be noted that these numbers refer to different portions of the catchments, belonging to two different landscape units (Sallmone: plain; Dam: mountain) and to two different time periods with almost no overlap. For these reasons, they are hardly comparable *sensu strictu*. However, they appear to be of a similar order of magnitude, also considering that the gap between the two numbers (about 6 times higher in Sallmone than at the dam) would considerably reduce if (i) only the bed material load would be considered (excluding the washload at least from the Sallmone estimate and (ii) considering that the period to which the Sallmone measurements refer was characterized by higher sediment loads, according to the estimates of Chapter 4 (Figure 4.22).

Multi-decadal flow variability

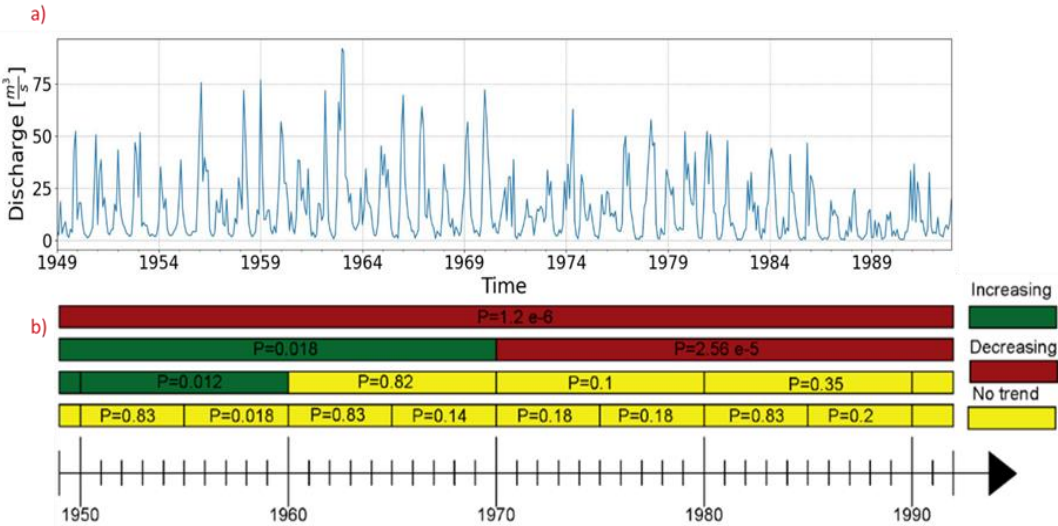


Figure 3. 31. Monthly average discharge and (b) results of the Mann-Kendall trend test on the same time series referring to Sallmone hydrometric station.

The monthly flow record in the lowest hydrometric station of Sallmone (reach 3) is reported in Figure 3.31a. Applying the Mann-Kendall trend test on a seasonal monthly basis revealed significant trends for the entire available period of data from 1949 to 1992. There was a strong decreasing trend observed, with a P-value of 1.2 e-6 for all period (53 years, upper red bar of figure 3.31b). Furthermore, when analysing trends over 20-year periods, the first half of the time frame (1949-1970) displayed a slight increasing trend (green portion of the second horizontal bar from top in figure 3.31b) with a P-value of 0.018, categorized as a moderate trend. Conversely, the second half of the period (1970-1992) showed a strong decreasing trend with a P-value of 2.56 e-5.

Additionally, the analysis was conducted at 10-year and 5-year intervals. In the 10-year analysis, the first decade (1949-1960) exhibited a moderate increase in trend, while no trend was observed in the subsequent years. The decrease in the flow regime and the magnitude of the floods after 1970 likely impacted channel narrowing and subsequently reduced sediment transport to the river.

Land cover change

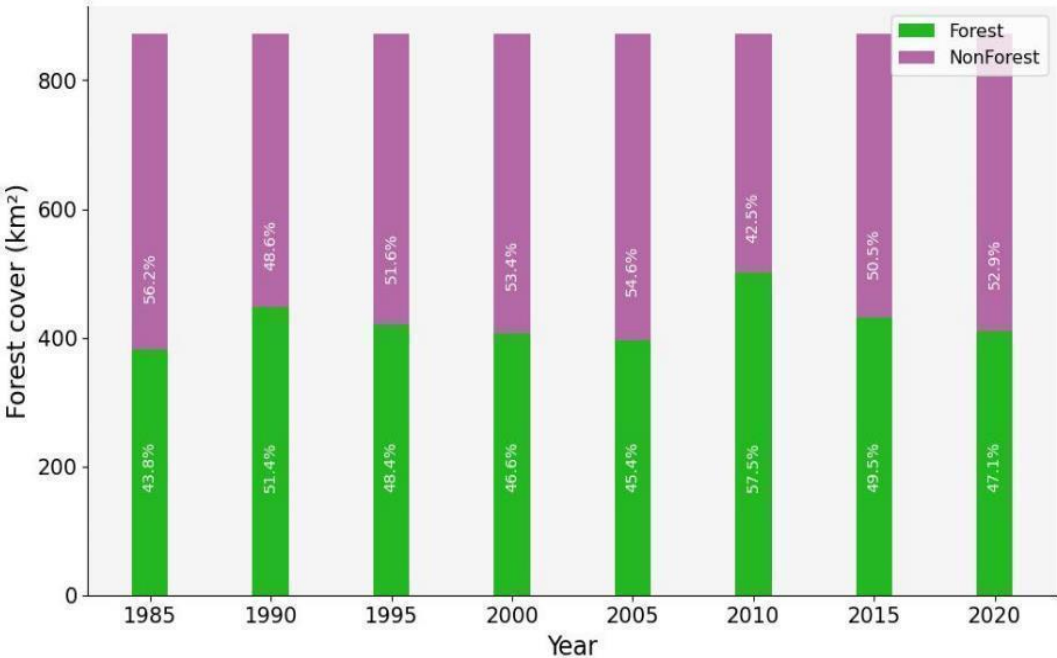


Figure 3. 32. Changes in forest cover Erzen basin

Using supervised classification with *LandTrendr* to assess forest cover based on 100 control points, the results indicated a relatively minor difference between forest gain and loss, with a range of around +/- 10%. This finding suggests a relatively balanced dynamics between areas where forest cover has increased and those where it has decreased. This result underscores the stability of forest cover changes within this range, indicating a relatively steady state of forest dynamics in the study area.

Urbanization

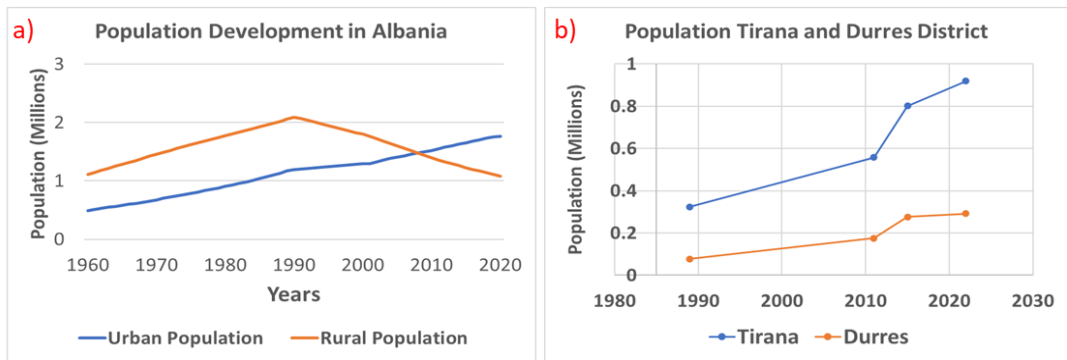


Figure 3.33. Urban and rural population Albania (figure a). Population of Tirana and Durres districts (figure b). World bank data, 2022.

The demographic increase in the country and in heavily urbanized parts can be used as a proxy of infrastructural development, to corroborate the semi-quantitative indications on the increase in sediment mining in the river channel. According to World Bank Open Data, 2022, the population of Albania experienced an increase from 1955 to 1990, reaching its peak in 1990 at 3.3 million. After 1990, there was a slight decrease in the population, reaching 2.8 million by 2023. Over the years, the urban population demonstrated a consistent upward trend. In 2010, the urban population surpassed the rural population. Conversely, the rural population displayed an increasing trend until 1990, followed by a constant decline, associated with both an increase in internal rural to urban migration and to migration outside the country.

Tirana, the capital city of Albania, and Durres are the two cities that stand out in terms of population concentration. These two districts collectively host around 40% of the population, with approximately 1.2 million people residing there. Tirana, in particular, accommodates nearly 30% of Albania's total population, amounting to around one million residents. Durres, with a population of 250,000, also contributes significantly to this urban concentration.

The population graphs for both Tirana and Durres illustrate consistent population growth. This growth can be attributed to the social-political changes in Eastern Europe, particularly the collapse of dictatorial regimes after 1990. Following this period, a substantial number of rural inhabitants, particularly from the northern regions of Albania, migrated to larger cities, seeking improved living conditions and access to better services.

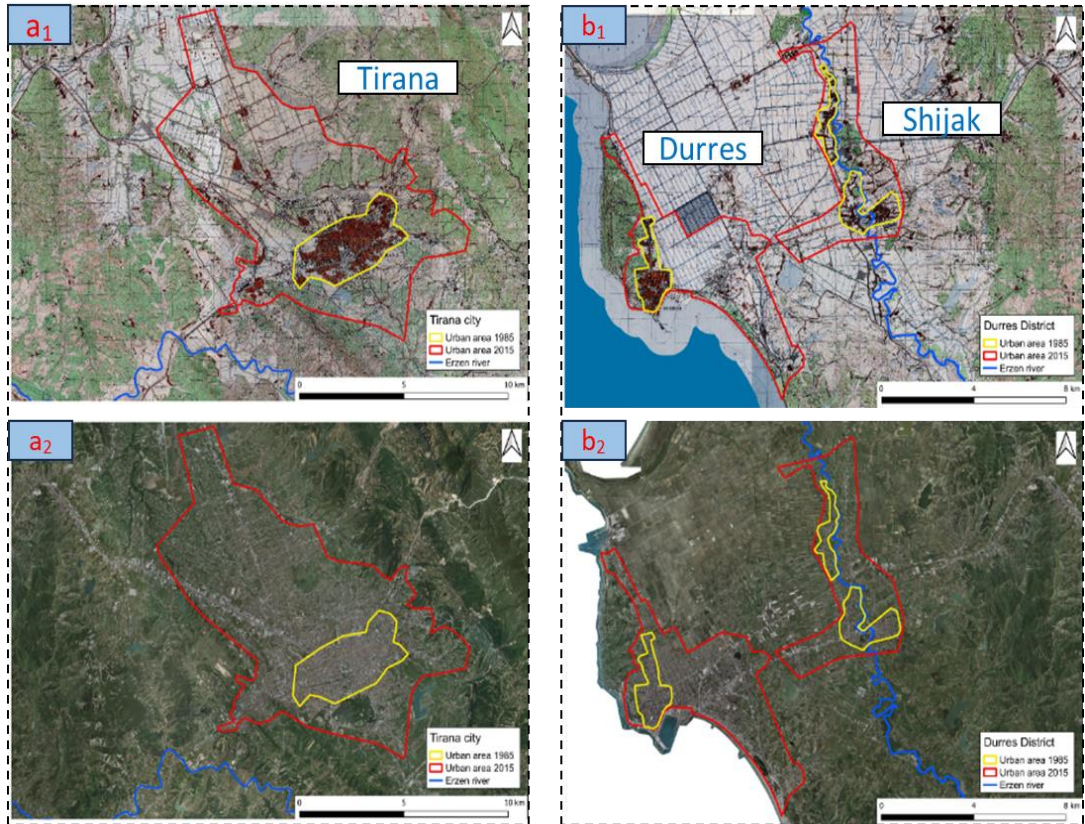


Figure 3. 34. Urban area Tirana and Durres district. Figure a₁ shows Tirana urban area with yellow in 1985 and figure b₁ with red line Tirana urban area in 2015. Figure b₁ shows the Durres district including two cities Durres and Shijak in 1985, urban area in yellow and figure b₂ shows in red Durres district urban area in red line.

Based on old military maps from 1985, the urban area of Tirana was roughly mapped at approximately 12 km². However, by looking at the orthophoto from 2015, it became evident that the urban area had expanded significantly to cover 97 km², marking an eight-fold increase in size. This rapid expansion is indicative of substantial urban growth and development over the observed 30-year period. Similarly, for the Durres district, the mapping of urban areas in 1985 encompassed approximately 3 km², including the cities of Durres and Shijak. In the present time, both cities, situated near the Erzen River, have seen their urban areas grow to cover a combined surface area of 8 km².

Furthermore, Durres city has experienced significant development from 1990 to 2010, particularly along the coastline near the Erzen river delta. This expansion has largely been driven by tourism, with many buildings operating for only 3-4 months during the peak tourist season in the summer. Despite having a limited number of year-round residents, this area experiences substantial construction activity due to its role in accommodating the seasonal influx of tourists.

3.5 Discussion

The work presented in this chapter aimed to quantify the characteristics of channel adjustments occurring in the lower Erzen river in Albania, a representative river system in the western Balkan area, with limited availability of historical data, and to investigate the potential driving factors. The results allow to clearly identify the occurring processes and provide a first quantification of their timescales and magnitude. The analysis of possible drivers also allows to identify which can be the main causes of the observed modifications of the active river channel. The present discussion focuses on: the quantification of the processes, also in relation to observed channel adjustments in other European regions and westernized countries, associated with the patterns of socio-economic development and related evolution of the hydromorphological pressures on river systems; (ii) the interpretation of the possible causal factors; (iii) a summary of the limitations of the present analysis and of the need for future work, and (iv) possible management implications of the observed phenomena.

3.5.1 Channel adjustments in the Erzen river and relation other contexts

The present analysis is one of the few that focused so far on the process of river channel adjustments in the Western Balkan region, and among the very few on Albanian rivers. Results for the Erzen suggest channel adjustment in Erzen River might have started in the late 1970s and is continuing up to now. The analysis cannot indicate to which extent it might have been occurring also previously, in the 1950s or earlier, due to the absence of accurate enough historical information. Given the known information on the country's history, channel adjustments in earlier times might have been caused by changes in the flow and/or sediment supply due to rather slow changes of the land cover due to internal country-scale mobilisation towards agricultural activities and related cooperative organization. A summary of the results on channel narrowing is reported in Table 2.8. Two phases can be distinguished. A first phase (1968-1985) when channel adjustments are milder, of different directions (narrowing – widening), in which the theoretical average narrowing rate is 0.1 meters per year in reaches 5, 8 and 11, with their narrowing rate decreasing upstream from reach 5 to 11. Such first phase is followed by a second phase characterized by much higher narrowing rates in the same reaches, for an average of 3.6 m/y, more than 30 times higher compared to the previous phase. During this second phase, a notable exception is represented by upstream reach 17, which displays narrowing rates that are instead of the same order of magnitude of those of reaches 5 and 8 in the first phase.

In Italy and several other western European countries channel adjustment has been documented already in the 19th century, with channel narrowing and without significant channel incision in the 1870 - 1950 period, and it has mainly been attributed to land cover change and a gradual reduction of flood magnitude and frequency with respect to the 1800s, especially in Alpine rivers (e.g. Marchese et al., 2017) to followed by dramatic changes in the 1950-1990 period. Such acceleration has mostly been driven by instream sediment mining and, in some cases, by large dam construction and operations in Italy, like in the Piave, Brenta, Cellina, Tagliamento, and Torre rivers (Surian, et al., 2009). These accelerated changes, however, started to decrease after 1990, when a more relaxed phase of

channel recovery has been observed in association with a reduced pace of anthropogenic pressures.

	Active channel width			1st phase		17	2nd phase		37	Entire period		54
	1968	1985	2022	1968-1985		narr. rate (m/y)	1985-2022		narr. rate (m/y)	1968-2022		narr. rate (m/y)
				Abs (m)	%		Abs (m)	%		Abs (m)	%	
R2	40	NA	15	NA	NA	NA	NA	NA	NA	25	63%	0.5
R5	180	150	50	30	17%	1.8	100	67%	2.7	130	72%	2.4
R8	260	250	60	10	4%	0.6	190	76%	5.1	200	77%	3.7
R11	195	230	120	-35	-18%	-2.1	110	48%	3.0	75	38%	1.4
R17	NA	180	120	NA	NA	NA	60	33%	1.6	NA	33	NA

Table 3. 8. Summary of observed channel narrowing in the five target reaches of the Erzen in absolute terms, percentage and average annual rates, for the two phases of adjustment and for the entire period of observation (abs: absolute difference; %: percentage relative to initial year: narrowing rate in meters per year).

Tables 3.9 and 3.10 summarize the magnitude of the documented narrowing (Table 3.9) and incision processes (Table 3.10) reported from different literature sources.

River Channel Narrowing in the World			
Country	River Name	Relative Narrowing (%)	Reference
Albania	Erzen	33-77	This work
Italy	Brenta	62	Surian et al. 2009b
	Piave	50	Surian et al. 2009b, Comiti et al. (2011)
	Orcia and Albegna	60-88	Surian and Rinaldi (2003)
	Trigno	75	Scorpio et al. (2015)
	Biferno	96	
	Volturno	84-87	
France	Arve	83	Peiry 1987 and Gurnell et al. 2009
	Eygues	59	Kondolf (2007) and Gurnell et al. (2009)
	Drôme	50	Piégay et al. (1997) and Landon et al. (1998) Kondolf et al. (2002) and Gurnell et al. (2009)
Poland	Dunajec	50	Zawiejska and Wyżga (2010)
	Porebianka	70	Korpak (2007) and Gurnell et al. (2009)

Austria	Danub	60	Hohensinner et al. (2004)
New Zealand	Waitaki	65	Hicks et al. (2007)
US	Pine Creek River	50	Kondolf et al. (2002)
Chile	Maipo	46	Arróspide Alarcón (2017)

Table 3. 9. Compilation of observed river channel narrowing rates in several European and World rivers. Adapted from Stecca et al. (2019) and other sources.

In the Erzen River in Albania, the evolutionary trajectory that emerges from the present study indicates relevant narrowing rates. The most intense changes have been shown in the period 1990-2015 in correspondence of the increased pace of economic growth, which led to intense sediment mining, which started to be regulated, with possible reduction, after 2010. Dams were built mostly after 1950 but so far, they have been much less affecting the river network compared to Italy or other European countries where the percentage of many catchment areas impounded by dams is often higher. The present study suggests that similar human pressures affect Albanian rivers compared to rivers in Italy and in Western Europe but they have initiated with a time lag of nearly 30 to 40 years, and within a period of 30 years for dam construction and 20 years of intense sediment mining. They have determined channel adjustments, in the Erzen River, of the same intensity, but occurring more rapidly, compared to the most impacted rivers from analogous human stressors, as previously documented in other European countries.

Compared with channel adjustment observed in other rivers of the world, the Erzen River stands in the range of the highest channel narrowing rates, particularly in its middle segment (50-60%) and in the lowland segment (range 60- 80 %).

River Channel Incision in the World			
Country	River Name	Channel Incision (m)	Reference
Albania	Erzen	4-5	This work
Italy	Piave Cellina, Tagliamento, Torre	2-4	Surian et al., (2009)
	Brenta	8.5	Surian et al., (2009)
	Trigno, Biferno, Volturno and Sinni	2-6	Scorpio et al. (2015) and Stecca et al., (2019)
France	Drôme	2-5	(Piégay et al. (1997), Landon et al. (1998), Kondolf et al. (2002)
	Arve	3-10	Gurnell et al. (2009) and Peiry (1987)
Poland	Dunajec	3.5	Wyżga (2008)

Spain	Cinca	2	Begueria et al. (2006)
New Zealand	Waitaki	3	Hicks et al. (2007)
Chile	Maipo	5	Arróspide Alarcón (2017)

Table 3. 10. Compilation of observed river channel narrowing rates in several European and World rivers. Adapted from Stecca et al. (2019) and other sources.

3.5.2 Possible driving factors of change

While multiple factors contribute to these transformations, one prominent influence is the impact of sediment mining activities. This correlation aligns notably with the accelerated urbanization and infrastructural development that emerged post-1990s. These anthropogenic interventions have likely introduced discernible disturbances to sediment transport patterns, yielding discernible effects on both the channel's morphology and sediment equilibrium.

Cukalla (2009) shows 22 mining sites along the Erzen river that are aligned with mapped sites observed from Google Earth and historical images (Geoportal Albania). The volume of sediment extraction from Erzen River till 2009 is estimated around 6 million m³, It accounts for 15% of total sediment transported every year.

In Albania, the huge growth of urbanisation occurred after 1990 when the dictatorial regime collapsed. Tirana alone in 30 years has been growing approximately by a factor of eight times, as it appears by comparing the military map of 1985 with the orthophoto of 2015. Durrës city has had the same very rapid growth. Coherently, the population data from the World Bank database show an increase in population in these two cities, and after 2010 urban population has overpassed the rural population in Albania. Further analyses have been performed using the Corine landcover images available for Albania for years 2000, 2006, 2012, 2018. Here artificial areas that represent the urban areas have shown a remarkable growth for both cities. Such indicators are proxy for the need of construction material which can be most conveniently mined from riverbeds close to the major urban centres.

At the same time, the financial crisis of 2009 has pushed many citizens of Albania who were previously living outside the country to invest in their homeland. This has determined an increase in building and investment in many sectors especially in the construction industry. Infrastructure development after 2000 has caused a growing demand for construction material, especially for gravel as primary resource for road stabilisation and building construction. During the period between 1990 and 2005, many rural roads remained unpaved, prompting local authorities to opt for river gravel as a cost-effective solution for road construction. This practice facilitated the use of river gravel as a readily available resource. However, a notable change occurred in 2005 with the implementation of a new legal reform. Under this reform, new roads were constructed using asphalt and gravel sourced from rocks, and a shift away from utilizing river gravel was initiated. This reform led, at least formally, to a reduction in the extraction of river gravel from significant rivers

in Albania. While specific data on this matter remains unreported, it underscores the impact of policy changes on resource use in the region.

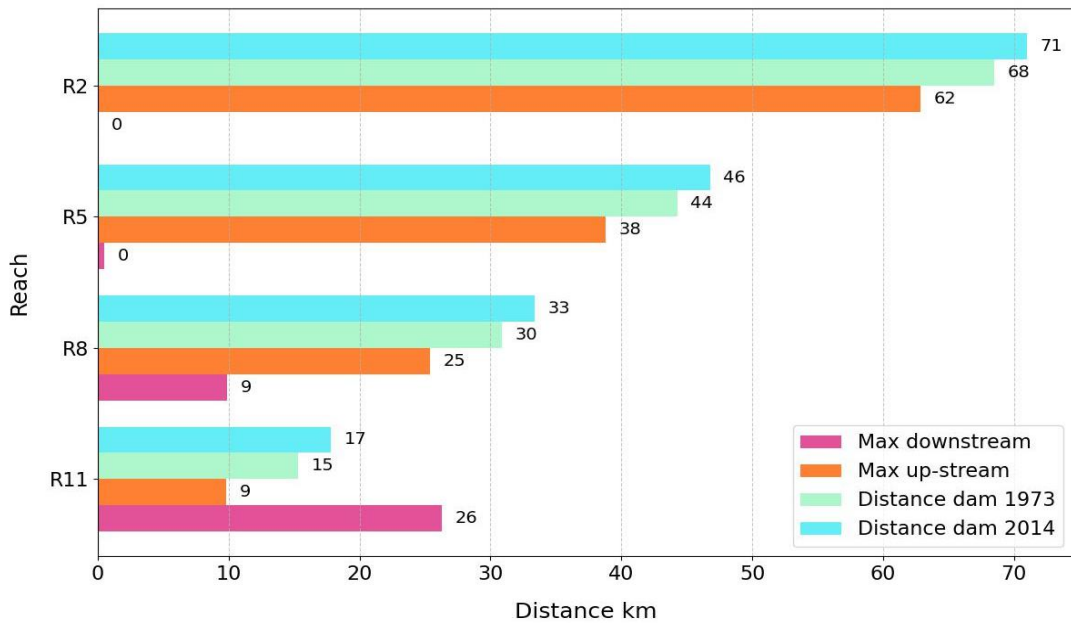


Figure 3. 35. Distance (km) of the downstream end of selected reaches from: the most downstream mapped sediment mining site in the catchment (“Max downstream”, violet bars); the most upstream mapped sediment mining site in the catchment (“Max upstream”, orange bars); the two dams built in 1973 (Skorana dam) and in 2014 (green and blue bars, respectively)

The dominant effect of sediment mining on the river channel adjustments, compared to the effect of the existing dams in the catchment, can be semi-quantitatively assessed referring to Figure 3.36. The most downstream mining site commences around reach 5, approximately 34 km upstream the river's delta, and extends upstream for further 42 km until reach 14. This equates to approximately 42 km of the river being exposed to mining activities. While there are two dams located further upstream, the Skorana dam (1973) is situated 5.5 km upstream, and the Mudhar dam (2014) is located 8 km upstream from the most upstream mapped mining site in the Erzen river. In essence, the lowest reaches, in which the processes of incision and narrowing have been most intense, are closer to the majority of the mining sites compared to the two dams. Furthermore, it may be deduced that the rate of sediment extraction by the mining activities from the riverbed is probably higher compared to the rate of sedimentation in the two dams.

For reach 2, Figure 3.35 reports that all 22 mining sites are positioned upstream along the river with the farthest site located 63 km upstream the downstream end of the reach, and all the other sites being closer, or much closer, to the reach. The Skorana dam (1973) is situated at 68.5 km, and the Mudhar dam (2014) is located at 71 km. Upon examining the map of sediment mining, it becomes apparent that 3 mining sites are within reach 5, while other 19

sites are located upstream. Reach 8 encompasses 2 mining sites downstream and 3 upstream, with 17 located upstream, spanning a significant 25.4 km. The two dams are positioned at 31 km and 33.5 km in this reach. In reach 11, 5 mining sites are present in the area, with 9 located downstream and 8 upstream, spanning a distance of 26.3 km downstream and 9.8 km upstream. The dams are situated at distances of 15.3 km and 17.8 km.

Upon evaluating these distances, it is likely that reaches 5, 8, and the lower reaches as well, are more significantly impacted by mining activities than by the other hydro-morphological stressors, as the two dams are located much farther upstream (Figure 3.35). Reach 11 is probably instead affected more relevantly by the two dams, due to its proximity to them. Quantifying the impact of sediment mining compared to other stressors on this middle course of the river is more challenging compared to the lower reaches, due to a more likely overlap between the two types of the stressors, dams and sediment mining.

The estimated annual gravel trapped by the dam is 60,000 m³, while mining activities are reported to contribute 300,000 m³/year, five times more than the Skorana dam. The other dam build in 2014 covers only 8% of the basin and is located on the Mudhar stream (tributary of Erzen). These numbers seems to imply that its effect is probably less dominant on reduction of the sediment supply downstream comparing to the sediment mining activities. The older Skorana dam, constructed in 1973, covers 22 % of the basin. and is situated in a very narrow canyon that might to have reduced the downstream passage of sediments, even in the absence of the dam.

Most of the hydropower plants in Erzen River are for the “run-of-the-river” type (two existing < 2 MW, and seven are planned). The envisioned hydroelectric power project presents potential challenges to the river's inherent dynamics.

Another examined factor that can cause channel adjustment that emerged from the analysis is the reduction in the monthly flow volumes, which may reflect a reduction in the frequency and magnitude of floods able to drive sediment transport. Floods reduction may could have started channel narrowing between 1965 and 1990, This factor seems to have been the dominant one only in the mountain reach 17, located way upstream the major dams and urban centres. Possibly, changes in forest cover in that part of the catchment might have added to the effect of gradually changing flow regimes. Both factors, in any case, are known to cause slow changes in the river trajectories, opposite from sediment mining or dams, which make the trajectories to “bend” more sharply. The observed trend in the upstream reach suggests assuming that, in the absence of rapid socio-political changes, and then of the related urban and infrastructural development, rivers would probably have narrowed also downstream, but at a much smaller rate than it has been actually observed. The differences between the trends observed in the upstream and downstream reaches can then be attributed to the direct human effects of sediment mining (in the lower reaches) and dams (in the middle reaches).

Mann-Kendall trend test applied to seasonal monthly data spanning 1949 to 1992 indicates a significant and consistent decreasing trend in the Erzen River's flow regime. The overarching 53-year period reflects a substantial decline, supported by a low P-value of 1.2

e-6. This long-term trend is characterized by a notable shift, with the first two decades (1949-1970) demonstrating a moderate increasing trend followed by a distinct and significant decrease from 1970 to 1992. Importantly, this trend in precipitation extends beyond the Erzen River, also other rivers observed in region with the data available have a decreasing trend of flow regime, such as Osum, Vjosa and Shkumbin river in Albania, showing similar discernible reduction in the annual and monthly flow volumes, which possibly correlate with a reduced frequency and magnitude of floods. The role of such reduction in flow volumes on the sediment transport capacity of the Erzen river is investigated in more detail in Chapter 4.

3.5.3 Limitations of the work

The limitations of this study predominantly stem from challenges related to data availability, which ultimately affect the accuracy and predictability of the river system's behaviour. The accuracy of our findings relies heavily on the data sources at hand. Our use of Landsat imagery with a resolution of 30 meters, along with orthophotos from geoportal Albania in 2007 and 2015 at a resolution of 20 centimetres, has provided valuable insights. Corona satellite images, although not comprehensively covering the entire river basin, have been extremely beneficial also thanks to their resolution of up to even 5-10 meters and offers a key opportunity to assess the active channel of the river back at the end of the 1960s, a key information that is lacking instead for historical cross-section data, which has made the task of precisely gauging channel incision. While trying to estimate incision over the past 30 years, the absence of clear historical cross-section information hampers the ability to discern the exact extent of channel evolution. The analysis of the accuracy of the classification has revealed that Landsat imagery was not suitable for the narrower, lower reaches, but also for the more recent configurations of initially wider reaches (like reach 5, see Appendix), for which the Landsat imagery were still rather accurate until the 1990s, but for which they became inaccurate because of the strong narrowing processes that occurred along the last decades in those intermediate reaches.

The availability of flow data also poses challenges. While accessed flow data span from 1950 to 1990 from three stations on a daily basis, data availability declines for the period thereafter. This data scarcity after 1990 poses difficulties in accurately predicting flow trends over the past two decades, limiting our ability to capture recent changes and trends in the river's flow regime.

Key areas warranting attention include monitoring (1) the river discharge in continuous and making the existing historical and recent data publicly available, at least for non-commercial, scientific purposes; (2) river sediment size distribution; (3) vertical channel adjustments through the monitoring of multi-temporal river cross sectional data, which were also measured in the past. Maintaining hydrometric station and providing accessible flow and topography data is pivotal in predicting flow trends, aiding flood mitigation, and maintaining a harmonious water balance among diverse stakeholders. Monitoring water turbidity emerges as an imperative task, as it directly informs water quality and sediment dynamics.

3.5.4 Management implications

The observed dynamics of the Erzen River present several challenges for river integrated management. Channel adjustment and reduction of sediment supply from the Erzen River likely significantly influences coastal erosion dynamics, causing a chain of interconnected processes. The decline in sediment transport due to factors like sediment mining disrupts the natural balance that sustains coastal equilibrium. The reduced sediment influx results in the weakening of protective coastal features, exposing the coastline to the erosive forces of waves and tides. This translates into the gradual erosion and recession of the shoreline, posing threats to coastal infrastructure and natural habitats. The study on Lazy Bay, Erzen river delta from (De Leo et al., 2017) found out up to 800 m of costal retreat by from 1985-2015 comparing historical satellite (Landsat) data. In this respect, future attention should be also paid must delve into the interplay between coastal erosion and other environmental processes.. For instance, a comprehensive examination of groundwater levels and the intricate interplay between saltwater intrusion and freshwater systems would be interesting, to assess possible effects of the nearby coastal erosion on the the availability of local freshwater resources and use of agricultural land. Indeed, the issue of drawing down the water table, prompted by the need for flood management, introduces another layer of complexity. Such measures might inadvertently intensify the challenges of coastal erosion. By lowering the water table, the interface between saltwater and freshwater can shift, allowing saltwater intrusion into freshwater sources. This not only affects the availability of drinking water, land use agriculture but also exacerbates erosion due to the corrosive nature of saltwater on the coastal terrain (Chang et al., 2011; Croucher and O’Sullivan, 1995).

Moreover, the implications of diminished sediment supply extend beyond mere incision. The muddy riverbed that replaces sandy areas due to insufficient sediment delivery impacts not only recreational activities along the river but also the broader coastal ecosystem. Reduced sediment availability affects the stability of coastal vegetation and habitats, compromising their resilience against erosion and contributing to habitat degradation. From the discussion with local habitants in the nearby of the lower reaches of the Erzen River, it was reported that the local population used to swim in the river until 1995, near 20 km upstream the delta, and the river water surface level at low flows was higher and the water much cleaner. Instead, now the riverbanks are vegetated, and water quality is dramatically worsened, and the river is deeply incised in the floodplain, much more than 20-30 years ago.

One of the key effects of channel adjustment is the reduction of the river's floodplain and its ability to absorb excess water during high-flow periods. Narrower and deeper channels may result in faster flow velocities, which can contribute to alter peak flows downstream. The low part of the Erzen River, Rrushkull and Jube village last ten years have an average to 3-4 times per year flooding, even with small intensity of the rainfall.

Maintenance of river structures poses a significant challenge for river managers, particularly in the context of channel adjustments. For instance, the bridge near Tirana at mainstream Erzen River, known as "Ura Peshkatarit," was replaced by another bridge adjacent to the old one. This replacement was necessitated by foundation damage caused by the altered channel

conditions. Similar concerns arise for other bridges along the river, where exposed foundations raise issues of structural integrity.

It is hoped that the present study can support a more sustainable planning of interventions to manage the river in the future with a multidimensional approach, which can account for the needs of the ecosystems that are more related to the river and to the local stakeholders.

3.6 Conclusion

In conclusion, analysis of the lower Erzen River underscores a series of profound alterations that have significantly reshaped its morphology and behaviour. Notably, the observed channel narrowing last 50 years, especially evident within the 30-60 % upstream range and spanning 60-80% downstream, Likewise, the extensive channel incision spanning nearly 40 km, averaging 4-6 meters up to 8 m, provides clear evidence to.

These pronounced alterations in river morphology carry consequential impacts. The substantial decrease in gravel areas implies potential habitat loss for aquatic life, posing challenges to biodiversity. Simultaneously, the noteworthy growth in vegetation. The findings underscore the urgent need for a comprehensive river management strategy and ongoing monitoring, encompassing sediment dynamics, urban expansion, hydrological intricacies, and potential impacts from both existing and planned infrastructure. As urbanization continues to exert influence, it is crucial to implement forward-looking and sustainable strategies that strike a balance between ecological preservation and societal needs, ensuring the ongoing equilibrium of the Erzen River ecosystem.

Chapter 4

4. Assessing the role of recent channel adjustments of Albanian rivers and of climatic oscillations on fluvial sediment inputs to the Adriatic Sea.

Abstract

This Chapter focuses on a sediment transport analysis focusing on the Albanian river with reported historical highest average annual sediment yield, of 5,222 tons/years/km², the Erzen River. The goal is twofold. The first goal is to propose a simple, repeatable approach to reconstruct the past temporal, inter-annual variability of yearly sediment loads to the sea from Albanian rivers, which accounts for the typical historical and present data availability for rivers in the country. The second goal is to assess the different roles of (i) the observed recent channel adjustments and (ii) climate and hydrological variability on the estimated sediment transport capacity of the river system in its lowland reaches, close to its mouth.

Historical streamflow data spanning from 1949 to 1992, data collection on site and from local agencies were used to calibrate a sediment transport capacity predictor that uses reach-averaged input parameter values and an instantaneous normal flow approximation. Few available historical data on recorded suspended sediment transport rates support the calibration of this predictor. It must be noted that the used data refer to the total measured turbidity of the stream, while the employed sediment transport predictor conceptually refers to the transport capacity of the suspended load only. Once calibrated, the predictor has been used to calculate the sediment transport capacity under various scenarios, taking into account changes in channel slope (aggradation or incision) and variations in channel width, which are the main characteristics of the lowland reaches of the Erzen river, as of many other ones in the region, which have been modified through channel adjustments resulting from increasing human pressures, as presented in Chapter 3. Predictions of changes in sediment transport rates, due to channel changes, can be of high relevance for effective river management and the implementation of sustainable practices. Estimates developed for the Erzen are compared with analogous ones from the nearby Shkumbin river, developed in another study. Results set an important baseline to further understand the sediment transport dynamics in the catchment. Such baseline could support studies aimed at quantifying the relationship between human activities at the river catchment scale and coastal erosion observed in the same landscape unit, considering the significant impact of fluvial sediment transport on coastal areas.

4.1 Introductions

Albania stands out globally with one of the highest rates of sediment transport per unit catchment area (Mulder and Syvitski, 1995), as exemplified, for instance, by the Erzen River, which records an impressive 5,222 ton/km² annually. Ishem River is reported to carry 3715 ton/km², and the Devoll River 3589 ton/km² (primary tributary of the Osum River).

This notable sediment yield suggests a likely high dynamicity of its streams, the need to properly account for sediment transport processes in river engineering measures, and also the potential implications for the dynamics of the coasts of the country, whose dynamics is likely supported by the high inputs of fluvial sediments. For this reason, investigating how the detected alterations in river channel morphology (Chapter 3) may affect the dynamics of sediment transport, and therefore, the related processes and implications, appears of some relevance. Such investigation is performed in the present chapter by drawing insights from established research on sediment transport capacity and applying simplifying sediment transport models to the Erzen River. Results allow to calibrate a predictive model of suspended sediment transport capacity for the Erzen river, to estimate the possible effects of the recent channel adjustments, and to formulate preliminary hypothesis that shall be further investigated in future work

Monitoring of sediment transport in Albania commenced regularly in 1948 and continued until 1992. After this period, measurements were irregular due to institutional changes, lack of funding, sociopolitical shifts in the country, collapse of the dictatorial regime after the 1990s and transition to the democracy and changing economic priorities. The institution responsible for these measurements was initially the Hydrometeorological Institute of Albania, now known as the Institute of Geoscience, which is presently formally an institution of the Polytechnic University of Tirana, and functioning as one of its departments. Before 1992 the Hydrometeorological Institute of Albania was a separate unit with an own Academy of Science, it had its budget and periodically published bulletins containing data on rivers, lakes, climate; it carried our research activities besides being responsible for monitoring hydrometeorological issues and analysing the data related data. The book "Hydrology of Albania," published in 1979, serves as a comprehensive compilation of water resource data in Albania from 1948 to 1975, summarizing periodic studies and measurements up to 1975. We use this book as a reference for long-term data on stream flows and sediment transport rates to calibrate the sediment transport capacity for Erzen river.

Additionally, the Institute of Hydrometeorology, through its Hydraulic Laboratory, played a crucial role in the design and modelling of the main dams in the Drin River (Drin cascade) constructed between 1970 and 1980. Notable examples include the Fierza Hydropower Plant (HPP) with 500 MW, Koman HPP with 400 MW, and Vau I Dejes HPP with 250 MW. It played a crucial role on to model the dams, and electrification of Albania in 1970.

During this time, the main focus was on collecting data to understand the specific characteristics of each river catchment. However, the scientific foundation for addressing sediment transport was somewhat limited, and the resulting knowledge may not have been

widely shared across the country. It's likely that fluid-mechanics-based and empirical sediment transport predictions were either unavailable or not widely used during this historical monitoring period and up to now limited study available in sediment transport area. Additionally, much of the literature used in academia originated from the Soviet Union (Albania relation with east countries) and was translated into Albanian. The literature on fluid mechanics in rivers primarily emphasized hydraulic design, with a stronger focus on designing hydraulic structures rather than focusing into comprehensive studies and predictions related to river engineering.

After the collapse of the dictatorial regime in 1992, the Institute of Hydrometeorology underwent significant changes. It transformed into a smaller unit, no longer receiving government financing as it had before (only covering staff wages), and its building was privatized for alternative purposes. The institute experienced a notable reduction in both budget and staff, leading to a less structured approach to data collection. From 1992 to 1994, regular data measurement in many stations stopped, and the office was relocated, resulting in some data loss. In this period until 1997, marked by the civil war in Albania, there was a lack of prioritization in hydrometeorology monitoring. The government's main focus during this time was stabilizing the country and establishing new "democratic institutions." Up until 1997, the country faced instability, with minimal foreign investment and donor support. Following this period, there was gradual improvement as the country stabilized economically, established institutions, and enacted new laws.

After 1997, data collection resumed but not consistently across all stations, data protocol procedures collection was not followed as before (1992), and accuracy were compromised. Budget constraints, staff shortages, and a lack of investment contributed to the decline in data quality. Since 2021, under new leadership, the institute has seen improvements. Some stations now use electronic measurements (smart hydrometric stations), but data accuracy remains a challenge due to maintenance fund shortages. Donations from organizations such as GIZ (German Agency for International Cooperation), AICS (Italian Agency for Development Cooperation), SIDA (Swedish International Development Cooperation Agency), UNDP (United Nations Development Programme). We can mention Italian cooperation have supported the water sector in Albania. Notably, the installation of a hydrometric station in Permet city on the Vjosa River in 2022, funded by AICS Albania in cooperation with the University of Trento (Italy), demonstrates ongoing efforts to enhance water monitoring capabilities.

As available sediment transport data refer to the pre-1990 period, and as considerable channel adjustments have occurred after that date, it is legitimate to wonder which impact on sediment transport rates were produced by these modifications of the channel geometry and morphology. Furthermore, as also some climatic variability has been detected with reduction of precipitation between the 1960s and the 1990s, also this effect may have contributed to alterations in the sediment transport regime of Albanian rivers. In the case of the Erzen River, extensive channel narrowing has been observed in the lowland and transitional reaches, ranging from 20% to 70% between 1985 and 2020. Additionally, there has been substantial channel incision, reaching depths of 5-6 meters. Over the period from

1985 to 2015, there has been an 800-meter coastal erosion in the mouth of the Erzen, specifically in Lalzi Bay (De Leo et al, 2017), accompanied by a decrease in the flow regime.

The goal of the work presented in this chapter is to develop an assessment of sediment transport of one of the highest sediment-producing river catchments in Albania, and in the entire Mediterranean, the Erzen River. The following specific aims are pursued:

- To review the available knowledge on the historical sediment transport measurements in the case study
- To explore the possible changes in the sediment transport capacity of the lower Erzen associated with the recent channel adjustments that have been analysed in Chapter 3

The above goals are achieved by calibrating and applying a simplified suspended sediment transport predictor for the Erzen River, and using historical hydrological data covering the period from 1949 to 1992, alongside on-site data collection from local agencies. The predictor utilizes reach-averaged input parameter values and a normal flow approximation.

The calibration process is supported by the limited historical data available on recorded total suspended matter or turbidity, which is conceptually different from the sole suspended sediment transport, mainly because of the washload contribution. Once calibrated, the predictor is employed to calculate suspended sediment transport capacity under various scenarios. These scenarios account for changes in channel slope (aggradation or incision) and variations in channel width, key characteristics of the observed channel adjustments of lowland river reaches in the Erzen River as it emerged from the analysis carried out in Chapter 3 of the present thesis.

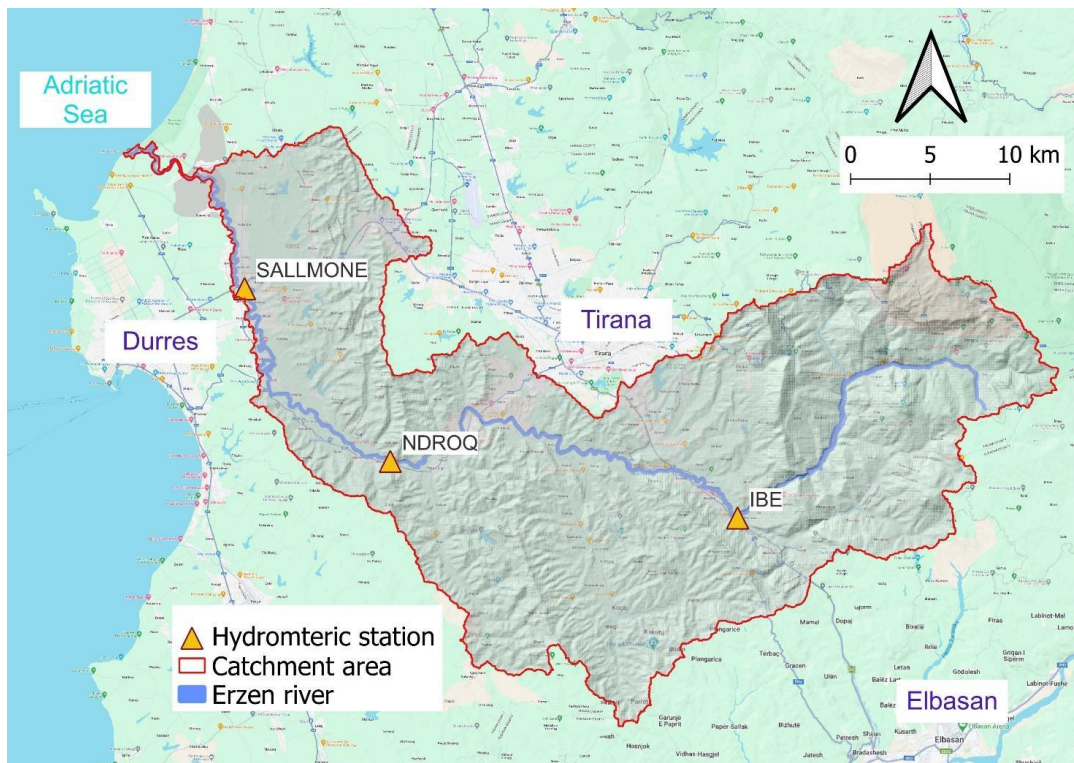


Figure 4. 1. Location of the main hydrometric stations in Erzen river. Sallmone hydrometric station located in lowland of the river that has been in operation since 1949; Ndroq hydrometric station starting from 1952 and Ibe from 1972.

4.2 Study Area and relevant gauging stations

The focus of the analysis is on the lower Erzen (Figure 4.1), with the aim to focus on the contribution of the fluvial sediment transport to its mouth, also because of its potential relevance for the coastal dynamics. The reasons for the choice of this station is that the sediment gauging station located in Sallmone is 15 km upstream the mouth of the river.

Historical measurements of the transported sediment grain size allow a characterization of some general features related to sediment transport. Figure 4.2 reports the grain size distributions of the suspended load and bedload as measured at the Ndroq and Sallmone stations based on a long-term average. These data are extracted from Hydrology of Albania, 1979 and represent the average of monitoring data from 1948 up to 1975. These data are used to calculate the sediment transport capacity in both station form Hydrometeorological Institute published on the book. The same information for the suspended load is reported in Figure 4.3 in the form of the cumulative distribution.

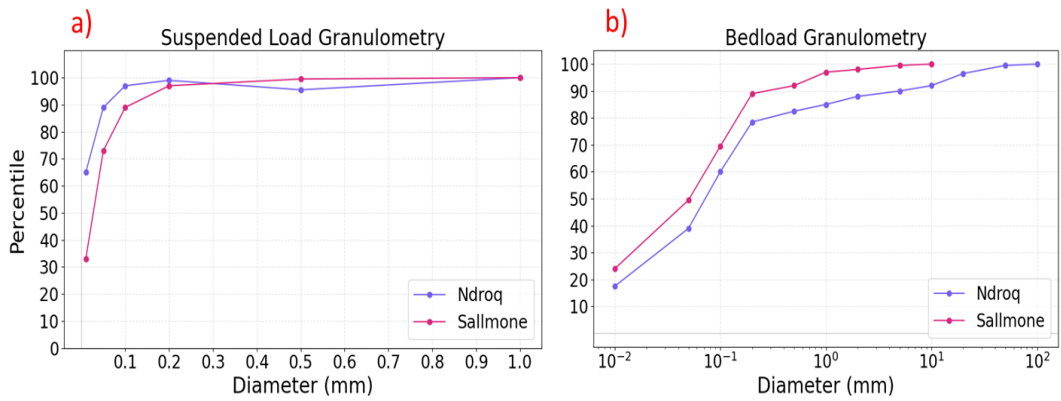


Figure 4. 2. Grain size distribution (mm) of at the hydrometric stations Ndroq and Sallmone. (a) suspended load grain size distribution. (b) bedload load composition grain size distribution.

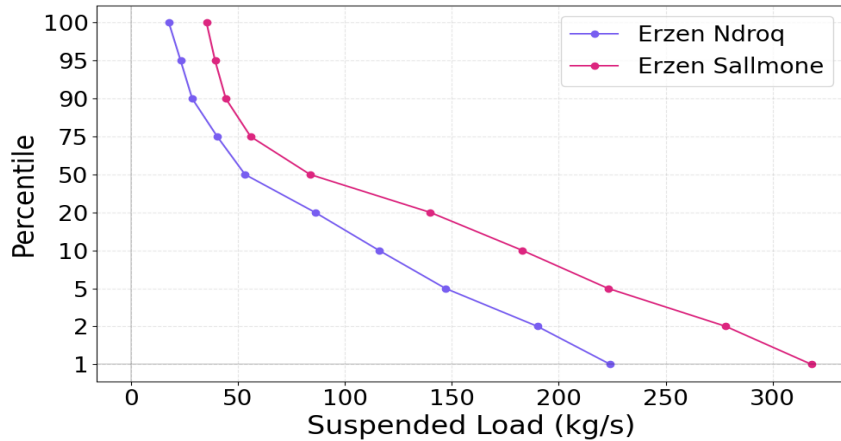


Figure 4. 3. Cumulative grain size distribution as measured for suspended load in Sallmone and Ndroq station. (Data Hydrology of Albania, 1979).

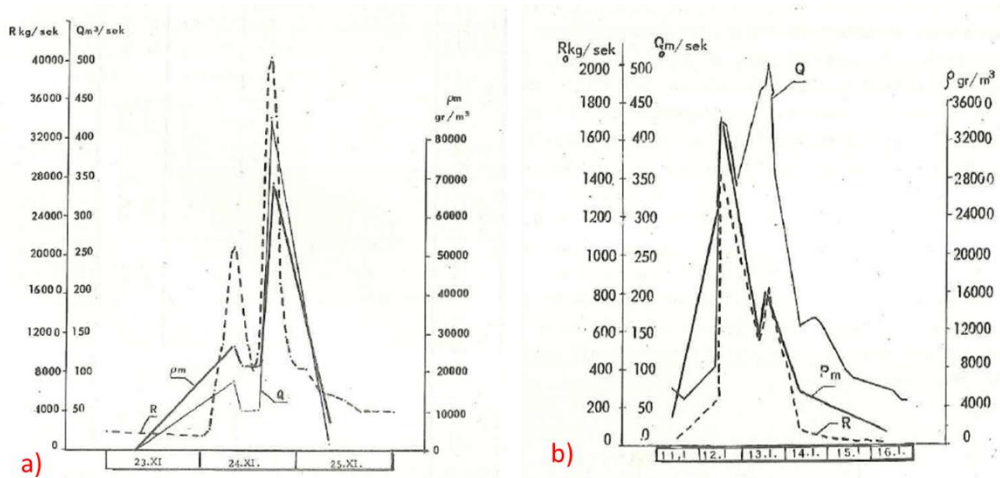


Figure 4. 4. (a) Ndroq from date 23-25.11.1966. Figure b) represent Sallmone 11-16.01.1966. R kg/s represent the sediment flow. Q m³/s represent the discharge and ρ gr/m³ represent the concentration measured.

Turbidity was collected regularly in the 1950s until the 1970s, and in some cases the frequency of measurements was intensified, as in correspondence of relevant flood events. Figure 4.4 shows two examples of monitored flood events in terms of instantaneous turbidity and flow discharge values. Maximum instantaneous turbidity for in Erzen has been recorded as 251000 gr/m³ in 28.08.1967 and in Sallmone 192000 gr/m³ in 14.09.1966.

Station	Year	Catchment area (km ²)	Q (m ³ /s)	Suspended Load (kg/s)	Concentration (gr/m ³)	Suspended load (ton/year)	Bedload (ton/year)	Washload (ton/year)	Total (ton/year)	Total (kg/s)
Ndroq	1964-1975	663.00	14.5	68.4	4720	2,150,000	430000	157000	2740000	87
Sallmone	1958-1975	755.00	18	101	5610	3,180,000	636000	195000	4010000	127

Table 4. 1. Main characteristics of hydrometric station Ndroq and Sallmone. The data refer to long term average values. (Hydrology of Albania, 1979).

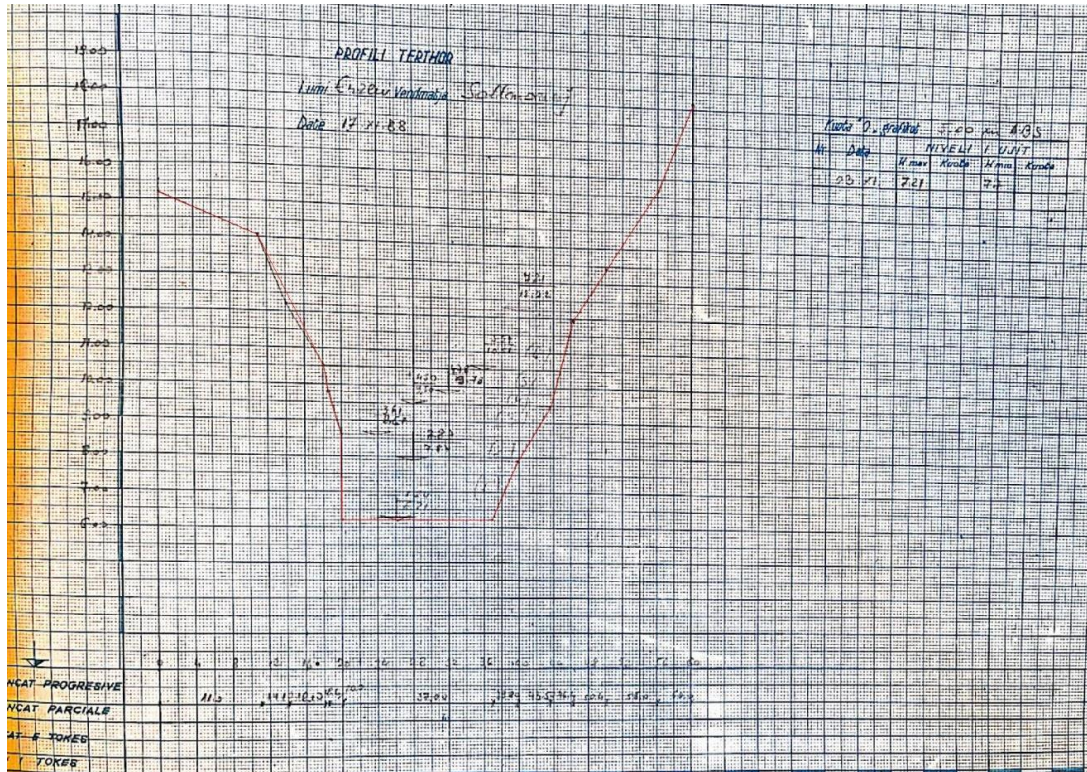


Figure 4. 5. Cross section Sallmone Hydro station 17.11.1988 (Archive institute of Geoscience Albania)

Also, the cross-sectional geometry was regularly surveyed, in association with discharge measurement campaigns (e.g. Figure 4.5)

3.3 Material and Methods

The description of Materials and Methods section is organized as follows. First, an overview about how sediment transport measurements in Albanian rivers were carried out in historical times is developed, by extracting and summarizing relevant methodological descriptions in the book Hydrology of Albania (1979). This allows to understand which type of sediment transport data are actually available from historical records (4.3.1). This is followed by a synthesis of the sediment transport data that were retrieved from the historical sources for the specific case of the Erzen river (4.3.2). The simple statistical methods used to analyse the historical flow records are then described (4.3.3), followed by a description of theoretical approaches to estimate incipient sediment mobility conditions (4.3.5) and sediment transport rates, with focus on predictors for the suspended sediment transport capacity (4.3.6).

4.3.1 Methods for historical hydrometric and sediment transport measurements in Albania

The primary literature source for estimating sediment transport in the Erzen River is "Hydrology of Albania," published in 1979 by the Academy of Science of the Hydrometeorological Institute. This book serves as a comprehensive compilation of data on water resources in Albania from 1948 to 1975. It extensively covers the characteristics of lakes, rivers, and lagoons, with a particular emphasis on the main rivers in Albania, including Drin, Mat, Ishem, Erzen, Shkumbin, Seman (which includes Devoll and Osum), and Vjosa. The text that follows is extracted and synthesized from this book.

The key parameters monitored for the rivers included discharge at gauge stations, suspended load, turbidity, water temperature, and physiochemical characteristics of the water. These parameters were measured on a daily basis (discharge, temperature, turbidity) and documented in periodical bulletins. The information was then compiled in book format and periodically archived.

The measurement of suspended sediment was conducted in conjunction with the measurement of the water discharge and separately from that. When taken during discharge measurements, turbidity samples were collected at the verticals where flow velocity was measured, while when they were collected separately from streamflow measurements, they were collected at a specific fixed location, where daily turbidity sample was collected. Through the calculated mass discharge of suspended sediment "R" (kg/s) and water discharge "Q" (m³/s), the average turbidity value ρ_m (kg/m³) representative for the entire river section is determined. Together with the mass of the solid matter present in the bottle samples, also its volume was measured to assess its density. Value " ρ_m " here represent the average of numbers measurement taken in the section daily where " ρ_v " represent just one sample and "n" number of samples taken in the section daily.

Turbidity measurements were taken once daily, with additional samples during extraordinary events associated with heavy rainfall. These samples, consistently collected from the same location, undergo pre-filtration and laboratory analysis. Daily turbidity tables are completed, capturing the volume of water sampled and the weight of suspended sediment.

At the conclusion of this procedure, for each measurement of suspended sediment discharge, which was carried out at different river levels throughout the year, we have the pair of data ρ_{vn} and ρ_m , where "n" is the number of measurements conducted during the year. With this data pair, the dependency $\rho_v=f(\rho_m)$ is established for the entire amplitude of the river level fluctuation throughout the year. This creates the possibility of converting daily turbidity to the point where the daily average turbidity sample is taken for the entire river section and especially to express turbidity values as volume concentrations (m³ sediments / m³ water), besides in the form of mass concentration (kg sediments /m³ water).

Subsequently, by having the daily average turbidity (g/m^3) and the daily discharge (m^3/second), it was possible to calculate the daily average suspended sediment inflow $R = \rho_m * Q$ and then the monthly and yearly average suspended sediment transport.

The manual summarized in Hydrology of Albania (1979) outlines the protocols and procedures employed at river gauging stations for the measurement of crucial parameters, including water level, discharge, temperature, turbidity, and suspended sediment. Water level readings were taken at least once daily, with additional measurements depending on station specifications. Timepoints for measurements could include three times daily at 08:00, 14:00, and 20:00, or in other cases twice daily at 07:00 and 17:00, or also one single measurement at 07:00. All measurements were recorded in a monthly summary table, and exceptional observations were documented separately for particular events which could be recorded when possible and outside fixed hours. The unit of measurement for water level is centimeters, and calculations were reported for daily averages, monthly averages, and maximum and minimum monthly levels.

For the measurement of water discharge, a range of tools, including flow meters, chronometer, tape measure, and calibrated pipe, were utilized. The process involved measuring the riverbed width, depth, calculating the sectional area and then integrating it with velocity measurements using a velocity-area method to determine the discharge. Technical staff typically conducted these measurements once a month or once every two months.

Simultaneously, water temperature was measured at the same intervals as water level, and daily averages were obtained from extreme hours. Monthly and yearly averages, along with maximum and minimum values, were determined at the conclusion of each period. The unit of measurement for water temperature was degrees Celsius.

4.3.2 Collection of historical discharge time series and digitalization for Erzen river in Albania

The first step of this analysis was made by searching the available historical sediment transport information, namely Hydrology of Albania (1979), archive data from Institute of Geoscience (former Hydrometeorological institute of Albania).

The data for the Erzen River were extracted/requested officially from the archives of the Institute of Geoscience, primarily based on daily flow discharge records from three main stations along the Erzen River. Subsequently, the data were digitized and pre-processed through discharge statistics analysis using the Gumbel method (Van Campenhout et al., 2020) (Clarke, 2002). The dataset covers the period from 1949 to 1992 for the Sallmone station, 1953 to 1992 for the Erzen station, and 1972 to 1990 for the Ibe station (Figure 4.6).

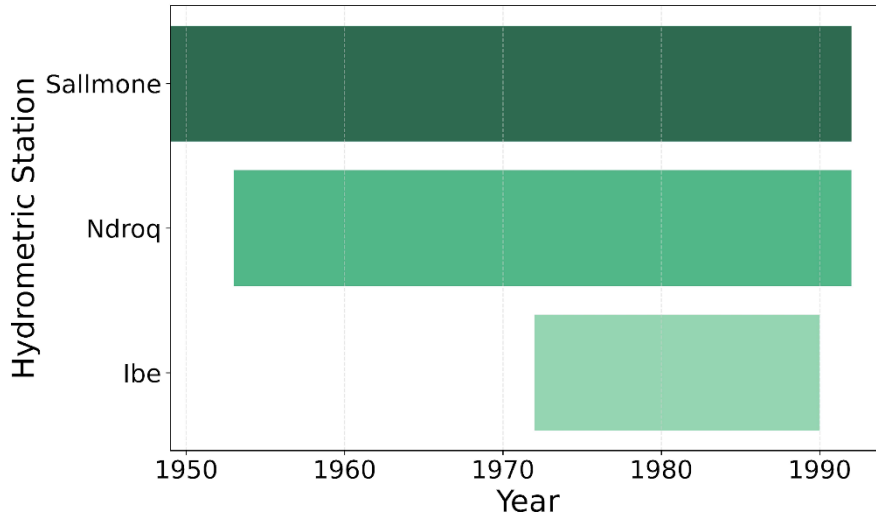


Figure 4. 6. Data digitalization daily/ data available for Erzen river

From the Hydrology of Albania 1979, the data on the average sediment transport average were extracted for two station available in the Erzen River Sallmone and Ndroq. The annual average data (calculated as average from 1949-1975), discharge (m^3/s), surface of the catchment at the gauge station, suspended matter transport rate (kg/s), concentration (gr/m^3), suspended load, washoad and bedload (ton/year) were calculated based on empirical coefficient for the lowland reaches of rivers (not Alpine river),

Because it could not be directly measured, the bedload was calculated as a fixed percentage (20%) of the measured suspended load and the total load was components of this three.

REPUBLIKA POPULLORE SOCIALISTE E SHQIPRISE
AKADEMIA E SHKENCËVE
Instituti Hidrometeorologjik

TH-10/1

PRURJA E UJIT m³/s

Lumi: Erzeni Vendndëzja: Sallmone VIII. 1976

Date	I	II	III	IV	V	VI	VII	VIII	IX	X	XI	XII
1	8.65	48.5	9.20	8.20	26.5	16.9	8.95	4.40	3.21	2.22	2.41	14.6
2	8.20	36.8	9.20	8.20	18.8	4.86	10.9	5.58	11.2	1.98	29.5	16.3
3	8.20	30.5	8.95	8.20	16.4	7.70	18.0	11.1	13.2	1.86	15.2	18.1
4	8.95	26.1	8.70	8.95	15.4	6.01	6.70	4.80	4.06	1.72	12.3	31.1
5	10.0	22.9	8.45	8.70	13.5	6.42	5.09	3.89	3.85	1.30	10.9	24.0
6	8.20	18.7	8.20	8.45	11.7	40.8	6.23	16.3	9.20	3.21	17.6	10.5
7	8.20	16.8	8.98	8.95	8.98	35.9	3.04	3.89	4.23	3.21	63.2	68.1
8	8.20	14.1	31.5	8.20	10.6	23.0	4.23	4.66	4.23	2.87	12.6	85.6
9	7.70	12.4	13.5	8.95	10.9	21.6	7.45	3.89	4.06	4.06	10.0	58.6
10	7.65	12.6	11.2	16.8	10.0	15.4	10.3	3.21	3.89	2.08	10.6	44.3
11	7.20	12.3	10.6	12.3	10.3	12.3	5.09	3.21	3.55	1.98	10.3	60.4
12	7.20	13.5	10.6	10.6	23.3	11.2	3.89	2.38	3.55	1.60	9.48	49.9
13	7.20	9.69	8.76	10.6	24.7	9.78	3.72	2.22	3.55	2.22	11.2	35.6
14	6.70	33.4	9.20	11.4	14.1	8.95	3.21	2.10	3.72	4.63	11.6	35.0
15	6.70	29.0	9.20	10.0	8.76	8.70	7.20	1.86	3.89	8.70	8.70	33.2
16	6.20	23.6	8.95	10.6	10.6	8.45	4.40	0.890	2.87	8.95	18.9	24.2
17	6.24	25.2	8.20	8.95	10.6	7.95	1.86	0.890	2.58	6.24	14.1	25.6
18	5.70	19.7	7.95	8.70	10.3	14.7	0.790	4.63	3.55	8.70	20.5	30.5
19	5.78	11.1	8.45	10.6	7.95	11.4	0.790	1.62	4.06	11.7	23.5	23.3
20	5.53	18.4	8.45	9.20	9.76	11.7	0.980	8.20	1.72	10.9	60.4	22.4
21	5.53	16.4	10.2	8.95	8.45	9.98	0.200	6.24	3.89	7.70	53.4	19.3
22	6.24	13.5	18.4	8.45	6.01	18.2	0.603	5.55	4.63	5.78	40.1	76.1
23	6.789	10.6	11.2	16.6	7.55	7.95	2.70	11.9	4.06	5.09	42.9	15.0
24	5.78	11.7	12.6	30.5	11.2	5.78	2.89	5.52	3.28	5.09	24.7	16.4
25	6.24	10.9	20.0	20.5	8.45	3.78	6.24	4.63	3.04	4.86	25.2	15.2
26	17.5	10.3	16.4	13.5	6.70	10.9	4.86	4.06	2.84	4.86	21.2	11.2
27	26.6	10.0	18.2	23.3	6.95	12.6	3.78	3.89	3.84	4.63	16.8	12.9
28	83.5	8.95	11.0	32.6	8.76	6.70	3.72	3.55	3.04	4.63	16.4	16.1
29	87.0	9.48	10.9	19.3	6.24	12.3	28.0	3.28	2.24	4.40	15.0	13.5
30	48.1	10.3	20.0	6.24	8.70	6.70	2.87	1.78	4.40	13.5	86.2	
31	47.1		5.76		5.78		4.63	2.70		39.5		30.5
MES	23.5	22.5	11.5	13.2	11.2	14.0	5.43	4.75	6.78	8.06	40.6	64.9
MIN	5.32	9.20	9.20	6.70	3.04	4.86	0.200	0.890	1.70	1.30	81.5	10.0
MAX	36.1	17.7	38.0	63.2	32.6	13.0	28.0	38.0	16.9	36.1	32.1	58.8

Prurja mesatare: 17.4 m³/s

Me e medha: 58.8 m³/s Me e vogel: 8.23 m³/s

Date: 8.11.1 Date: 31.11

Figure 4. 7. Example of data record sheet for 1976 for Sallmone station in Erzen river. Data representation are daily data in m³/s. The Sallmone hydrometric station, located near the town of Shihak in the Durres municipality of Albania, was operational from 1949 to 1992.

Having the daily flow data and relation between discharge and the sediment transport the sediment transport daily was calculated.

4.3.3 Flow Data processing

Daily Flows

An initial data quality check was performed to verify the presence of unrealistic flow rate values and/or sudden jumps from one day to the next. Subsequently, an examination was conducted to identify trends in the time series, as it is a main driver of river system dynamics and therefore an important driver of possible changes in sediment transport (Hussain and Mahmud, 2019). A plot of the daily flows in the three stations is reported in Figure 4.8.

Monthly Flows

Monthly discharge statistics were obtained from daily data, and the mean, median, standard deviation, and relevant percentiles were calculated. These parameters were graphically represented, and the following simple statistics are also reported: the coefficient of variation (Cv), and the second is the comparison of normalized flows between stations. Multidecadal trends in monthly flows were also examined, both across the entire series and by checking for trends within each month throughout the entire time series.

Annual Flows

Monthly flows were averaged per year, and a comparison was made between the three hydrometric stations using normalized flows. Additionally, the coefficient of variation (Cv) was calculated. Trends in annual flows were also assessed, both across the entire series and by investigating the presence of trends within each month over the entire time series.

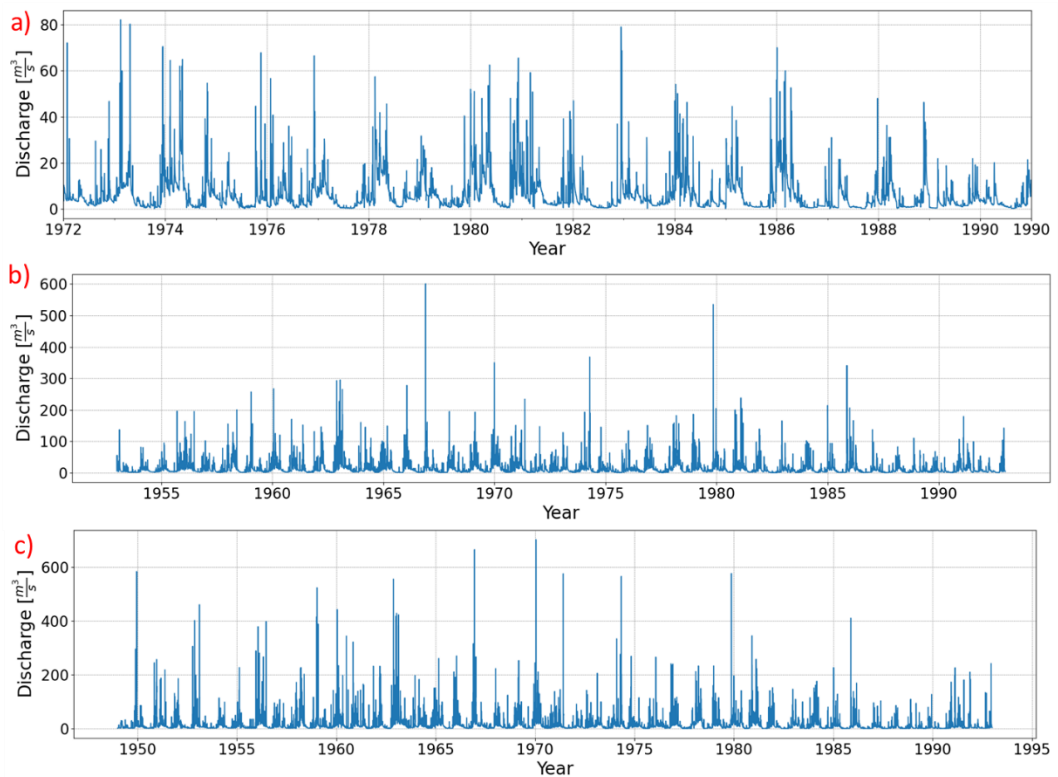


Figure 4. 8. Daily flow discharge (m^3/s) in the used three main hydrometric stations in Erzen River. a) Ibe hydrometric station; b) Ndroq hydrometric station; c) Sallmone hydrometric station.

Basic flow data pre-processing

The parameter Q^* - Normalized discharge was computed using the mean (Q) and standard deviation (s) of each time series, as follows:

$$Q^* = \frac{Q(t) - \underline{Q}}{\sigma} \quad (4.1)$$

- $Q(t)$ is the daily time series
- \underline{Q} is the mean of the time series.
- σ is the standard deviation of the time series.

$$\sigma = \sqrt{\frac{\sum_{i=1}^N (Q(t)_i - \underline{Q})^2}{N}} \quad (4.2)$$

The coefficient of variation, C_v (or relative standard deviation), is a descriptive statistical measure that quantifies the variability of the data record relative to its mean. In other words, it is a dimensionless numerical descriptive index that provides information about the variability of a quantitative variable, in our case, the flow rates.

$$C_v = \frac{\sigma(Q(t))}{\underline{Q}} \quad (4.3)$$

Among the most important parameters for discharge are magnitude, frequency, and duration. Therefore, in addition to a general statistical analysis, an analysis of events above threshold has been conducted, focusing on verifying these parameters. Only the Sallmone station has been considered, as it provides data on both discharge and information on grain size and cross-sectional area. The calculated thresholds include:

1. Discharges with return periods (TR) of 2, 2.5, 3, 5, 10, and 20 years.

Gumbel and discharges with different return periods

The Gumbel distribution is widely used in hydrology to analyse data related to extreme events, such as river floods. It is a two-parameter distribution with real parameters α for scale and u for location, and it is valid for $x \in \mathbb{R}$.

Given a variable X and a specific value x , it is possible to define the Probability Density Function (PDF), which represents the probability density, and the Cumulative Distribution Function (CDF), which is the probability of not exceeding a value x $P(X \leq x)$, indicating the probability that the variable X does not exceed the assigned value x . For the Gumbel distribution, the following relations apply:

CDF (Cumulative Distribution Function) $P(X \leq x; \alpha, u) = e^{-e^{-\alpha(x-u)}}$ (4.4)

Mode $m = u$ (4.5)

Median $\mu_X = u + \frac{\gamma}{\alpha}$ (4.6)

Variance $\sigma_X^2 = \frac{\pi^2}{6\alpha^2}$ (4.7)

The estimation of parameters of the distribution can be performed using various methods, including:

- Method of Moments
- Least Squares Method
- Maximum Likelihood Method

The Method of Moments allows parameter estimation by equating the sample moments to their corresponding population moments. The following relations are defined:

Sample Mean $\bar{x} = \frac{\sum_{i=1}^N x_i}{N}$ (4.8)

Sample Variance $S_X^2 = \frac{\sum_{i=1}^N (x_i - \bar{x})^2}{N - 1}$ (4.9)

First-order Sample Moment $M_{X1(\text{par})} = \int_{-\infty}^{+\infty} xp(x; \text{par})dx$ (4.10)

Second-order Sample Moment

$$M_{X^2(par)} = \int_{-\infty}^{+\infty} (x-M_{X^2})p(x; par)dx \quad (4.11)$$

The parameters are determined by solving the following system, in which the moments of the distribution are equalled to the moments of the sample:

$$\begin{cases} M_{X^1(par)} = \bar{x} \\ M_{X^2(par)} = S_X^2 \end{cases} \quad (4.12)$$

The least squares method allows finding a function that closely approximates a set of data. In particular, the function aims to minimize the sum of the squares of the distances between the observed data points and those on the curve representing the function. Specifically, it is necessary to order the available data in ascending order and calculate their frequency.

$$F_j = \frac{j}{N+1} \quad (4.13)$$

where F_j is the frequency of the data located at the j -th position, N is the number of data points; after which, the minimization proceeds by minimizing the sum of squared residuals (SSR), which is the sum of the squares of the differences between the observed and predicted values.

$$SSR = \sum_{j=1}^N (P(x_j, par) - F_j)^2 \quad (4.14)$$

where P is the chosen probability distribution, par indicates its unknown parameters, the values of which are to be determined, and x_j is the value of the j data point.

The maximum likelihood method starts with the assumption that the data are statistically independent, allowing the transition from conditional probability to the product of individual probabilities.

$$P(x_1, x_2, \dots, x_N \vee par) = \prod_{i=1}^N P(x_i \vee par) \quad (4.15)$$

Subsequently, maximization is performed through partial derivatives, which can be simplified by applying the logarithm function:

$$L = \text{Ln} \left(\prod_{i=1}^N P(x_j \vee \text{par}) dx^n \right) \quad (4.16)$$

$$= \sum_{i=1}^N L_n (P(x_j \vee \text{par}))$$

After calculating the derivatives, they are set equal to zero. Solving the resulting system allows for the identification of the unknown parameters. To determine which method to use, we use the Pearson test, a non-parametric test that helps identify the best method for parameter estimation.

$$\chi^2 = \sum_{i=1}^k \frac{(n_i - n_{pi})^2}{n_{pi}} \quad (4.17)$$

Where k is the number of intervals, n_i is the number of data falling into the i interval, and n_{pi} is the expected number of values based on the considered distribution. Once the best method is identified, the calculation of the return period can be carried out.

The return period T_R is defined as the average time interval, typically expressed in years, that must be waited for an event equal to or exceeding a certain intensity to occur.

$$T_R = \frac{1}{P(X > x)} = \frac{1}{1 - P(X < x)} \quad (4.18)$$

The following thresholds, based on the percentiles of the distribution of the streamflow values in the record, have been used for the identification of return periods for all three stations:

- Discharges greater than the 25th percentile.
- Discharges greater than the 50th percentile.
- Discharges greater than the 75th percentile.
- Discharges greater than the mean.
- Discharges greater than the 95th percentile.

4.3.4 Estimate of incipient sediment mobility conditions

The concept of the sediment motion threshold refers to the specific flow and boundary conditions at which sediment transport initiates. While it cannot be precisely defined with absolute certainty, empirical observations from various experiments have yielded reasonably accurate and consistent results in laboratory conditions, (Chanson, 2004) but the prediction of such a threshold in field conditions, as for sediment transport rates, is known to represent a serious open challenge (Gomez and Church, 1988).

From a theoretical, fluid-mechanics based viewpoint, the initiation of sediment motion can be estimated through a force balance acting on the individual sediment particle:

- Drag force is the hydrodynamic resistance force represented by R and calculated using the equation (4.20)
- Lift force is represented as P and calculated using the equation (4.21)
- Gravity force is denoted as G and calculated using the equation (4.22)
- Buoyancy is represented by B and calculated using the equation (4.23)

The frictional resistance (4.19) assumed to be proportional (Coulomb friction) to the resultant of the normal components of the forces acting on the particle, through a suitable friction coefficient C_A . This coefficient depends on the nature and shape of the particles. The particle begins to move when C_A reaches the value of the tangent of the friction angle ϕ : $C_A = \tan(\phi)$.

$$A = \tan\phi(G-B-P) \quad (4.19)$$

$$R = C_R\alpha_2d^2\rho\frac{u^2}{2} \quad (4.20)$$

$$P = C_P\alpha_2d^2\rho\frac{u^2}{2} \quad (4.21)$$

$$G = g\rho_s\alpha_3d^3 \quad (4.22)$$

$$B = g\rho_s\alpha d^3 \quad (4.23)$$

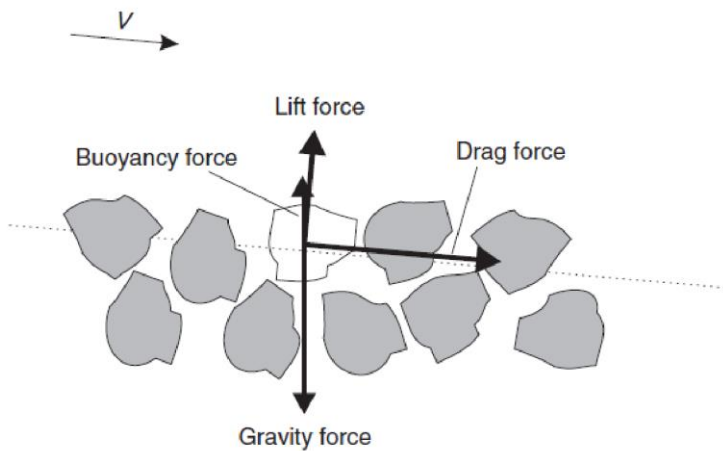


Figure 4. 9. Forces acting on a sediment particle (Chanson, 2004)

The gravity force and the buoyancy force act both in the vertical direction while the drag force acts in the flow direction and the lift force in the direction perpendicular to the flow direction (Fig. 4.9). The inter-granular forces are related to the grain disposition and packing.

Within the equations determining the forces, $\alpha_2 d^2$ represents the cross-sectional area of the particle, where α_2 is an appropriate shape factor; α_3 is the volume of the particle. C_R and C_P are the coefficient of hydrodynamic resistance and the coefficient of lift respectively.

On the other hand, the hydrodynamic forces tend to move the material, transporting it downstream. At the moment of detachment, the resistance force R is equal to the Coulomb friction force A (Eq. 4.24)

$$R = \tan\phi(G-B-P) \quad (4.24)$$

Shields (1936), through experimental analysis, where he used homogeneous non-cohesive particles, a horizontal bed, and a logarithmic velocity profile, determined the critical bed shear stress by proposing a dimensionless mobility parameter q , which could be used to assess whether sediments were moving by the flow under the condition of q being larger than a threshold q_c . The Shields dimensionless mobility parameter is defined as follows:

$$\theta = \frac{U_*^2}{g\Delta d} \quad (4.25)$$

The threshold Shields parameter θ_c has been determined to weakly depend on the particle Reynolds number under controlled laboratory conditions. Such dependence is represented in figure 4.10. The parameter Re is the particle Reynolds number, which is defined as follows:

$$Re = \frac{U_* d}{\nu} \quad (4.26)$$

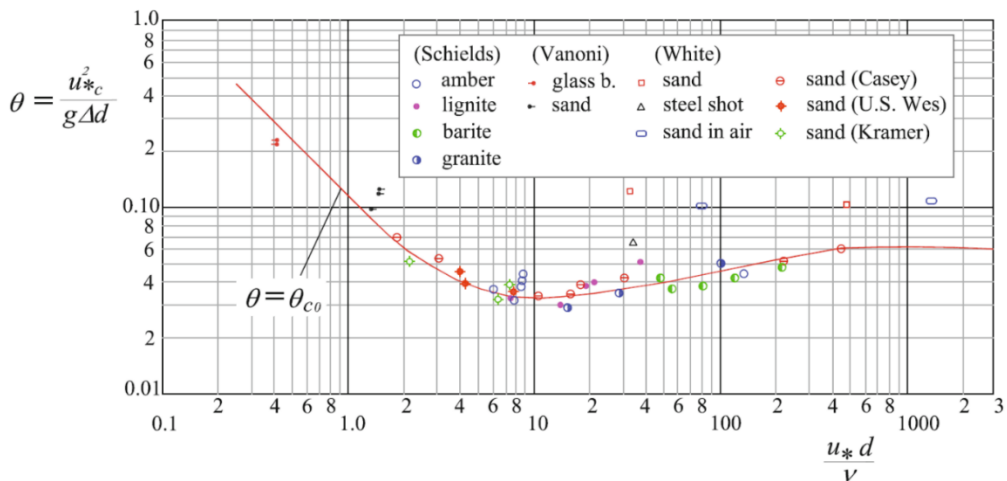


Figure 4. 10. Threshold Shields stress for sediment mobility or “Shields diagram” (reprinted from Armanini, 2018, and based on Shields, 1936).

Figure 4.10 distinguishes between the region of particle mobility (points below the line $\theta=\theta_c$) and the immobility zone (above the line $\theta=\theta_c$). The discharge at which bed material movement initiates $\theta=\theta_c$ is known as the critical streamflow / flow rate that determines the critical shear stress. Moreover, the graph can be further divided into three distinct zones:

- When $R_e \leq 2$ is a hyperbolic relationship. The friction velocity is independent of the particle diameter but depends on the fluid viscosity:

$$\theta_c = \frac{0.12}{R_e} \quad (4.27)$$

- When $2 < R_e < 200$, where the mobility condition depends on both the fluid viscosity and the sediment diameter. The minimum value occurs around $R_e \approx 8 \sim 10$, corresponding to $\theta_c \approx 0.03 \sim 0.04$.
- When $R_e \geq 200$, in which the mobility condition is not dependent on the fluid viscosity and tends to a nearly constant, asymptotic value:

$$\theta_c \approx 0.057 \quad (4.28)$$

To determine the critical flow rate in the Sallmone, reference is made to the constant part of the curve since $R_e > 200$. By substituting Equation 4.29 into Equation 4.28, Equation 4.30 is obtained, which is set equal to the bed shear stress with the assumption of a wide rectangular channel (Eq: 4.31). The equality of τ_c is then systematized with the Chezy formula for flow parameterized according to Gauckler-Strickler (Eq: 4.32).

$$U_*^2 = \frac{\tau_c}{\rho} \quad (4.29)$$

$$\tau_c = 0.057 \rho g \Delta d \quad (4.30)$$

$$\tau_c = \rho g i_f h_c \quad (4.31)$$

$$Q_c = K_s B \left(\frac{\tau_c}{\rho g i_f h_c} \right)^{5/3} \sqrt{i_f} \quad (4.32)$$

The Shields theory presented so far refers to incipient bedload conditions. The historical sediment transport measurements refer to what could be called “suspended matter” (e.g., Figure 4.11), which includes both the sediments transported as suspended load, which can settle within the flow once the Shields parameter reduce, the washload, the set of dissolved

sediments in water, and, possibly, organic material. In this thesis the threshold $\theta_c = 0.057$ has been chosen as a reference for the computation of a reference discharge value above which it is likely that some suspended load transport occurs, and does not pretend to represent the exact discharge value at which sediment mobility actually initiates in that particular section. It is rather a conventional value that allows to develop a realistic estimate of the characteristics of flood events able to determine sediment transport.

4.3.5 Estimation of Sediment Transport capacity

Sediment transport in rivers and streams involves the movement of materials like silt, sand, gravel, and boulders, categorized into bed load and suspended load. Bed load refers to grains rolling along the riverbed, while suspended load consists of grains kept in suspension by turbulence. Sediment transport begins when the bed shear stress surpasses a critical value, leading initially to bed-load transport and, for higher flows, also to suspended-load transport. Particle motion in bed load occurs by rolling, sliding, and saltation, with the particle keeping in frequent contact with the riverbed. The threshold of sediment motion defines the conditions under which sediment transport starts. Sediment suspension occurs when turbulent agitation keeps particles surrounded by fluid without frequent bed contact. Wash load refers to fine particles in suspension that do not interact with the bed material and are mainly dissolved in water (Chanson, 2024).

Sediment transport based on the magnitude of hydrodynamic forces and resisting forces, can be classified into three modes:

- Bedload transport
- Suspended load transport
- Wash load transport



Figure 4. 11. Conceptual diagram of the different modes of sediment transport in rivers (Chanson, 2004)

Wash load transport when, with an increase in flow velocity, the fine material may not be readily available in sufficient quantity at the bed to meet the transport capacity requirements.

It depends on the amount of material coming from upstream. This chapter does not consider the wash load transport due to the lack of data availability.

Bedload transport can occur through rolling or saltation. Armanini reports as follows: in the case of rolling, typically, the submerged weight of the particle is greater than the buoyancy force. In saltation, on the other hand, the buoyancy force acting on the particle exceeds its submerged weight. As the particle lifts, the buoyant force decreases, and the particle falls back to the bed after covering a relatively short distance, roughly on the order of its diameter. Because the buoyancy force is closely related to the flow velocity, and gravity force can be related to the fall velocity in stagnant water of a body, the transport mode essentially depends on the ratio between the fall velocity (W_s) and the shear velocity (U^*) of the flow (Armanini, 2021).

- Rolling bedload transport

$$6 > \frac{W_s}{U^* > 2} \quad (4.33)$$

- Saltation Bedload transport

$$2 > \frac{W_s}{U^* > 0.8} \quad (4.34)$$

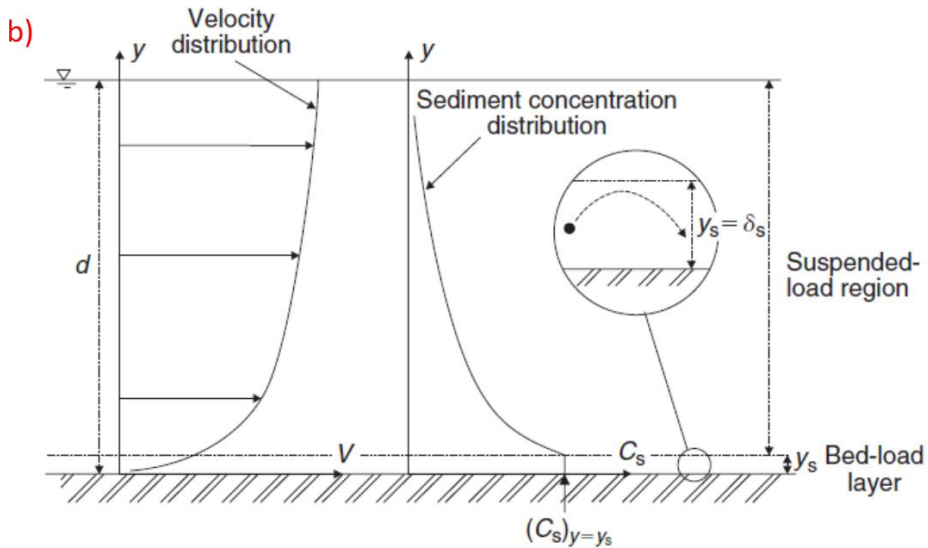
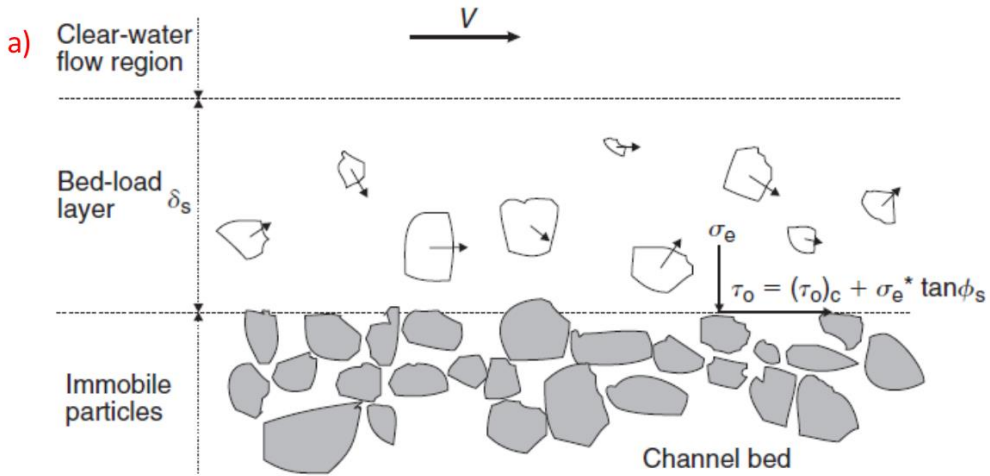


Figure 4. 12. Bed-load motion layer (a) and (b) definition sketch of the suspended load layer (Chanson, 2004)

The bed-load transport rate per unit width may be defined, in a general form as:

$$q_s = C_s \delta_s V_s \quad (4.35)$$

Where C_s is sediment concentration in the bedload layer, d_s is the thickness of the same layer and V_s is the average speed of the sediments in the same layer.

Sediment suspension can be described as the motion of sediment particles during which the particles are surrounded by the fluid. The grains are maintained within the mass of fluid by turbulent agitation without (frequent) bed contact. Sediment suspension takes place when

the flow turbulence is strong enough to balance the particle weight. According to Bagnold, a particle is transported in suspension when its fall velocity in stagnant water (W_s) is lower than the local turbulence intensity. Since the turbulence intensity is scaled by the shear velocity, the indicative parameter for the onset of suspended transport is a mobility index expressed in terms of the fall velocity (Eq. 4.36). The threshold value of the Shields mobility parameter can be expressed in this case (suspended load) as:

$$(\theta_c) = \frac{W_s^2}{g\Delta d_{s0}} \quad (4.36)$$

Suspended load transport occurs when in the force balance acting on particles, the buoyancy force (induced by turbulence) significantly outweighs gravity. In this case, the trajectory of a single particle is at least on the order of the water depth. The main force acting on suspended particles is the buoyancy force induced by turbulence, and since it depends on the shear velocity (U^*), it is reasonable to assume that there exists a critical value of shear velocity for particles of a certain diameter, beyond which they are transported in suspension.

The critical mobility parameter value for suspended transport depends on the characteristic diameter, according to Equation 4.36, for values below 40-100. However, it becomes independent of the characteristic diameter for higher values.

According to Bagnold, the threshold value of the ratio W_s to u^* for suspended load initiation is 1, while according to Van Rijn, it falls between 0.15 and 0.25. For our work, the shear velocity has been considered equal to the fall velocity of a particle in stagnant water, and the critical parameter is set as the curve derived from Shields. Therefore, it is assumed that suspended transport occurs when bedload transport is also present. For the concentration distribution, the Rouse solution has been used, where the diffusion coefficient is derived from the logarithmic velocity law and the triangular distribution of Reynolds stresses, following classical equilibrium assumptions. The Rouse vertical concentration profile reads:

$$C_s = (C_s)_{y=y_0} \left(\frac{\frac{h}{y} - 1}{\frac{h}{y_s} - 1} \right)^{\frac{W_s}{K U^*}} \quad (4.37)$$

Where h is the water depth, y is the depth, and y_s is the distance from the bottom where suspended transport is considered. Rouse assumes that the ratio of the water depth to this distance from the bottom is 0.05. The suspended transport is given by:

$$q_s = \int_a^h C_s U dy \quad (4.38)$$

Where q_s is the suspended sediment transport per unit length. The concentration $(C_s)_{y=y_0}$ is determined using the Van Rijn closure formulas:

$$(C_s)_{y=y_0} = \frac{0.117}{d_s} \left(\frac{\nu^2}{(s-1)g} \right)^{\frac{1}{3}} \left(\frac{\tau^*}{\tau_c^*} - 1 \right) \quad (4.39)$$

$$a = 0.3d_s \left(d_s \left(\frac{(s-1)g}{\nu^2} \right)^{\frac{1}{3}} \right)^{0.7} \sqrt{\frac{\tau^*}{\tau_c^*} - 1} \quad (4.40)$$

Where s is the ratio of the particle density to the water density ρ_s/ρ . A ratio of 0.65 is imposed on the sediment concentration at the bottom (Chanson, 2004).

In this chapter, sediment transport has been estimated in Sallmone station as a time series from the time series of discharges available (1949-1992). Since the station is located in the lower part of the Erzen river, the major part of total sediment transport is suspended load and bedload is likely to represent a small proportion, which historically was assumed to be about 20% of total load. Such assumption, though reasonable, however cannot be verified.

4.3.6 Calibration of the simplified model for sediment transport capacity

The calculation of suspended sediment transport was carried out only for the Sallmone station, because it combines both the longest and more complete data availability in terms of channel cross-section and discharge and the fact of being the one located most downstream and therefore closer to the mouth of the Erzen river. For this reason, estimates of sediment transport at this station represent the best information that could be used also to assess possible effect of changing sediment transport patterns on the dynamics of the nearby coastline. The model was calibrated by adjusting the two variables that presented the highest uncertainty in their estimation, at least with reference to the historical conditions to which the flow record refers: sediment diameter and channel slope. The data used for calibration has been the average annual suspended and bedload transport from the "Hydrology of Albania 1979", a reference value ($3810 \cdot 10^3$ ton/year) for suspended load. Bedload was calculated based on simplified formula of Nielson 1992, considering a simplified model.

Therefore this was a different method from the highly simplified approach used in "Hydrology of Albania 1979", in which bedload was computed as a fixed percentage, 20%, of the suspended load. For the calibration of suspended load, we accepted an error of 2%. The Nielson (1992) formula for bedload reads:

$$C_s = 0.65$$

$$\frac{\delta s}{ds} = 2.5(\tau^* - (\tau^*)_s) \quad (4.41) \text{ Nielson (1992), simplified formula for bedload}$$

$$\frac{\delta s}{ds} = 4.8$$

$$q_s = C_s \delta_s V_s \quad (4.42) \text{ Equation of Van Rijn for bedload, 1984}$$

$$\tau^* > (\tau^*)_s$$

The used discharge data of the Sallmone station for calibration were those from 1949 to 1975 because sediment load data used for calibration were obtained by averaging measurements corresponding to these years.

From the calibration of suspended sediment load, a sediment diameter of 0.0014 m and a slope of 0.00045 m/m were obtained, as those providing the best representation of the long term average, These values were kept unchanged for all the period. For bedload transport, the diameter was chosen as slightly higher, 0.002 m and clearly the same channel slope was maintained.

The cross section of the channel in Sallmone hydro station was taken from archive of the Institute of Geoscience, surveyed in 1988. Other available cross-sectional surveys showed that the topographic profile of the section has been rather stable across several decades. An equivalent rectangular cross section with identical discharge under uniform flow was derived from the original, irregular cross-section, and was used for the suspended sediment transport computations. An implicit assumption has been that such cross section maintained its transport capacity for the entire calibration period (1949-1975). An equivalent width of 23m was obtained for the rectangular cross section in Sallmone.

The calibration was carried out using the Python package "channelflowlib" for a rectangular channel. This package relies on the assumption of a wide rectangular channel, possibly leading to underestimation of the actual normal flow depth.

The calibration was carried out using the Python package "channelflowlib" for a rectangular channel. This package relies on the assumption of a wide rectangular channel, which is a limit.

Table 4. 2 summarizes the parameters and calibration results, while Figure 4.13 illustrates the volume of transport.

Qs ton/year (Hydrology of Albania,1975)	Qs ton/year (calibrated)	Error (%)	d (mm)	Slope (m/m)	B (m)
$3810 \cdot 10^3$	$3816 \cdot 10^3$	2	0.0014	0.00045	23

Table 4. 2 Calibration parameters for suspended load in Sallmone hydrostation

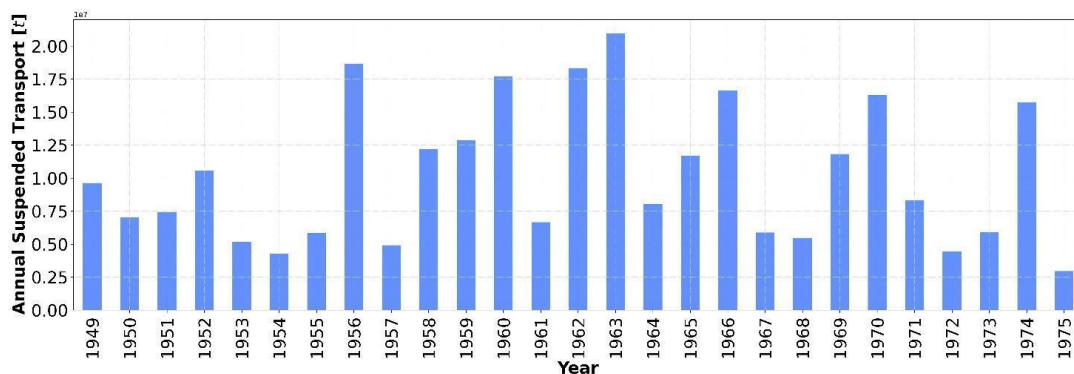


Figure 4. 13. Calibrated suspended sediment transport in Sallmone station as average of year

Once the model is calibrated, the estimation of suspended sediment transport is conducted for the entire discharge time series, spanning from 1948 to 1992. The Mann-Kendall statistical test is then applied to these estimates to detect the presence of any trends. As from Chapter 3, several indications that incision and narrowing of the channel has been occurring, possibly also during the latest part of this time period, the predicted estimates of the sediment transport capacity were plotted against different values of channel width and slope, which are likely to have been affected by the incision and narrowing process, and also assessed against discharge variation.

4.4 Results

4.4.1 Discharge statistics

Analysing the normalized discharge rates from the three hydrometric stations 4.14 reveals coherence. To assess whether there is indeed a good correlation between the data from the three stations, the R-squared (coefficient of determination) and the MSE (mean squared error) are calculated.

In Figure 4.15, pairwise comparisons of the stations are made by plotting the normalized discharge rates on a scatter plot. The R-squared values range from 0.736 for the comparison between Sallmone and Ndroq station, to 0.527 for the comparison between Ibe and Ndroq station. This difference is attributed to the percentage and distribution of watershed areas covered by each hydrometric station. Ndroq and Sallmone are closest stations between each-

other, Sallmone station covers the biggest catchment area with 780 km², Ndroq 663 km² and Ibe with 247 km², while the distance between Sallmone and Ndroq is 24 km, and between Ndroq and Ibe is 31.1 km. We see a better correlation between Sallmone and Ndroq stations because they are closer to each other and the length of the data record is much longer compared with that of the upstream Ibe station. The correlation of Sallmone and Ibe station has an $R^2 = 0.67$ and the one between Ibe and Ndroq stations has an $R^2 = 0.527$. Such difference may not be an indication of poor data quality, since there are contributing subcatchments between the closest stations of Sallmone and Ndroq, between which, in addition, a relevant water intake for irrigation purposes is present since several decades, thus potentially reducing the correlation between the monthly average discharge values, particularly during the irrigation season.

The MSE (mean squared error), ranging from 0.26 Sallmone and Ndroq correlation, 0.33 Ibe and Sallmone while for Ibe and Ndroq to 0.49, is relatively high that can be contributed to the dam build and the Ibe station length of data only for 20 years, while for Ndroq and Sallmone the data are for 50 years.

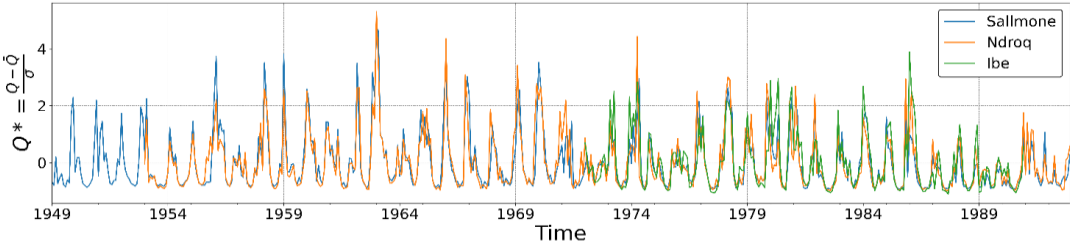


Figure 4.14. Monthly normalized discharge for the three hydrometric stations

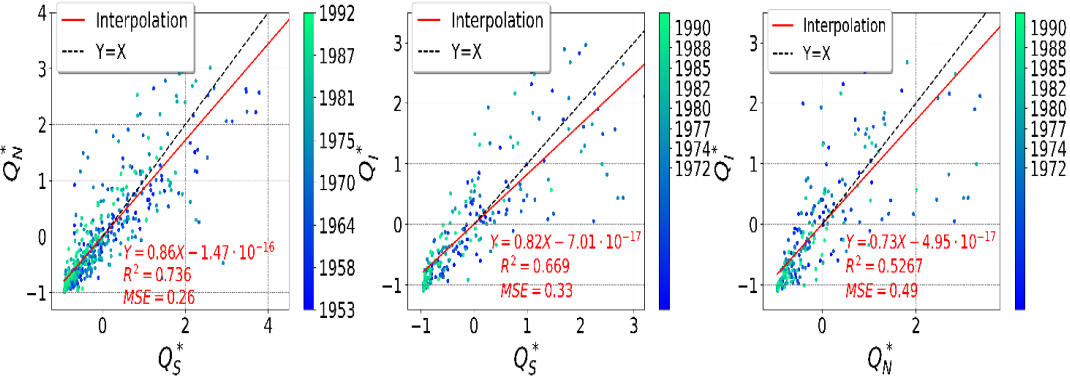


Figure 4.15. Correlation of monthly normalised discharge between pairs of the three hydrometric stations.

The hydrological regime of the Erzen river is that of a typical Mediterranean river, with high discharge in the winter period and low discharge in the summer (see the normalized flow rates in Figure 4.14 and the distributions in figure 4.16).

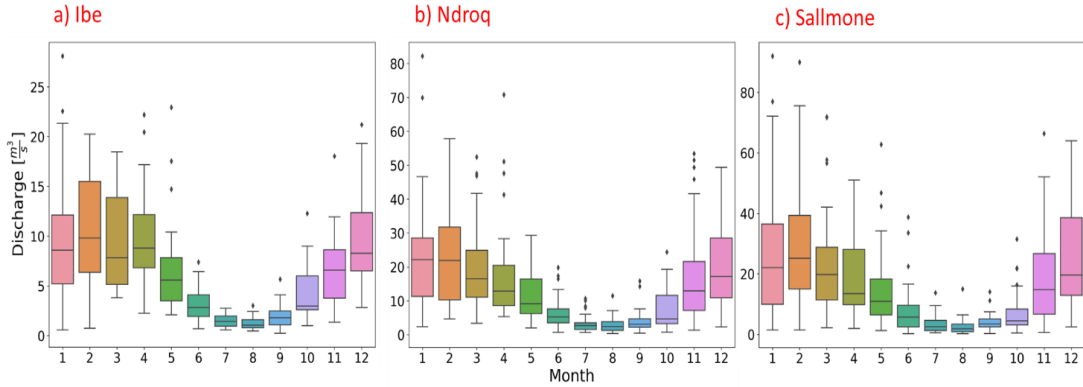


Figure 4. 16. Monthly distributions of daily discharge values for each of the three examined gauging stations in the Erzen River.

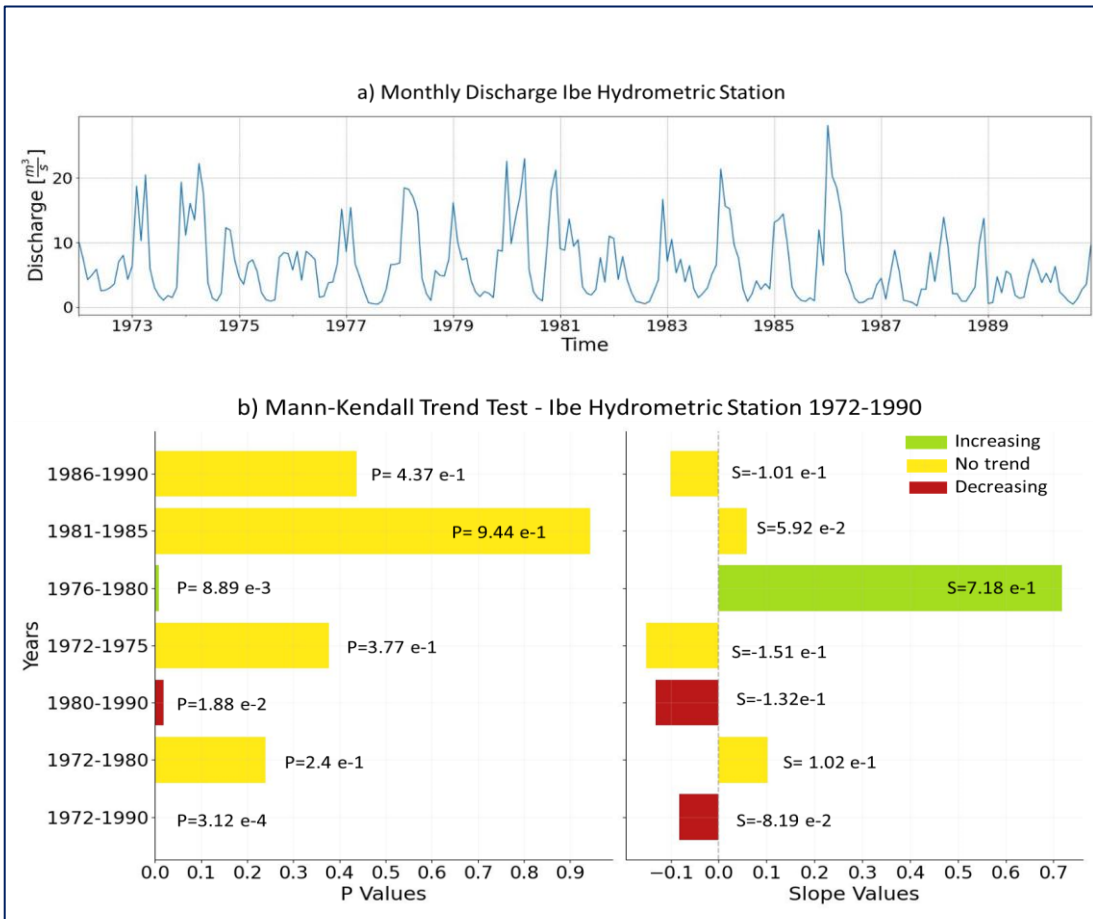


Figure 4. 17. Discharge (m^3/s) information for the Ibe hydrometric station in Erzen River. (a) monthly mean discharge time series. (b) Results of the Man-Kendall trend test for the Ibe hydrometric station between 1972-1990 applied to mean monthly data computed from daily data.

The Mann-Kendall test was applied to each data record in each station separately for different time periods: the entire period (1972-1990 for Ibe, different for the other stations), each twenty years (for long enough flow records), ten years, and five years. In the Ibe station (Figure 4.17), for the entire period (1972-1990), a significant decreasing trend was observed, with a very small p-value of $3.12e-4$, indicating the significance of the trend. The corresponding Mann-Kendall test score (Slope) was found to be $-8.919e-2$. From 1980 to 1990, there was also a decreasing trend observed, with a p-value of $1.88e-2$ and a Mann-Kendall test score of $-1.32e-1$. During the period 1976-1980, there was a significant decreasing trend with a p-value of $8.89e-3$ and a Mann-Kendall test score of $7.18e-1$. However, for other periods analyzed, there were no considerable trends observed.

For the analysis of discharge trends at the Sallmone hydro station, already conducted in Chapter 3, the results closely mirror those of the Ndroq Station. This similarity can be attributed to the proximity of these two stations to each other.

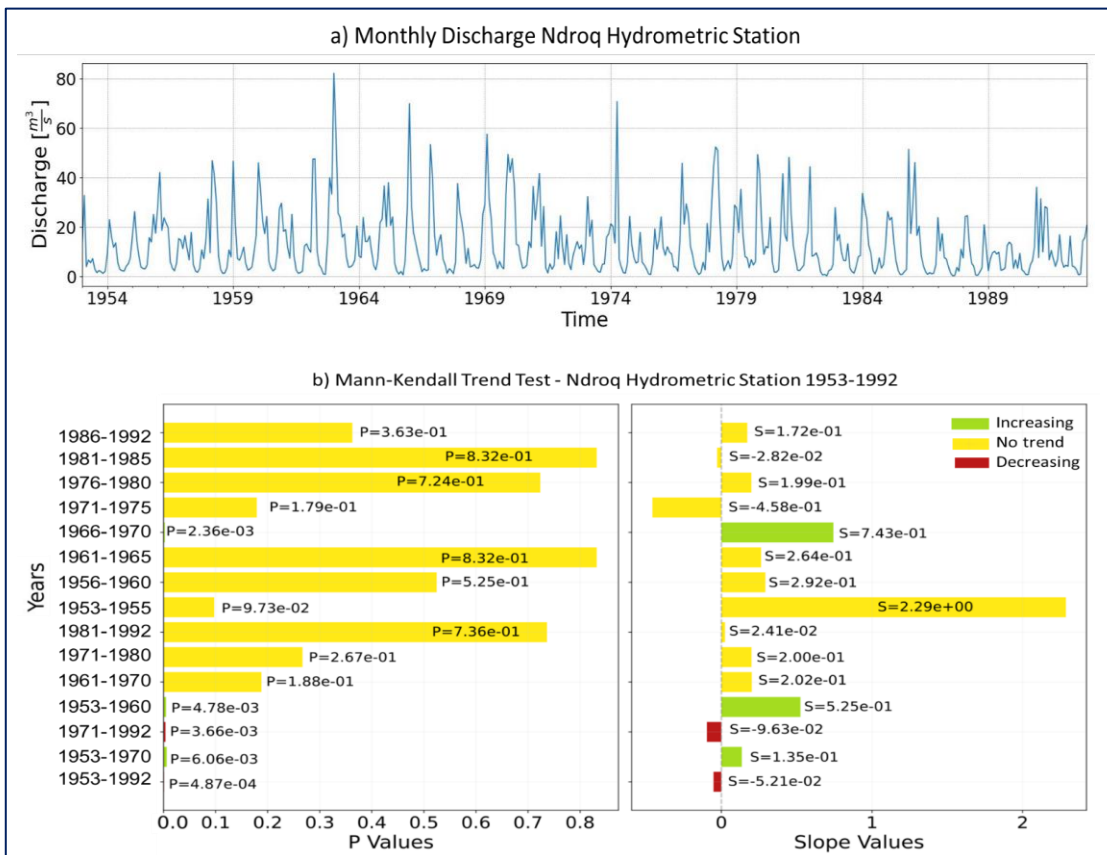


Figure 4. 18. Discharge (m^3/s) information for the Ndroq hydrometric station in Erzen River. (a) monthly mean discharge time series. (b) Results of the Man-Kendall trend test for the Ndroq hydrometric station between 1953-1992 applied to mean monthly data computed from daily data.

The Mann-Kendall test conducted for the Ndroq station data, covering the entire available period from 1953 to 1992, revealed a consistent decreasing trend in discharge. The test yielded a p-value of $4.87e-04$ and a Mann-Kendall test score (Slope) of $-5.21e-2$, indicating the significance and magnitude of this downward trend. Similarly, focusing on the period from 1970 to 1992, the Mann-Kendall test also indicated a decreasing trend in discharge, with a p-value of $3.66e-3$ and a Mann-Kendall test score of $-9.63e-2$. This aligns with the findings from Chapter 3, where the analysis of the Sallmone Station data demonstrated a consistent decreasing trend in discharge after 1970. However, prior to 1970, there were periods of varying trends observed at the Ndroq station. From 1953 to 1970, there was an increasing trend in discharge, as evidenced by a p-value of $6.06e-3$ and a Mann-Kendall test score of $1.35e-1$ (tested over a 20-year period). Additionally, from 1953 to 1960, there was a notable increasing trend, with a p-value of $4.78e-3$ and a Mann-Kendall test score of $5.25e-1$.

Further analysis using shorter time intervals (5-year periods) also revealed an increasing trend in discharge from 1966 to 1975.

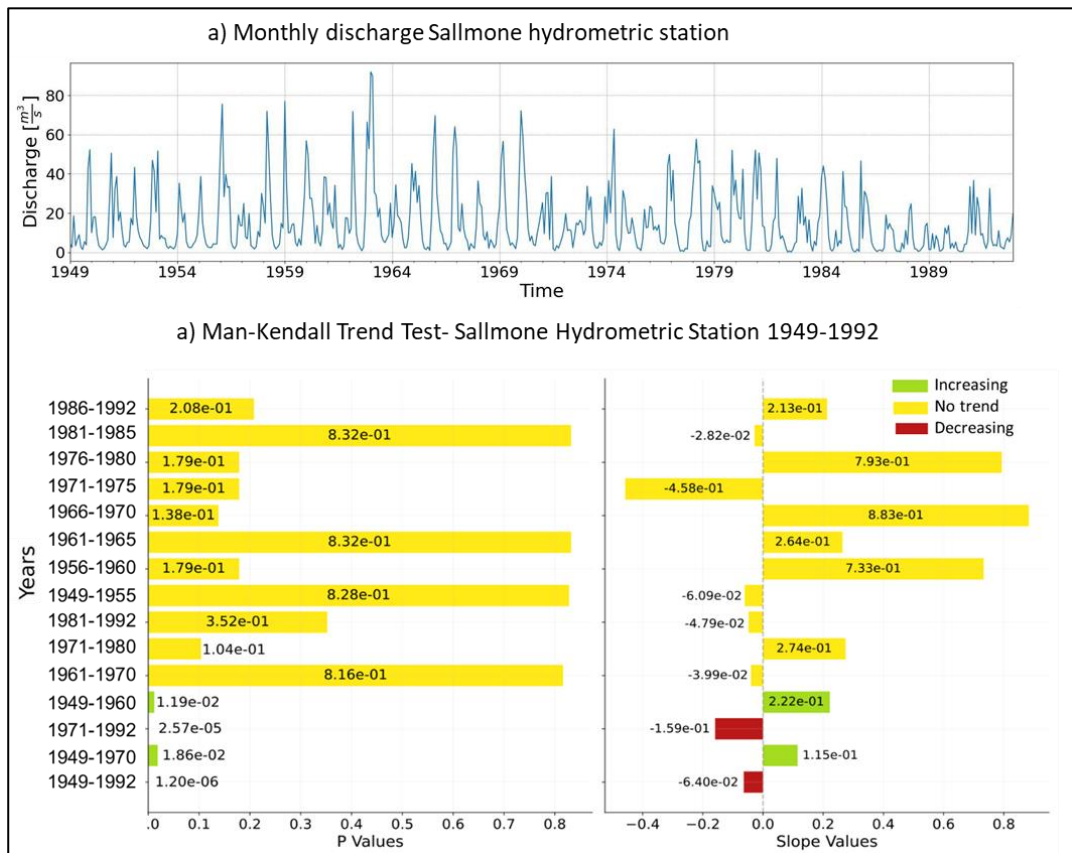


Figure 4.19. Discharge (m^3/s) information for the Sallmone hydrometric station in Erzen River. (a) monthly mean discharge time series. (b) Results of the Man-Kendall trend test for the Sallmone hydrometric station between 1949-1992 applied to mean monthly data computed from daily data.

4.4.2 Return times analyses of discharge

In Figure 4.20, the Gumbel distributions for the daily discharge for the Sallmone station are presented. The figures depicts the Gumbel distributions for various percentiles: the 25th percentile is shown in Figure a, the 75th percentile in Figure b, the 95th percentile in Figure c, and the mean in Figure d. These analyses were conducted using three different methods: the method of moments, maximum likelihood, least squares, and the empirical cumulative distribution function (ECDF).

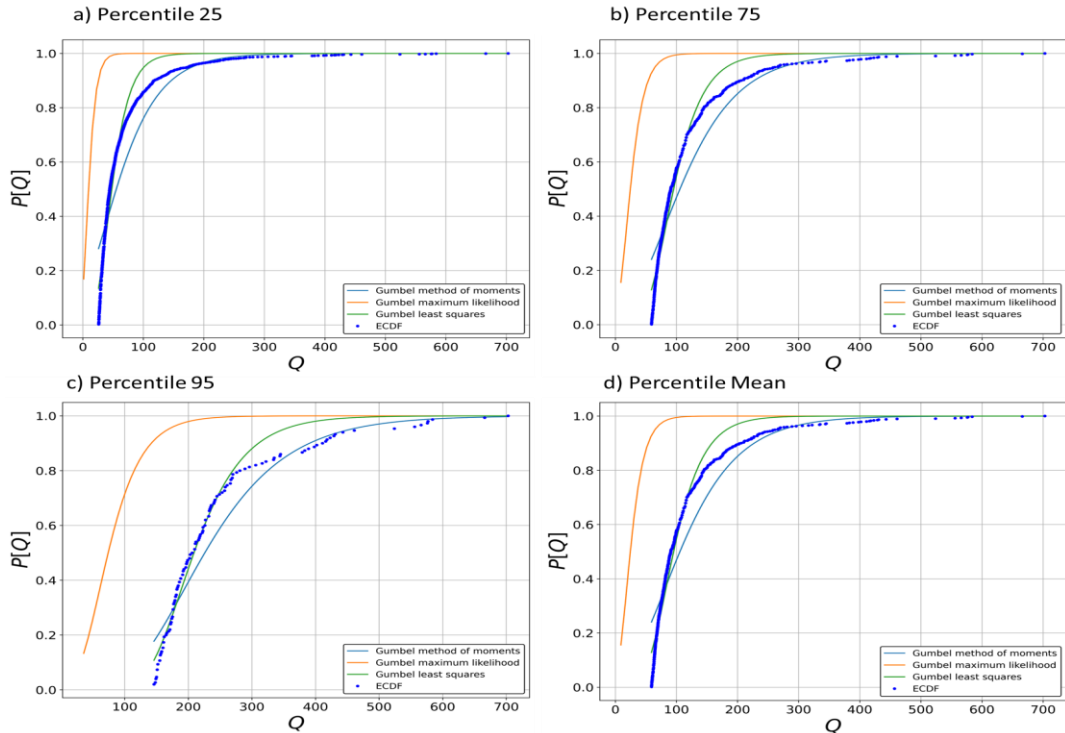


Figure 4. 20. Gumbel distribution of different discharge percentiles for Sallmone hydrometric station (data record: 1949-1992).

The return time of discharge for different periods derived from the Gumbel distribution analysis can be calculated using the inverse of the cumulative distribution function (CDF). They are reported in figure 4.21. Given that the bankful discharge typically occurs between 1.5 and 3 years return time in single-thread rivers (e.g. Bertoldi et.al, 2020) the discharge corresponding to a return time of 2, 2.5, and 3 years, considering a percentile of 95%, can be taken as a realistic representation for the bankfull discharge.

For the Sallmone station the following values are obtained:

- Discharge with a return time of 2.5 years (95th percentile): $89.4 \text{ m}^3/\text{s}$
- Discharge with a return time of 2.5 years (mean value): $30.6 \text{ m}^3/\text{s}$

Similar analyses are performed for all the stations to determine the discharge values corresponding to the specified return times and percentiles.

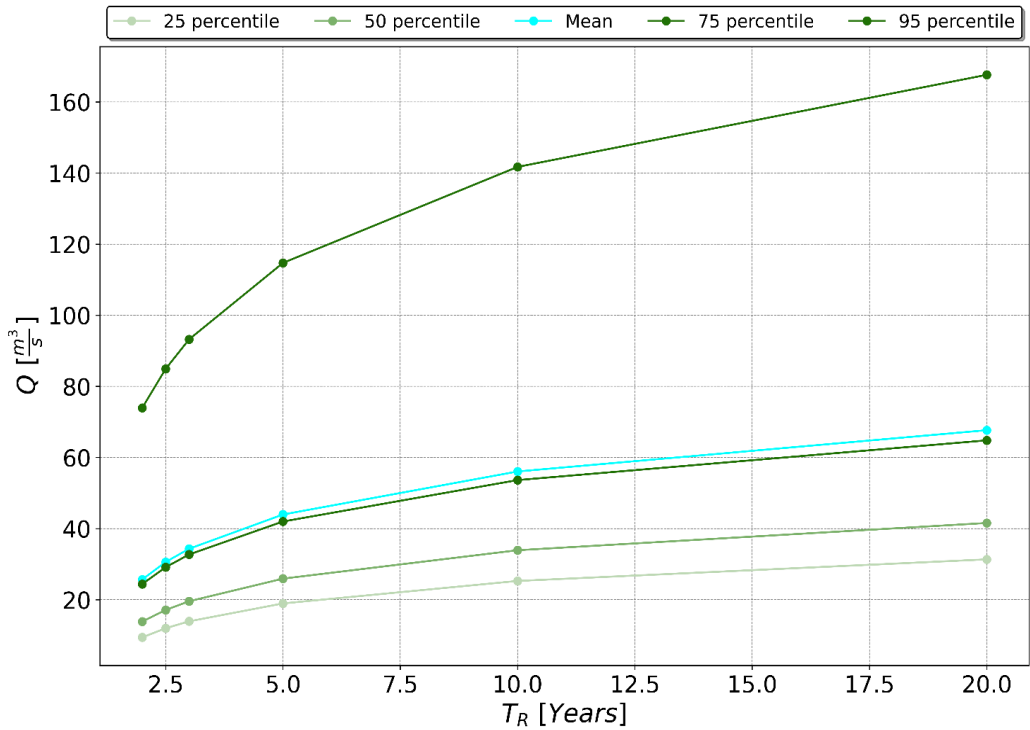


Figure 4. 21. Return times of discharge for Sallmone station derived from Gumbel distribution.

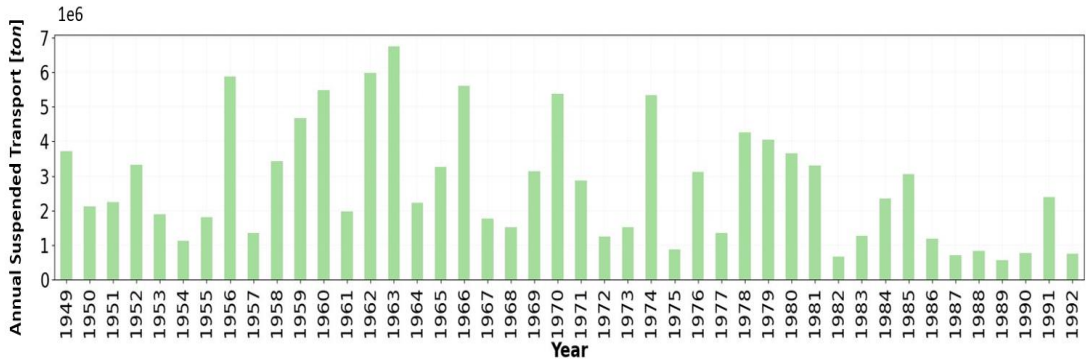
Return (years)	Percentile 25	Percentile 50	Percentile 75	Percentile 95	Mean
2	9.4	24.4	62.5	73.9	25.7
2.5	12.0	29.1	70.2	84.9	30.6
3	13.9	32.7	76.0	93.2	34.3
5	19.0	42.0	91.0	114.7	44.0
10	25.3	53.6	109.9	141.7	56.1
20	31.3	64.8	128.0	167.6	67.7

Table 4. 3. Return time discharge of Sallmone hydrometric station data 1949-1992, with different percentile, using the Gumbel distribution as a results of Pearson test of three methods used: (i) Method of Moments (ii) Least Squares Method and (iii) Maximum Likelihood Method.

4.4.3 Estimates of Sediment transport capacity

Figures 4.22 and 4.23 show the simulated annual suspended load (figure 4.22) and bedload (Figure 4.23) for the Sallmone station (panels a) and the respective outcomes of the Mann-Kendall trend test (panels b) performed on the same simulated time series. The only trend that is statistically significant (p value < 0.005) is the decreasing one that is detected for the entire period (1949 – 1992) with reference to the estimates of the suspended sediment transport capacity (Figure 4.22b). A trend with a similar sign (decreasing) also emerges for the estimates of the annual bedload transport capacity, though this is not significant (p value > 0.005 ; Figure 4.23b). Because all reach-averaged parameters (channel width, slope, mean sediment diameter) have been kept constant within these simulations, and the only one that varies is the flow discharge, on a daily basis, then the above trends are solely determined by the variability in the flow regime.

a) Suspended sediment loads yearly Sallmone Station 1949-1992



b) Mann-Kendall Trend Test - Sallmone Hydrometric Station Suspended Load 1949-1992

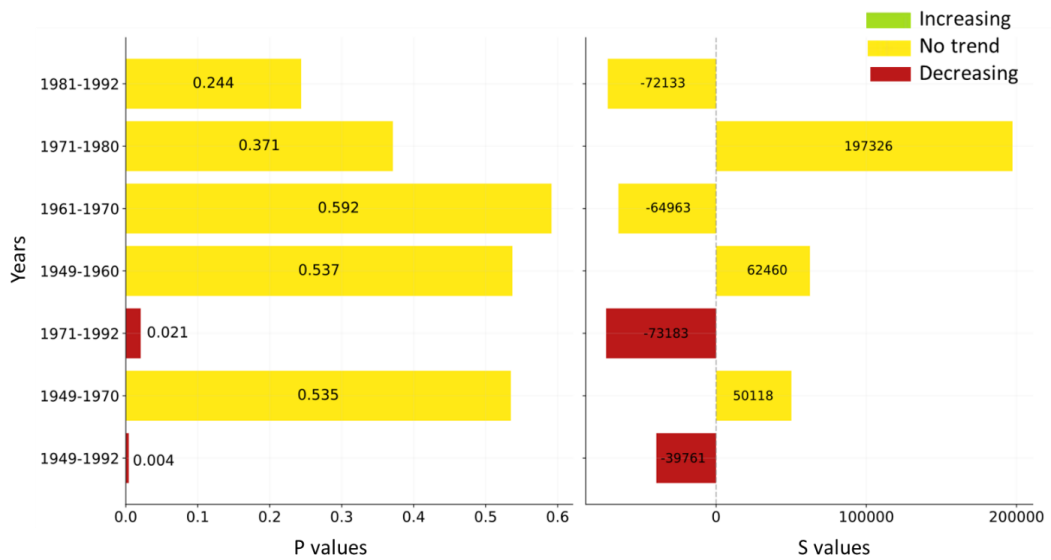


Figure 4. 22. Predicted annual suspended load capacity for Sallmone Hydrometric station. (a) Annual suspended sediment transport using Van Rijn method. (b) Mann-Kendall trend test for suspended sediment transport prediction in the Sallmone hydrometric station showing P and Slope values of the test.

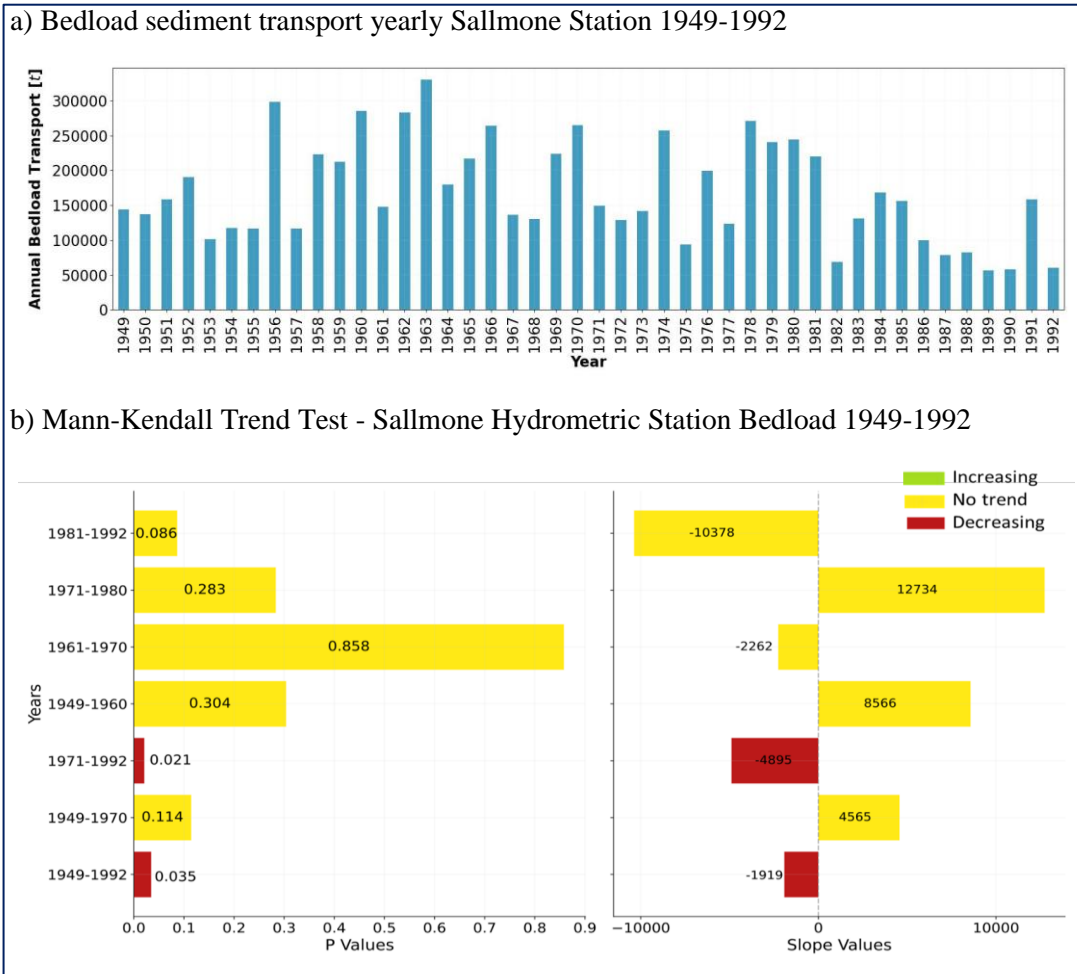


Figure 4. 23. Annual bedload transport capacity for Sallmone Hydrometric station. (a) Annual bedload sediment transport capacity using Van Rijn method. (b) Mann-Kendall trend test for simulated annual bedload in Sallmone hydrometric station showing P and Slope values of the test.

4.4.3 Effects of channel adjustments on sediment transport capacity

In Chapter 3, when analyzing the reaches of the Erzen River, notable phenomena were observed, including marked channel adjustments characterized by narrowing and incision. These changes suggest dynamic adjustments within the river system, likely resulting in changes in the channel slope and channel width.

We have therefore tested to which extent, at least theoretically, the computed sediment transport capacity varies with the two main quantities that are affected by the observed process of channel adjustments, namely channel width and slope, within realistic ranges of their variability. Figure 4.24, The observed narrowing and incision may be attributed to

changes in sediment transport regime, alterations in channel slope, and variations in discharge over time.

Figures 4.24 to 4.26 report the results of the analysis. The observed channel adjustments may have affected the sediment transport capacity in a maximum range of 20-25%, also considering that: narrowing might have increased the unit suspended sediment transport capacity of the channel, while the possible reduction in slope, due to riverbed incision, might have reduced it. The actual extent to which these two opposite effects may have actually affected the total sediment transport capacity of the reach needs further investigation.

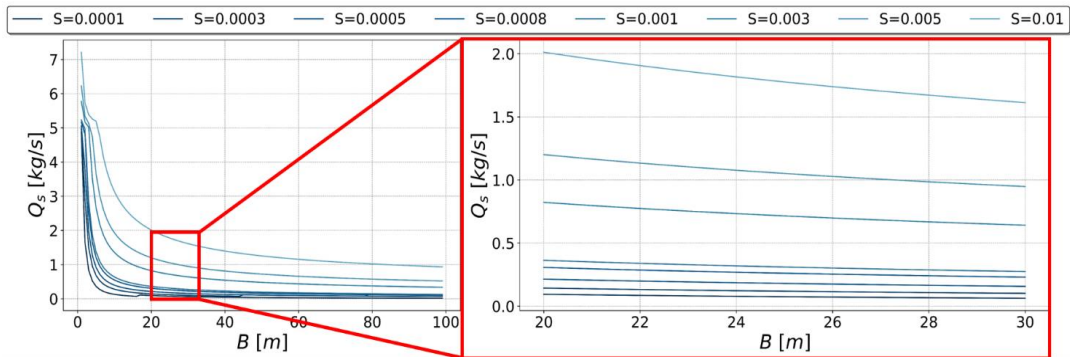


Figure 4. 24. Modelled suspended load transport capacity as function of the channel width B for different values of the channel slope and a fixed discharge Q corresponding to estimated bankfull conditions. The panel on the right is an enlargement of the red box on the left that corresponds to the relevant range of variability for the channel width in the lower Erzen (reach 3 as from Chapter 2) as it emerged from the analysis of channel adjustments.

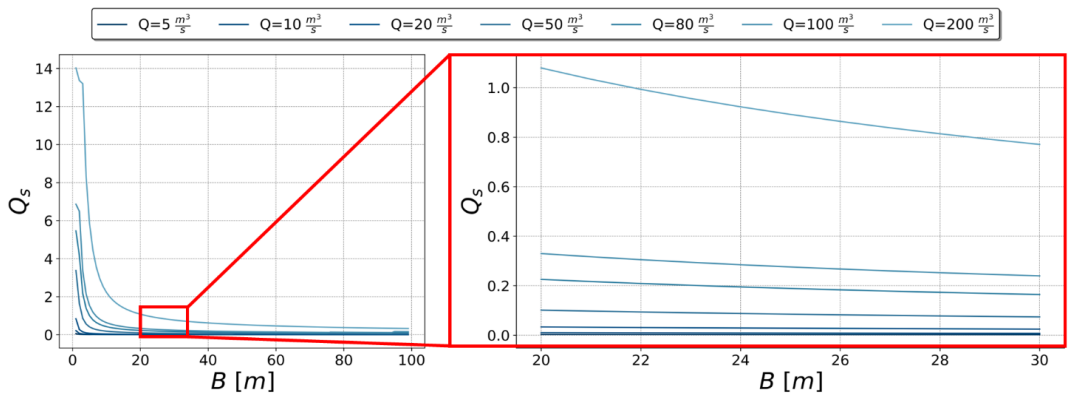


Figure 4. 25. Modelled suspended load transport capacity as function of the channel width B for different values of the reference discharge Q and a fixed channel slope corresponding to the value emergin from the calibration procedure. The panel on the right is an enlargement of the red box on the left that corresponds to the relevant range of variability for the channel width in the lower Erzen (reach 3 as from Chapter 2) as it emerged from the analysis of channel adjustments.

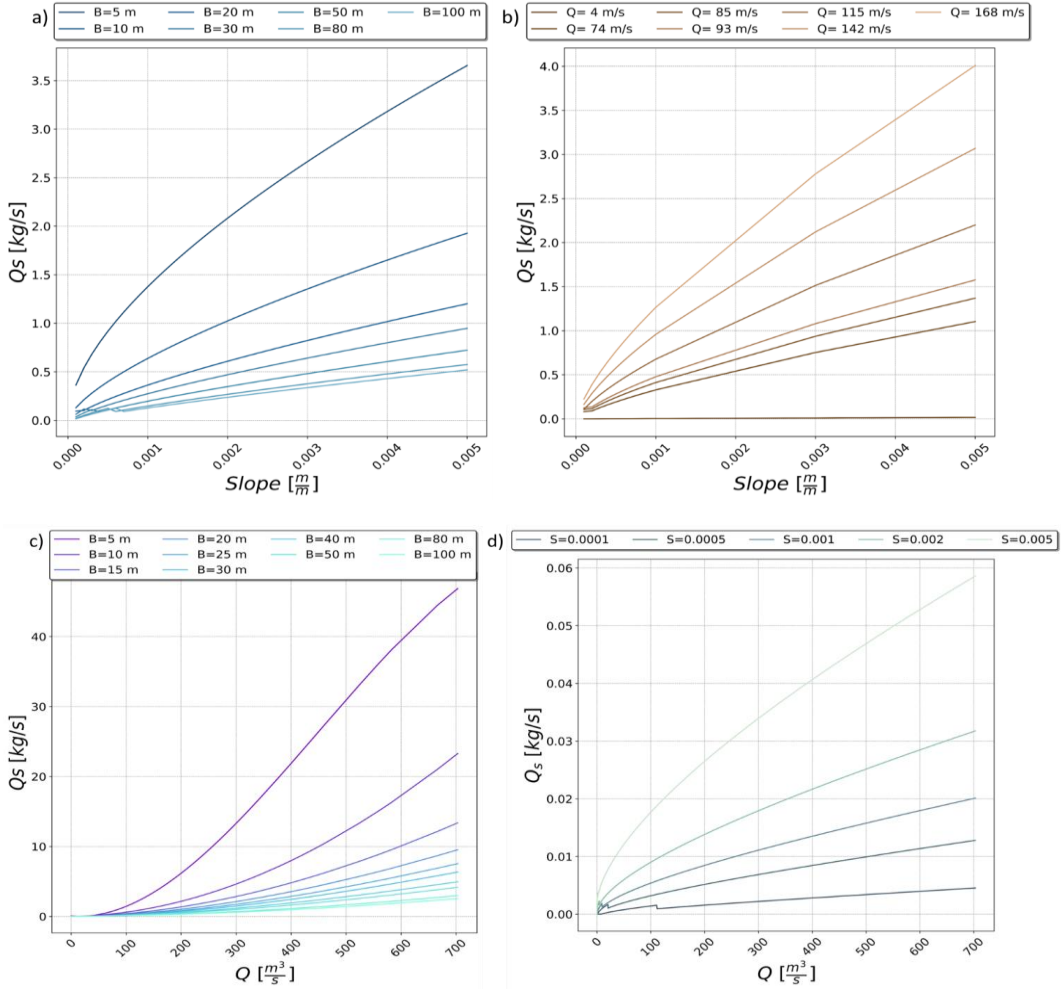


Figure 4. 26. Computation of main channel parameters in different channel condition. Figure a) represent suspended Q_s sediment transport in function of slope S and different channel width B , while discharge is constant Q . Figure b) plotted suspended sediment transport Q_s with Slope S and different discharge Q with fixed channel width B . Figure c) plotted sediment transport Q_s with discharge Q with different channel width B and slope S constant. Figure d) plotted suspended sediment transport Q_s with discharge Q and different slope S and channel width B constant.

4.5 Discussion

The analysis of sediment transport processes and discharge trends in the Erzen River basin yields valuable insights into the dynamics of fluvial systems and their implications for river management and conservation. In this discussion, we delve into the results obtained from our investigation, highlighting key findings, interpreting trends, and discussing their significance in the context of hydrological variability and channel dynamics.

4.5.1 Suspended Sediment Load Analysis

The estimation of the annual variability of the suspended sediment transport capacity with constant representative values of channel width, slope and sediment size at the Sallmone hydrometric station from 1949 to 1992 provides interesting information on sediment transport dynamics in the Erzen River. The calibrated sediment diameter of 0.0014 m and channel slope of 0.00045 m/m yield an average annual suspended sediment load of $3816 * 10^3$ tons/year, closely matching (2% difference) the reference value from the "Hydrology of Albania 1979.". It must be noted that this cannot be taken as a demonstration of the accuracy of the sediment transport model used, because the sediment size and channel slope have been varied on purpose to match the estimate from the measurements. Therefore, the resulting channel slope and sediment size values have to be viewed more as calibration parameters rather than accurate estimates of their actual values. The preliminary exercise presented in this chapter uses this proxy, calibration parameters to develop a predictor of the sediment transport capacity that can allow to reconstruct in a realistic way the inter-annual variability of the sediment transport capacity of the reach in which Sallmone is located under some representative conditions. Also, must be stressed that these estimates do not refer to the actually transported sediment load, which may deviate from the theoretical capacity of transport by the channel, and which has instead been the information that was measured within historical times. Nevertheless, this represents a first attempt, though with a highly simplified approach, to set up a calibrated tool to quantify the possible multi-decadal variations in the sediment fluxes transported by the Erzen river, and more in general by an Albanian river, to the sea.

Analogous comments apply to the estimate of the bedload sediment transport capacity, which reveals a relatively minor contribution to the total sediment load in the Erzen River basin, accounting for less than 10% of the total load. The calibrated sediment diameter of 0.002 m, consistent with the reference value, allows for the calculation of bedload transport using the simplified formula of Nielson (1992). While bedload transport is comparatively low, it remains an essential component of sediment dynamics, particularly in shaping channel morphology and substrate composition.

4.5.2 Discharge Trends and Statistics

Statistical analysis of discharge trends at multiple hydrometric stations along the Erzen River highlights significant temporal variability in flow dynamics. The Mann-Kendall trend test reveals varying trends over different time periods, with both increasing and decreasing trends observed, which aren't always statistically significant. Notably, a consistent decreasing trend in discharge is observed at the Sallmone and Ndroq stations from the 1970s onwards, indicative of potential hydrological changes within the basin.

The return time analyses of discharge events provide critical information for detecting relevant discharge values to be used in the sediment transport predictors. Furthermore, though not examined in the present study, its outputs can support the assessment of flood risks and the design of resilient infrastructure. Utilizing Gumbel distribution analysis, we estimate discharge values corresponding to specific return times and percentiles, offering

insights into the frequency and magnitude of extreme flow events. The approach assume from the literature that bankfull discharge typically occurs between 1.5 and 3 years return time, with corresponding discharge values computed from the Gumbel analysis ranging from 89.4 to 114.7 m³/s.

4.5.3 Effects of Channel Adjustments on Sediment Transport Capacity

The observed channel adjustments (Chapter 3), including narrowing and incision, reflect dynamic responses to changes in sediment transport regimes and discharge variability. Using the developed simplified sediment transport predictor in this Chapter, we assess to which extent the observed modifications of the channel geometry, mainly due to narrowing and incision might have affected the sediment transport capacity of the reach. It emerges that channel narrowing, and riverbed incision separately create opposite effects on the sediment transport capacity by a maximum of 20-25%, and the overall effect of these two competing factors will need further investigations.

4.6 Conclusion

The study on transport in the Erzen River represents a significant step forward in understanding the intricate interplay between channel morphology, climatic variations, and human-induced alterations. Leveraging historical hydrology data spanning from 1949 to 1992, and extending the analysis up to 2008 in Albania, this study delved into the calibration of a highly simplified sediment transport capacity predictor. The predictor, utilizing reach-averaged input parameters and an instantaneous normal flow approximation, became a first, preliminary tool in quantifying sediment fluxes from the river system to the Adriatic Sea.

The calibration process, anchored in on-site data collection from local agencies, produced rough estimates of the channel slope, and diameter of sediment of Sallmone reach of the Erzen River that can shall be taken more as calibration parameters rather than accurate estimates. The calibrated suspended sediment transport for the period 1949-1976 stood at 3186×10^3 tons per year, with difference as low as 0.2%. These calibrated parameters may support future studies to assess the likely sediment fluxes, making this work a starting point for future river management strategies that consider the dynamic river response in Albania to rapid environmental and socio-economic changes.

Statistical analyses of discharge trends at multiple hydrometric stations uncovered significant temporal variations. For instance, the Mann-Kendall trend tests demonstrated both increasing and decreasing trends in discharge over different time spans. Notably, at the Sallmone station, the discharge exhibited a significant decreasing trend from 1972 to 1990, with a Mann-Kendall test score (Slope) of $-8.919e-2$ and a p-value of $3.12e-4$. These findings underscore the necessity for adaptive management strategies to cope with changing hydrological conditions.

Return time analyses of discharge events provided critical information on the frequency and magnitude of extreme flow events. For instance, discharge with a return time of 2.5 years (95th percentile) at the Sallmone station was estimated to be approximately 89.4 m³/s, with the mean value around 30.6 m³/s. Besides the presented sediment transport analysis, these insights can also support assessing flood risks and designing effective mitigation measures tailored to the specific characteristics of the basin.

Moreover, the examination of channel adjustments effects on sediment transport capacity represents a first, though rough and simplified, attempt to isolate the different role of changing climate conditions, and man-made alterations of the sediment regime in affecting the sediment transport capacity of the river in its low reach close to the mouth.

. Similar results were found by Bajrami et al (2023) on the Shkumbin River, a nearby counterpart studied independently, added a layer of coherence with the present findings. This comparative approach can be used to support our understanding of the broader relationship between human activities, river adjustments, and coastal erosion within the region.

This study shall be viewed as a preliminary investigation on the topic, in view of its many simplified assumptions and approximations. The following list includes some needed future developments of this research.

- **Extended Temporal Analysis:** Expanding the temporal scope of the study beyond 2008 can provide a more comprehensive understanding of long-term trends and the influence of recent climate fluctuations. This requires that the recently measured discharge data on Albanian rivers must be made readily and freely available for research purposes by monitoring agencies.
- **updated data from sediment transport monitoring:** the practice of sediment transport or turbidity monitoring should be again part of the institutional monitoring activities in Albanian rivers. Incorporating high-resolution data, especially on suspended sediment transport rates, can surely enhance the accuracy of predictive models and contribute to more physically based river basin management plans.
- **Climate Change Considerations:** As climate change becomes more pronounced, future studies could delve deeper into how changing climatic patterns might impact streamflow variability and therefore sediment transport dynamics.

As Albania grapples with the delicate balance between development and environmental preservation, the insights derived from this study are an important step towards more informed decision-making in river management and aligned with EU directives.

Chapter 5

5. Conclusion

The general goal of this thesis has been to advance the development of systematic quantitative knowledge on the morphology of major Albanian rivers at the country scale, and also to support understanding the possible drivers of the observed recent, multidecadal changes in the channel morphology, focusing on understanding the main underlying physical processes.

Chapter 2 has focused on answers to the following questions:

- (i) What are the morphologies of Albanian rivers, and how are they distributed in the different physiographic regions?
- (ii) To which extent and in which ways have river reaches changed their channel patterns after rapid socio-economic development occurring after the 1990s?
- (iii) How can the concept of “reference conditions” be conceptually and operationally developed in the case of Albanian rivers?

The main stems and largest tributaries of the Vjosa, Devoll, Osum, Seman, Shkumbin, Erzen, Ishem, and Mat rivers have been analysed for this purpose.

This research work offers a comprehensive quantitative analysis of the morphological evolution of six major Albanian rivers spanning over 1300 km. It has provided the first country-scale updated census of the river channel morphologies. BY Utilizing the IDRAIM methodology, aligned with the Water Framework Directive and commonly used for Italian rivers, the study sheds light on the hydromorphological landscape of Albanian rivers at two distinct times: the 1960s and 2015. Examining river channels exceeding 650 km² in catchment area, the findings reveal a diversity of patterns such as single-thread (22%), sinuous (17%), meandering (15%), and wandering (11%) morphologies, with braided reaches (24%) exhibiting significant presence across physiographic units. Notable changes over the studied 60-year period include a 59% reduction in braided reaches and a 52% decrease in wandering reaches, indicating substantial alterations in river morphology. A discernible trend towards channel narrowing is evident, with a 39% shift from braided to wandering and a 10% transformation from braided to sinuous reaches. Human interventions, including channelization, land cover changes, and natural cut-offs, have led to approximately 53 km of river channels transitioning into abandoned reaches over five decades. Through diachronic analysis, this study not only clarifies the main morphological modifications but also provides a historical reference period for assessing recent changes. These findings contribute to the assessment of hydro-morphological quality elements in line with the EU Water Framework Directive, facilitating a better understanding of river dynamics and informing management strategies for sustainable river ecosystems.

Chapter 3 has addressed in depth the morphological changes occurring in one of the river systems analysed in Chapter 2, the Erzen river, which is the one historically reported to have the highest annual average sediment yield per unit catchment area to the sea in the entire country. The aim was to develop an in-depth understanding of the hydro-morphological dynamics of a representative river system in the area, after the large-scale analysis of the

previous chapter. The specific aim was to quantify the characteristics of the channel adjustments and river trajectories in terms of time evolution, magnitude, possible drivers, and to relate it to analogous processes that have been documented in westernized countries, to understand similarities and differences among contexts characterized by different phases of development.

The analysis of Chapter 3 has then been performed on the Erzen river in the central part of Albania. The analysis of the lower Erzen River reveals profound alterations in its morphology and behaviour over the past decades. The observed channel narrowing resulted within 30-60% of the initial active corridor width in the intermediate course, and up to 60-80% in the downstream segment of the river. Additionally, extensive channel incision, averaging 4-6 meters and reaching up to 8 meters in some reaches, provides clear evidence of the dynamic processes of the river response to changing external conditions. Sediment mining activities, intensified by urbanization and infrastructural development post-1990s, emerge as the main drivers of these changes in the lowest segment. The substantial growth in urban areas, particularly in cities like Tirana and Durrës, has led to increased demand for construction material, driving sediment extraction from riverbeds. The financial crisis of 2009 further fuelled this demand as citizens returned to invest in their homeland, leading to increased construction activities and infrastructure development. Moreover, the construction of dams, albeit to a lesser extent compared to other European countries, might have also had some effect on the sediment dynamics in the river. The dams, however, cover a relative small proportion of the basin (22% and 8%) and were constructed primarily for hydropower and water irrigation purposes. An observed trend of decreasing flow volumes and flood magnitudes post-1970 is consistent across the catchment. This decline in flow regime, coupled with changes in land cover and flow regimes, has likely contributed to channel narrowing, particularly in the mountainous upstream reaches. These pronounced alterations are likely to have impacts on the river ecosystem. The substantial decrease in gravel areas implies potential habitat loss for aquatic life, posing challenges to biodiversity. Simultaneously, the noteworthy growth in vegetation along the riverbanks signifies a shift in habitat characteristics. The implications of these alterations extend beyond the river ecosystem. Coastal erosion dynamics are significantly influenced by sediment supply from the Erzen River, affecting shoreline stability and coastal habitats. Additionally, reduced floodplain capacity can exacerbate flood risks in downstream areas, impacting local communities and infrastructure. Addressing these challenges requires a holistic approach to integrated river management.

Monitoring sediment dynamics, flow regimes, and coastal erosion trends is crucial for informed decision-making and proactive management strategies. Furthermore, maintaining hydrometric stations and providing accessible flow and topography data are essential for predicting flow trends and aiding flood mitigation efforts. Analysis of the lower Erzen River underscores the urgent need for reinforced monitoring of streamflow and sediment transport rates, and the difficulties in collecting existing data indicate the importance of making these data accessible for non commercial, research purposes, because at the moment of writing this thesis, they are actually not easily available.

Finally, Chapter 4 focused on attempting at quantifying the possible effects of the detected changes in the flow regime and in the channel morphology over the last six decades on the sediment transport in the Erzen River, and looking at the possible implications for effective

river basin management. By calibrating a simplified sediment transport capacity predictor using historical hydrology data spanning from 1949 to 1992, this study has provided a preliminary calibration of a simplified suspended sediment transport model based on the Rouse vertical sediment concentration profile. Return time analyses of discharge events provided critical insights into the frequency and magnitude of extreme flow events, with discharge events with a return time of 2.5 years (95th percentile) at the Sallmone station estimated to be approximately 89.4 m³/s. From historical data on suspended matter monitoring in the 1950 – 1975 period, the calibrated suspended sediment transport for the period 1949-1976 was estimated to be 3186 x 10³ tons per year. Application of simplified bedload transport prediction for the lower reaches (Sallmone station) suggests that bedload may approximately represent 10% or less of the total sediment load.

Statistical analyses of discharge trends at various hydrometric stations unveiled significant temporal variations, such as the notable decreasing trend in discharge observed at the Sallmone station from 1972 to 1990. Application of the calibrated sediment transport model suggests that decreasing streamflow trends from the 1960s to 1990 may account for an approximate 20% reduction of the mean annual sediment transport capacity of the lowest reaches of the Erzen. Moreover, the examination of the possible channel adjustments on sediment transport capacity elucidated dynamic responses to changes in sediment transport regimes, channel slope, and discharge variability.

The insights derived from this study not only deepen our understanding of sediment transport intricacies in the Erzen River but also lay a solid foundation for holistic river basin management plans. As Albania navigates the delicate balance between development and environmental preservation, the findings presented in this chapter are invaluable for informed decision-making aligned with EU directives.

Further research work of the current analysis shall entail a comprehensive study of the morphology of the entire Drin River basin, thus contributing to the completion of an Albanian Morphological Atlas. This work plan should extend the morphological assessments to cover not only the main channels of the major rivers in Albania but also their main tributaries. While the ongoing analyses have provided valuable insights into the morphological characteristics of the main river channels, expanding the scope to encompass the tributaries will offer a more complete understanding of river morphology dynamics across the Albanian landscape. Such baseline information is a key prerequisite to develop river basin management plans that can carefully consider the possible impacts of planned development in hydropower plants, sediment mining sites, river engineering works, and the future management of water abstractions and intake structures.

Last, but not least, an extension of the ongoing research involves integrating the analysis of sediment transport connectivity with coastal erosion dynamics in Lalzy Bay. Understanding the complex relationship between sediment dynamics within river systems and coastal erosion processes is critical, particularly in coastal areas susceptible to environmental fluctuations and anthropogenic influences. By investigating the impact of sediment transport from the Erzen River on coastal erosion patterns in Lalzy Bay, a prediction of possible future scenarios can be achieved for the coastal dynamics of the region in response to management actions that are implemented in the upstream river catchments. This expanded analysis will shed light on how sediment transported by the Erzen River interacts with the coastal currents,

wave actions, and shoreline morphology, ultimately influencing erosion and sedimentation processes along the Lalzy Bay coastline. Such insights are crucial for developing effective coastal management strategies that are fully coupled with the river basin management, which is of particular relevance given the increasing value of tourism on Albanian coasts and the fundamental need to preserve its unique ecosystems.

Appendix



Figure A1. Orthophoto 2015 representing the result of the classification of the river reach morphology using a combination of the computation of the sinuosity index and subjective expert judgement. a) Anabranching morphology in a reach of the Drin River. b) Braided morphology in a reach of the Mat River. c) Another braided morphology in a reach of the Devoll river. d) Sinuous morphology in Shkumbin River. e) Wandering morphology in a reach of the Shkumbin river.

- Sinuosity index (S_i): is defined as the ratio between the distance l_a measured along the (main) channel and the distance l_n measured following the direction of the overall planimetric course;

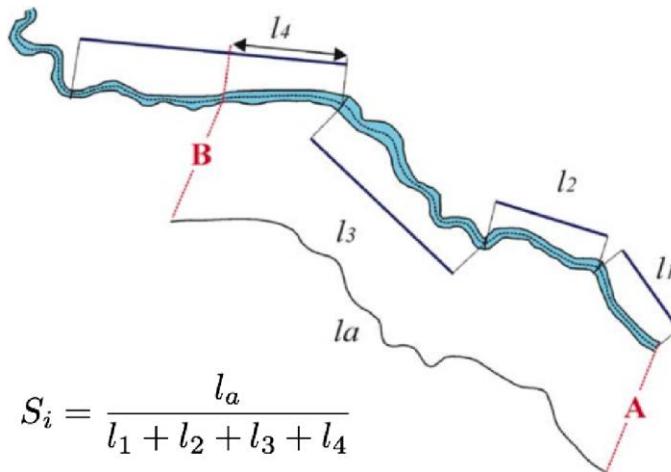


Figure A2. Sinuosity Index

- Braiding index (B_i): is defined as the number of wet channels at baseflow separated by bars.

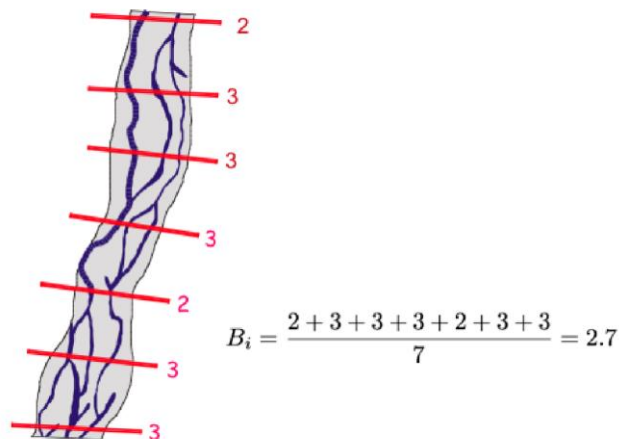


Figure A3. Braided index

- Anabranching index (A_i) is defined as the number of active channels at the baseflow separated by vegetated islands.

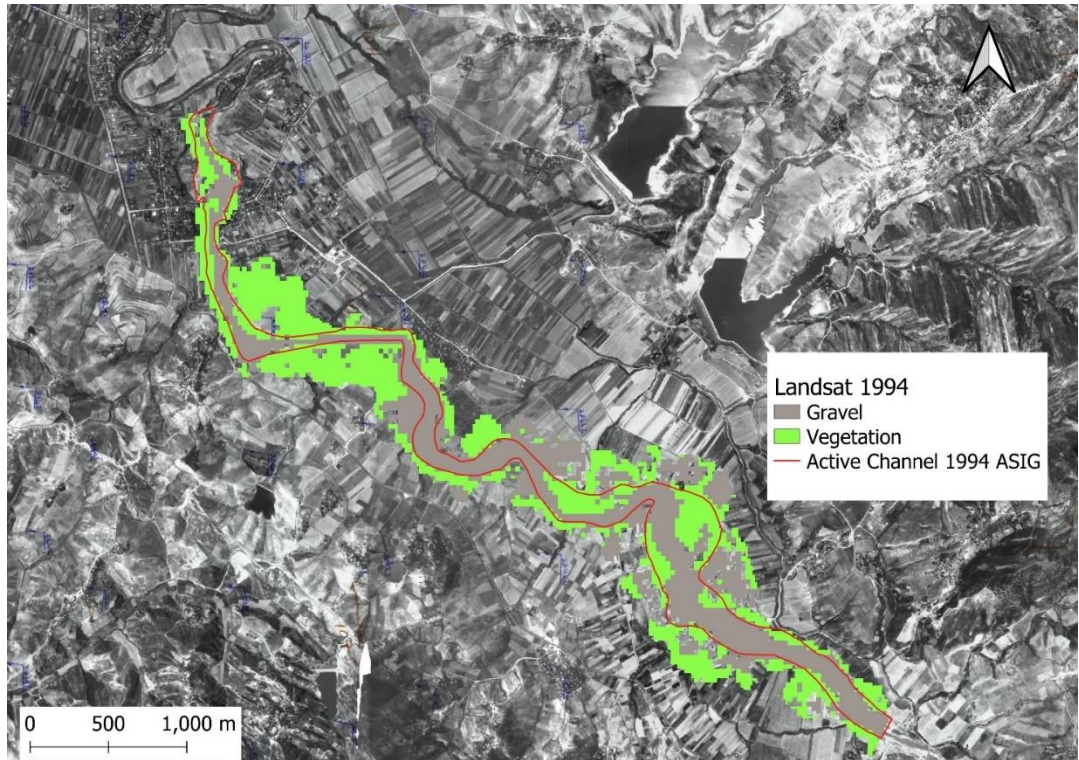


Figure A4. Comparison of two methods Semi-automatic (Landsat) and manual mapping of active channel referring orthophoto 1994 Geoportal Albania and classification from Landsat same year. Location reach 5 Erzen river. With red list shows active channel 1994 geoportal Albania, grey colour active channel (ravel and water) and with green vegetation.

By comparing these 2 methods we do not see a big change since the active channel mapped from Landsat shows some pixel out from what is mapped form orthophoto but some of these pixel in orthophoto shows water pools, small reservoirs that farmers use for agricultural. Need to be highlighted when we compare this in 2015 year the channel is narrow, and we do not see a clear active channel to compare with manual mapped from the orthophoto. So, this method can be applied to the rivers with an river corridor over 100 m to give a better results.

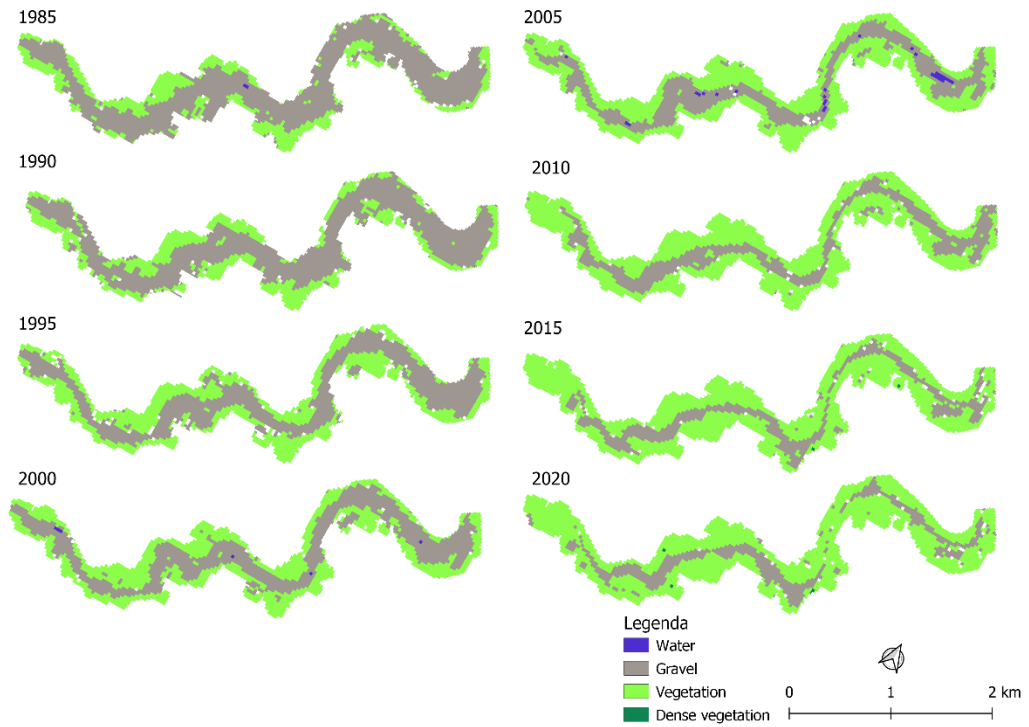


Figure A5. Evolution of land cover in reach 8 Erzen river, visualized by images obtained every five years from the analysis of Landsat imagery.

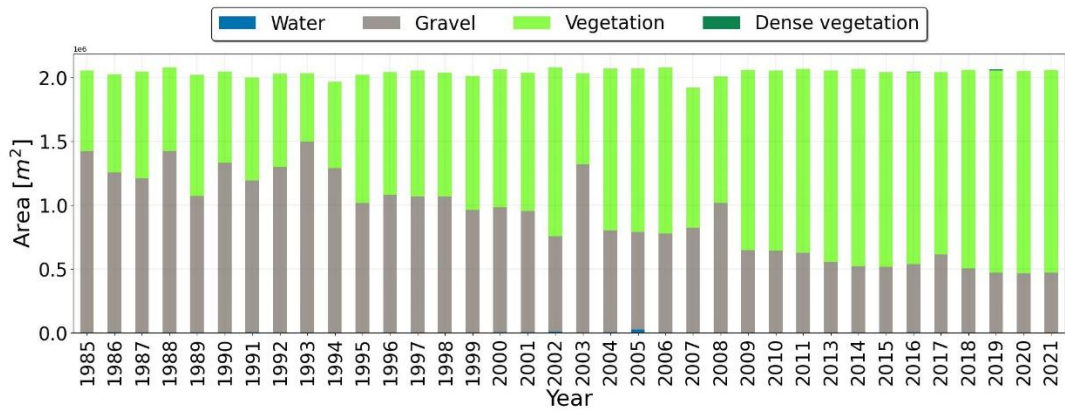


Figure A6. Annual time series of land cover classes in reach 8 Erzen river obtained from the analysis of Landsat imagery.

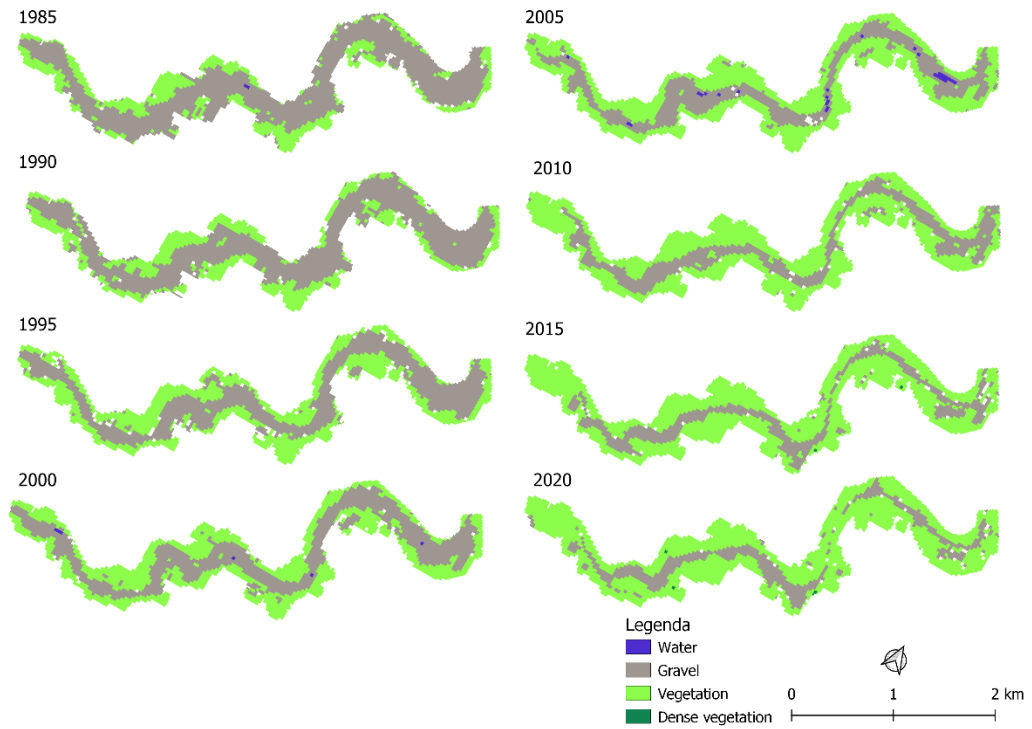


Figure A7. Evolution of land cover in reach 11 Erzen river, visualized by images obtained every five years from the analysis of Landsat imagery.

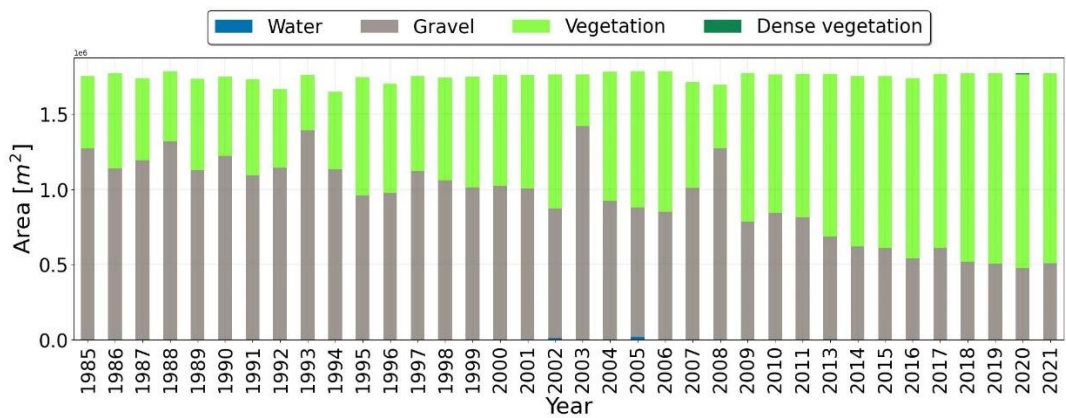


Figure A8. Annual time series of land cover classes in reach 11 Erzen river obtained from the analysis of Landsat imagery.

Reach_No	PU	Conf	Ci	Cd	Length_m	Distance_m	SI	Morphology_2015	Slope%	Av_AC_m	Av_FL_m	Elevation_m
1	Plain	UC	360.0	≤ 10%	5295	2521	2.1	Abandoned	0.05	26	6391	0.5
2	Plain	UC	410.0	≤ 10%	1210	672	1.8	Abandoned	0.14	18	7528	2
3	Plain	UC	361.0	≤ 10%	10110	5773	1.78	Meander	0.05	26	6391	3.1
4	Plain	UC	427.2	≤ 10%	3188	1890	1.69	Meander	0.14	18	7528	6.7
5	Plain	UC	268.0	≤ 10%	7055	5159	1.37	Sinuuous	0.04	24	6100	10.2
6	Plain	UC	181.1	≤ 10%	10757	5129	2.1	Meander	0.19	27	3213	14.5
7	Plain	UC	43.8	≤ 10%	8075	5755	1.4	Sinuuous	0.10	42	1325	21
8	Plain	UC	21.6	≤ 10%	2373	2255	1.05	Straight	0.14	38	805	28.8
9	Plain	SC	6.0	10+90%	2671	2249	1.19	Sinuuous	0.61	34	204	35.3
10	Plain	SC	8.1	10+90%	6575	4487	1.47	Sinuuous Alternate Bars	0.23	47	327	48.9
11	Plain	SC	4.8	10+90%	4175	2658	1.57	Sinuuous	0.37	35	149	66.3
12	Plain	SC	3.0	10+90%	5719	3793	1.51	Sinuuous	0.31	57	154	84.8
13	Hill	SC	4.2	10+90%	5773	4440	1.3	Sinuuous	0.48	67	246	109.6
14	Hill	SC	3.9	10+90%	5409	4658	1.16	Sinuuous	0.70	46	170	139.1
15	Hill	SC	6.7	10+90%	4209	3382	1.24	Sinuuous Alternate Bars	0.81	53	294	174.9
16	Hill	C	2.4	> 90%	2982	2748	1.08	Wandering	1.03	72	135	210.2
17	Hill	C	1.6	> 90%	2677	2507	1.07	Straight	3.38	24	41	272.6
18	Mountain	C	1.2	> 90%	1052	1017	1.06	Damed-up	0.16	183	220	314.1
19	Mountain	C	1.6	> 90%	5453	5062	1.07	Braided	1.47	160	245	351.5
20	Mountain	C	1.6	> 90%	5190	4775	1.09	Wandering	2.68	94	133	463.6
21	Mountain	C	1.5	> 90%	2503	4249	1.16	Sinuuous	5.07	15	29	701.5
22	Mountain	C	1.2	> 90%	3910	871	1.35	Single thread	6.4	6	7	732
23	Mountain	C	1.2	> 90%	955	863	1.11	Single thread	28.7	6	7	995

Table A1. Morphology analyses workflow for main indicator shown in the table for Erzen river.

PU- Physiographist unit

Conf- Confinement class, Unconfinement (UC), Semi Confinement (SC), Confinement channel (C)

Length_m – Length of the central river for each reach

Distance- Distance of the reach by taking 2 extreme point.

SI- Sinuuous index

Morphology_2015- Morphology assess in 2015 taking in consideration orthophoto 2015 from Geoportal Albania

Slope% - Slope of the reach in % taken form DTM 10 M.

Av_AC m- Average active channel in (m)

Av_FL_m- Average floodplain in (m)

Elevation_m- Average elevation in m taken from DTM 10 m by taking downstream and upstream elevation of the reach.

These analyses for as performed for other rivers (chapter 2) Mat, Ishem, Erzen, Shkumbin, Seman, Devoll, Osum and Vjosa. Additionally the morphology of 1960 year and active channel was assessed as described in chapter 2.

References

3rd Environmental Performance Review of Albania | UNECE [WWW Document], n.d. URL <https://unece.org/environment-policy/publications/3rd-environmental-performance-review-albania> (accessed 11.19.23).

Albania - Climatology | Climate Change Knowledge Portal [WWW Document], n.d. URL <https://climateknowledgeportal.worldbank.org/country/albania/climate-data-historical> (accessed 11.19.23).

Aleko, M., Gunnar, P., n.d. OVERVIEW OF WATER QUALITY OF ALBANIAN RIVERS.

Arnaud, F., Schmitt, L., Johnstone, K., Rollet, A.-J., Piégay, H., 2019. Engineering impacts on the Upper Rhine channel and floodplain over two centuries. *Geomorphology* 330, 13–27. <https://doi.org/10.1016/j.geomorph.2019.01.004>

Baena-Escudero, R., Rinaldi, M., García-Martínez, B., Guerrero-Amador, I.C., Nardi, L., 2019. Channel adjustments in the lower Guadalquivir River (southern Spain) over the last 250 years. *Geomorphology* 337. <https://doi.org/10.1016/j.geomorph.2019.03.027>

Belletti, B., Nardi, L., Rinaldi, M., 2016. Diagnosing problems induced by past gravel mining and other disturbances in Southern European rivers: the Magra River, Italy. *Aquatic Sciences* 78. <https://doi.org/10.1007/s00027-015-0440-5>

Biodiversity Days: Europe's last big wild river to be explored [WWW Document], n.d. URL <https://riverwatch.eu/de/general/news/biodiversity-days-europe%E2%80%98s-last-big-wild-river-be-explored> (accessed 11.29.23).

Boothroyd, R., Nones, M., Guerrero, M., 2021. Deriving planform morphology and vegetation coverage from remote sensing to support river management applications. *Frontiers in Environmental Science* 9. <https://doi.org/10.3389/fenvs.2021.657354>

Boothroyd, R.J., Williams, R.D., Hoey, T.B., Barrett, B., Prasojo, O.A., 2021. Applications of Google Earth Engine in fluvial geomorphology for detecting river channel change. *WIREs Water* 8, e21496. <https://doi.org/10.1002/wat2.1496>

Bornette, G., Amoros, C., Rostan, J.-C., 1996. River incision and vegetation dynamics in cut-off channels. *Aquatic Science* 58, 31–51. <https://doi.org/10.1007/BF00877639>

Brown, A.G., Lespez, L., Sear, D.A., Macaire, J.-J., Houben, P., Klimek, K., Brazier, R.E., Van Oost, K., Pears, B., 2018. Natural vs anthropogenic streams in Europe: History, ecology and implications for restoration, river-rewilding and riverine ecosystem services. *Earth-Science Reviews* 180, 185–205. <https://doi.org/10.1016/j.earscirev.2018.02.001>

Carolli, M., Gelmini, F., Pellegrini, S., Deriu, M., Zolezzi, G., 2021. Prioritizing reaches for restoration in a regulated Alpine river: Locally driven versus hydro-morphologically based actions. *River Research and Applications* 37. <https://doi.org/10.1002/rra.3737>

Carolli, M., Leaniz, C.G. de, Jones, J., Belletti, B., Huđek, H., Pusch, M., Pandakov, P., Börger, L., Bund, W. van de, 2023. Impacts of existing and planned hydropower dams on river fragmentation in the Balkan Region. *Science of the Total Environment* 871. <https://doi.org/10.1016/j.scitotenv.2023.161940>

Catchment-scale cumulative impact of human activities on river channels in the late Anthropocene: implications, limitations, prospect - ScienceDirect [WWW Document], n.d. URL <https://www.sciencedirect.com/science/article/pii/S0169555X19301217?via%3Dihub> (accessed 7.29.23).

Chang, S.W., Clement, T.P., Simpson, M.J., Lee, K.-K., 2011. Does sea-level rise have an impact on saltwater intrusion? *Advances in Water Resources* 34, 1283–1291. <https://doi.org/10.1016/j.advwatres.2011.06.006>

Changes in the channel-bed level of the eastern Carpathian rivers: Climatic vs. human control over the last 50 years - ScienceDirect [WWW Document], n.d. URL <https://www.sciencedirect.com/science/article/pii/S0169555X1300202X?via%3Dihub#bb0345> (accessed 7.22.23).

Comiti, F., 2012. How natural are Alpine mountain rivers? Evidence from the Italian Alps. *Earth Surface Processes and Landforms* 37, 693–707. <https://doi.org/10.1002/esp.2267>

Comiti, F., Da Canal, M., Surian, N., Mao, L., Picco, L., Lenzi, M.A., 2011. Channel adjustments and vegetation cover dynamics in a large gravel bed river over the last 200years. *Geomorphology* 125, 147–159. <https://doi.org/10.1016/j.geomorph.2010.09.011>

Crivellaro, M., Serrao, L., Cekrezi, B., Vitti, A., Bertoldi, W., Skrame, K., Hauer, C., Zolezzi, G., 2021. How does the morphology of natural rivers evolve? The wild Vjosa river in the last five decades, in: *AGU Fall Meeting Abstracts*. pp. EP45D-1547.

Croucher, A.E., O’Sullivan, M.J., 1995. The Henry Problem for Saltwater Intrusion. *Water Resources Research* 31, 1809–1814. <https://doi.org/10.1029/95WR00431>

Cullaj, A., Hasko, A., Miho, A., Schanz, F., Brandl, H., Bachofen, R., 2005a. The quality of Albanian natural waters and the human impact. *Environment International* 31, 133–146. <https://doi.org/10.1016/j.envint.2004.06.008>

Cullaj, A., Hasko, A., Miho, A., Schanz, F., Brandl, H., Bachofen, R., 2005b. The quality of Albanian natural waters and the human impact. *Environment international* 31, 133–46. <https://doi.org/10.1016/j.envint.2004.06.008>

Cullaj, A., Hasko, A., Miho, A., Schanz, F., Brandl, H., Bachofen, R., 2005c. The quality of Albanian natural waters and the human impact. *Environment international* 31, 133–46. <https://doi.org/10.1016/j.envint.2004.06.008>

Drescher, A., 2018. The Vjosa (Vjosë)-the floodplains of an outstanding gravel bed river in southern Albania 85–105.

Dufour, S., Rinaldi, M., Piégay, H., Michalon, A., 2015. How do river dynamics and human influences affect the landscape pattern of fluvial corridors? Lessons from the Magra River, Central-Northern Italy. *Landscape and Urban Planning* 134. <https://doi.org/10.1016/j.landurbplan.2014.10.007>

Earth Surface Processes and Landforms | *Geomorphology Journal* | Wiley Online Library [WWW Document], n.d. URL <https://onlinelibrary.wiley.com/doi/full/10.1002/esp.5225> (accessed 8.11.23a).

Earth Surface Processes and Landforms | *Geomorphology Journal* | Wiley Online Library [WWW Document], n.d. URL <https://onlinelibrary.wiley.com/doi/full/10.1002/esp.5225> (accessed 8.21.23b).

Effects of deposited wood on biocomplexity of river corridors - Gurnell - 2005 - *Frontiers in Ecology and the Environment* - Wiley Online Library [WWW Document], n.d. URL <https://esajournals.onlinelibrary.wiley.com/doi/full/10.1890/1540-9295%282005%29003%5B0377%3AEODWOB%5D2.0.CO%3B2> (accessed 7.22.23).

Eftimi, R., 2010. HYDROGEOLOGICAL CHARACTERISTICS OF ALBANIA. *AQUAmundi* 79–92. <https://doi.org/10.4409/Am-007-10-0012>

European Parliament criticizes Albania’s hydropower policies [WWW Document], 2015. . EuroNatur. URL <https://www.euronatur.org/en/what-we-do/news/european-parliament-criticizes-albanias-hydropower-policies> (accessed 11.29.23).

Forti, L., Mariani, G.S., Brandolini, F., Pezzotta, A., Zerboni, A., 2022. Declassified intelligence satellite imagery as a tool to reconstruct past landforms and surface processes: The submerged riverscape of the Tigris River below the Mosul Dam Lake, Iraq. *Earth Surface Processes and Landforms* 47. <https://doi.org/10.1002/esp.5389>

Gregory, K.J., 2019. Human influence on the morphological adjustment of river channels: The evolution of pertinent concepts in river science. *River Research and Applications* 35, 1097–1106. <https://doi.org/10.1002/rra.3455>

Gurnell, A., Tockner, K., Edwards, P., Petts, G., 2005. Effects of deposited wood on biocomplexity of river corridors. *Frontiers in Ecology and the Environment* 3, 377–382. [https://doi.org/10.1890/1540-9295\(2005\)003\[0377:EODWOB\]2.0.CO;2](https://doi.org/10.1890/1540-9295(2005)003[0377:EODWOB]2.0.CO;2)

Gurnell, A.M., 1998. The hydrogeomorphological effect of beaver dam-building activity. *Progress in Physical Geography* 22. <https://doi.org/10.1177/030913339802200202>

Gurnell, A.M., 1983. Downstream Channel Adjustments in Response to Water Abstraction for Hydro-Electric Power Generation from Alpine Glacial Melt-Water Streams. *The Geographical Journal* 149. <https://doi.org/10.2307/634009>

Gurnell, A.M., Hill, C.T., 2022. River channel changes through time and across space: Using three commonly available information sources to support river understanding and management in a national park. *Earth Surface Processes and Landforms* 47. <https://doi.org/10.1002/esp.5267>

Gurnell, A.M., Rinaldi, M., Belletti, B., Bizzi, S., Blamauer, B., Braca, G., Buijse, A.D., Bussettini, M., Camenen, B., Comiti, F., Demarchi, L., Jalón, D.G. de, Tánago, M.G. del, Grabowski, R.C., Gunn, I.D.M., Habersack, H., Hendriks, D., Henshaw, A.J., Klösch, M., Lastoria, B., Latapie, A., Marcinkowski, P., Martínez-Fernández, V., Mosselman, E., Mountford, J.O., Nardi, L., Okruszko, T., O'Hare, M.T., Palma, M., Percopo, C., Surian, N., Bund, W. van de, Weissteiner, C., Ziliani, L., 2016. A multi-scale hierarchical framework for developing understanding of river behaviour to support river management. *Aquatic Sciences* 78. <https://doi.org/10.1007/s00027-015-0424-5>

Gurnell, A.M., Scott, S.J., England, J., Gurnell, D., Jeffries, R., Shuker, L., Wharton, G., 2020. Assessing river condition: A multiscale approach designed for operational application in the context of biodiversity net gain. *River Research and Applications* 36. <https://doi.org/10.1002/rra.3673>

Hamed, K.H., Ramachandra Rao, A., 1998. A modified Mann-Kendall trend test for autocorrelated data. *Journal of Hydrology* 204, 182–196. [https://doi.org/10.1016/S0022-1694\(97\)00125-X](https://doi.org/10.1016/S0022-1694(97)00125-X)

Hannah, D.M., Smith, B.P.G., Gurnell, A.M., McGregor, G.R., 2000. An approach to hydrograph classification. *Hydrological Processes* 14. [https://doi.org/10.1002/\(SICI\)1099-1085\(20000215\)14:2<317::AID-HYP929>3.0.CO;2-T](https://doi.org/10.1002/(SICI)1099-1085(20000215)14:2<317::AID-HYP929>3.0.CO;2-T)

Harezlak, V., Geerling, G.W., Rogers, C.K., Penning, W.E., Augustijn, D.C.M., Hulscher, S.J.M.H., 2020. Revealing 35 years of landcover dynamics in floodplains of trained lowland rivers using satellite data. *RIVER RES APPL* 36, 1213–1221. <https://doi.org/10.1002/rra.3633>

Hauer, C., Skrame, K., Fuhrmann, M., 2021. Hydromorphological assessment of the Vjosa river at the catchment scale linking glacial history and fluvial processes. *CATENA* 207, 105598. <https://doi.org/10.1016/j.catena.2021.105598>

Hooke, J.M., 2006. Human impacts on fluvial systems in the Mediterranean region. *Geomorphology*, 37th Binghamton Geomorphology Symposium 79, 311–335. <https://doi.org/10.1016/j.geomorph.2006.06.036>

Human impacts on fluvial systems in the Mediterranean region - ScienceDirect [WWW Document], n.d. URL <https://www.sciencedirect.com/science/article/pii/S0169555X0600256X?via%3Dihub> (accessed 7.29.23).

Hussain, M.M., Mahmud, I., 2019. pyMannKendall: a python package for non parametric Mann Kendall family of trend tests. *Journal of Open Source Software* 4, 1556. <https://doi.org/10.21105/joss.01556>

IJGI | Free Full-Text | Multi-Temporal Image Analysis for Fluvial Morphological Characterization with Application to Albanian Rivers [WWW Document], n.d. URL <https://www.mdpi.com/2220-9964/7/8/314> (accessed 7.22.23).

IUCN helps protect Vjosa in Albania, the last wild free-flowing river in Europe - Story | IUCN [WWW Document], n.d. URL <https://www.iucn.org/story/202209/iucn-helps-protect-vjosa-albania-last-wild-free-flowing-river-europe> (accessed 11.19.23).

Kabo, M., 1990. *Physical geography of Albania*. page 400.

Leo, F.D., Besio, G., Zolezzi, G., Bezzi, M., 2019. Coastal vulnerability assessment: Through regional to local downscaling of wave characteristics along the Bay of Lalzit (Albania). *Natural Hazards and Earth System Sciences* 19. <https://doi.org/10.5194/nhess-19-287-2019>

Leo, F.D., Besio, G., Zolezzi, G., Bezzi, M., Floqi, T., Lami, I., 2017. COASTAL EROSION TRIGGERED BY POLITICAL AND SOCIO-ECONOMICAL ABRUPT CHANGES: THE CASE OF LALZIT BAY, ALBANIA. *Coastal Engineering Proceedings*. <https://doi.org/10.9753/icce.v35.management.13>

Liu, J., Kuang, W., Zhang, Z., Xu, X., Qin, Y., Ning, J., Zhou, W., Zhang, S., Li, R., Yan, C., Wu, S., Shi, X., Jiang, N., Yu, D., Pan, X., Chi, W., 2014. Spatiotemporal characteristics, patterns, and causes of land-use changes in China since the late 1980s. *Journal of Geographical Sciences* 24. <https://doi.org/10.1007/s11442-014-1082-6>

Lobera, G., Besné, P., Vericat, D., López-Tarazón, J.A., Tena, A., Aristi, I., Díez, J.R., Ibisate, A., Larrañaga, A., Elosegi, A., Batalla, R.J., 2015. Geomorphic status of regulated rivers in the Iberian Peninsula. *Science of The Total Environment* 508, 101–114. <https://doi.org/10.1016/j.scitotenv.2014.10.058>

M., Serrao, L., Bertoldi, W., Bizzi, S., Vitti, A., Hauer, C., Skrame, K., Cekrezi, B., Zolezzi, G.(C., 2022. Catchment-scale, multidecadal morphological trajectories of the large near-natural vjosa river in south-east europe. *Geomorphology* . Under-review.

Mavroulis, S., Lekkas, E., Carydis, P., 2021. Liquefaction Phenomena Induced by the 26 November 2019, Mw = 6.4 Durrës (Albania) Earthquake and Liquefaction Susceptibility Assessment in the Affected Area. *Geosciences* 11, 215. <https://doi.org/10.3390/geosciences11050215>

Miho, A., Kupe, L., Jaupaj, O., Karjalainen, S., Hellsten, S., Gunnar, P., 2008. Overview of Water Quality of Albanian Rivers.

Monegaglia, F., Zolezzi, G., Güneralp, I., Henshaw, A.J., Tubino, M., 2018. Automated extraction of meandering river morphodynamics from multitemporal remotely sensed data. *Environmental Modelling and Software* 105. <https://doi.org/10.1016/j.envsoft.2018.03.028>

Morphological response to river engineering and management in alluvial channels in Italy - ScienceDirect [WWW Document], n.d. URL <https://www.sciencedirect.com/science/article/pii/S0169555X02002192?via%3Dihub> (accessed 7.29.23).

Mulder, T., Syvitski, J.P.M., 1995. Turbidity Currents Generated at River Mouths during Exceptional Discharges to the World Oceans. *The Journal of Geology* 103, 285–299. <https://doi.org/10.1086/629747>

Nabaei, S., Saghafian, B., 2019. Cellular time series: A data structure for spatio-temporal analysis and management of geoscience information. *Journal of Hydroinformatics* 21. <https://doi.org/10.2166/hydro.2019.012>

Nilsson, C., Reidy, C.A., Dynesius, M., Revenga, C., 2005. Fragmentation and Flow Regulation of the World's Large River Systems. *Science* 308, 405–408. <https://doi.org/10.1126/science.1107887>

Pessenlehner, S., Liedermann, M., Holzapfel, P., Skrame, K., Habersack, H., Hauer, C., 2022. Evaluation of hydropower projects in Balkan Rivers based on direct sediment transport measurements; challenges, limits and possible data interpretation – Case study Vjosa River/Albania. *River Research and Applications* 38, 1014–1030. <https://doi.org/10.1002/rra.3979>

Peters, R., Berlekamp, J., Lucía, A., Stefani, V., Tockner, K., Zarfl, C., 2021. Integrated Impact Assessment for Sustainable Hydropower Planning in the Vjosa Catchment (Greece, Albania). *Sustainability* 13, 1514. <https://doi.org/10.3390/su13031514>

Phillips, J.D., Slattery, M.C., Musselman, Z.A., 2005. Channel adjustments of the lower Trinity River, Texas, downstream of Livingston Dam. *Earth Surface Processes and Landforms* 30. <https://doi.org/10.1002/esp.1203>

Piégay, H., Walling, D.E., Landon, N., He, Q., Liébault, F., Petiot, R., 2004. Contemporary changes in sediment yield in an alpine mountain basin due to afforestation (the upper Drôme in France). *CATENA, Geomorphic Impacts of Rapid Environmental Change* 55, 183–212. [https://doi.org/10.1016/S0341-8162\(03\)00118-8](https://doi.org/10.1016/S0341-8162(03)00118-8)

Poff, N.L., Allan, J.D., Bain, M.B., Karr, J.R., Prestegard, K.L., Richter, B.D., Sparks, R.E., Stromberg, J.C., 1997. The Natural Flow Regime A paradigm for river conservation and restoration The ecological integrity of river ecosystems depends on their natural dynamic character. *BioScience* 47.

Reduced braiding of rivers in human-modified landscapes: Converging trajectories and diversity of causes - ScienceDirect [WWW Document], n.d. URL

<https://www.sciencedirect.com/science/article/pii/S0012825217304312?via%3Dihub>
(accessed 7.22.23).

REFORM in a nutshell | REFORM [WWW Document], n.d. URL
<https://www.reformrivers.eu/> (accessed 11.26.23).

REFORM wiki [WWW Document], n.d. URL
https://wiki.reformrivers.eu/index.php?title=Main_Page (accessed 11.26.23).

Rinaldi, M., Surian, N., Comiti, F., Bussetini, M., 2015. A methodological framework for hydromorphological assessment, analysis and monitoring (IDRAIM) aimed at promoting integrated river management. *Geomorphology* 251.
<https://doi.org/10.1016/j.geomorph.2015.05.010>

Rinaldi, M., Surian, N., Comiti, F., Bussetini, M., 2013. A method for the assessment and analysis of the hydromorphological condition of Italian streams: The Morphological Quality Index (MQI). *Geomorphology* 180–181. <https://doi.org/10.1016/j.geomorph.2012.09.009>

Rosgen, D.L., 1994. A classification of natural rivers. *CATENA* 22, 169–199.
[https://doi.org/10.1016/0341-8162\(94\)90001-9](https://doi.org/10.1016/0341-8162(94)90001-9)

Schiemer, F., Beqiraj, S., Drescher, A., Graf, W., Egger, G., Essl, F., Frank, T., Hauer, C., Hohensinner, S., Miho, A., Meulenbroek, P., Paill, W., Schwarz, U., Vitecek, S., 2020. The Vjosa River corridor: a model of natural hydro-morphodynamics and a hotspot of highly threatened ecosystems of European significance. *Landscape Ecol* 35, 953–968.
<https://doi.org/10.1007/s10980-020-00993-y>

Schneider, C., Laizé, C.L.R., Acreman, M.C., Flörke, M., 2013. How will climate change modify river flow regimes in Europe? *Hydrology and Earth System Sciences* 17, 325–339.
<https://doi.org/10.5194/hess-17-325-2013>

Scorpio, V., Surian, N., Cucato, M., Prá, E.D., Zolezzi, G., Comiti, F., 2018. Channel changes of the adige river (Eastern Italian Alps) over the last 1000 years and identification of the historical fluvial corridor. *Journal of Maps* 14.
<https://doi.org/10.1080/17445647.2018.1531074>

Sediment transport at the network scale and its link to channel morphology in the braided Vjosa River system - Bizzi - 2021 - *Earth Surface Processes and Landforms* - Wiley Online Library [WWW Document], n.d. URL
<https://onlinelibrary.wiley.com/doi/10.1002/esp.5225> (accessed 7.22.23).

Shuker, J.L., Moggridge, H.L., Gurnell, A.M., 2015. Assessment of hydromorphology following restoration measures in heavily modified rivers: Illustrating the potential contribution of the Urban River Survey to Water Framework Directive investigations. *Area* 47. <https://doi.org/10.1111/area.12185>

Stecca, G., Zolezzi, G., Hicks, D.M., Surian, N., 2019. Reduced braiding of rivers in human-modified landscapes: Converging trajectories and diversity of causes. *Earth-Science Reviews* 188, 291–311. <https://doi.org/10.1016/j.earscirev.2018.10.016>

Surian, N., 2022. 9.24 - Fluvial Changes in the Anthropocene: A European Perspective, in: Shroder, J. (Jack) F. (Ed.), *Treatise on Geomorphology (Second Edition)*. Academic Press, Oxford, pp. 561–583. <https://doi.org/10.1016/B978-0-12-818234-5.00109-7>

Surian, N., Rinaldi, M., Pellegrini, L., 2011. Channel adjustments and implications for river management and restoration. *Geografia Fisica e Dinamica Quaternaria* 34.

Surian, N., Ziliani, L., Comiti, F., Lenzi, M.A., Mao, L., 2009. Channel adjustments and alteration of sediment fluxes in gravel-bed rivers of north-eastern Italy: Potentials and limitations for channel recovery. *River Research and Applications* 25. <https://doi.org/10.1002/rra.1231>

The Vjosa River at a Crossroad – Dam Tsunami or National Park? [WWW Document], 2015. . EuroNatur. URL <https://www.euronatur.org/en/what-we-do/news/the-vjosa-river-at-a-crossroad-dam-tsunami-or-national-park> (accessed 11.29.23).

Vörösmarty, C.J., McIntyre, P.B., Gessner, M.O., Dudgeon, D., Prusevich, A., Green, P., Glidden, S., Bunn, S.E., Sullivan, C.A., Liermann, C.R., Davies, P.M., 2010. Global threats to human water security and river biodiversity. *Nature* 467. <https://doi.org/10.1038/nature09440>

Wohl, E., 2020. Rivers in the Anthropocene: The U.S. perspective. *Geomorphology, The Binghamton Geomorphology Symposium: 50 years of Enhancing Geomorphology* 366, 106600. <https://doi.org/10.1016/j.geomorph.2018.12.001>

Wu, H., Lu, C., Shen, C., Ye, Y., 2023. Using a subsurface barrier to control seawater intrusion and enhance groundwater extraction in coastal aquifers: An analytical study. *Journal of Hydrology* 621, 129537. <https://doi.org/10.1016/j.jhydrol.2023.129537>

Wyżga, B., 2001. Impact of the channelization-induced incision of the Skawa and Wisłoka Rivers, southern Poland, on the conditions of overbank deposition. *Regulated Rivers: Research & Management* 17, 85–100. [https://doi.org/10.1002/1099-1646\(200101/02\)17:1<85::AID-RRR605>3.0.CO;2-U](https://doi.org/10.1002/1099-1646(200101/02)17:1<85::AID-RRR605>3.0.CO;2-U)

Xu, H., 2006. Modification of normalised difference water index (NDWI) to enhance open water features in remotely sensed imagery. *International Journal of Remote Sensing* 27, 3025–3033. <https://doi.org/10.1080/01431160600589179>

Zalasiewicz, J., Waters, C.N., Summerhayes, C.P., Wolfe, A.P., Barnosky, A.D., Cearreta, A., Crutzen, P., Ellis, E., Fairchild, I.J., Gałuszka, A., Haff, P., Hajdas, I., Head, M.J., Ivar do Sul, J.A., Jeandel, C., Leinfelder, R., McNeill, J.R., Neal, C., Odada, E., Oreskes, N., Steffen, W., Syvitski, J., Vidas, D., Wagreich, M., Williams, M., 2017. The Working Group on the Anthropocene: Summary of evidence and interim recommendations. *Anthropocene* 19, 55–60. <https://doi.org/10.1016/j.ancene.2017.09.001>

Ziliani, L., Surian, N., 2012. Evolutionary trajectory of channel morphology and controlling factors in a large gravel-bed river. *Geomorphology* 173–174, 104–117. <https://doi.org/10.1016/j.geomorph.2012.06.001>

Ziliani, L., Surian, N., Botter, G., Mao, L., 2020. Assessment of the geomorphic effectiveness of controlled floods in a braided river using a reduced-complexity numerical model. *Hydrology and Earth System Sciences* 24, 3229–3250. <https://doi.org/10.5194/hess-24-3229-2020>.

List of figures

Figure 1. 1. Hydrological map of Albania (Ozdemir, 2013). The eight river basins are highlighted by different colours.	7
Figure 1. 2. Monthly climate information of Albania based on the 1991-2020 period, data from the World Bank, Climate Change Knowledge Portal (2023)	9
Figure 1. 3. Illustrative images of the landscape of the Buna river in the left (a), part of Drin basin (source https://medwet.org/) and of the Vjosa river (b), (source: https://www.muchbetteradventures.com/magazine/vjosa-national-park-now-announcement/)	10
Figure 1. 4. Kukes City located in the North-East of Albania. (a) the city before creation of the Fierza hydropower dam in 1978. (b) the city after the completion of the dam.	11
Figure 1. 5. (a) Sediment mining in Shkumbin river. (b) Exposure of the “Bridge Zogu” foundation in Mat River associated with channel incision.....	11
Figure 1. 6. Terkuze River (Ishem river basin) near Tirana Airport. (a) Corona images 1973 (reach 5) and (b) satellite image of 2015, showing urbanization and buildings very close to the river channel, which at the same time has been dramatically narrowed.	12
Figure 1. 7. Examples of flooding in Albania. (a) flooding in lower part of Drin River, south of Shkodra city 23.11.22. (b) flooding in city of Tirana 03.11.2023, Lana River.	12
Figure 1. 8. Run off river hydro power plant in Valbona River (tributary of Drin River) in Albania. Valbona valley is a National Park. (a) construction phase in 2018 of hydropower plants in Valbona valley. (b) people from NGO that protest against hydropower plants that are being built in the same national Park (2022).....	13
Figure 1. 9. Coastal Erosion Impact, Lalzi Bay, Albania (Leo et al., 2017). (a) depicts the notable movement of Lalzi Bay's coastal line from 1985 to 2015, indicating an 800-meter loss. (b) photo taken in 2020, a bunker built before the 1990s on the local sand beach, is now submerged in the sea, illustrating the drastic effects of coastal erosion.	14
Figure 1. 10. Organizational chart for institutional framework on water resources management, Albania (Ministry of Agriculture and Rural Development, Albania, 2019).	17
Figure 1. 11. Morphological patterns of major Alpine rivers (Hohensinner et al., 2021) (a) historical patterns in the early 19 th century; (b) present-day patterns as detected in a 2017 satellite image.(Hohensinner et al., 2021).....	20
Figure 1. 12. Channel Trajectory concept. (a) Tagliamento river (Italy) channel width evolution in time (Ziiani, and Surian, 2012). (b) incision of Arno River (Italy) as documented by the comparison of the cross-sectional bed elevations over time in different years (Surian and Rinaldi 2002).....	20
Figure 2. 1. Map of the analysed river catchments.....	30
Figure 2. 2. a) Average annual discharge (m ³ /s) per catchment area; b) Total sediment load (ton/year) for each analysed catchment.....	33
Figure 2. 3. Results of the main steps of the watershed delineation workflow.	38
Figure 2. 4. Example of the output of the subdivision of a river catchment area into landscape or “physiographic” units (Mat River, Albania).....	39
Figure 2. 5. Illustration of the employed confinement parameters. Floodplain denoted in green, hillslopes / ancient terraces denoted in brown. From Rinaldi et al. (2014). Cd; Confinement degree; CI: Confinement index	42

Figure 2. 6. Transects generated for calculating the Confinement Index, Reach 13, Mat river. ...	43
Figure 2. 7. Map of confinement classes (Mat River, Albania)	44
Figure 2. 8. The eight river types of the Basic River Typology (BRT) defined by Rinaldi et al., (2016).....	45
Figure 2. 9. Nine typologies of the morphology to quantify the present morphology of Albanian river.....	46
Figure 2. 10. Measurement of the Sinuous Index.....	47
Figure 2. 11. (1) Hydrological discontinuity due to a major tributary; (2) discontinuity in bed slope; (3) change in size of the floodplain; change in channel width. From Rinaldi et al., (2015)	48
Figure 2. 12. An illustrative example of the used cartographic and satellite / aerial imagery sources. The example shows the evolution of river morphology and urban areas for a reach of the Tirana river, Ishem river basin.....	50
Figure 2. 13. Change of River Morphology from Braided to Channelized, Terkzue River, Ishem basin.....	51
Figure 2. 14. Geology characterization at catchment scale for rivers analysed	52
Figure 2. 15. Main geology classes (km ² and percentage of the total area) per catchment. Devoll and Osum river are catchments of Seman river.	53
Figure 2. 16. (a) Annual Sediment yield , per catchment area. (b) Annual sediment yield plotted against the % of some chosen geological categories, expected to be more erodible (red circles) and less erodible (blue circles).	54
Figure 2. 17. Map of the physiographic units of the analysed river catchments.	56
Figure 2. 18. Percentage area of each physiographic unit type relative to the total catchment area of the examined Albanian rivers.....	57
Figure 2. 19. Physiographic unit of the Albanian rivers in km ²	58
Figure 2. 20. Confinement map for major Albanian rivers.....	59
Figure 2. 21. Length of confinement classes in km	60
Figure 2. 22. Confined classes per each catchment (C-confined; SC- semi-confined; UC-unconfined).....	61
Figure 2. 23. River morphology atlas 1960 for majority rivers in Albania	63
Figure 2. 24. Albanian River morphological classes 1960	64
Figure 2. 25. Albanian river morphological atlas for 2015.....	65
Figure 2. 26. Albanian River Morphology classes 2015	66
Figure 2. 27. Morphology classes for two periods 1960 in the left and 2015 on the right with lighter colour.	67
Figure 2. 28. The Metamorphosis of Main Albanian River Morphologies: A Heat map comparison between 1960 and 2015.....	68
Figure 2. 29. Sequence relation diagram of river morphology changes from 1960 to 2015 changes	69
Figure 2. 30. Osum River-Reach 5, changes from braided to wandering morphology.....	70
Figure 2. 31. Devoll River-Reach 2, changes from wandering to sinuous morphology.....	71
Figure 3. 1. Erzen River catchment area.....	80
Figure 3. 2. Geological map of Erzen basin according to the reclassified six classes described in Chapter 2.....	82
Figure 3. 3. Semi-automatic method to study extract of the hydromorphological evolutionary trajectories of a reach (reproduced from Crivellaro et al., 2023).	84

Figure 3. 4. Visualization of the correspondence between the normalized difference vegetation index NDVI and the likely presence and type of vegetation. (source: https://eos.com/blog/ndvi-faq-all-you-need-to-know-about-ndvi/).....	85
Figure 3. 5. Envelope of active channel extracted for the selected reaches.	86
Figure 3. 6. Classification in four classes on reach 5, referring to year 2020.....	87
Figure 3. 7. Transects generated by mask for active channel (reach 17, 1985 Landsat). (a) transects generated with a spacing of 200m along the river centerline. (b) transects with length determined after the <i>r.mapcalc</i> command has been applied, which cuts the transects cut based on the active channel mask. (c) transect are inside the active channel and ready to export and calculated the average length. This is done for every 5 years of active channel.	89
Figure 3. 8. View of the available Corona images covering the Erzen river catchment.....	91
Figure 3. 9. Low-res view of the full spectrum of Corona images used for our reaches. Original images were further georeferenced.	91
Figure 3. 10. A visual impression of channel incision occurred in the lower Erzen river. (A) photo taken in November 2022 near Hardhishte village, in reach 4, at cross section 6 (B) photo taken in September 2020, in reach 1, at cross section 3 (figure 3.13 for cross-sections location).....	92
Figure 3. 11. Images of the GPS Sokkia GRX2 used for the topographic survey(Sokkia GRX2 Operator Manual, 2012)	94
Figure 3. 12. Location of the surveyed cross sections. Cross-sections number and distance along the river are progressively measured starting from the mouth. The first number in each white box indicates the cross-section number and the second number (+xy) indicate the distance (km) from the mouth measured along the river course.	94
Figure 3. 13. Illustrative example of scanned sheet of daily flow record in 1982 for Sallmone hydrometric station	97
Figure 3. 14. Evolution of land cover in reach 5 visualized by images obtained every five years from the analysis of Landsat imagery.	99
Figure 3. 15. Evolution of land cover in reach 17 (upstream of the Skorana dam) visualized by images obtained every five years from the analysis of Landsat imagery.	99
Figure 3. 16. Annual time series of land cover classes in reach 5 obtained from the analysis of Landsat imagery.	100
Figure 3. 17. Annual time series of land cover classes in reach 17 obtained from the analysis of Landsat imagery.	101
Figure 3. 18. Background image: Corona image (1968). Boundaries of the active river channel indicated in red (1968), blue (2015) and green (2022). (a) Reach 5; (b) reach 8.....	102
Figure 3. 19. Evolution of the distributions of reach-scale active channel width. Reach 5 (a), reach 8 (b), reach 11 (c) and reach 17 (d).....	103
Figure 3. 20. Time series of the active channel width distributions obtained from manual digitalisation of ASIG imagery reach 2. Year 2022 with light green colour, active channel width is extracted from google maps imagery.....	105
Figure 3. 21. Time series of the active channel width distributions obtained from manual digitalisation of ASIG imagery (a) and from the automated analysis of the Landsat imagery (b) for reach 5.....	105
Figure 3. 22. Longitudinal (instream coordinate) profiles of a representative low flow water level, of the floodplain elevation in the same transects and of their difference. The location of reaches R1 – R9 is reported on the top of the figure, together with the corresponding channel morphology, as it results from the analysis of Chapter 2 (M= Meander, S= Sinuous, ST= Straight, SAB= Sinuous with alternated bars).	106

Figure 3. 23. Ratio channel width and channel depth in m.....	107
Figure 3. 24. Cross-section Sallmone reach 3, 15 km from mouth (a1), cross-section Hardhishte reach 4, 19.7 km from mouth (b1), cross section Ura e Beshirit reach 9, 43.3 km from mouth (c1). Figures A2, B2 9taken in November 2022) and c2 (taken September 2020), represent the photos per each cross-section.....	108
Figure 3. 25. Illustrations of the artificial cutoff occurred in the meandering reach 2, and of the related indirect estimation of channel incision occurring afterwards. (a-c) Historical evolution of the artificial meander cut-off that occurred in reach 2 at the end of the 1960s; (d) Cross-section surveyed in November 2022, reach 2, which extends into the floodplain until the abandoned meandering channel, showing the difference in elevation between the former channel bed in the abandoned meander and the present riverbed of the active channel. (e) view of the present channel from the left bank of the right bank; (f) view of the banks in the right of the cross-section; (g) middle portion of the cross-section of the abandoned arm of the river.	109
Figure 3. 26. Map of anthropic pressures Erzen Basin.....	111
Figure 3. 27. View of some representative sediment mining sites in the Erzen River from the Orthophoto 2007. (a), reach 11, (b) reach 12). Source Geoportal Albania.	112
Figure 3. 28. Visual signs of the riverbed incision downstream of the reaches where the strongest concentration of sediment mining sites is observed. Both images show emergence of the bedrock. (a) Photo Riverbed Erzen River reach 7, November 2022. (b) Photo riverbed Erzen River reach 11, 2020.	112
Figure 3. 29. Catchment areas covered by dams. (a) areas drained by the two dams. (b) view of Skorana dam, used for irrigation and built in 1972; (c) Mudhar dam, built in 2014 for hydroelectricity.....	113
Figure 3. 30. Reach 16, immediately upstream the irrigation Skorana dam. Results of the Landsat imageries analysis showing the temporal changes in the land cover classes.	114
Figure 3. 31. Monthly average discharge and (b) results of the Mann-Kendall trend test on the same time series referring to Sallmone hydrometric station.	115
Figure 3. 32. Changes in forest cover Erzen basin	116
Figure 3. 33. Urban and rural population Albania (figure a). Population of Tirana and Durres districts (figure b). World bank data, 2022.....	117
Figure 3. 34. Urban area Tirana and Durres district. Figure a ₁ shows Tirana urban area with yellow in 1985 and figure b ₁ with red line Tirana urban area in 2015. Figure b ₁ shows the Durres district including two cities Durres and Shijak in 1985, urban area in yellow and figure b ₂ shows in red Durres district urban area in red line.	118
Figure 3. 35. Distance (km) of the downstream end of selected reaches from: the most downstream mapped sediment mining site in the catchment ("Max downstream", violet bars); the most upstream mapped sediment mining site in the catchment ("Max upstream", orange bars); the two dams built in 1973 (Skorana dam) and in 2014 (green and blue bars, respectively)	123

Figure 4. 1. Location of the main hydrometric stations in Erzen river. Sallmone hydrometric station located in lowland of the river that has been in operation since 1949; Ndroq hydrometric station starting from 1952 and Ibe from 1972.132

Figure 4. 2. Grain size distribution (mm) of at the hydrometric stations Ndroq and Sallmone. (a) suspended load grain size distribution. (b) bedload load composition grain size distribution.133

Figure 4. 3. Cumulative grain size distribution as measured for suspended load in Sallmone and Ndroq station. (Data Hydrology of Albania, 1979).	133
Figure 4. 4. (a) Ndroq from date 23-25.11.1966. Figure b) represent Sallmone 11-16.01.196. R kg/s represent the sediment flow. Q m ³ /s represent the discharge and ρ gr/m ³ represent the concentration measured.	134
Figure 4. 5. Cross section Sallmone Hydro station 17.11.1988 (Archive institute of Geoscience Albania)	135
Figure 4. 6. Data digitalization daily/ data available for Erzen river	138
Figure 4. 7. Example of data record sheet for 1976 for Sallmone station in Erzen river. Data representation are daily data in m ³ /s. The Sallmone hydrometric station, located near the town of Shijak in the Durres municipality of Albania, was operational from 1949 to 1992.	139
Figure 4. 8. Daily flow discharge (m ³ /s) in the used three main hydrometric stations in Erzen River. a) Ibe hydrometric station; b) Ndroq hydrometric station; c) Sallmone hydrometric station.	140
Figure 4. 9. Forces acting on a sediment particle (Chanson, 2004)	145
Figure 4. 10. Threshold Shields stress for sediment mobility or "Shields diagram" (reprinted from Armanini, 2018, and based on Shields, 1936).	146
Figure 4. 11. Conceptual diagram of the different modes of sediment transport in rivers (Chanson, 2004)	148
Figure 4. 12. Bed-load motion layer (a) and (b) definition sketch of the suspended load layer (Chanson, 2004)	150
Figure 4. 13. Calibrated suspended sediment transport in Sallmone station as average of year	154
Figure 4. 14. Monthly normalized discharge for the three hydrometric stations	155
Figure 4. 15. Correlation of monthly normalised discharge between pairs of the three hydrometric stations.	155
Figure 4. 16. Monthly distributions of daily discharge values for each of the three examined gauging stations in the Erzen River.	156
Figure 4. 17. Discharge (m ³ /s) information for the Ibe hydrometric station in Erzen River. (a) monthly mean discharge time series. (b) Results of the Man-Kendall trend test for the Ibe hydrometric station between 1972-1990 applied to mean monthly data computed from daily data.	156
Figure 4. 18. Discharge (m ³ /s) information for the Ndroq hydrometric station in Erzen River. (a) monthly mean discharge time series. (b) Results of the Man-Kendall trend test for the Ndroq hydrometric station between 1953-1992 applied to mean monthly data computed from daily data.	157
Figure 4. 19. Discharge (m ³ /s) information for the Sallmone hydrometric station in Erzen River. (a) monthly mean discharge time series. (b) Results of the Man-Kendall trend test for the Sallmone hydrometric station between 1949-1992 applied to mean monthly data computed from daily data.	158
Figure 4. 20. Gumbel distribution of different discharge percentiles for Sallmone hydrometric station (data record: 1949-1992).	159
Figure 4. 21. Return times of discharge for Sallmone station derived from Gumbel distribution.	160
Figure 4. 22. Predicted annual suspended load capacity for Sallmone Hydrometric station. (a) Annual suspended sediment transport using Van Rijn method. (b) Mann-Kendall trend test for	

suspended sediment transport prediction in the Sallmone hydrometric station showing P and Slope values of the test.....162

Figure 4. 23. Annual bedload transport capacity for Sallmone Hydrometric station. (a) Annual bedload sediment transport capacity using Van Rijn method. (b) Mann-Kendall trend test for simulated annual bedload in Sallmone hydrometric station showing P and Slope values of the test163

Figure 4. 24. Modelled suspended load transport capacity as function of the channel width B for different values of the channel slope and a fixed discharge Q corresponding to estimated bankfull conditions. The panel on the right is an enlargement of the red box on the left that corresponds to the relevant range of variability for the channel width in the lower Erzen (reach 3 as from Chapter 2) as it emerged from the analysis of channel adjustments.164

Figure 4. 25. Modelled suspended load transport capacity as function of the channel width B for different values of the reference discharge Q and a fixed channel slope corresponding to the value emergin from the calibration procedure. The panel on the right is an enlargement of the red box on the left that corresponds to the relevant range of variability for the channel width in the lower Erzen (reach 3 as from Chapter 2) as it emerged from the analysis of channel adjustments.....164

Figure 4. 26. Computation of main channel parameters in different channel condition. Figure a) represent suspended Q_s sediment transport in function of slope S and different channel width B , while discharge is constant Q . Figure b) plotted suspended sediment transport Q_s with Slope S and different discharge Q with fixed channel width B . Figure c) plotted sediment transport Q_s with discharge Q with different channel width B and slope S constant. Figure d) plotted suspended sediment transport Q_s with discharge Q and different slope S and channel width B constant.165

List of tables

Table 1. 1. Main characteristic of major Albanian rivers (Kabo. M, 1990; Hydrology of Albania, 1979).....	8
Table 2. 1. Main characteristic of River studied.....	29
Table 2. 2. Summary of general setting and segmentation procedure in the IDRAIM approach (modified from Rinaldi et al., 2013).	36
Table 2. 3. Criteria used to outline the main physiographic units by the IDRAIM method (e-elevation).	38
Table 2. 4. Selected criteria for physiographic categorization.	41
Table 2. 5. Definition of final confinement classes as obtained by combining the value ranges of confinement degree and confinement index. Reworked from Rinaldi et al., (2014)	42
Table 2. 6. Special data source used for the study.....	49
Table 3. 1. Main morphological properties of the selected reaches for the analysis. Confinement: UC- Unconfined, PC – Partially Confined, C- Confined, CI- Confinement Index; L- reach Length (km); Reach average elevation taken from DEM 10 m ASIG Albania; SI- Sinuosity index, Floodplain W- Floodplain average width in (m) are old terraces of the river created during the years, Active channel W- average width in m is the river corridor including water, gavel and sometimes vegetation.	81
Table 3. 2. Threshold values of NDVI and MNDWI used for determining the computation domain.	85
Table 3. 3. Pixel values after reclassification with their respective classes and pixel values before reclassification after merging the masks using the expression (3).....	88
Table 3. 4. Mann-Kendell trend test P Value range	90
Table 3. 5. Image ID, Acquisition date, Root-mean square error and covered reaches of the Corona Images Georeferencing procedure.	91
Table 3. 6. Results of the Mann-Kendall trend test for the time series of the different land cover classes for all reaches analysed.....	101
Table 3. 7. Values of the 25th, 50th and 75th percentiles of the reach-scale distributions of the active channel width as obtained from the semi-automated method (Landsat imagery) and from manual extraction on high-resolution orthophoto. Data refer to reach 5, which has experienced a strong narrowing in the period of observation.....	106
Table 3. 8. Summary of observed channel narrowing in the five target reaches of the Erzen in absolute terms, percentage and average annual rates, for the two phases of adjustment and for the entire period of observation (abs: absolute difference; %: percentage relative to initial year: narrowing rate in meters per year).....	120
Table 3. 9. Compilation of observed river channel narrowing rates in several European and World rivers. Adapted from Stecca et al. (2019) and other sources.....	121
Table 3. 10. Compilation of observed river channel narrowing rates in several European and World rivers. Adapted from Stecca et al. (2019) and other sources.....	122
Table 4. 1. Main characteristics of hydrometric station Ndroq and Sallmone. The data refer to long term average values. (Hydrology of Albania, 1979).	134

Table 4. 2 Calibration parameters for suspended load in Sallmone hydrostation154
Table 4. 3. Return time discharge of Sallmone hydrometric station data 1949-1992, with
different percentile, using the Gumbel distribution as a results of Pearson test of three methods
used: (i) Method of Moments (ii) Least Squares Method and (iii) Maximum Likelihood Method.
.....161